

TCAD Parameters for 4H-SiC: A Review

Jürgen Burin,¹ Philipp Gaggl,¹ Simon Waid,¹ Andreas Gsponer,¹ and Thomas Bergauer¹

Institute of High Energy Physics, Austrian Academy of Sciences, Nikolsdorfer Gasse 18, 1050 Wien

(*e-mail: juergen.burin@oeaw.ac.at)

(Dated: 2 December 2024)

In this paper we review the models and their parameters to describe the relative permittivity, bandgap, impact ionization, mobility, charge carrier recombination/effective masses and incomplete dopant ionization of 4H silicon carbide in computer simulations. We aim to lower the entrance barrier for newcomers and provide a critical evaluation of the status quo to identify shortcomings and guide future research. The review reveals a rich set of often diverging values in literature based on a variety of calculation and measurement methods. Although research for all the selected parameters is still active, we show that sometimes old values or those determined for other kinds of silicon carbide are commonly used.

Keywords: 4H-SiC, TCAD simulations, simulation parameters, silicon carbide

CONTENTS

I. Relative Permittivity	4
A. Theory	4
B. Results	5
C. Discussion	7
II. Density-of-States Effective Mass	11
A. Theory	12
1. Effective Masses along Principal Directions	12
2. Density-of-States (DOS) Mass	12
3. Conductivity Effective Mass	13
4. Polaron Mass	14
B. Results	15
1. Effective Mass along Principal Directions	15
2. DOS Mass	17
3. Temperature	20
4. Effective DOS Mass for TCAD Tools	21
C. Discussion	21
III. Band Gap	23
A. Theory	25
1. Temperature Dependency	26
2. Doping Dependency	27
B. Results & Discussion	29
1. Temperature Dependency	31
2. Doping Dependency	34
3. TCAD Values	36
IV. Impact Ionization	40
A. Theory	41
B. Results	43
C. Discussion	49

V. Charge Carrier Recombination	51
A. Theory	52
1. Shockley-Read-Hall Recombination	52
2. Bimolecular Recombination	57
3. Auger Recombination	58
4. Analysis	59
B. Results & Discussion	60
1. SRH Lifetime	61
2. Doping Dependency of SRH Lifetime	65
3. Temperature Dependency of SRH Lifetime	69
4. Surface Recombination Velocity	71
5. Bimolecular Recombination	74
6. Auger Recombination	74
VI. Incomplete Ionization	77
A. Theory	79
B. Results	81
C. Discussion	86
References	92

I. RELATIVE PERMITTIVITY

The permittivity ϵ describes the dielectric properties that influence electromagnetic wave propagation within a material and their reflections on interfaces². These effects are, for example, essential to describe the impact of an external electric field, which determines the capacitance values in a device. In general, the user has to provide the relative permittivity $\epsilon_r = \epsilon/\epsilon_0$, i.e., the ratio compared to the vacuum permittivity $\epsilon_0 = 8.854 \times 10^{-12} \text{ F/m}$, to the TCAD tools.

A. Theory

In the frequency domain, the complex relative permittivity can be written as

$$\epsilon_r^*(\omega) = \epsilon'(\omega) + i\epsilon''(\omega).$$

The real part ϵ' represents the energy stored in the material when exposed to an electric field and the imaginary part ϵ'' the losses (e.g., absorption and attenuation)². ϵ' and ϵ'' are tightly interconnected via the Kramers-Kronig (KK) relation³

$$\epsilon'(\omega) = 1 + \frac{2}{\pi} \int_0^\infty \frac{\omega' \epsilon''(\omega')}{\omega'^2 - \omega^2} d\omega' \quad (1a)$$

$$\epsilon''(\omega) = -\frac{2\omega}{\pi} \int_0^\infty \frac{\epsilon'(\omega')}{\omega'^2 - \omega^2} d\omega' \quad (1b)$$

In TCAD simulations of semiconductor devices ϵ'' is of diminishing importance, but ϵ' is required to calculate capacitances or the electric field distribution. Consequently, we will focus on ϵ' in the sequel.

In the literature the static (ϵ_s) and high-frequency resp. optical (ϵ_∞) relative permittivity are distinguished. The former is $\epsilon'(\omega \rightarrow 0)$ but a definition of the latter is more complicated. It denotes ϵ' at the end of the reststrahlen range towards higher frequencies, where the real part of the refractive index is null⁴. In publications that focus on optical high-frequency analysis ϵ_∞ is sometimes denoted as $\epsilon'(0)$ ⁵, which must not be confused with ϵ_s . These inconsistencies were explained in the following fashion⁶: “We shall use ϵ_∞ to denote the extrapolation … to zero frequency. This somewhat contradictory notation arose because ϵ_∞ the “optical” dielectric constant, was often set … at a frequency much higher than the lattice frequency, but low compared with electronic transition frequencies. In many substances no suitable frequency exists, and it is preferable to extrapolate optical data to zero frequency …”

To clarify: ϵ_∞ is measured at frequencies well above the long-wavelength longitudinal optical (LO) phonon frequency ω_{LO} ³. ω_{LO} translates ϵ_s into ϵ_∞ and vice versa in conjunction with the transversal optical (TO) phonon frequency ω_{TO} and the Lyddane-Sachs-Teller (LST) relationship⁷

$$\frac{\epsilon_s}{\epsilon_\infty} = \left(\frac{\omega_{\text{LO}}}{\omega_{\text{TO}}} \right)^2. \quad (2)$$

For ω_{LO} we encountered the energy values 120 meV (approximately 29 THz)^{8–12}, 104 to 121 meV¹³ and 104.2 meV¹⁴ in our search. Instead of the energy often the respective wave numbers are presented, i.e., (in cm^{-1}) $\omega_{\text{TO}} = 793$ and $\omega_{\text{LO}} = 974$ ¹⁵, $\omega_{\text{LO}}^{\parallel} = 964.2$, $\omega_{\text{LO}}^{\perp} = 966.4$, $\omega_{\text{TO}}^{\parallel} = 783$ and $\omega_{\text{TO}}^{\perp} = 798$ ¹⁶, $\omega_{\text{TO}} = 783$ and $\omega_{\text{LO}} = 964$ ¹⁷ and $\omega_{\text{LO}} \in [967, 971]$ ¹⁸.

B. Results

Various approaches have been used to determine the relative permittivity: One possibility are calculations using the density functional theory (DFT) based local density approximation (LDA)^{5,8,19–24} or the effective mass theory²⁵. With these the band structure and, thus, ϵ'' is calculated and then transformed into ϵ' using the Kramers-Kronig relations (Eq. (1)). Measurements use either some form of resonator (RES)^{26–28}, spectroscopy (SPEC)^{29–31}, spectroscopic ellipsometry (SE)^{32,33} or the refractive index (RI)^{6,16,34}. In some cases the transversal and longitudinal optical phonon frequencies are determined and used in the LST relationship (Eq. (2))^{32,33}. Furthermore, the tight relationship between relative permittivity and complex refractive index, i.e., $n^*(E) = \sqrt{\epsilon(E)}$ ³, with $E = \hbar\omega$, is utilized if ϵ'' is negligible. For fitting purposes the representation

$$n^2 = 1 + \frac{\epsilon_g}{1 - (hf/E_g)^2} \approx \epsilon_\infty + \epsilon_g \left(\frac{hf}{E_g} \right),$$

with hf the photon energy, E_g an "average band gap" and ϵ_g proportional to the oscillator strength⁶, is used to extract ϵ_∞ ^{6,16,30,34}. Finally, fitting to $\ln(J/E)$ ³⁵, with J the current density, is also deployed.

The relative permittivity was furthermore investigated at mm-wave frequencies (MM) (10 GHz to 10 THz)^{27,36–39} (nicely summarized by Li *et al.*²⁸, Yanagimoto *et al.*⁴⁰). Unfortunately, there are often fluctuations in the data or just single data points available, which makes an interpolation to zero frequency ($= \epsilon_s$) not possible. For these reasons we had to discard most of the respective data. We also excluded publications whose values got refined in succeeding experiments^{41,42}, that

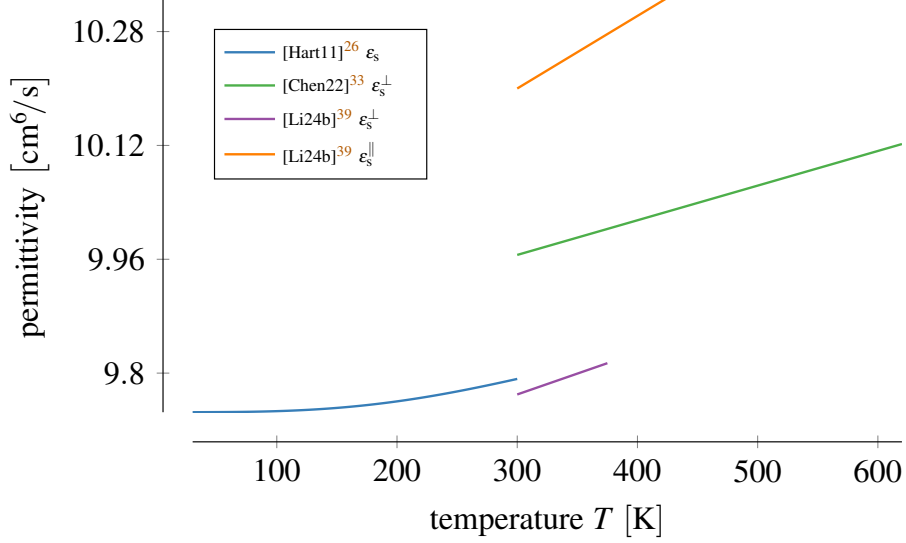


FIG. 1. Temperature dependency of the permittivity.

did not specify the investigated polytype^{43–46} or where an extraction of the data values was not possible⁴⁷.

With the listed characterization approaches values in the range of [9.6, 10.65] for the static relative permittivity and [6.25, 7.61] for the high-frequency one have been achieved (Table I). In the table we also show two references that exclusively provide 6H values because these are often referenced for 4H investigations. Wherever necessary we calculated the relative permittivity according to $\epsilon_s = (\epsilon_s^\parallel \epsilon_s^\perp)^{\frac{1}{2}}$ resp. $\epsilon_\infty = (\epsilon_\infty^\parallel \epsilon_\infty^\perp)^{\frac{1}{2}}$ ^{48–52}, which far more often used than $\epsilon_s = (\epsilon_s^\parallel \epsilon_s^\perp)^{\frac{1}{2}}$ proposed by Ivanov *et al.*²⁵.

In TCAD tools the permittivity is a constant although research showed that there is a frequency²⁶ and temperature^{26,33} dependency. For a frequency around 40 GHz Hartnett *et al.*²⁶ provided the approximation

$$\epsilon_s(T) = 9.7445 + 3.1862 \times 10^{-5} T - 6.3026 \times 10^{-7} T^2 + 5.9848 \times 10^{-9} T^3 - 8.2821 \times 10^{-12} T^4 ,$$

with the temperature T in K. Cheng, Yang, and Zheng³³ approximated $\epsilon_s^\perp = 9.82 + 4.87 \times 10^{-4} T$ and Li *et al.*³⁹ $\epsilon_s^\perp = 9.77 * (1 + 6 \times 10^{-5}(T - 300\text{K}))$ and $\epsilon_s^\parallel = 10.2 * (1 + 1 \times 10^{-4}(T - 300\text{K}))$. All approximations show an increase of the permittivity with temperature (Fig. 1).

TABLE I. Published relative permittivity values.

ref.	ϵ_s	ϵ_s^{\parallel}	ϵ_s^{\perp}	ϵ_{∞}	$\epsilon_{\infty}^{\parallel}$	$\epsilon_{\infty}^{\perp}$	method ^a	SiC	doping
[Patr70] ^b	9.78 ^c	10.03	9.66	6.58 ^c	6.7	6.52	RI	6H	-
[Ikeda80] ³⁴	9.94 ^c	10.32	9.76	-	-	-	RI	4H	-
[Nino94] ³²	9.83 ^c	9.98	9.76	6.62 ^c	6.67	6.59	SE	6H	-
[Hari95] ¹⁶	-	-	-	6.63 ^c	6.78	6.56	RI	4H	-
[Karc96] ¹⁹	10.53 ^c	10.9	10.352	7.02 ^c	7.169	6.946	DFT-LDA	4H	-
[Well96] ²⁰	-	-	-	7.02 ^c	7.17	6.95	DFT-LDA	4H	-
[Adol97] ²¹	-	-	-	7.56 ^c	7.61	7.54	DFT-LDA	4H	-
[Ahuj02] ⁸	-	-	-	7.11 ^c	7.47	6.94	DFT-LDA	4H	n-type
[Peng04] ²²	-	-	-	6.31 ^c	6.44	6.25	DFT	4H	-
[Pers05] ⁵³	9.73 ^c	9.94	9.63	6.47 ^c	6.62	6.4	DFT-LDA	4H	intrinsic
[Chin06] ⁵	-	-	-	6.81	-	-	DFT-LDA	4H	intrinsic
[Dutt06] ³⁶	9.97 ± 0.02 ^b	-	-	-	-	-	MM	4H	high purity
[Ivan06] ²⁵	9.93 ± 0.01	-	-	-	-	-	EMT	4H	intrinsic
[Hart11] ²⁶	9.77 ^d	-	-	-	-	-	RES	4H	high purity
[Jone11] ²⁷	9.6	-	-	-	-	-	RES	4H	high purity
[Naft16] ²⁹	10.11 ^c	10.53 ^f	9.91 ^f	-	-	-	SPEC	4H	undoped
[Cout17] ²⁴	10.13 ^c	10.65	9.88	-	-	-	DFT-LDA	4H	-
[Tare19] ³⁰	-	-	-	6.587 ± 0.003	-	-	SPEC	4H	-
[Chen22] ³³	9.97 ^g	-	-	-	-	-	SE	4H	-
[Gao22a] ³¹	-	-	-	6.51	-	-	SPEC	4H	-
[Yang22a] ³⁵	10.21	-	-	-	-	-	$\ln(J/E)$	4H	p-type
[Li23] ²⁸	-	10.27 ± 0.03	-	-	-	-	RES	4H	high purity
[Li24b] ³⁹	9.91 ^c	10.20 ± 0.05	9.77 ± 0.01	-	-	-	RES	4H	high purity

^a description of the single methods in the text

^b frequency range 131–145 GHz, for lower resp. higher frequencies $\epsilon_s = 9.74$ was achieved

^c $\epsilon_s = (\epsilon_s^{\perp 2} \epsilon_s^{\parallel})^{1/3}$

^d temperature and frequency dependent

^e calculated from refractive index n as $\epsilon_s = n^2$

^f wavelength-dependent refractive index presented

^g temperature dependent

C. Discussion

We identified two very influential publications, largely dominating the permittivity values found in literature. Ikeda, Matsunami, and Tanaka³⁴ published, based on measurements from Shaffer⁵⁸, in 1980 the first 4H-SiC permittivity data. Although these values are broadly used in liter-

ature^{23,59–63}, we never found a citation of that particular paper. Not even cross-references among the citing publications exist.

In 1970, so ten years prior to the first 4H values, Patrick and Choyke⁶ determined, based on measurements published in 1944⁶⁴, the permittivity of the 6H polytype. Many publications on 4H-SiC used these results (see Fig. 2) despite the deviating polytype. Some authors claimed that dedicated 4H values were not available^{13,49,65–68}, a mistake as we showed before. Nevertheless, it is still claimed up to this day³³. This shows, how hard it is to get a comprehensive overview over 4H-SiC TCAD parameters. In contrast to early analysis, that clearly highlight that 6H values were used⁶⁹, the majority of publications simply adopts the parameters without further remark, which leaves the false impression that proper 4H values were used.

Rounding of the original values, e.g., $9.66 \rightarrow 9.7 \rightarrow 10^{72,83}$ (see Fig. 2), and mere typographical errors, e.g., turning 9.66 into 9.67⁹² (a comprehensive analysis of all encountered inconsistencies is shown in ??), expanded the range of available values (see Figs. 3 and 4). In these figures we connected those values where at least one direct connection could be found. Due to missing references we can, however, not guarantee that all authors made their selection based on the same data. In many cases, e.g., for the prominent values $\epsilon_s = 9.7$ or $\epsilon_s = 10$, it is not unreasonable to assume that simply the permittivity in one principal direction was picked.

An interesting case is $\epsilon_s = 8.5584^{93,94}$, which is supposed to be based on $\epsilon_s^\perp = 9.66$ and $\epsilon_s^\parallel = 10.03^{57}$. We were not able to achieve this value analytically since the result is lower than both constituents. Only when we added the high-frequency relative permittivity to the calculations we achieved a somewhat close value of 8. Such a combination is, however, not justifiable.

Overall, the missing awareness regarding 4H related permittivity values is striking. One explanation why the same old values are reused over and over again are the often very long citation (see Fig. 2). Combined with often missing references this makes it difficult to pinpoint the origin of a value and thus assess its suitability. Another interpretation of the achieved results is that the permittivity has little impact in TCAD simulations, such that somewhat accurate 6H values are already sufficient. Nevertheless, even if this was the case, we highly encourage the scientific community to adopt the most recent measurement 4H-SiC in future publications to make these values more prominently known and, thus, lead to a wider distribution.

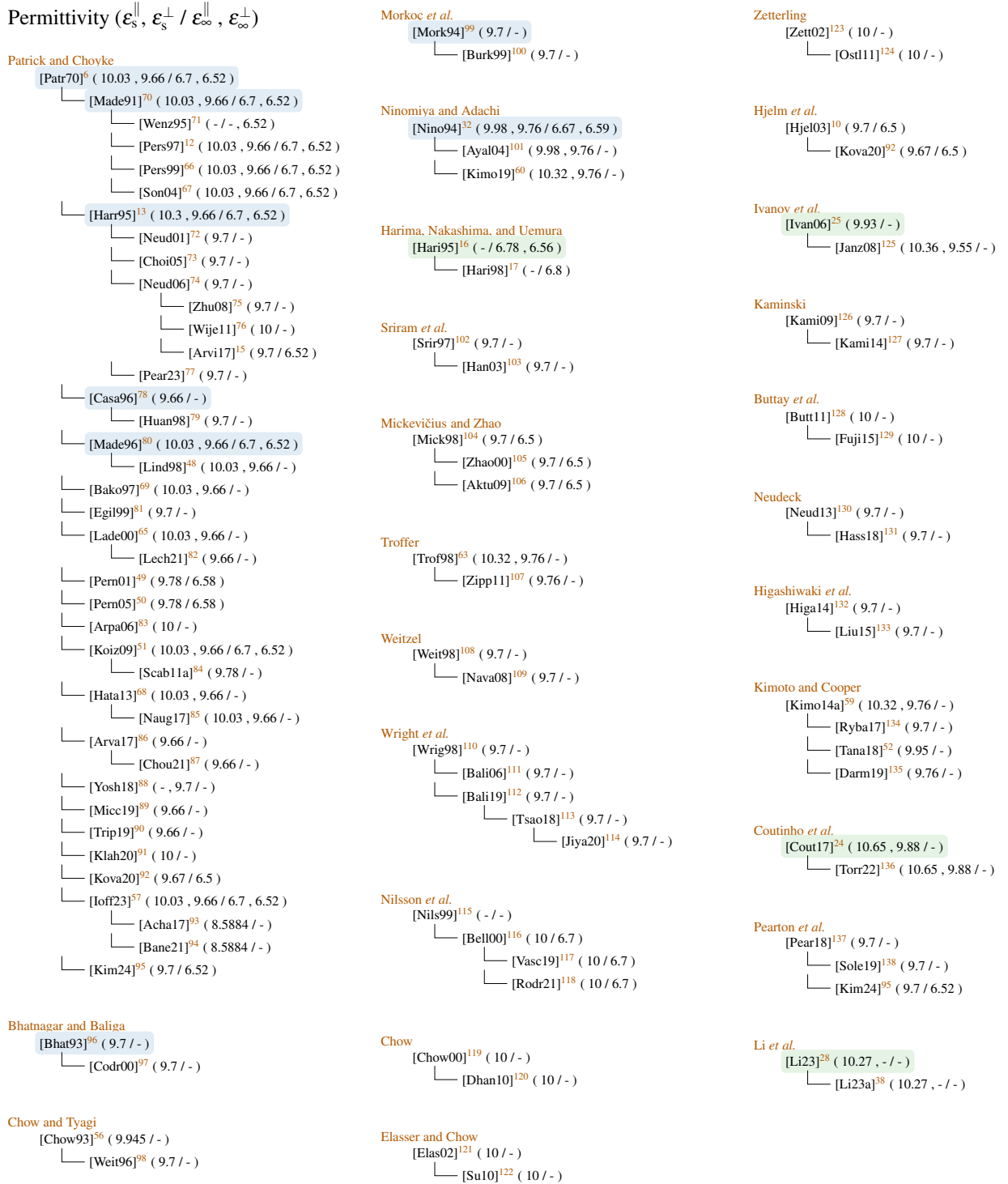


FIG. 2. Reference chains found for the relative permittivity. Publications with blue background are not focused on 4H-SiC, while those in green are novel analyses on 4H-SiC.

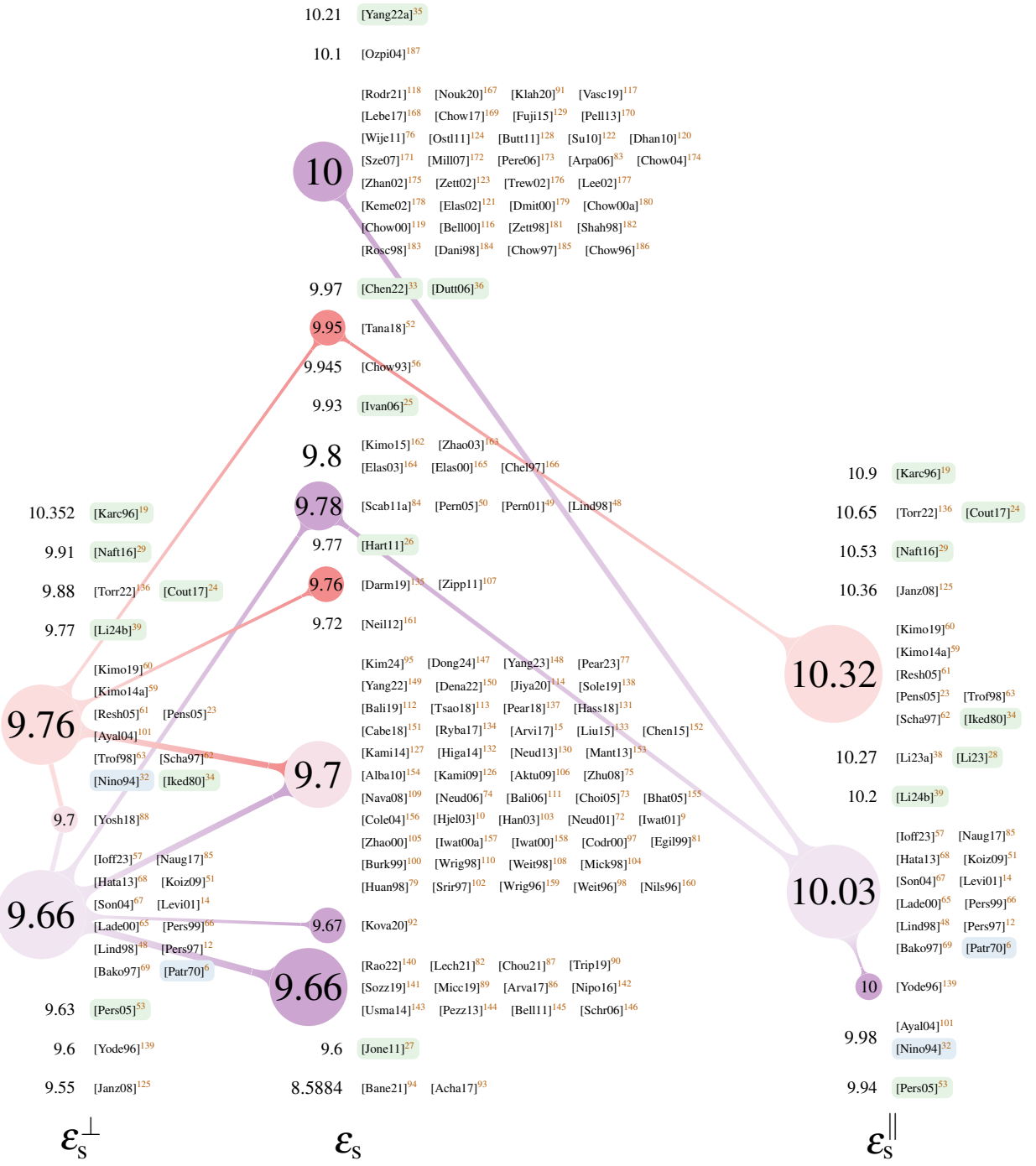


FIG. 3. Published values for the static permittivity. Connected values indicated that at least one connection has been found. References with blue background indicate investigations of non-4H silicon carbide while green background denotes basic 4H-SiC investigations.

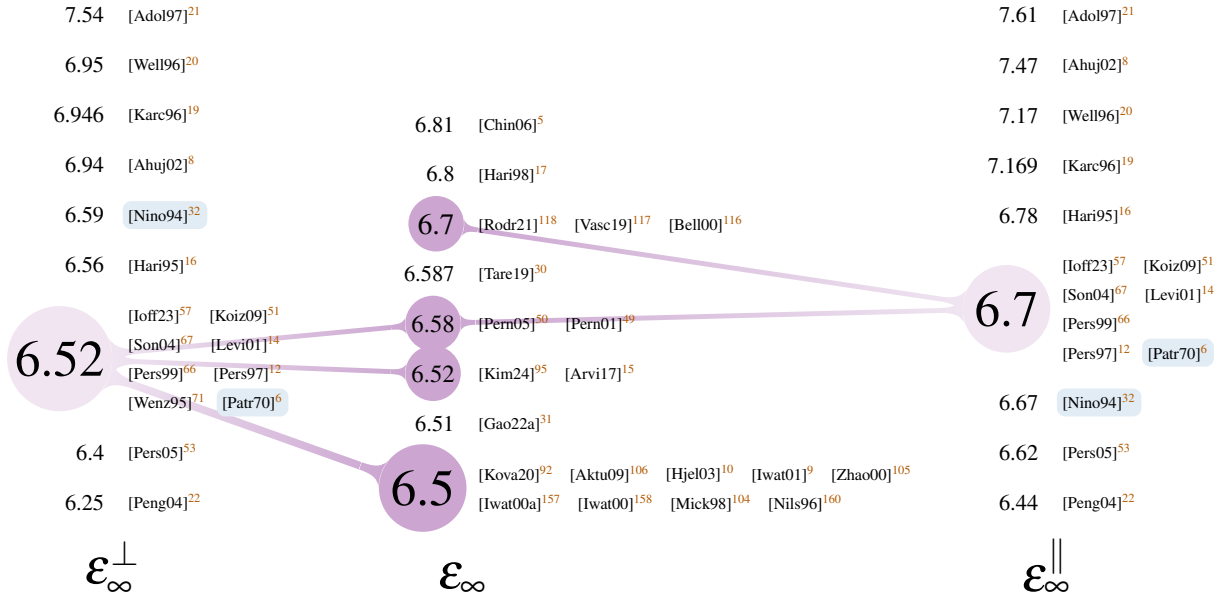


FIG. 4. Published values for the high-frequency permittivity. Connected values indicated that that at least one connection has been found. References with green background indicate investigations of non-4H silicon carbide while blue background denotes basic 4H-SiC investigations.

II. DENSITY-OF-STATES EFFECTIVE MASS

The effective mass of charge carriers is defined as the reciprocal of the second derivative of the spherically averaged dispersion relation⁴⁸ and, thus, dependent on the shape of the conduction/valence band. Because the latter are not uniform in a semiconductor deviating masses for each principal direction are achieved. These direction-dependent values are then further combined to end up with more simplistic descriptions³.

In this section we investigate the effective mass of electrons and holes in each principal direction and how these get merged into the density-of-states (DOS) and conductivity mass. We extend earlier overview publications^{13,23,62,63,188–190} and focus primarily on the DOS masses because they are used in TCAD simulations in various occasions, e.g., the calculation of the charge carrier concentration or impact and incomplete ionization. We want to highlight that in TCAD tools many additional effective masses are used, e.g., tunneling masses, quantum well masses, effective mass at the contact or in a channel or thermionic relative masses, which must not be confused.

A. Theory

In the sequel we start with a short theoretical analysis of effective masses. For further information the interested reader is referred to the dedicated literature^{3,13,23,53,62,67,188,189,191}. To increase the readability the effective masses are denoted relative to the free electron mass m_0 , i.e., $m^* = m/m_0$ ¹⁹².

1. Effective Masses along Principal Directions

For electrons the mass is specified in the directions starting in the conduction band minimum at the M point^{101,189,193–195} (cp. ??) towards the Γ , K and L point, denoted in the sequel as m_{MF}^* , m_{MK}^* and m_{ML}^* . The first two are perpendicular to the c-axis and the last one parallel^{69,101,196,197}. In the M point two conduction bands are very close together, such that both can influence the effective mass^{62,195}. Zhao *et al.*¹⁰⁵ even used three conduction bands. If not otherwise stated we will focus in this paper solely on the lowest one.

The valence band maximum is in the Γ point^{63,69,101}. Consequently, the three relative masses are termed m_{TM}^* , m_{TK}^* (perpendicular) and m_{TA}^* (parallel) indicating the directions towards the M, K and A point^{195,198}. At the Γ point three separate bands meet^{67,69,193,198,199}, whereat the two topmost are called heavy-hole (hh) and light-hole (lh) and the third one crystal split off (so)^{67,199}. Although all have to be considered for an accurate estimation often only a subset is used.

2. Density-of-States (DOS) Mass

The effective density of states for conduction (N_C) and valence (N_V) band^{65,84,107,201,202}

$$N_C = 2 M_C \left(\frac{2\pi m_{\text{de}}^* k_B T}{h^2} \right)^{3/2}$$

$$N_V = 2 \left(\frac{2\pi m_{\text{dh}}^* k_B T}{h^2} \right)^{3/2},$$

with M_C the number of conduction band minima in the first Brillouin zone²⁰², is, for example, used to evaluate the electron and hole concentration. The utilized effective density-of-states masses m_{de}^* and m_{dh}^* are defined as^{23,69,81,191}

$$m_{\text{de}}^* = (m_{\text{de}\perp}^* m_{\text{de}\parallel}^*)^{1/3} = (m_{\text{MF}}^* m_{\text{MK}}^* m_{\text{ML}}^*)^{1/3}$$

$$m_{\text{dh}}^* = (m_{\text{dh}\perp}^* m_{\text{dh}\parallel}^*)^{1/3} = (m_{\text{TM}}^* m_{\text{TK}}^* m_{\text{TA}}^*)^{1/3}$$

with⁶⁷

$$\begin{aligned} m_{de\perp}^* &= \sqrt{m_{MF}^* m_{MK}^*}, & m_{de\parallel}^* &= m_{ML}^* \\ m_{dh\perp}^* &= \sqrt{m_{TM}^* m_{TK}^*}, & m_{dh\parallel}^* &= m_{TA}^*. \end{aligned}$$

In this case m_{de}^* is called the *single valley* DOS electron effective mass^{23,68,81,101}, as the factor M_C is not considered. It is also very common, e.g., in some TCAD tools, to add M_C to the effective mass^{3,69,154,204,205}, i.e.,

$$m_{de}^* = (M_C^2 m_{de\perp}^* {}^2 m_{de\parallel}^*)^{1/3}.$$

In this review we will only present the single valley values and highlight all publications where we found expressions including M_C .

For an effective mass of the holes it is also necessary to combine the masses of heavy (m_{hh}^*) and light (m_{lh}^*) holes, which can be achieved by^{48,50,171}

$$m_{dh}^* = \left(m_{hh}^* {}^{3/2} + m_{lh}^* {}^{3/2} \right)^{2/3}. \quad (3)$$

This expression is already a simplification, because for accurate results the energy difference between the bands has to be considered⁶⁹. This leads to

$$m_h^*(T) = \left[m_{h1}^{3/2} + m_{h2}^{3/2} \exp\left(-\frac{\Delta E_2}{k_B T}\right) + m_{h3}^{3/2} \exp\left(-\frac{\Delta E_3}{k_B T}\right) \right]^{2/3} \quad (4)$$

where ΔE_2 and ΔE_3 denote the energy separation between the bands.

a. Temperature Dependency The changing amount of charge carriers with temperature can be compactly modeled by using a *thermal DOS effective mass*^{191,206}. There is no explicit form available but it was calculated by Wellenhofer and Rössler¹⁹¹ (electrons and holes separately) and Tanaka *et al.*⁵² (average effective mass). Later Schadt⁶², Hatakeyama, Fukuda, and Okumura⁶⁸ fitted the results from Wellenhofer and Rössler¹⁹¹ with an equation of the form

$$m^*(T) = \left(\frac{z_0 + z_1 T + z_2 T^2 + z_3 T^3 + z_4 T^4}{1 + n_1 T + n_2 T^2 + n_3 T^3 + n_4 T^4} \right)^\eta \quad (5)$$

for both electrons and holes. Such a change in the effective DOS mass is not yet covered in TCAD simulations suites.

3. Conductivity Effective Mass

For investigations of the mobility in 4H-SiC^{9,52,62,79,157,158,207–211} the mobility mass is a crucial simplification, e.g., in¹⁸⁹

$$\mu = \frac{e\tau}{m_c^*},$$

with μ the mobility, e the elementary charge and τ the lifetime (see ??). The conductivity mass must not be confused with the DOS mass since its definition^{3,212}

$$m_{ce}^* = \frac{3m_{ce\perp}^* m_{ce\parallel}^*}{m_{ce\perp}^* + 2m_{ce\parallel}^*}$$

$$m_{ch}^* = \frac{3m_{ch\perp}^* m_{ch\parallel}^*}{m_{ch\perp}^* + 2m_{ch\parallel}^*}$$

with^{207,208}

$$\frac{2}{m_{ce\perp}^*} = \frac{1}{m_{MK}^*} + \frac{1}{m_{M\Gamma}^*}, \quad m_{ce\parallel}^* = m_{ML}^*$$

$$\frac{2}{m_{ch\perp}^*} = \frac{1}{m_{\Gamma M}^*} + \frac{1}{m_{\Gamma K}^*}, \quad m_{ch\parallel}^* = m_{\Gamma A}^*$$

which results in⁷⁹

$$\frac{3}{m_{ce}^*} = \frac{1}{m_{M\Gamma}^*} + \frac{1}{m_{MK}^*} + \frac{1}{m_{ML}^*}$$

$$\frac{3}{m_{ch}^*} = \frac{1}{m_{\Gamma M}^*} + \frac{1}{m_{\Gamma K}^*} + \frac{1}{m_{\Gamma A}^*}.$$

is fundamentally different. In the sequel we will solely concentrate on the DOS mass.

4. Polaron Mass

In the Si-C bond of silicon carbide, carbon atoms are more electronegative than silicon ones. This results in a partly ionic crystal⁶⁷. Within this surrounding a charge carrier, together with its self-induced polarization, forms a quasiparticle, which is called a polaron²¹³. This can also be described by longitudinal optical vibrations that generate an electric field along the direction of the vibration which interacts with the charge carriers^{67,192}. Effectively, the carrier is “dressed” by a charge leading to a deviating effective mass¹². The adapted mass m_p , called *polaron mass*, is slightly higher than the bare mass m and can be calculated as^{12,53,67}

$$m_p = m \frac{1 - 8 \times 10^{-4} \alpha^2}{1 - \alpha/6 + 3.4 \times 10^{-3} \alpha^2} \approx m \left(1 - \frac{\alpha}{6}\right)^{-1}$$

with the Fröhlich constant α defined as

$$\alpha = \frac{1}{2} \left(\frac{1}{\epsilon_\infty} - \frac{1}{\epsilon_s} \right) \frac{e^2}{\hbar \omega_{LO}} \left(\frac{2m\omega_{LO}}{\hbar} \right)^{1/2} \frac{1}{4\pi\epsilon_s}.$$

In the latter e denotes the elementary charge, $\epsilon_s/\epsilon_\infty$ the static/high-frequency dielectric constant and ω_{LO} the longitudinal optical phonon frequency (see Section I). We want to highlight that in some definitions in literature^{213–215} the last term $1/4\pi\epsilon_s$ is missing due to a differing unit system.

Note that in (optically detected) cyclotron resonance measurements always the polaron mass is extracted. For a better comparability it is thus necessary to adapt non-polaron masses, e.g., those achieved by calculations¹⁹⁵.

B. Results

In the following we show the results of our investigations. Note that we discarded conductivity masses, e.g., by Mikami, Kaneko, and Kimoto²¹⁷, and solely concentrate on the DOS mass here. We also did not include the results by Son *et al.*²¹⁸ since Son *et al.*⁶⁷ later stated that the smaller values are due to “errors caused by a broad and asymmetric ODCR line shape with the peak position slightly shifted to lower magnetic fields”.

1. Effective Mass along Principal Directions

To determine the effective masses mainly band structure calculations are used. The most common ones are based on the density functional theory (DFT) local density approximation (LDA)^{71,106,160,191,194–196,219}. Differing methods, e.g., projector augmented wave (PAW)^{198,220}, (full-potential) linearized augmented plane wave ((FP)LAPW)^{12,53,67,193,221}, (orthogonalized) linear combination of atomic orbital ((O)LCAO)^{5,222}, full-potential linear muffin-tin orbital method (FPLMTO)²²³ and hybrid pseudo-potential and tight-binding (HPT)²²⁴, were utilized in this context. Other calculations include empirical pseudo potentials (EPM)^{116,225} and RSP Hamiltonians (RSPH)¹⁹⁹.

Results achieved by these calculations are sometimes combined using Monte Carlo (MC)^{106,160} simulations or genetic algorithm fitting (GAF)^{228,229}. In some cases the literature values were used as starting point for further analyses. Based on the data from Son *et al.*²¹⁸ such a refinement was executed by Nilsson, Sannemo, and Petersson¹⁶⁰, whose results then served as starting point for a fitting by Mickevičius and Zhao¹⁰⁴. Similarly, Mikami, Kaneko, and Kimoto²¹⁷ calculated the hole mass as the second derivative of the E-k dispersion by Persson and Lindefelt¹⁹³.

The calculations are complemented by measurements, for example by optically detected cy-

TABLE II. Effective masses in principal directions. Multiple values for the same band are calculated by differing algorithms.

ref.	electron				band	hole				method ^a	polaron
	m_{MF}^* [m_0]	m_{MK}^* [m_0]	m_{ML}^* [m_0]			$m_{\Gamma\text{M}}^*$ [m_0]	$m_{\Gamma\text{K}}^*$ [m_0]	$m_{\Gamma\text{A}}^*$ [m_0]			
[Kack94] ²¹⁹	0.62	0.13	0.39	-	-	4.23	2.41	1.73	hh	DFT-LDA	-
	-	-	-	-		0.45	0.77	1.73	lh	DFT-LDA	-
	-	-	-	-		0.74	0.51	0.21	so	DFT-LDA	-
[Karc95] ¹⁹⁴	0.66	0.31	0.3	-	-	-	-	-	-	DFT-LDA	-
[Lamb95] ²²³	0.58	0.28	0.31	-	-	-	-	-	-	DFT-LDA	-
[Wenz95] ⁷¹	0.6	0.28	0.19	-	-	-	-	-	-	DFT-LDA	-
[Nils96] ¹⁶⁰	0.43	0.43	0.28	1	-	-	-	-	-	DFT-LDA	-
	0.52	0.21	0.45	2		-	-	-	-	DFT-LDA	-
[Pers96] ¹⁹³	0.57	0.28	0.31	-	-	-	-	-	-	DFT-LDA	-
[Volm96] ²²⁶	0.58 ± 0.01	0.31 ± 0.01	0.33 ± 0.01	-	-	-	-	-	-	ODCR	y
[Chen97] ²²⁴	1.2	0.19	0.33	-	-	-	-	-	-	DFT-LDA	-
[Pers97] ¹²	0.57	0.28	0.31	1	-	-	-	-	-	DFT-LDA	-
	0.59	0.31	0.34	1		-	-	-	-	DFT-LDA	-
	0.61	0.29	0.33	1		-	-	-	-	DFT-LDA	y
	0.78	0.16	0.71	2		-	-	-	-	DFT-LDA	-
	0.8	0.18	0.75	2		-	-	-	-	DFT-LDA	-
	0.85	0.17	0.77	2		-	-	-	-	DFT-LDA	y
[Pers98a] ²²⁷	-	-	-	-	-	0.7	3.04	1.64	1	fit	-
	-	-	-	-		0.6	0.34	1.64	2	fit	-
[Bell00] ¹¹⁶	0.57	0.23	0.27	-	-	-	-	-	-	EPM	-
[Zhao00a] ²²²	0.62 ± 0.03	0.27 ± 0.02	0.31 ± 0.02	-	-	-	-	-	-	DFT-LDA	-
[Penn01] ²²⁵	0.60 ± 0.05	0.20 ± 0.02	0.36 ± 0.02	-	-	-	-	-	-	EPM	-
[Iwat03] ¹⁹⁶	0.59	0.29	-	-	-	-	-	-	-	DFT-LDA	-
[Iwat03a] ²⁰⁹	0.58	0.3	-	-	-	-	-	-	-	Hall	-
[Dong04] ¹⁹⁵	0.53	0.27	0.3	-	-	0.86	0.95	1.58	1	DFT-LDA	-
	-	-	-	-		0.55	0.52	1.32	2	DFT-LDA	-
	-	-	-	-		1.13	1.30	0.21	3	DFT-LDA	-
[Chin06] ⁵	0.47	-	0.38	-	-	-	-	-	-	DFT-LDA	-
[Ng10] ²²⁸	0.66	0.31	0.34	-	-	-	-	-	-	GAF	-
[Kuro19] ¹⁹⁸	0.54	0.28	0.31	-	-	0.54	0.54	1.48	-	DFT-LDA	-
[Lu21] ²²⁰	0.54	0.3	-	-	-	2.77	1.82	1.52	-	DFT-LDA	-

^a for explanation see text

clotron resonance (ODCR)^{192,211,218,226,230}, photoluminescence⁸¹, infrared absorption (IR)²⁰², Raman scattering¹⁶ and Hall effect measurements^{51,209,231,232}. However, for the relative masses in the principal directions (see Table II) calculations clearly dominate. Only two measurements^{209,226} could be found for the electron masses whereat not a single experimental evaluation for hole masses was achieved.

In literature the hole bands are either denoted as heavy-hole (hh), light-hole (lh) and crystal split-off (so) or simply as 1, 2, 3. According to the found values we are confident to say that $1 \equiv \text{hh}$, $2 \equiv \text{lh}$ and $3 \equiv \text{so}$.

2. DOS Mass

For a comprehensive overview on DOS masses we combine calculations based on the effective masses in the principal directions and values presented in literature (see Table III and Table IV). Again, calculations clearly dominate, however, an increased amount of measurements^{51,192,209,218,226,231,232}, including some for the hole mass, could be acquired.

The values show significant deviation. In addition Schadt⁶² stated that they are only valid close to the band minimum/maximum as they are calculated there or at very low temperature. Furthermore, Son *et al.*⁶⁷ claimed that if the polaron effect is added to the results from Persson and Lindefelt^{193,221} the values $m_{\text{dh}\perp}^* = 0.66$ and $m_{\text{dh}\parallel}^* = 1.76$ are achieved, which fit the results from ODCR measurements well. In the opinion of these authors it is also important to consider spin-orbit couplings for holes. Zhao *et al.*¹⁰⁵ is the only publication that also provided parameters for a third conduction band, which is, however, 2 eV above the lowest one in the M-point.

According was achieved over the last decades regarding the value of M_C . Although in early publications rather high values of $M_C = 12$ ^{233,234} or $M_C = 6$ ^{190,235,236} were encountered, almost all more recent publications agree upon $M_C = 3$ ^{9,14,23,48,57,62,65,68,69,84,107,142,204,206,227,237-239}.

We found some deviations among the utilized formalisms. Pennington and Goldsman²⁴⁰ used $\sqrt{m_{\text{ML}}^* m_{\text{MK}}^*}$ as the DOS effective mass of electrons, i.e., $m_{\text{de}}^* = m_{\text{de}\perp}^*$. Tilak, Matocha, and Dunne²⁴¹ reused the value of m_{de}^* but calculated the perpendicular one themselves, which lead to almost identical values. Persson and Lindefelt²²⁷ used for the calculation of the effective mass, i.e., $m_{\text{de}}^* = (m_{\text{de}\perp 1}^* m_{\text{de}\parallel}^*)^{1/3}$ only one of the perpendicular masses, which was in the sequel reused⁵⁰. In contrary, Gao *et al.*³¹ used $m_{\text{de}}^* = m_{\text{de}\parallel}^*$. Ivanov, Magnusson, and Janzén⁴² used $m_{\text{de}\perp}^* = \sqrt{m_{\text{ML}}^* m_{\text{MK}}^*} = 0.32$ resp $m_{\text{de}\parallel}^* = m_{\text{ML}}^* + 0.58$ by citing Faulkner²⁴². We were unable

TABLE III. First half of DOS masses. Multiple values for the same band are calculated by differing algorithms.

ref.	electron				hole				method ^h	polaron
	m_{de}^* [m_0]	$m_{de\perp}^*$ [m_0]	$m_{de\parallel}^*$ [m_0]	band	m_{dh}^* [m_0]	$m_{dh\perp}^*$ [m_0]	$m_{dh\parallel}^*$ [m_0]	band		
[Loma73] ²³¹	0.20 ^a	0.21	0.19	-	-	-	-	-	Hall	-
[Loma74] ²³²	0.20 ^a	0.21	0.19	-	-	-	-	-	Hall	-
[Gotz93] ²⁰²	0.19	0.176	0.224	-	-	-	-	-	IR	-
[Kack94] ²¹⁹	0.31 ^a	0.28 ^b	0.39 ^c	-	2.60 ^a	3.19 ^b	1.73 ^c	hh	DFT-LDA	-
	-	-	-	-	0.84 ^a	0.59 ^b	1.73 ^c	lh	DFT-LDA	-
	-	-	-	-	0.43 ^a	0.61 ^b	0.21 ^c	so	DFT-LDA	-
[Hari95] ¹⁶	0.35 ^a	0.30 ± 0.07	0.48 ± 0.12	-	-	-	-	-	Raman	-
[Karc95] ¹⁹⁴	0.39 ^a	0.45 ^b	0.30 ^c	-	-	-	-	-	DFT-LDA	-
[Kord95] ²¹¹	-	0.42	-	-	-	-	-	-	ODCR	y
[Lamb95] ²²³	0.35 ^a	0.4	0.27	-	-	-	-	-	DFT-LDA	-
[Son95] ²¹⁸	0.37 ^a	0.42	0.29 ± 0.03	-	-	-	-	-	ODCR	y
[Wenz95] ⁷¹	0.32 ^a	0.41 ^b	0.19 ^c	-	-	-	-	-	DFT-LDA	-
[Nils96] ¹⁶⁰	0.37 ^a	0.43 ^b	0.28 ^c	1	-	-	-	-	DFT-LDA	-
	0.37 ^a	0.33 ^b	0.45 ^c	2	-	-	-	-	DFT-LDA	-
[Pers96] ¹⁹³	0.37 ^a	0.40 ^b	0.31 ^c	-	-	-	-	-	DFT-LDA	-
[Volm96] ²²⁶	0.39 ^a	0.42 ^b	0.33 ^c	-	-	-	-	-	ODCR	y
[Bako97] ⁶⁹	-	-	-	-	0.84	-	-	1	-	-
	-	-	-	-	0.79	-	-	2	-	-
	-	-	-	-	0.78	-	-	3	-	-
[Chen97] ²²⁴	0.42 ^a	0.48 ^b	0.33 ^c	-	-	-	-	-	DFT-LDA	-
[Hemm97] ²⁰⁴	-	-	-	-	1	-	-	-	-	-
[Lamb97] ¹⁹⁹	-	-	-	-	0.85 ^a	0.62	1.6	hh	RSPH	-
	-	-	-	-	0.84 ^a	0.62	1.55	lh	RSPH	-
	-	-	-	-	0.81 ^a	1.58	0.21	so	RSPH	-
[Pers97] ¹²	0.37 ^a	0.40 ^b	0.31 ^c	1	0.82 ^a	0.59	1.56	1	DFT-LDA	-
	0.40 ^a	0.43 ^b	0.34 ^c	1	0.82 ^a	0.59	1.6	1	DFT-LDA	-
	0.39 ^a	0.42 ^b	0.33 ^c	1	0.82 ^a	0.59	1.56	2	DFT-LDA	y
	0.44 ^a	0.35 ^b	0.71 ^c	2	0.82 ^a	0.59	1.6	2	DFT-LDA	-
	0.48 ^a	0.38 ^b	0.75 ^c	2	0.78 ^a	1.49	0.21	3	DFT-LDA	-
	0.48 ^a	0.38 ^b	0.77 ^c	2	0.79 ^a	1.49	0.22	3	DFT-LDA	y

$$^a m_{de}^* = (m_{de\perp}^* m_{de\parallel}^*)^{1/3}$$

$$^b m_{de\perp}^* = \sqrt{m_{MI}^* m_{MK}^*}$$

$$^c m_{de\parallel}^* = m_{ML}^*$$

$$^d m_{dh}^* = (m_{dh\perp}^* m_{dh\parallel}^*)^{1/3}$$

$$^e m_{dh\perp}^* = \sqrt{m_{TM}^* m_{TK}^*}$$

$$^f m_{dh\parallel}^* = m_{TA}^*$$

^h explanation see text

TABLE IV. Second half of DOS masses. Multiple values for the same band are calculated by differing algorithms.

ref.	electron				hole				method ^h	polaron
	m_{de}^* [m_0]	$m_{de\perp}^*$ [m_0]	$m_{de\parallel}^*$ [m_0]	band	m_{dh}^* [m_0]	$m_{dh\perp}^*$ [m_0]	$m_{dh\parallel}^*$ [m_0]	band		
[Well97] ¹⁹¹	0.394	-	-	-	-	-	-	-	DFT-LDA	-
[Lind98] ⁴⁸	-	-	-	-	1.7	-	-	hh	DFT-LDA	-
-	-	-	-	-	0.48	-	-	lh	DFT-LDA	-
[Pers98a] ²²⁷	-	-	-	-	0.94	1.46 ^b	1.64 ^c	1	fit	-
-	-	-	-	-	0.84	0.45 ^b	1.64 ^c	2	fit	-
-	-	-	-	-	0.88	-	-	3	fit	-
[Egil99] ⁸¹	0.37	-	-	-	-	-	-	-	PL	-
[Pers99b] ²²¹	-	-	-	-	0.85 ^a	0.62	1.61	1	DFT-LDA	-
-	-	-	-	-	0.84 ^a	0.61	1.62	1	DFT-LDA	-
-	-	-	-	-	0.78 ^a	0.56	1.52	2	DFT-LDA	-
-	-	-	-	-	0.78 ^a	0.58	1.42	2	DFT-LDA	-
-	-	-	-	-	0.78 ^a	1.5	0.21	3	DFT-LDA	-
-	-	-	-	-	0.76 ^a	1.46	0.21	3	DFT-LDA	-
[Bell00] ¹¹⁶	0.33 ^a	0.36 ^b	0.27 ^c	-	-	-	-	-	EPM	-
[Son00] ¹⁹²	0.39 ^a	0.45 ± 0.02	0.30 ± 0.02	-	0.91 ^a	0.66 ± 0.02	1.75 ± 0.02	-	ODCR	y
[Zhao00] ¹⁰⁵	0.37 ^a	0.42	0.28	1	-	-	-	-	-	-
-	0.44 ^a	0.35	0.71	2	-	-	-	-	-	-
-	0.40 ^a	0.66	0.15	3	-	-	-	-	-	-
[Zhao00a] ²²²	0.37 ^a	0.41 ± 0.02	0.31 ^c	-	-	-	-	-	DFT-LDA	-
[Penn01] ²²⁵	0.34 ^a	0.35 ± 0.02	0.31 ± 0.05	-	-	-	-	-	EPM	-
[Iwat03] ¹⁹⁶	-	0.41 ^b	-	-	-	-	-	-	DFT-LDA	-
[Iwat03a] ²⁰⁹	-	0.42 ^b	-	-	-	-	-	-	Hall	-
[Dong04] ¹⁹⁵	0.35 ^a	0.38 ^b	0.30 ^c	-	1.09 ^a	0.90 ^b	1.58 ^c	1	DFT-LDA	-
-	-	-	-	-	0.72 ^a	0.53 ^b	1.32 ^c	2	DFT-LDA	-
-	-	-	-	-	0.67 ^a	1.21 ^b	0.21 ^c	3	DFT-LDA	-
[Chin06] ⁵	-	-	0.38 ^c	-	-	-	-	-	DFT-LDA	-
[Aktu09] ¹⁰⁶	0.40	-	-	-	-	-	-	-	DFT-LDA	-
[Koiz09] ⁵¹	-	-	-	-	0.5	-	-	-	Hall	-
[Ng10] ²²⁸	0.41 ^a	0.45 ^b	0.34 ^c	-	-	-	-	-	GAF	-
[Kuro19] ¹⁹⁸	0.36 ^a	0.39 ^b	0.31 ^c	-	0.76 ^a	0.54 ^b	1.48 ^c	-	DFT-LDA	-
[Lu21] ²²⁰	-	0.40 ^b	-	-	1.97 ^a	2.25 ^b	1.52 ^c	-	DFT-LDA	-

$$^a m_{de}^* = (m_{de\perp}^*{}^2 m_{de\parallel}^*)^{1/3}$$

$$^b m_{de\perp}^* = \sqrt{m_{\Gamma M}^* m_{MK}^*}$$

$$^c m_{de\parallel}^* = m_{ML}^*$$

$$^d m_{dh}^* = (m_{dh\perp}^*{}^2 m_{dh\parallel}^*)^{1/3}$$

$$^e m_{dh\perp}^* = \sqrt{m_{\Gamma M}^* m_{\Gamma K}^*}$$

$$^f m_{dh\parallel}^* = m_{\Gamma A}^*$$

^h explanation see text

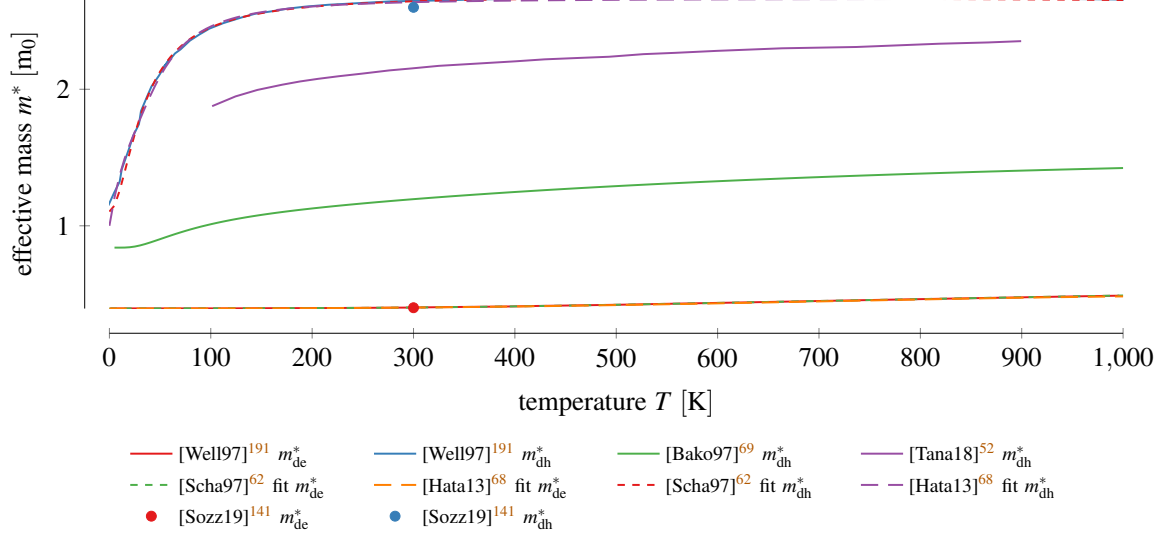


FIG. 5. Temperature dependency of the DOS mass.

TABLE V. Fitting parameters in Eq. (5) to calculations by Wellenhofer and Rössler¹⁹¹.

ref.	mass	z_0	z_1	z_2	z_3	z_4	n_1	n_2	n_3	n_4	η
[Scha97] ⁶²	m_{de}^*	0.3944	-6.822×10^{-4}	1.335×10^{-6}	3.597×10^{-10}	0	-1.776×10^{-3}	3.65×10^{-6}	0	0	1
[Scha97] ⁶²	m_{dh}^*	1.104	1.578×10^{-2}	3.087×10^{-3}	-7.635×10^{-8}	0	1.387×10^{-2}	1.126×10^{-3}	0	0	1
[Hata13] ⁶⁸	m_{de}^*	0.394	0	3.09×10^{-8}	2.23×10^{-10}	-1.65×10^{-13}	0	0	0	0	1
[Hata13] ⁶⁸	m_{dh}^*	1	6.92×10^{-2}	0	0	1.88×10^{-6}	0	6.58×10^{-4}	0	4.32×10^{-7}	2/3

to retrace these equations. Transformed to the set of equations used in this paper we, thus, get $m_{\text{de}\perp}^* = 0.42$ and $m_{\text{de}\parallel}^* = 0.33$. A more comprehensive listing of all inconsistencies is presented in ??.

3. Temperature

The temperature dependency of the DOS masses was calculated by Tanaka *et al.*⁵² and Wellenhofer and Rössler¹⁹¹ (see Fig. 5). Since these calculations can not be described implicitly there exist two fittings for the latter^{62,68} using Eq. (5). The respective parameters are shown in Table V.

The temperature scaling of the hole mass considering the separation between the three valence bands in the Γ point⁶⁹ (see Eq. (4), also shown in the figure) is described by the coefficients $m_{\text{h}1} = 0.84$, $m_{\text{h}2} = 0.79$, $m_{\text{h}3} = 0.78$, $\Delta E_2 = 9 \text{ meV}$ and $\Delta E_3 = 73 \text{ meV}$. Bakowski, Gustafsson, and Lindefelt⁶⁹ stated that these are only valid for low temperatures, which might explain the big

deviations compared to the calculations by Wellenhofer and Rössler¹⁹¹. Also shown in the figure are the parameters extracted by Sozzi *et al.*¹⁴¹ from Wellenhofer and Rössler¹⁹¹ at 300 K, i.e., $m_{de}^* = 0.4$ and $m_{dh}^* = 2.6$.

4. Effective DOS Mass for TCAD Tools

For TCAD simulations solely the effective electron and hole masses are interesting. We, therefore, collected all values found for m_{de}^* and m_{dh}^* (see Fig. 6). We also added values that we calculated from fundamental masses according to the formalism presented earlier. We just used the first conduction band for m_{de}^* and Eq. (3) to calculate m_{dh}^* considering the first two valence bands only.

For electrons the masses are dominantly using values of 0.37 ± 0.05 . For holes the spread is more significant. Although the majority used 1 ± 3 there are also values > 2.6 available. This can be retraced to the significant temperature dependency. Ambivalent in this context is $m_{dh}^* = 1.2$. While Bakowski, Gustafsson, and Lindefelt⁶⁹ calculated this value for the mass at 300 K others^{154,243} seemingly calculated $m_{dh}^* = \sqrt{m_{dh\perp}^* m_{dh\parallel}^*}$, i.e., twice the parallel instead of the perpendicular component, resulting in $m_{dh}^* = 1.26^{61}$ based on the masses by Son *et al.*¹⁹². Crude rounding then leads to the desired value.

C. Discussion

The majority of the investigations on the density-of-states masses in 4H-SiC have been conducted in a time frame of one decade between 1994 and 2004. Although the earliest studies in the 70s were measurements, nowadays dominantly calculations are utilized. For the hole mass, actually, up to this day only two measurements could be identified.

Our investigations showed that the value for m_{dh}^* has to be carefully picked, as a significant change with temperature was observed. Many of the available values, especially those based on calculations, are only valid close to 0 K. For more realistic results a much higher mass has to be used. Nevertheless, almost all temperature dependency fittings are based on the same calculation by Wellenhofer and Rössler¹⁹¹. Despite these large variations, temperature is rarely considered^{63,107}. Rakheja *et al.*²⁴⁷ explicitly claims the presented values to correspond to 300 K, although the reference investigation¹⁹² was carried out at 4.4 K.

From the references (see Fig. 8 and Fig. 7) we are able to identify the publications by Persson

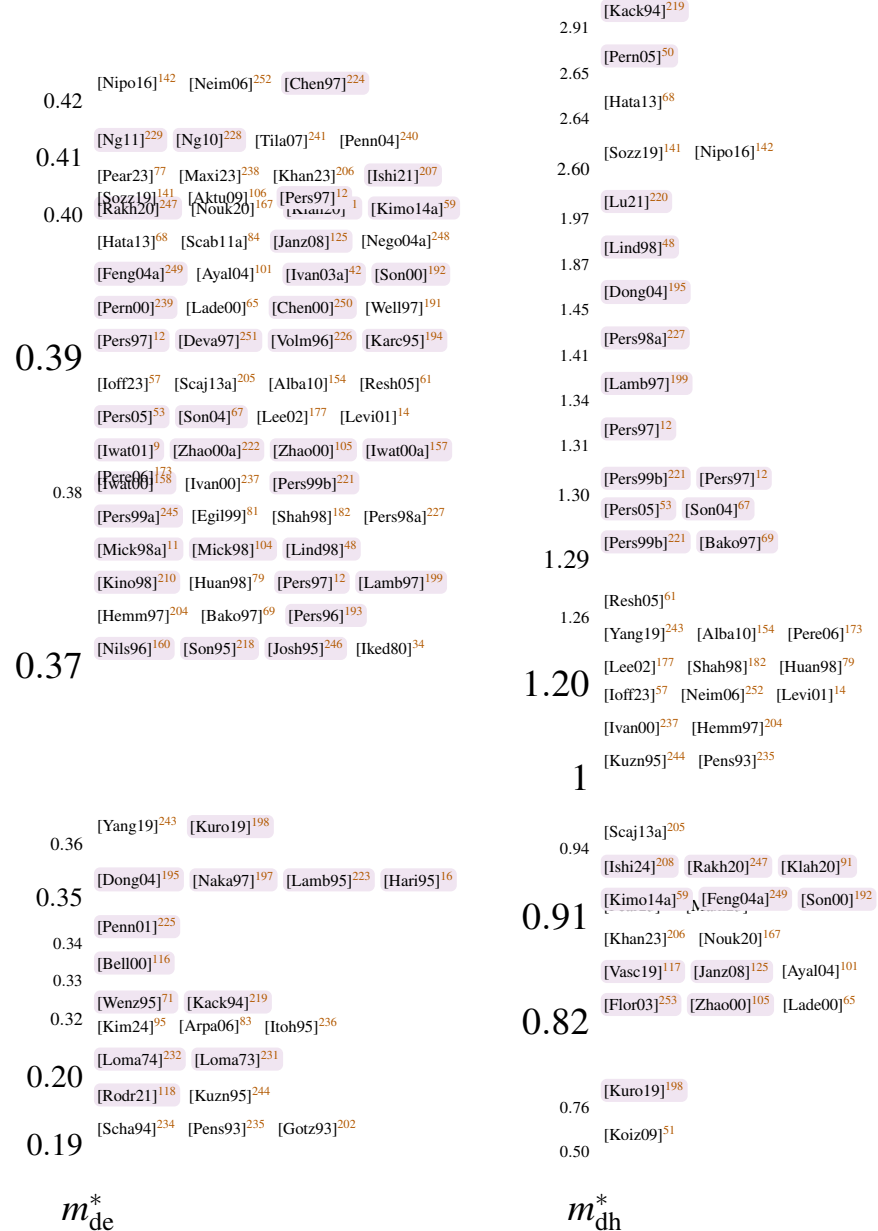


FIG. 6. Effective DOS masses for TCAD tools. A purple background denotes values that we calculated from more fundamental masses using the equations presented in this paper.

et al.^{12,193,221,227} but also by Volm *et al.*^{226,191} and¹⁹² as very influential.

At last we shortly want to notice that there have been hints that the DOS mass is also doping dependent³. This was shown for 6H-SiC²⁴⁵ but not yet for 4H.

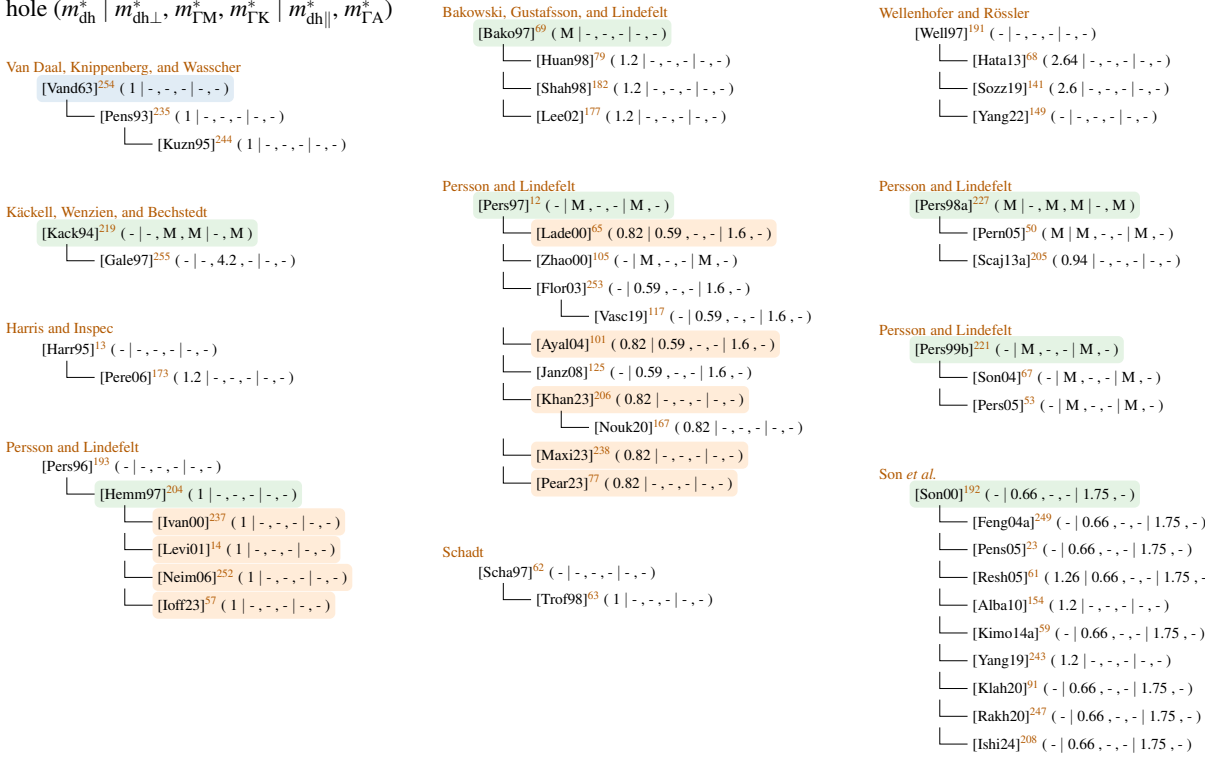


FIG. 7. DOS reference chain for holes. 'M' denotes that multiple values are found in the publication. Entries with green background show fundamental investigations, orange references we inferred based on the used data.

III. BAND GAP

The band diagram of a material specifies the energy of a charge carrier for a given direction-dependent momentum. The electrons are described by the *conduction band* and the holes by the *valence band*. If both touch the material is called a conductor while a large gap, called the *band gap*, characterizes an insulator. Materials having a band gap in between these two extremes are called semiconductors. This shows that an exact knowledge of the band gap is instrumental to describe the electronic properties of 4H-SiC.

In TCAD simulations the band gap E_g is essential for the carrier concentration, in the drift diffusion equation and also for the barrier heights in Schottky contacts. Because E_g is often stated in the exponent, where small changes can have a huge impact, a high accuracy is desired. In this section we are, thus, going to investigate band gap energies published in literature by extending existing overviews^{130,257}. Overall, we conclude that the majority of the currently used values are, with high confidence, based on measurement from the year 1964. Despite various variations and

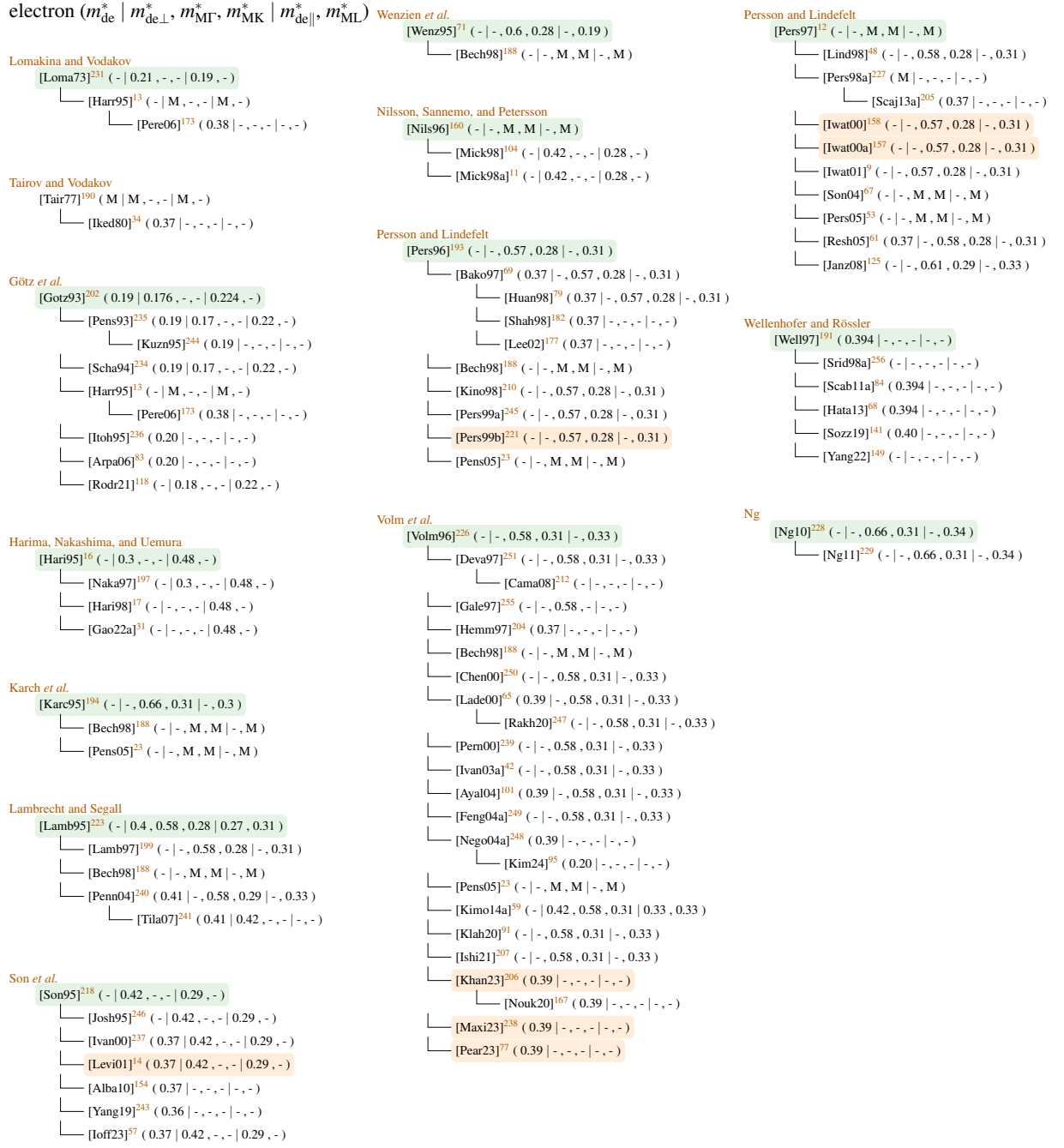


FIG. 8. DOS reference chain for electrons. 'M' denotes that multiple values are found in the publication. Entries with green background show fundamental investigations, orange references we inferred based on the used data and blue investigation based not on 4H.

changes the most commonly used value coincidentally fits latest measurements, however further investigations are required for proper confirmation.

A. Theory

The band gap is measured between the highest energy value of the valence band in the Γ point (see ??) and the lowest one of the conduction band in the M-point^{5,57,67}. Because these are not at the same location 4H-SiC is a so-called indirect semiconductor, which means that some transfer of moment, e.g., by a phonon, is required for the minimum energy difference. Electrons can also be lifted from the valence to the conduction band in the Γ point and then gradually relax towards the minimum, however, in that case more than the band gap energy is required to create an electron-hole pair. An overview of ionization energies for these cases is provided by Gsponer *et al.*²⁵⁸, who extracted a value of (7.83 ± 0.02) eV from their own measurements.

Our statement that electrons are lifted from the valence to the conduction is not completely correct. Actually, the electron first forms an exciton by Coulomb interactions with the hole it left behind^{259–262}. This setup can be compared to the hydrogen atom but with much larger radii due to the much lower effective masses. Additional energy has to be provided before the electron can move freely within the conduction band. Consequently, the band gap energy E_g is the sum of the energy required to generate the exciton, i.e., the exciton band gap energy E_{gx} , and the energy to free the electron from the exciton, i.e., the *free exciton binding energy* E_x (see Eq. (6)¹⁵⁴).

$$E_g = E_{gx} + E_x \quad (6)$$

The free exciton binding energy E_x must not be confused with the *bound* exciton binding energy^{34,91,202,211,233,259,263–268}. An exciton, which is neutral and thus can relatively easily travel through the lattice, can achieve an energetically better configuration when attaching itself to an impurity²⁵⁹. The energy reduction relative to E_{gx} is represented by the bound exciton binding energy, which depends on the impurity atom, the lattice site and the charge state²⁶⁹. Typical values reported in literature are comparable to the free exciton binding energy (in the range of a few meV). Because the same symbol E_x is used it is challenging to distinguish bound and free exciton binding energy.

The band gap energy is not a constant. First and foremost it varies among the polytypes of silicon carbide. It was empirically shown that the band gap scales linearly with the degree of

hexagonality, i.e., the ratio of hexagonal to cubic lattice sites^{59,270–272}. Because 4H-SiC has a hexagonality of 50 %²⁷³ (cp. Section VI) its band gap energy is located halfway between the extreme values. In addition the band gap changes with pressure³, under strain¹⁹⁸ and for varying temperature and doping concentrations. These have a significant effect on the device behaviour as the shift in the band edges create, for example, potential barriers which influence the carrier transport across junctions²⁷⁴.

In the sequel we are going to investigate band gap narrowing described by Eq. (7), whereat $E_g(T)$ denotes the temperature induced variation and $\Delta E_g(N_D^+, N_A^-)$ the doping-induced one.

$$E_g(T, N_D^+, N_A^-) = E_g(T) - \Delta E_g(N_D^+, N_A^-) \quad (7)$$

1. Temperature Dependency

Lattice vibrations cause a shift of the band energies and changes in the electron-lattice interaction energy²⁷⁵. Because these changes differ among energy levels the effective band gap changes²⁷⁶. The temperature dependent band gap (see Eq. (8))³ contains effects from thermal expansion ($\Delta E_{\text{th}}(T)$) and electron-phonon interaction ($\Delta E_{\text{ph}}(T)$).

$$E_g(T) = E_g(0) - \Delta E_{\text{th}}(T) - \Delta E_{\text{ph}}(T) \quad (8)$$

These effects are hard to separate in experiments³, which was, so far, only achieved by Cheng, Yang, and Zheng³³. Because $\Delta E_{\text{th}}(T)$ has a much weaker impact²⁷⁷ and the scaling of both contributions is comparable²⁷⁸ the models for $\Delta E_{\text{ph}}(T)$ are, in general, used to describe both with reasonable accuracy. Arvanitopoulos *et al.*⁸⁶ extended Eq. (8) by adding an additive term Δ_g^{Fermi} to account for carrier statistics. This is, however, only necessary for devices whose size is close to the de-Broglie wavelength.

For high temperatures the band gap decreases linearly^{65,279,280} while for low temperatures non-linear behavior, i.e., quadratic²⁸⁰ or plateau-like behavior²⁸¹ is observed. Quadratic behavior is described by the empirical Varshni relation in Eq. (9)²⁸² with T_g some arbitrary characterization temperature.

$$E_g(T) = E_g(T_g) + \alpha \left(\frac{T_g^2}{T_g + \beta} - \frac{T^2}{T + \beta} \right) \quad (9)$$

Multiple authors^{277,278,281} criticize that it is not possible to retrace the parameters of this model to physical mechanism-specific quantities (e.g., β was said to be approximately the Debye temperature which turned out to be not the case, since it sometimes even got negative^{143,283,284}) and

the model is unable to provide adequate interpretation of available data sets at low and high temperature^{285,286}. For example, Pässler²⁸⁶ tried to match the values from Choyke, Hamilton, and Patrick²⁷⁰ but achieved only unrealistic results.

A physically based approach describing a plateau-like behavior at cryogenic temperature is a model of Bose-Einstein type in Eq. (10)^{281,287} with Θ_B the mean frequency of the involved phonons and α_B the strength of the electron-phonon interaction³.

$$E_g(T) = E_B - \alpha_B \left(1 + \frac{2}{e^{\Theta_B/T} - 1} \right) \quad (10)$$

The rate of change of the band gap at low temperatures is strongly material specific and depends on the phonon dispersion Δ ²⁸⁶. Eq. (9) is most accurate for $\Delta \gg 1$ ^{280,288}, while Eq. (10) represents the lower limit ($\Delta \rightarrow 0$) and is most suitable for $\Delta < \frac{1}{3}$ ²⁸⁶. Because most semiconductors show a dispersion in the range of 0.3–0.6²⁸⁶ Pässler^{277,286} proposed the model shown in Eq. (11) with ε the entropy and Θ_p the average phonon temperature.

$$E_g(T) = E_g(0) - \frac{\varepsilon \Theta_p}{2} \left[\sqrt[p]{1 + \left(\frac{2T}{\Theta_p} \right)^p} - 1 \right] \quad (11)$$

$$p \approx \sqrt{\frac{1}{\Delta^2} + 1}$$

This model was subsequently extended by Pässler²⁸⁰ to cover a wider range of the phonon dispersion Δ and, thus, promises to bridge the gap between Eq. (9) and Eq. (10).

2. Doping Dependency

The band gap also changes due to many-body effects of free carriers, i.e., their interactions among each other and with dopants, which become dominant for small carrier-to-carrier distances (high doping concentrations)²⁸⁹. Examples are interactions within a band, across bands and with ionized dopants^{48,289,290}. The single effects were investigated extensively on their own²⁸⁹ and got eventually merged, based on a similar analysis for silicon²⁹⁰, for 4H-SiC by Lindefelt⁴⁸ to the

model shown in Eq. (12).

$$\begin{aligned}
\Delta E_g(N_D^+, N_A^-) &= -\Delta E_{(n/p)c}(N_D^+) + \Delta E_{(n/p)v}(N_A^-) \\
\Delta E_{nc}(N_D^+) &= A_{nc} \left(\frac{N_D^+}{10^{18}} \right)^{1/3} + B_{nc} \left(\frac{N_D^+}{10^{18}} \right)^{1/2} < 0 \\
\Delta E_{nv}(N_D^+) &= A_{nv} \left(\frac{N_D^+}{10^{18}} \right)^{1/4} + B_{nv} \left(\frac{N_D^+}{10^{18}} \right)^{1/2} > 0 \\
\Delta E_{pc}(N_D^+) &= A_{pc} \left(\frac{N_A^-}{10^{18}} \right)^{1/4} + B_{pc} \left(\frac{N_A^-}{10^{18}} \right)^{1/2} < 0 \\
\Delta E_{pv}(N_D^+) &= A_{pv} \left(\frac{N_A^-}{10^{18}} \right)^{1/3} + B_{pv} \left(\frac{N_A^-}{10^{18}} \right)^{1/2} + C_{pv} \left(\frac{N_A^-}{N_{A0}} \right)^{1/4} > 0
\end{aligned} \tag{12}$$

ΔE_{nc} and ΔE_{pc} denote the change of the conduction band due to *n* and *p* type doping. Because the conduction band energy level drops these factors are negative and thus have to be subtracted from the increase of the valence band denoted by ΔE_{nv} and ΔE_{pv} .

The term featuring C_{pv} was added in an extension proposed by Persson, Lindefelt, and Sernelius⁶⁶. The authors define the validity of this model for ionized charge carrier concentrations (see Section VI) above a few $10^{18}/\text{cm}^3$ and claim that a larger displacement is observable in 4H compared to other polytypes. More specifically, the valence band displacement is larger than the conduction band one. Other publications distribute the band gap narrowing equally across valence and conduction band⁸⁶ or chose a contribution of $\Delta E_c/E_g = 0.7$ ²⁹¹.

Some TCAD tools merge the prefactor and the denominator 10^{18} often called Jain-Roulston model²⁹⁰, as shown in Eq. (13). We get $A_{xc}^j/A_{xc} = 10^{-6}$ and $B_{xy}^j/B_{xy} = 10^{-9}$ with $x \in \{n, p\}, y \in \{c, v\}$. For the remaining parameters the correlation is not so simply, i.e., we get $A_{xc}^j/A_{xc} = \approx 3.162 \times 10^{-5}$. For better comparison we transferred all parameters of Eq. (13) back to their respective counterparts in Eq. (12), except the sum of B_{xy} , which could obviously not be separated.

$$\begin{aligned}
\Delta E_{gn} &= -A_{nc}^j (N_D^+)^{1/3} + (B_{nv}^j - B_{nc}^j) (N_D^+)^{1/2} + A_{nv}^j (N_D^+)^{1/4} \\
-\Delta E_{gp} &= A_{pc}^j (N_A^-)^{1/3} + (B_{pv}^j - B_{pc}^j) (N_A^-)^{1/2} + A_{pv}^j (N_A^-)^{1/4}
\end{aligned} \tag{13}$$

An alternative approach to describe the doping dependency is to use the Slotboom model (see Eq. (14)), which was originally developed for Si. Ruff, Mitlehner, and Helbig²⁹² first did it for 6H and Lades⁶⁵ later followed for 4H-SiC by fitting to the results in Eq. (12) with N the and $N_{n,p}$.

$$\Delta E_g = C_{n,p} \left(\ln \left(\frac{N}{N_{n,p}} \right) + \sqrt{\left(\ln \left(\frac{N}{N_{n,p}} \right) \right)^2 + G} \right) \tag{14}$$

A more physically based approach is to interpret the band gap reduction as renormalization due to electron-electron interactions alone. To describe this effect Schubert²⁸⁹ proposed the band gap narrowing described by Eq. (15).

$$\Delta E_g = \frac{e^2}{4\pi\epsilon r_s} \quad (15)$$

The screening radius r_s is given by the Debye and Thomas-Fermi radii leading to the descriptions for the non-degenerate (see Eq. (16)) and degenerate (see Eq. (17)) case with n the charge carrier concentration.

$$\Delta E_g = \frac{e^3 \sqrt{n}}{4\pi\epsilon^{3/2} \sqrt{k_B T}} \quad (\text{Debye, non-degenerate}) \quad (16)$$

$$\Delta E_g = \frac{e^3 \sqrt{m_{de}^*(3n)^{1/3}}}{4\pi^{5/3} \epsilon^{3/2} \hbar} \quad (\text{Thomas-Fermi, degenerate}) \quad (17)$$

We want to highlight that in state-of-the-art TCAD tools only Eq. (9) and Eq. (14) are supported out of the box, although some feature the possibility to write custom code for band gap narrowing.

B. Results & Discussion

Multiple methods to determine the band gap, which were partially discussed by Nava *et al.*¹⁰⁹, De Napoli¹⁵⁰, were used in literature. Most of them focus on measurements, e.g., transmission spectroscopy (TS)^{8,33}, spectroscopic ellipsometry²⁹³, photo absorption (PA)^{269,270,285,294}, optical admittance (OA)²⁹⁵, exciton electroabsorption (EE)²⁶⁸, free carrier absorption (FCA)²⁷⁹, free exciton luminescence (FEL)²⁶⁷, photoluminescence (PL)^{211,266,296}, photoconductivity (PC)²⁹⁷ and wavelength-modulated absorption (WMA)^{91,298}. Sometimes the results of multiple measurements are combined to improve the accuracy²⁶³. Stefanakis and Zekentes²⁹⁹ states that the free carrier absorption method overestimates the band gap while optical absorption studies deliver more accurate results.

An alternative are calculations, which include empirical pseudopotentials (EP)^{116,300–302}, density functional theory local density approximation (DFT-LDA)^{5,12,67,136,195,198,220,222,224,303}, rectangular barrier of finite height (RB)³⁰⁴, fitting (FT)^{14,59,65,68} and genetic algorithm fitting (GAF)²²⁸.

With these methods mainly results for low temperatures were achieved (see Table VI). Predominantly the exciton band gap energy was measured, whereat the achieved values seem to agree on $E_{gx} = (3.265 \pm 0.002)$ eV. For the band gap energy only two investigations could be found which deliver $E_g = 3.285$ eV respectively $E_g = 3.28$ eV. The calculations show a much larger spread,

however, the latest investigations all propose significantly lower values of $E_g = (3.15 \pm 0.03)$ eV. For room temperature only few dedicated measurements are available^{8,279,285,293,305}, whereas the ones by Ahuja *et al.*⁸ have a quite big uncertainty of 98 meV. We only found one publication that investigated the anisotropy²⁸⁵ achieving the same exciton (band gap) energy for fields parallel resp. perpendicular to the c-axis. The doping induced band gap narrowing is in general not known for these measurements.

TABLE VI: Band gap energies and their temperature dependency fittings. If no temperature dependency parameters (for Eq. (9)) are shown T_g represents the measurement temperature for the shown energies. Highlighted lines represent no 4H results and calculations.

ref.	band gap			temperature dep.			interval	method ³⁰⁶
	E_g [eV]	E_{gx} [eV]	E_x [meV]	T_g [K]	α [eV/K]	β [K]		
[Choy57] ^{294 307}	-	-	-	-	3.3×10^{-4}	-	-	PA
[Choy64] ²⁷⁰	-	3.263 ± 0.003	-	4	-	-	-	PA
[Choy64a] ^{269 308}	-	3.265	-	4.7	-	-	-	PA
[Jung70] ³⁰¹	2.8	-	-	0	-	-	-	EP
[Dubr75] ²⁶⁸	-	-	20 ± 15	2	-	-	-	EE
[Dubr77] ³⁰⁴	3.2	-	-	0	-	-	-	RB
[Ikeda80b] ²⁶⁷	-	3.2639	10	77	-	-	-	FEL
[Gavr90] ³⁰⁹	2.89	-	-	0	-	-	-	DFT-LDA
[Back94] ³⁰⁰	3.28	-	-	0	-	-	-	EP
[Park94] ³¹⁰	2.14	-	-	0	-	-	-	EP
[Kord95] ²¹¹	-	3.265	-	4.2	-	-	-	PL
[Wenz95] ⁷¹	3.56	-	-	0	-	-	-	DFT-LDA
[Evwa96] ²⁹⁵	3.41 ± 0.03	-	-	40	-	-	-	OA
[Itoh96] ^{266 308}	-	3.265	-	4.25	-	-	-	PL
[Kaec96] ³¹¹	2.18	-	-	0	-	-	-	DFT-LDA
[Bako97] ⁶⁹	3.19	-	-	300	3.3×10^{-4}	0	300–700	FT
[Chen97] ²²⁴	3.27	-	-	0	-	-	-	DFT-LDA
[Pers97] ¹²	2.9	-	-	0	-	-	-	DFT-LDA
[Vanh97] ³⁰²	3.28	-	-	0	-	-	-	EP
[Ivan98] ²⁹⁶	-	3.266	-	2	-	-	-	PL
[Bell00] ¹¹⁶	3.05	-	-	0	-	-	-	EP
[Lade00] ^{65 312}	-	3.265	40	0	3.3×10^{-4}	1.05×10^3	4–200	FT
	-	3.265	40	0	3.3×10^{-2}	1×10^5	4–600	FT
	-	3.342	40	0	3.3×10^{-4}	0	300–700	FT
[Srid00] ²⁹⁸	-	3.267	-	2	-	-	-	WMA
[Zhao00a] ²²²	3.11	-	-	0	-	-	-	DFT-LDA
[Levi01] ^{14 313}	3.23	-	-	300	6.5×10^{-4}	1300	-	FT
[Ahuja02] ⁸	3.260 ± 0.098	-	-	300	-	-	-	TS
[Gale02] ²⁷⁹	3.285	-	-	0	3.5×10^{-4}	1100	0–650	FCA
	3.2625	-	-	300	2.4×10^{-4}	0	300–650	FCA
[Ivan02] ²⁹⁷	3.285	-	20.5 ± 1.0	2	-	-	-	PC

[Shal02] ³⁰⁵	3.18	-	-	300	-	-	-	-	PL
[Dong04] ¹⁹⁵	2.194	-	-	0	-	-	-	-	DFT-LDA
[Son04] ⁶⁷	3.35	-	-	0	-	-	-	-	DFT-LDA
[Bala05] ^{283 314}	3.26	-	-	300	4.15×10^{-4}	-131	-	-	-
[Chin06] ⁵	2.433	-	-	0	-	-	-	-	DFT-LDA
[Griv07] ²⁸⁵	-	3.267	30 ± 10	0	-	-	0–500	-	PA
[Tama08a] ^{315 314}	3.23	-	-	300	7.036×10^{-4}	1509	-	-	-
[Ng10] ²²⁸	3.28	-	-	0	-	-	-	-	GAF
[Hata13] ^{68 313}	3.285	3.265	20	0	9.06×10^{-4}	2030	0–800	-	FT
[Kimo14a] ^{59 313}	-	3.265	20	2	8.2×10^{-4}	1800	-	-	FT
[Yama18] ³⁰³	3.12	-	-	0	-	-	-	-	DFT-LDA
[Kuro19] ¹⁹⁸	3.15	-	-	0	-	-	-	-	DFT-LDA
[Klah20] ⁹¹	-	3.2659	40	1.4	-	-	-	-	WMA
[Lech21] ^{82 314}	3.265	-	-	0	10.988×10^{-3}	32744.3	-	-	FT
[Lu21] ²²⁰	3.17	-	-	0	-	-	-	-	DFT-LDA
[Chen22] ³³	3.44	-	-	0	5.27×10^{-4}	0	300–620	-	TS
[Huan22b] ³¹⁶	3.18	-	-	0	-	-	-	-	DFT-LDA
[Torr22] ¹³⁶	3.17	-	-	0	-	-	-	-	DFT-LDA
[Khan23] ^{206 314}	3.285	-	-	0	3.3×10^{-4}	240	-	-	-
[Main24] ²⁹³	3.30 ± 0.02	-	-	300	-	-	-	-	SE

The free exciton binding energy E_x was first estimated by Hagen, Van Kemenade, and Van Der Does De Bye³¹⁷ to be around 20 meV, with the side note that further investigations are needed. Later, five measurements were published^{91,267,268,285,297}. The achieved values range from 10–40 meV. The value of 10 meV²⁶⁷ was determined for the activation energy for thermal quenching of free excitons, however, Devaty and Choyke²⁵¹ argue that these values are too low to be free exciton binding energies.

1. Temperature Dependency

Very few measurements on the temperature dependency are available^{33,269,279,285}. The remaining models^{14,59,65,68} fit the data published by Choyke²⁶³, Choyke, Patrick, and Hamilton²⁶⁹, Choyke, Hamilton, and Patrick²⁷⁰ from the 1960s. Surprisingly, the model development only started at the beginning of the 2000s. In 1997 Bakowski, Gustafsson, and Lindefelt⁶⁹ were still forced to use the 6H values. In 2004 Ayalew¹⁰¹ stated that not reliable data are available.

The origin of some of the proposed model parameters^{82,206,283} could not be traced back to any scientific publication. Occasionally, we were able to them back to prominent TCAD simulation suites, where these were used as default values. Although Tamaki *et al.*³¹⁵ provides a reference

for the used model⁷⁸, we were unable to verify the parameters. By comparison we found that the results are very close to those predicted by Kimoto and Cooper⁵⁹ (see Fig. 9).

To describe the temperature dependency the majority resorts to the Varshni model (see Eq. (9)). We would like to highlight that the value $\alpha = 3.3 \times 10^{-4}$ eV/K was determined by Choyke and Patrick²⁹⁴ for an undefined polytype of SiC. According to the utilized band gap we suspect it to be 21R-SiC device although Bakowski, Gustafsson, and Lindefelt⁶⁹ argued that it was 6H. Nevertheless, a wide range of fittings utilizes this value, i.e., that 4H and 6H share the same temperature dependency¹⁶³. Nallet *et al.*³¹⁸ even references 6H values directly²⁹², which, however, go back to the same data by Choyke and Patrick²⁹⁴.

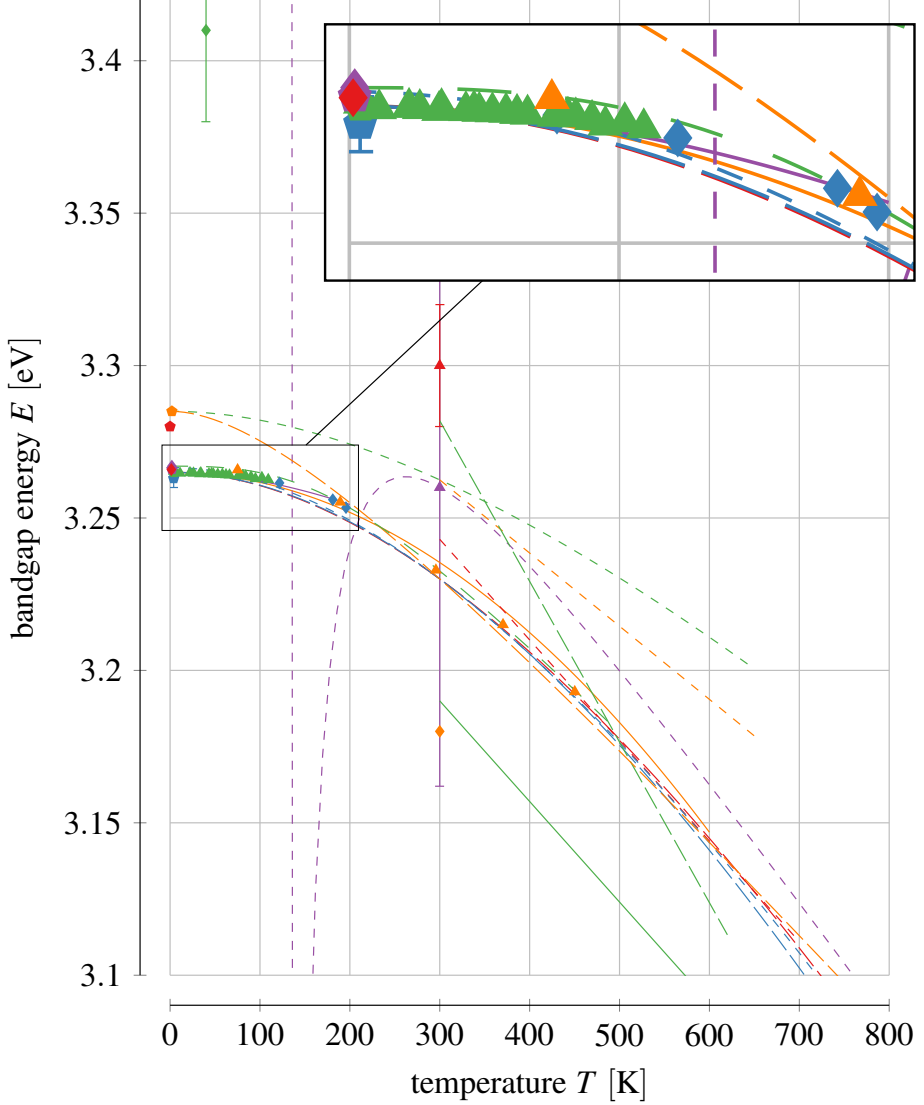
The model presented in Eq. (11) is solely used by Grivickas *et al.*²⁸⁵ with the parameters shown in Eq. (18).

$$\Theta_p = 450\text{ K}, \quad \epsilon = 3 \times 10^{-4} \text{ eV/K}, \quad p = 2.9 . \quad (18)$$

From a graphical representation of the band gap energy versus temperature (see Fig. 9) the deviations of the models becomes evident. We do not show the fitting by Hatakeyama, Fukuda, and Okumura⁶⁸ which is identical to the one by Kimoto and Cooper⁵⁹. Similarly, the parameters provided by Lechner⁸² reproduce the fitting from Lades⁶⁵ (4–600 K).

First of all it has to be noted that the measurements nicely distinguish E_g and E_{gx} . The same can not be said for the fittings. For example, Levinstejn, Rumyantsev, and Shur¹⁴ denoted to describe E_g but the values agree more to E_{gx} . Also the fitting by Bakowski, Gustafsson, and Lindefelt⁶⁹, who simply took the band gap at 0 K and applied the scaling factor α , turns out to underestimate the band gap. Newer models, e.g., the one by Cheng, Yang, and Zheng³³, suggest a much different slope with temperature, actually crossing the traces of E_{gx} with E_g . The model by Khanna²⁰⁶ matches E_g at low temperatures but at around 200 K it is equal to E_{gx} and follows that value from there onward. The fitting by Balachandran, Chow, and Agarwal²⁸³ is only feasible for $T \geq 300\text{ K}$ as it has a singularity at 131 K.

The plateau achieved by the Pässler model in Eq. (11) is barely visible, showing that the deviations are only subtle. Lades⁶⁵ approximated the shape with the Varshni model by just fitting it in a very narrow temperature range. The phonon dispersion of 4H-SiC $\Delta = 0.29^{285}$ is rather low, which would actually indicates that Eq. (10) is the most suitable, however, Eq. (11) seems to be accurate as well. Even more, Stefanakis and Zekentes²⁹⁹ compared the single models and identifies Eq. (9) as the most suitable one. In fact, we did not find a single instance where Eq. (10) was used to describe 4H-SiC.



- | | | |
|---|--|--|
| • [Choy64] ²⁷⁰ E_{gx} | • [Choy64a] ²⁶⁹ E_{gx} | • [Ikeda80b] ²⁶⁷ E_{gx} |
| • [Kord95] ²¹¹ E_{gx} | • [Evwa96] ²⁹⁵ E_g | • [Itoh96] ²⁶⁶ E_{gx} |
| • [Ivan98] ²⁹⁶ E_{gx} | • [Srid00] ²⁹⁸ E_{gx} | • [Ahuja02] ⁸ E_g |
| • [Ivan02] ²⁹⁷ E_g | • [Shal02] ³⁰⁵ E_g | • [Griv07] ²⁸⁵ E_{gx} |
| • [Ng10] ²²⁸ E_g | • [Klah20] ⁹¹ E_{gx} | • [Main24] ²⁹³ E_g |
| — [Bako97] ⁶⁹ E_g (V) | — [Lade00] ⁶⁵ E_{gx} (V) | — [Lade00] ⁶⁵ E_{gx} (V) |
| - - - [Lade00] ⁶⁵ E_{gx} (V) | - - - [Levi01] ¹⁴ E_g (V) | - - - [Gale02] ²⁷⁹ E_g (V) |
| - - - [Gale02] ²⁷⁹ E_g (V) | - - - [Bala05] ²⁸³ E_g (V) | - - - [Tama08a] ³¹⁵ E_g (V) |
| - - - [Hata13] ⁶⁸ E_{gx} (V) | - - - [Chen22] ³³ E_g (V) | - - - [Khan23] ²⁰⁶ E_g (V) |
| - - - [Griv07] ²⁸⁵ E_{gx} (P) | | |

FIG. 9. Band gap measurements and models. The latter are, if available, only shown in the specified confidence interval. (V) denotes a fitting using the Varshni model and (P) fitting with the Pässler model.

TABLE VII. Parameters for ionized dopants induced band gap narrowing.

ref.	method	n-type				p-type				
		A_{nc}	B_{nc}	A_{nv}	B_{nv}	A_{pc}	B_{pc}	A_{pv}	B_{pv}	C_{pv}
		[meV]								
[Lind98] ⁴⁸	calculation	-15	-2.93	19	8.74	-15.70	-0.39	13	1.15	-
[Pers99] ⁶⁶	calculation	-17.91	-2.20	28.23	6.24	-16.15	-1.07	-35.07	6.74	56.96

TABLE VIII. Parameters for ionized dopants induced band gap narrowing Slotboom model.

ref.	type	C	N	G
		[eV]	[1/cm ³]	[1]
[Lade00] ⁶⁵	n	2×10^{-2}	10^{17}	0.5
	p	9×10^{-3}	10^{17}	0.5

2. Doping Dependency

Two fittings for the doping dependent narrowing model in Eq. (12) could be found (see Table VII). We want to highlight that these are solely based on calculations. Measurement results are available^{285,319}, but due to their sparsity (see Fig. 11) they are not suitable to verify the calculations.

The main issue we identified regarding the parameters is an incorrect sign, as often all parameters become negative (see Fig. 10). The fact that in some cases, e.g., by Lophitis *et al.*³²⁰, the Jain-Roulston form is used (see Eq. (13)) makes a direct comparison of the parameters challenging. Furthermore, the parameter for the term with exponent 1/2 are sometimes combined^{144,145,154}, which makes it potentially impossible to apply them accurately in certain TCAD tools. A detailed analysis of all the inconsistencies we found in literature is provided in ??.

For the Slotboom model, that is used by various publications^{65,82,101}, one set of parameters is available⁶⁵ (see Table VIII). In contrast to the other models the band gap narrowing is linear in the semi-logarithmic plot (see Fig. 11). In a reasonable doping concentration range the deviation for p-type material is quite low but for n-type material considerable. The models of⁴⁸ and⁶⁶ only differ by a small amount.

Lindfelft ($A_{\text{nc}}, A_{\text{nv}}$) ($B_{\text{nc}}, B_{\text{nv}}$) ($A_{\text{pc}}, A_{\text{pv}}$) ($B_{\text{pc}}, B_{\text{pv}}$) (C_{pv})

Lindfelft

- [Lind98]⁴⁸ ($-1.5 \times 10^{-2}, 1.9 \times 10^{-2}$) ($-2.93 \times 10^{-3}, 8.74 \times 10^{-3}$) ($-1.57 \times 10^{-2}, 1.3 \times 10^{-2}$) ($-3.87 \times 10^{-4}, 1.15 \times 10^{-3}$) (-)
 - └─ [Levi01]¹⁴ ($-1.5 \times 10^{-2}, 1.9 \times 10^{-2}$) ($-2.93 \times 10^{-3}, 8.74 \times 10^{-3}$) ($-1.57 \times 10^{-2}, 1.3 \times 10^{-2}$) ($-3.87 \times 10^{-4}, 1.15 \times 10^{-3}$) (-)
 - └─ [Well01]³²¹ (-, -) (-, -) (-, -) (-)
 - └─ [Cha08]³²² ($-1.5 \times 10^{-2}, 1.9 \times 10^{-2}$) ($-2.93 \times 10^{-3}, 8.74 \times 10^{-3}$) (-, -) (-, -) (-)
 - └─ [Chen12]³²³ ($-1.5 \times 10^{-2}, 1.9 \times 10^{-2}$) ($-2.93 \times 10^{-3}, 8.74 \times 10^{-3}$) (-, -) (-, -) (-)
 - └─ [Alba10]¹⁵⁴ ($-1.5 \times 10^{-2}, 1.9 \times 10^{-2}$) (1.7×10^{-2}) ($1.57 \times 10^{-2}, 1.3 \times 10^{-2}$) (1.54×10^{-2}) (-)
 - └─ [Zhan10]³²⁴ ($-1.5 \times 10^{-2}, 1.9 \times 10^{-2}$) ($-2.93 \times 10^{-3}, 8.74 \times 10^{-3}$) (-, -) (-, -) (-)
 - └─ [Bell11]¹⁴⁵ ($-1.5 \times 10^{-2}, 1.9 \times 10^{-2}$) (1.17×10^{-2}) ($1.57 \times 10^{-2}, 1.3 \times 10^{-2}$) (1.54×10^{-3}) (-)
 - └─ [Habi11]²⁷⁴ ($-1.5 \times 10^{-2}, 1.9 \times 10^{-2}$) ($-2.93 \times 10^{-3}, 8.74 \times 10^{-3}$) ($-1.57 \times 10^{-2}, 1.3 \times 10^{-2}$) ($-3.87 \times 10^{-4}, 1.15 \times 10^{-3}$) (-)
 - └─ [Buon12]³²⁵ ($-1.5 \times 10^{-2}, -1.9 \times 10^{-2}$) ($-2.93 \times 10^{-3}, -8.74 \times 10^{-3}$) (-, -) (-, -) (-)
 - └─ [Pezz13]¹⁴⁴ ($1.5 \times 10^{-2}, 1.9 \times 10^{-2}$) (1.17×10^{-2}) ($1.57 \times 10^{-2}, 1.3 \times 10^{-2}$) (1.54×10^{-3}) (-)
 - └─ [Stef14]²⁹⁹ ($-1.5 \times 10^{-2}, 1.9 \times 10^{-2}$) ($-2.93 \times 10^{-3}, 8.74 \times 10^{-3}$) ($-1.57 \times 10^{-2}, 1.3 \times 10^{-2}$) ($-3.87 \times 10^{-4}, 1.15 \times 10^{-3}$) (-)
 - └─ [Zegh19]³²⁶ ($-1.5 \times 10^{-2}, 1.9 \times 10^{-2}$) (1.17×10^{-2}) ($-1.37 \times 10^{-2}, 1.3 \times 10^{-2}$) (1.54×10^{-3}) (-)
 - └─ [Zegh20]³²⁷ ($-1.5 \times 10^{-2}, 1.9 \times 10^{-2}$) (1.17×10^{-2}) ($-1.37 \times 10^{-2}, 1.3 \times 10^{-2}$) (1.54×10^{-3}) (-)
 - └─ [Ioff23]⁵⁷ ($-1.5 \times 10^{-2}, -1.9 \times 10^{-2}$) ($-2.93 \times 10^{-3}, -8.74 \times 10^{-3}$) ($-1.57 \times 10^{-2}, -1.3 \times 10^{-2}$) ($-3.87 \times 10^{-4}, -1.15 \times 10^{-3}$) (-)
 - └─ [Maxi23]²³⁸ ($-1.5 \times 10^{-2}, -1.9 \times 10^{-2}$) ($-2.93 \times 10^{-3}, -8.74 \times 10^{-3}$) ($-1.57 \times 10^{-2}, -1.3 \times 10^{-2}$) ($-3.87 \times 10^{-4}, -1.15 \times 10^{-3}$) (-)

Persson, Lindfelft, and Sernelius

- [Pers99]⁶⁰ ($-1.791 \times 10^{-2}, 2.823 \times 10^{-2}$) ($-2.2 \times 10^{-3}, 6.24 \times 10^{-3}$) ($-1.615 \times 10^{-2}, -3.507 \times 10^{-2}$) ($-1.07 \times 10^{-3}, 6.74 \times 10^{-3}$) (5.696×10^{-2})
 - └─ [Nipo16]¹⁴² (-, -) (-, -) (-, -) (-, -) (-)
 - └─ [Loph18]³²⁰ ($-1.791 \times 10^{-2}, 2.823 \times 10^{-2}$) ($-2.2 \times 10^{-3}, 6.24 \times 10^{-3}$) ($-7.311 \times 10^{-2}, 3.507 \times 10^{-2}$) ($-1.07 \times 10^{-3}, 6.74 \times 10^{-3}$) (-)

Slotboom ($C_{\text{n}}, N_{\text{n}} \mid C_{\text{p}}, N_{\text{p}} \mid G$)

Lades

- [Lade00]⁶⁵ ($2 \times 10^{-2}, 1 \times 10^{17} \mid 9 \times 10^{-3}, 1 \times 10^{17} \mid 5 \times 10^{-1}$)
 - └─ [Ayal04]¹⁰¹ ($2 \times 10^{-2}, 1 \times 10^{17} \mid 9 \times 10^{-3}, 1 \times 10^{17} \mid 5 \times 10^{-1}$)
 - └─ [Lech21]⁸² ($2 \times 10^{-2}, 1 \times 10^{17} \mid -, - \mid 5 \times 10^{-1}$)

FIG. 10. Citations and extracted parameters for the doping dependency of the band gap. If solely a single value is shown for parameter B then the publication only provides $B_{\text{c}} + B_{\text{v}}$. are fundamental investigations and connections predicted from the used values.

The band gap narrowing according to Eq. (17) is also shown, because it also occasionally used^{291,299}, whereat Stefanakis and Zekentes²⁹⁹ used a slightly different form of the Thomas-Fermi radius shown in Eq. (19) with n_0 the equilibrium carrier density.

$$\Delta E_{\text{g}} = \frac{e^2}{4\pi\epsilon_0\epsilon_s} \left(\frac{3n_0 e^2}{2\epsilon_0 E_F} \right)^{1/2} \quad (19)$$

Unfortunately our calculations did not succeed to reproduce the results achieved in these publications so we extracted the curve from Donnarumma, Palankovski, and Selberherr²⁹¹. Surprising for us is also the shape of the narrowing, which becomes almost linear in the semi-logarithmic plot for high doping concentrations. With the simple assumption $n = N_{\text{D}}^+$ resp. $n = N_{\text{A}}^-$ this does not

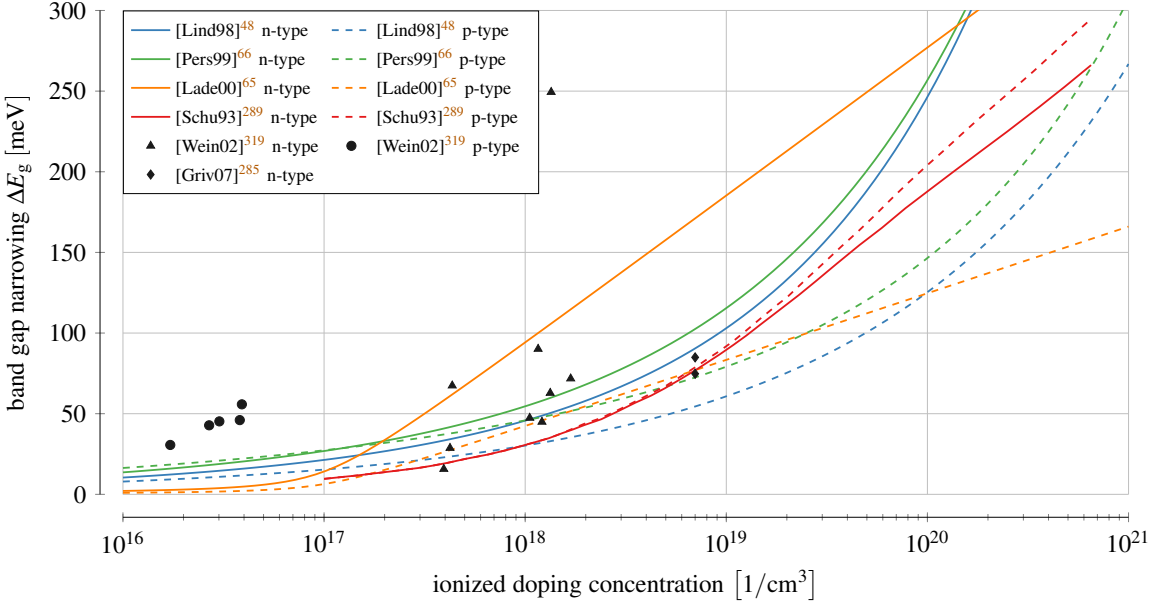


FIG. 11. Doping induced band gap narrowing. The different models complemented by measurement results for p- and n-type material are shown.

seem to be possible. Last Johannesson and Nawaz³²⁸ used the Debye radius from Eq. (16), based on the calculations by Lanyon and Tuft³²⁹.

3. TCAD Values

An overwhelming amount of band gap values can be found in literature (see Fig. 12). Measurements mainly focused on the exciton band gap energy E_{gx} at low temperatures, resulting in values of (3.265 ± 0.002) eV. Using the broadly accepted value of $E_x = 20$ meV (see also Fig. 15) a band gap energy of $E_g = 3.285$ eV is achieved, which has also been confirmed by dedicated measurements. The additional higher and lower values mainly stem from temperature dependency models, which were designed for higher temperatures and, thus, lack accuracy at low one. In general, only a few values for the parameters α and β are used (see Fig. 13), however, the energy value ($E_g(T_g)$) in Eq. (8)) is varied resulting in this wide range of values. Also calculations often deviate significantly. At room temperature few measurements are available such that values are dominated by model fitting.

The question that remains to be answered is on which values the various models for the band gap E_g are based upon, since there are very few measurements available. Our analysis revealed

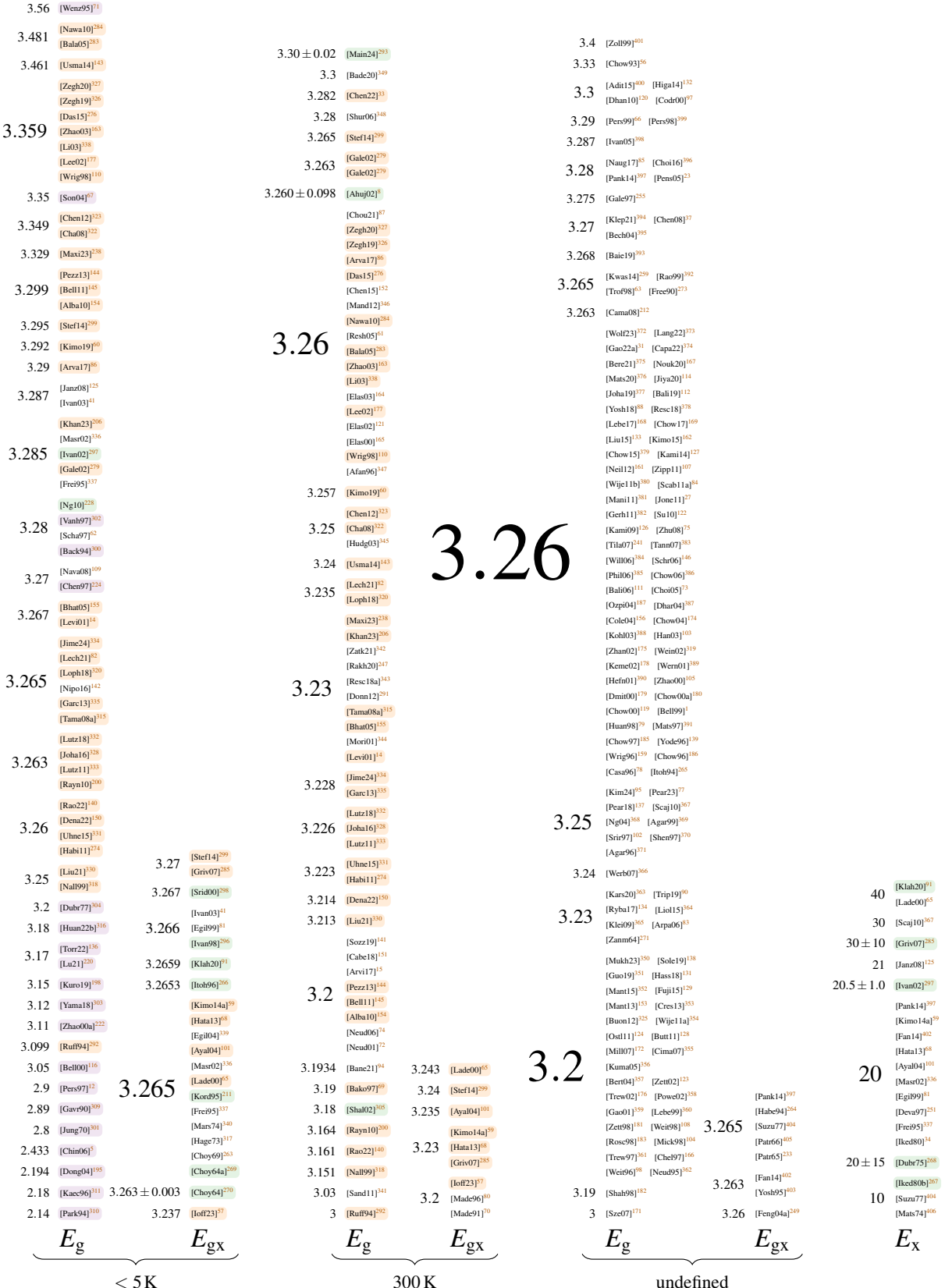


FIG. 12. Values for band gaps at varying temperatures. values correspond to calculations, ones to measurements and ones are values calculated from models.

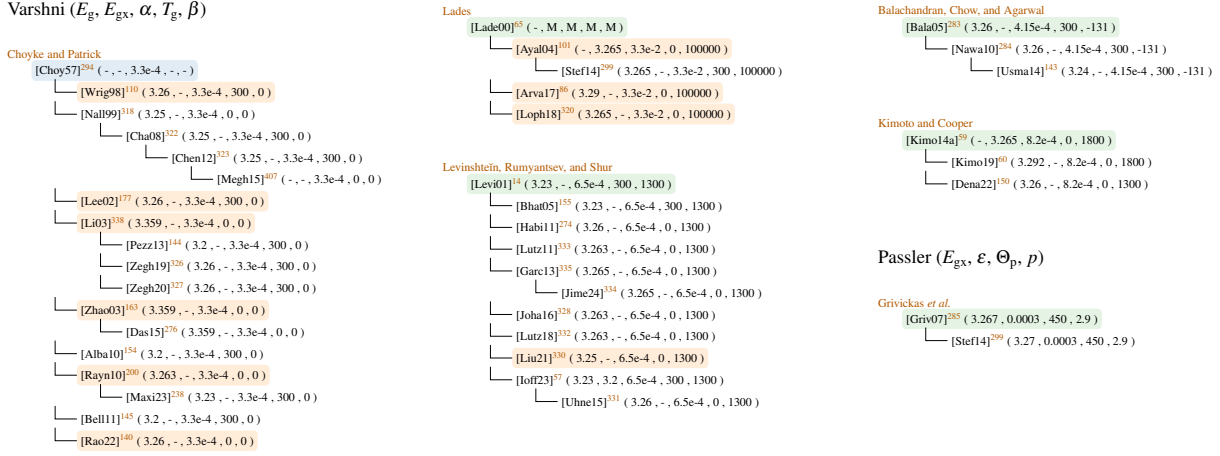


FIG. 13. Citations and the respective values for the temperature dependency. entries indicate values that have not been determined for 4H-SiC, are fundamental investigations and connections predicted from the used values.

that it sound to assume, that all the values currently in use go back to the investigations of E_{gx} by Choyke, Patrick, and Hamilton²⁶⁹, Choyke, Hamilton, and Patrick²⁷⁰ in 1964. Already in 1970 Junginger and Van Haeringen³⁰¹ rounded the achieved values of $E_{\text{gx}} = 3.263 \text{ eV}$ to $E_g = 3.26 \text{ eV}$. The same things were observed for the results from Choyke, Patrick, and Hamilton²⁶⁹, i.e., $E_{\text{gx}} = 3.263 \text{ eV}$. Stunningly, not only the value was changed but the exciton band gap energy was turned into the band gap energy, completely neglecting the free exciton binding energy. In fact, the excitonic values are nowadays only encountered in sophisticated publications.

Zanmarchi²⁷¹ introduced in 1964 for the first time the value $E_g = 3.23 \text{ eV}$, which is also commonly used today. Due to missing data at that time it is reasonable to assume that it was derived based on low temperature measurements of the exciton band gap. Also $E_g = 3.2 \text{ eV}$ seems to result from rounding $E_g = 3.265 \text{ eV}$. This was values was also achieved by Dubrovskii and Lepneva³⁰⁴ who added the exction band gap $E_{\text{gx}} = 3.265 \text{ eV}$ ²⁶³ and $E_x = 20 \text{ meV}$ to achieve $E_g = 3.2 \text{ eV}$. Solely for $E_g = 3.25 \text{ eV}$ we have no clear explanation, but maybe it is simply the result of a typographical error when transferring $E_g = 3.265 \text{ eV}$.

The outcome of our analysis is thus, that it is possible that the room temperature band gap energies commonly used in literature go back to low temperature exciton band gap energy measurements six decades ago. The fact that Ahuja *et al.*⁸ achieved the same value of $E_g = 3.23 \text{ eV}$ as Zanmarchi²⁷¹ 60 years ago shows, that multiple avenues to a specific values are possible and thus such statements not easy to prove. Nevertheless, since we did not find any other derivations,

Band Gap (E_g , E_{gx} , T)

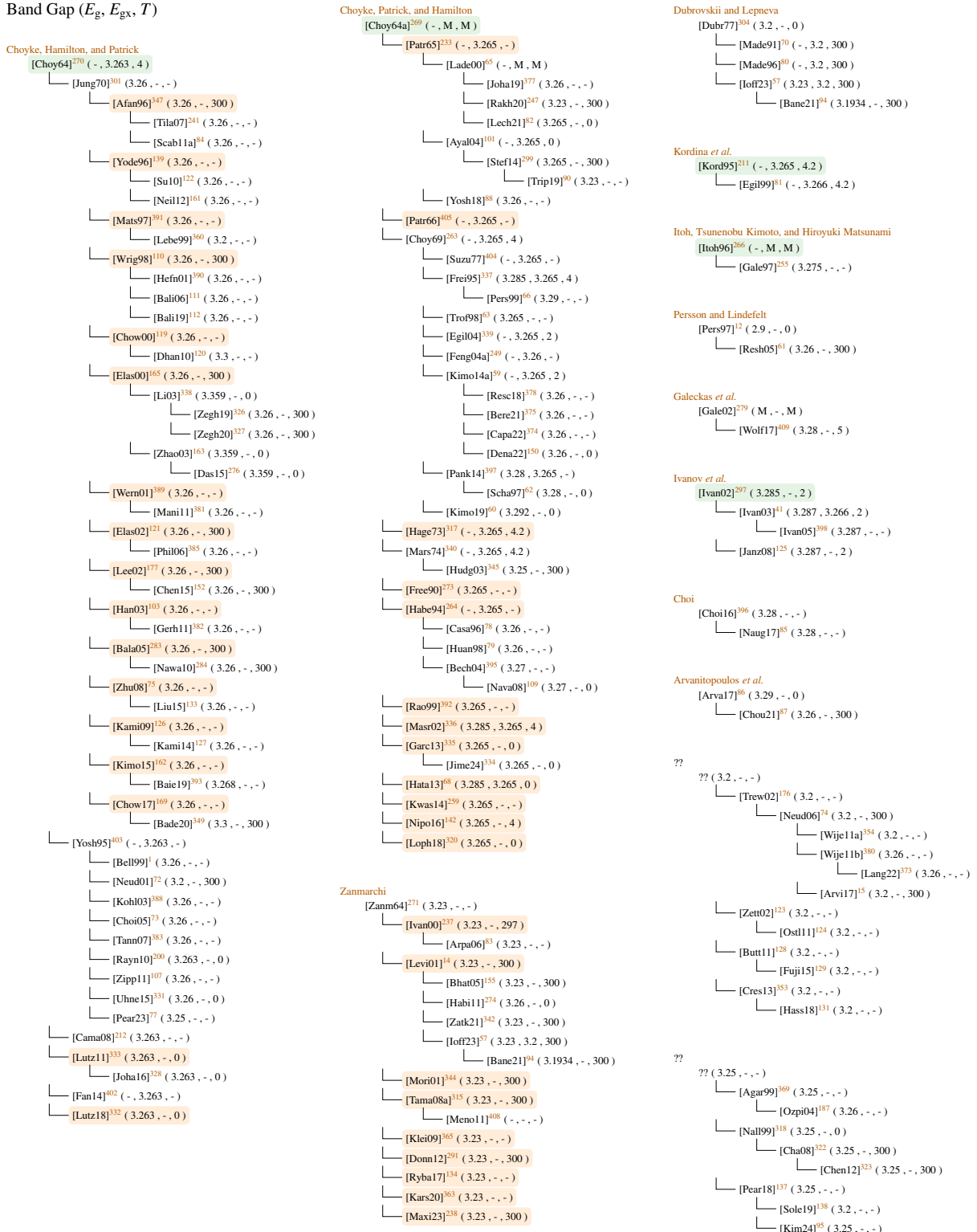


FIG. 14. Citations and values for band gap energies. Green boxes represent fundamental investigations and orange boxes represent connections predicted from the used values. We collect publications that share the same value but that do not provide a reference under ??.

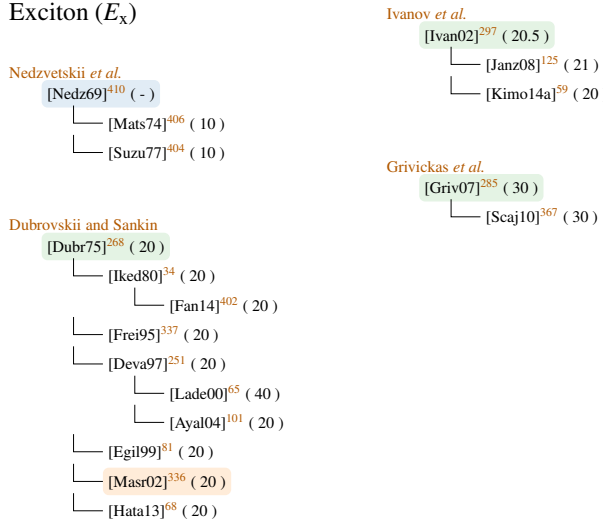


FIG. 15. Citations and values of the free exciton binding energy E_x . entries indicate values that have not been determined for 4H-SiC, are fundamental investigations and connections predicted from the used values.

we think that the chances that our hypothesis is true is quite high.

Aren't that horrifying news? Well, coincidentally recent measurements by Galeckas *et al.*²⁷⁹ and Ahuja *et al.*⁸ actually suggest that the band gap energy at 300 K is approximately 3.26 eV, whereat it has to be noted that the result by the latter have an uncertainty of 98 meV and thus have to be handled with care. To confirm that $E_{gx}(0) \approx E_g(300)$ holds, additional verifications are required. In our opinion this also includes an investigation of E_x versus temperature, which is assumed constant at the moment. The newest models (see Fig. 9), however, suggest an increasing distance between the band gap energies.

An additional avenue for future research would be an investigation of the differences between measurements and calculations. If the latter achieve the actually more accurate results the band gap energy for 4H-SiC might need significant corrections.

IV. IMPACT IONIZATION

In high electric fields, charge carriers are able to pick up enough kinetic energy to create an additional electron-hole pair, which is called impact ionization. This effect is sometimes deliberately used, e.g., in avalanche diodes, to increase the responsiveness³ but often is an undesired effect that leads to breakdown and the destruction of the device. Consequently, impact ionization

simulations are crucial to predict the safe operation regions of a device. In TCAD tools impact ionization is modeled as a (electric field dependent) multiplicative factor that denotes the increase of charge carriers per unit distance.

A. Theory

The impact ionization is described by the charge carrier generation rate^{69,325}

$$G_{II} = \frac{1}{q} (\alpha J_n + \beta J_p) = \frac{1}{q} (\alpha n v_n + \beta p v_p)$$

with n resp. p the amount of electron resp. holes, v_n resp. v_p their velocity and J_n resp. J_p the electron resp. hole current. The impact ionization coefficients for electrons (α) and holes (β) represent the number of secondary carriers a single charge carrier generates per cm in an electric field F , i.e.,³

$$\alpha = \frac{1}{n} \frac{dn}{dx} 1/\text{cm} \quad , \quad \beta = \frac{1}{p} \frac{dp}{dx} 1/\text{cm} .$$

Many models to describe α and β were proposed. We will provide a short introduction to the topic, whereat more detailed descriptions are available in literature^{3,161,249,411,412}. One of the earliest models is the still very popular empirical Chynoweth's law^{413,414}

$$\alpha, \beta(F) = a \exp\left[-\frac{b}{F}\right] , \quad (20)$$

often also called Van Overstraeten-de Man model⁴¹⁵. This empirical fitting was a necessity at the time of its publication because a physical explanation was only available for strong electric fields as⁴¹⁶

$$\alpha, \beta(F) = \frac{eF}{E_i} \exp\left[-\frac{3E_p E_i}{(eF\lambda)^2}\right] .$$

This changed with Shockley⁴¹⁷ who modeled the impact ionization coefficient by

$$\alpha, \beta(F) = \frac{eF}{E_i} \exp\left[-\frac{E_i}{eF\lambda}\right] , \quad (21)$$

In this case, e denotes the electron charge, λ the mean free path and E_i the ionization energy, i.e., the energy to create an electron-hole pair. The prefactor is the inverse of the length required to gain the ionization energy, i.e., how often per unit length this energy is reached, while the exponential term denotes the chance of doing that without collisions. This model is often called Shockley's "lucky electron"⁴¹⁸. In Lackner⁴¹⁹ the close relationship between Eq. (20) and Eq. (21), which can

be easily retraced by setting $a = eF/E_i$ and $b = E_i/e\lambda$, is highlighted, leading to a physically based calculation of parameters a and b . The author suggests an additional scaling factor, depending on the electric field and the parameter b for both α and β , to cover the parameter variations with changing electric field strength.

The low- and high-field cases were finally combined in Baraff's theory⁴²⁰, which expresses $\alpha, \beta \propto \exp[-b/F]$ for low fields and $\alpha, \beta \propto \exp[-c/F^2]$ for high ones. It was later extended by Thornber⁴²¹ to the expression⁴¹¹

$$\alpha, \beta(F) = \frac{eF}{\langle E_i \rangle} \exp \left[-\frac{\langle E_i \rangle}{[(eF\lambda)^2/3E_p] + eF\lambda + E_{k_B T}} \right], \quad (22)$$

with $\langle E_i \rangle$ the effective ionization threshold⁴¹¹, E_p the optical phonon energy and $E_{k_B T}$ a temperature contribution that is often neglected in the literature. Konstantinov *et al.*⁴¹⁸ even only used the high-field part for the electrons and dropped the factor $3E_p$ for the holes in the equation presented in the paper. We assume a typographical error as the division sign is still visible. For the ionization energy E_i originally a value of $3/2E_g$ (E_g the band gap; see Section III) was assumed, which represents the ideal case¹⁶⁷. Recent measurements, however, revealed for 4H-SiC values between 7.28 and 8.6 eV²⁵⁸.

Since Baraff's theory was not able to satisfy all demands⁴²², Okuto and Crowell⁴²³ extended Chynoweth's law by adding the electric field as a multiplicative factor, an exponential parameter m and a temperature dependency via c and d . The overall fitting model has the form

$$\alpha, \beta(F) = a\{1 + c(T - 300)\} F^n \exp \left[-\left(\frac{b\{1 + d(T - 300)\}}{F} \right)^m \right] \quad (23)$$

where T denotes the temperature in Kelvin. In all investigated publications $n = 0$ so we will not consider this parameter any further, leading to a simplified model that is often referred to as Selberherr model⁴¹².

More advanced models were also proposed, which are, however, not yet used in TCAD simulations. These include a more sophisticated temperature dependency in Eq. (23)⁴²⁴ and models based on multi-stage⁴²⁵ and inelastic collision events⁹³. Other popular methods to investigate the effects of impact ionization are Monte Carlo simulations^{10,104–106,116,426–431}, non-localized models^{432,433} and the impact of defects⁴³⁴ in the presence of a magnetic field^{435,436}. Some researchers^{333,437,438} even combine α and β to an effective coefficient and model it by a power law, i.e., $\alpha, \beta \propto E^n$, to achieve an analytic expression suitable for calculations.

The impact ionization is anisotropic, meaning that the breakdown field in $\langle 11\bar{2}0 \rangle$ is about three quarters of the one in $\langle 0001 \rangle$ direction⁴³⁹. For that reason the impact ionization coefficients have

been determined parallel and perpendicular to the c-axis. These can be combined, using a formalism introduced by Hatakeyama⁴⁴⁰, to achieve suitable amplification factors for any desired lattice direction. Jin *et al.*⁴⁴¹ reused the parameter values but introduced a new approach to calculate the "driving force" by considering also the field direction for constant carrier temperature. Nida and Grossner⁴⁴² adapted the field strength to an effective $F^* = (m/m_{\parallel})^{1/2}F$, with m resp m_{\parallel} the effective masses (see Section II).

To depict the changing behavior with temperature either the built-in parameters, as is the case for the Okuto-Crowell model (see Eq. (23)), or a multiplicative factor⁴⁴³

$$\gamma = \frac{\tanh\left(\frac{\hbar\omega_{\text{OP}}}{2k_B T_0}\right)}{\tanh\left(\frac{\hbar\omega_{\text{OP}}}{2k_B T_L}\right)} \quad (24)$$

to scale the parameters a and b of Eq. (20) is used^{65,101,318,440} with T_0 a reference temperature (often 300 K), T_L the lattice temperature and ω_{OP} the optical phonon energy. We are very confident that the latter corresponds to the longitudinal optical phonon energy ω_{LO} (see Section I) as their respective values match well. Hatakeyama⁴⁴⁰, however, pointed out that for a good fit $\omega_{\text{OP}} = 190$ meV had to be used, which contradicts experimental results of $\omega_{\text{LO}} = 120$ meV. Niwa, Suda, and Kimoto⁴⁴⁴ use a polynomial of degree two to scale the parameters while Bartsch, Schörner, and Dohnke⁴³⁷ utilize the ratio $T/300$ K for this purpose. In contrast, Hamad *et al.*⁴⁴⁵ explicitly present parameter values for different temperatures. Nida and Grossner⁴⁴² scaled the mean free path by $\sqrt{\gamma}$ and the ionization energy by the ratio of the bandgap at temperature T_L and at 300 K.

B. Results

To measure the impact ionization coefficients an equal amount of charge carriers is generated in a space charge region, either by (pulsed) electron (electron beam induced current (EBIC))⁴⁴⁸ or optical beams (optical beam induced current (OBIC))^{418,444,445,449–455}. Defects have a significant impact on the coefficients such that EBIC is used to extract parameters at defect-free regions¹¹².

The charge carrier generation is executed at varying field strengths. Recording the respective terminal currents enables a comparison against the no-field current and, thus, the determination of the effective amplification. The readout of the current can be executed in DC mode^{418,449} (whereat Raghunathan and Baliga⁴⁴⁸ state that elimination of leakage current in this case is hard), AC mode^{448,452,453} or both combined^{450,451}. Additional challenges are the selection of a suitable

test structure, e.g., p-n/n-p diodes or pnp/npn transistors) and the proper separation of electron and hole multiplication phenomena, which we will not further cover in this review. Instead we refer the interested reader to the dedicated literature^{418,444,452,454,456,457}.

Monte Carlo simulations are also used for the investigation of the impact ionization. While some are able to extract the impact coefficients as the reciprocal of the average distance^{431,458} others solely present simulated values without fitting to any of the earlier presented model^{10,104–106,116,426–430,459}. Fitting is, however, crucial to use the results in TCAD simulations tools. For this purpose Stefanakis *et al.*⁴⁶⁰ provides fittings to Monte Carlo simulation^{116,461}, Nouketcha *et al.*¹⁶⁷ used a genetic algorithm to fit to multiple sources^{442,449–451,462,463}, Nida and Grossner⁴⁴² fitted their model to values from^{418,440,448,450,462} and Stefanakis *et al.*⁴⁶⁰ achieved a "global fit" in regard to many 4H investigations^{418,450,451,453,455,463}, but also a 6H one²⁹², and Monte Carlo simulations^{116,461}. Kyuregyan⁴⁵⁶ calculated the average of available parameter values without conducting any fitting. According to the authors this is supposed to remove statistical inaccuracies and uncertainties introduced by the characterization methods. Even multiple fittings on the same data were executed. Choi *et al.*⁷³, Banerjee⁹⁴, Baliga¹¹², Zhao *et al.*¹⁶³, Morisette³⁴⁴, Sheridan *et al.*⁴⁶⁴ all used the data from Konstantinov *et al.*⁴¹⁸, however, the ones for Sheridan *et al.*⁴⁶⁴ exactly match values achieved for 6H by Ruff, Mitlehner, and Helbig²⁹².

TABLE IX. Parameters for fundamental fittings of the Okuto-Crowell model found in literature. If only a single value spanning across two columns is presented the crystal direction was not specified.

ref.	electron							hole							F region
	a_{\parallel}	a_{\perp}	b_{\parallel}	b_{\perp}	c	d	m	a_{\parallel}	a_{\perp}	b_{\parallel}	b_{\perp}	c	d	m	
	[$10^6/\text{cm}$]	[MV/cm]	[10^{-3}]	[10^{-3}]	[1]	[$10^6/\text{cm}$]	[MV/cm]	[10^{-3}]	[10^{-3}]	[1]	[MV/cm]				
[Ragh99] ⁴⁴⁸	-	-	-	-	0	0	1	3.09		17.9 ± 0.4		-3.46	0	1	2.5–3.2
[Bert00] ^{465j}	0.4	48	15		0	0	1.15	1.8	45	15		0	0	1	-
[Sher00] ^{464dl}	-	-	-	-	0	0	1	5.18	-	14	-	0	0	1	-
[Mori01] ^{344d}	-	-	-	-	0	0	1	-	-	-	-	0	0	1	-
[Ng03] ⁴⁵¹	1.98		9.46	-2.02 ^a	0	1.42		4.38		11.4	-0.913 ^a	0	1.06		1.8–4
[Zhao03] ^{163d}	7.26		23.4	0	0	1		6.85		14.1	0	0	0	1	-
[Hata04] ⁴⁶⁶	176	21	33	17	0	0	1	341	29.6	25	16	0	0	1	2–5
[Choi05] ^{73d}	16.5		25.8	0	0	1		5.5		13.5	0	0	0	1	1.5–5
[Loh08] ⁴⁵⁰	2.78		10.5	0	0	1.37		3.51		10.3	0	0	0	1.09	1–5
[Loh09] ⁴⁶⁷	-	-	-	-	0	0	1	3.321		10.385	-2.78	0.48 ^k	1.09		1.33–2
[Nguy11] ⁴⁵²	0.46		17.8	0	0	1		15.6		17.2	0	0	0	1	1.5–2.7
[Gree12] ^{457h}	0.019		2.888	0	0	4.828		0.06		1.387	0	0	0	0.96	1.6–4
[Nguy12] ⁴⁵³	3.36		22.6	0	0	1		8.5		15.97	0	0	0	1	1.5–4.8
[Sun12] ⁴³¹	1.803		13.52	0	0	1.2		1.861		9.986	0	0	0	1.11	1.5–5
[Niwa14] ⁴⁴⁴	8190		39.4	0	0	1		4.513		12.82	0 ^f	0	0	1	1.4–2.7
[Hama15] ⁴⁴⁵	0.99		12.9	0	0	1		1.61		11.5	0	0	0	1	2.5–7
[Niwa15] ⁴⁶²	0.143	-	4.93	-	0 ^e	0 ^e	2.37	3.14	-	11.8	-	6.3 ^c	1.23 ^c	1.02	1–2.8
[Shar15] ⁴⁶⁸	186	-	28	-	0	0	1	301	-	20.5	-	0	0	1	-
[Kyur16] ⁴⁵⁶ⁱ	38.6 ± 15.0		25.6 ± 0.1	0	0	1		5.31 ± 0.30		13.10 ± 0.01	0	0	0	1	1–5
[Zhan18] ⁴⁶⁹	1.31		13	-1.47	0	1		2.98		13	-1.56	0	0	1	-
[Bali19] ^{112d}	313		34.5	0	0	1		8.07		15	0	0	0	1	1.1–5
[Zhao19] ⁴⁵⁵	0.339	-	5.15	-	0	0	2.37	3.56	-	11.7	-	6.19	1.15	1.02	1–3.2
[Stef20] ⁴⁵⁴	-	6.4	-	12.5	0	0	1	-	6	-	13.3	0	0	1	1.3–2
[Bane21] ^{94d}	100		40.268	0	0	1		41.915		46.428	0	0	0	1	0.1–1
[Chea21] ^{458g}	0.932		7.19	0	0	1.95		1.75		6.56	0	0	0	1.45	1.6–10
[Stef21] ^{460e}	2.8	-	20.7	-	-1 ^b	-0.29 ^b	1	2.5	-	12.1	-	1.74 ^b	0.59 ^b	1	-

^a provided by Cha *et al.*⁴⁷⁰

^b provided by Steinmann *et al.*⁴⁷¹

^c different values suggested by Steinmann *et al.*⁴⁷¹

^d values fitted to Konstantinov *et al.*⁴¹⁸

^e values fitted to^{116,292,418,450,451,453,455,461,463}

^f temperature dependency stated in the paper that could not be transferred to model formalism

^g a and b presumably stated in 1/m and MV/m in paper, converted to 1/cm and MV/cm

^h for $F > 2.5 \text{ MV}/\text{cm}$ the parameters α from Ng *et al.*⁴⁵¹ are used

ⁱ values achieved by averaging of^{368,418,444,449–451,457,467}

^j fitted to Nilsson *et al.*¹¹⁵

^k we changed $b = 8.9 \times 10^6 - 4.95 \times 10^3 T$ to $b = 8.9 \times 10^6 + 4.95 \times 10^3 T$ to better match the results in the paper

^l same values achieved as 6H investigation by Ruff, Mitlehner, and Helbig²⁹²

TABLE X. Parameters for fundamental fittings of the Thurnber model found in literature. For $E_{k_B T} = k_B T$ this parameter scales with temperature.

ref.	dir	electron				hole				F region
		$\langle E_i \rangle$	λ	E_p	$E_{k_B T}$	$\langle E_i \rangle$	λ	E_p	$E_{k_B T}$	
		[eV]	[Å]	[meV]	[meV]	[eV]	[Å]	[meV]	[meV]	
[Kons97] ^{418f}		10	29.9	120	0	7	32.5	120	0	1.5–10
[Nida19] ^{442a}		10.61	27	120	$k_B T$	10.87	39.49	85	$k_B T$	1–10
[Nouk20] ^{167c}	-	7.5	10	92.5	14	6.62	4.8	9	102	0.9–10
[Stei23] ^{471e}	-	10.6	27	87	$k_B T$	10.9	80	87	$k_B T$	1–10

^a values picked from specified ranges, fitting to^{418,440,448,450,462}

^c $3/2 E_g$ instead of $\langle E_i \rangle$ used in the exponential, fitting to^{442,449–451,462,463}

^e initial values taken from Nida and Grossner⁴⁴²

^f linear term in denominator not used for α

A wide range of Okuto-Crowell (see Table IX) and Thornber (see Table X) model parameters could be identified in literature. In one case we were unable to match the temperature variation of β with $b = 8.9 \times 10^6 - 4.95 \times 10^3 T^{467}$ with the data presented in the same publication. We achieved much better results with $d = 8.9 \times 10^6 + 4.95 \times 10^3 T$ with T the temperature in Kelvin. In Stefanakis *et al.*⁴⁵⁴ the fitting for α also deviates slightly from the plots in the paper. Due to the minor deviation we kept the values as they were. In Cheang, Wong, and Teo⁴⁵⁸ the values of parameters a and b are two orders of magnitude too high. We suspect that they are specified in 1/m resp. MV/m although in the paper it is explicitly stated as 1/cm resp. MV/cm. Despite these changes we were not able to exactly recreate the plots shown in the paper. We had to exclude the publication by Ng *et al.*³⁶⁸ as no data are shown in the paper and Cheong *et al.*⁴⁴⁷, Kimoto *et al.*⁴⁷² who only specify that SiC is investigated but not the polytype.

A graphical representation of the models describing the impact ionization coefficient for electrons (see Fig. 16) show a spread of approximately one order of magnitude, whereat the deviations increase for low fields. For the crystal direction perpendicular to the c-axis much higher values are determined. This matches qualitatively early estimations, however, the quantities of $\alpha_\perp/\alpha_\parallel = 3.5$ used by Lades⁶⁵, Bakowski, Gustafsson, and Lindefelt⁶⁹ seems to be too low. For low resp. high fields the fittings of Zhang and You⁴⁶⁹ resp. Sharma, Hazdra, and Popelka⁴⁶⁸ are too high meaning that the models have to be handled with care in these regions.

For holes (see Fig. 17) the spread in values is much smaller, especially close to a field strength

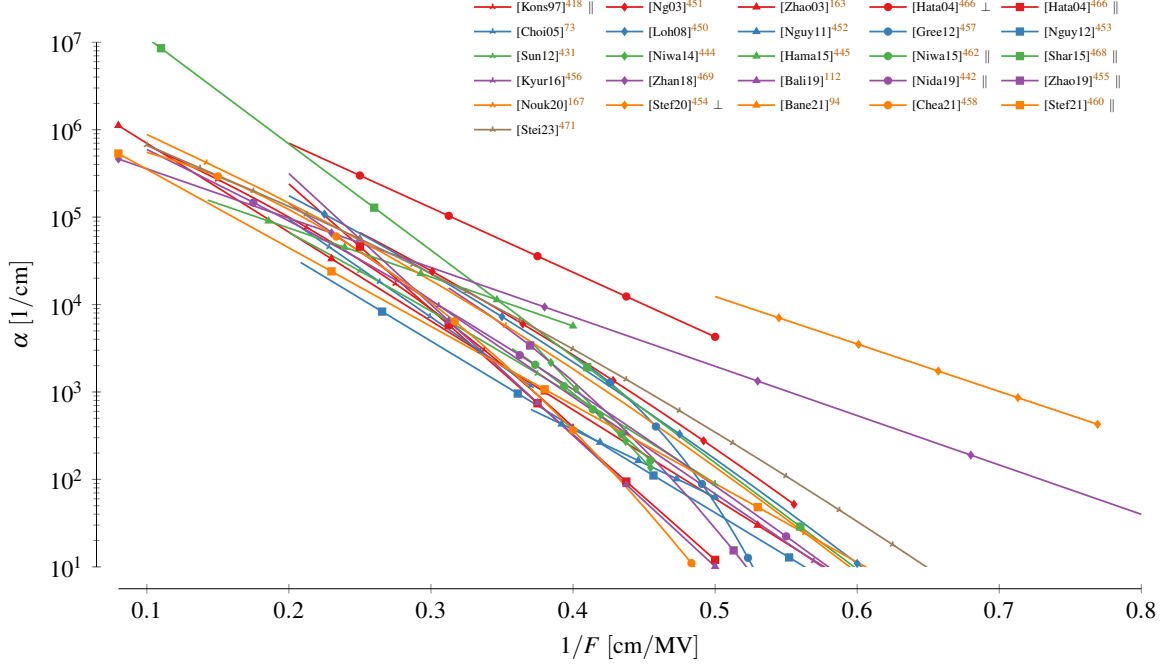


FIG. 16. Impact ionization coefficient α for electrons. Each model is limited to the interval used for characterization. The colors are altered to increase the readability.

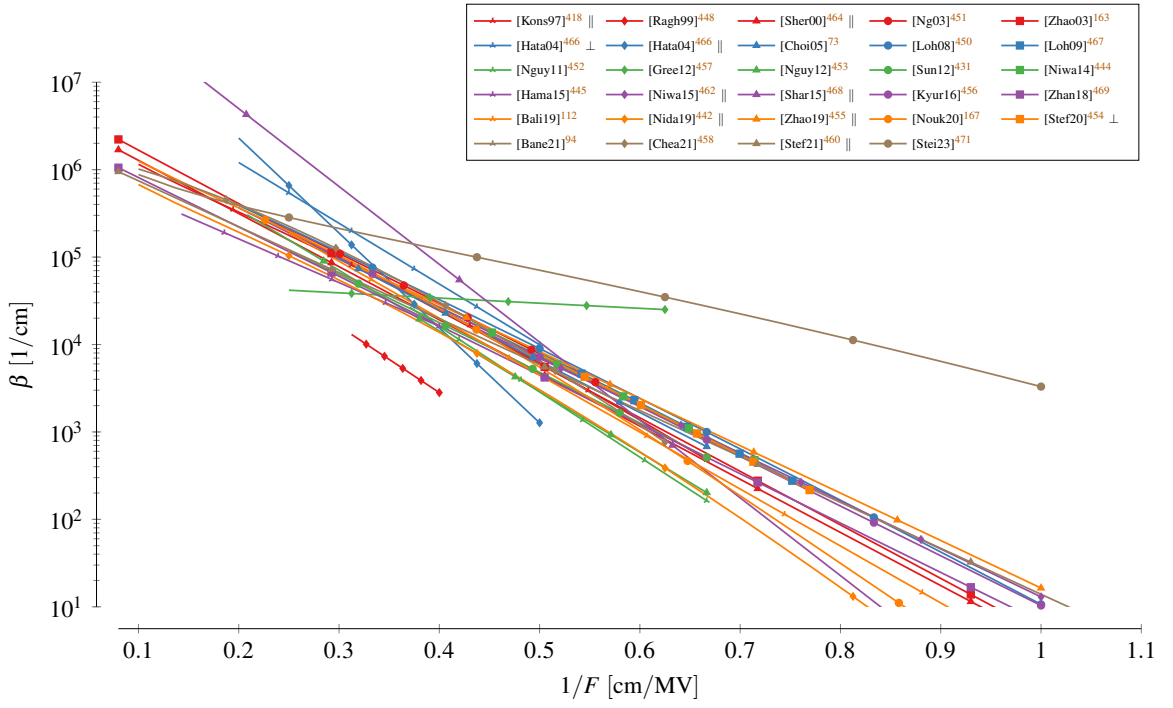


FIG. 17. Impact ionization coefficient β for electrons. Each model is limited to the interval used for characterization. The colors are altered to increase the readability.

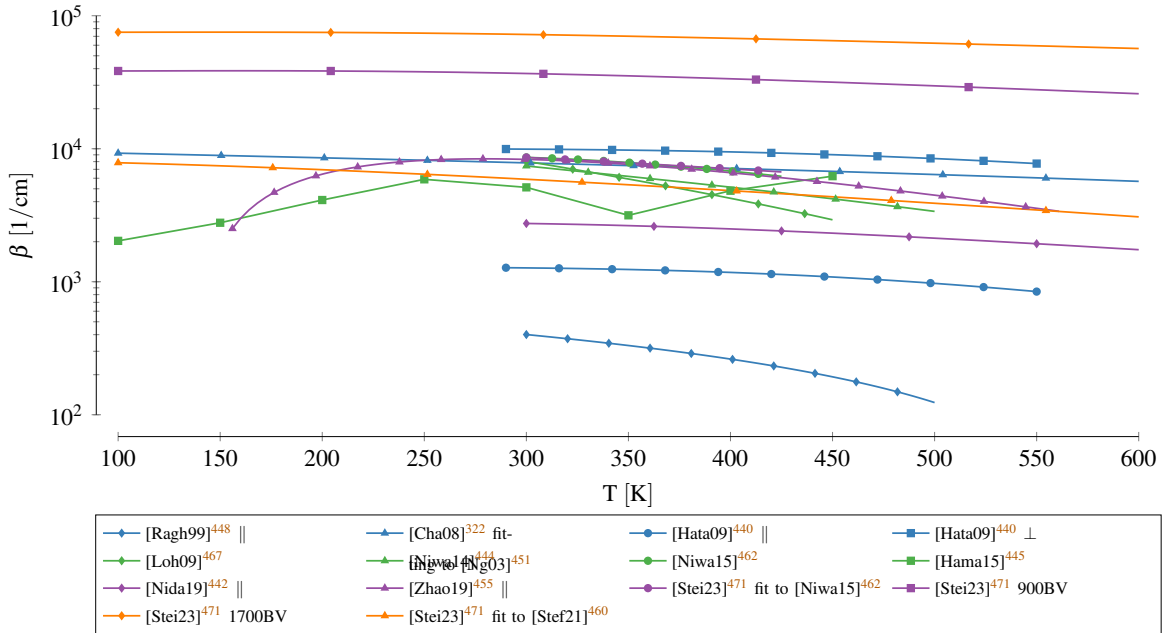


FIG. 18. Temperature dependence of the hole impact ionization coefficient. The single models are evaluated for an electric field of 2 MV/cm and are ordered according to their publication date. The colors simply are used to improve the readability.

around 2 MV/cm. Nevertheless, there are also fittings we want to highlight. The results of Steinmann *et al.*⁴⁷¹ are too high possibly correlating to the fitting of a rather high breakdown voltage. The values from Raghunathan and Baliga⁴⁴⁸ are too low, which was attributed to the direction dependency of α ^{249,465}, i.e., that the coefficient in the direction perpendicular to the c-axis is much stronger. Feng and Zhao²⁴⁹ thus conclude that the results in⁴⁴⁸ deviate from practical results since the focused beam used in the analyses caused them to miss a large share of the intrinsic defects. Although Fig. 17 supports this statement, the statement that the perpendicular impact ionization of holes is a lot stronger, could not be confirmed. The results suggest rather $\beta_{\perp} = \beta_{\parallel}$, which was also used for 6H⁶⁹. Finally, the fittings by Green *et al.*⁴⁵⁷ show a significantly slower increase with field than all other models.

Important for TCAD simulations is also the temperature dependency of the impact ionization coefficients. For holes (see Fig. 18) all models predict a decreasing value, which matches the reports of increasing breakdown voltage with increasing temperature^{322,473} and prevents thermal runaway. Hatakeyama⁴⁴⁰ uses the temperature scaling shown in Eq. (24) (multiplication with γ), which is also used by Lades⁶⁵, Schröder¹⁴⁶. Clearly visible is the decline of β with increasing temperature. Steinmann *et al.*⁴⁷¹ proposed two fittings for two different breakdown voltages of

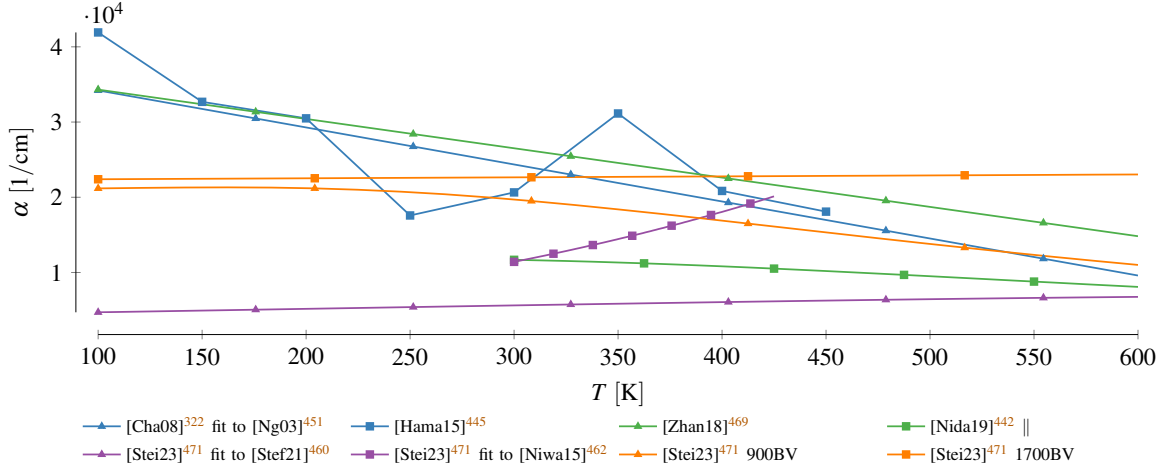


FIG. 19. Temperature dependence of the electron impact ionization coefficient. The single models are evaluated for an electric field of 3.33 MV/cm and are ordered according to their publication date. The colors simply are used to improve the readability.

the investigated device, i.e., 900 V and 1700 V.

For electrons (see Fig. 19) the results are quite inconclusive. Some models even propose an increase of α with temperature. This is, however, compensated by the decrease in β with increasing temperature due to the relatively small variations of α compared to β (linear vs. logarithmic y-axis).

C. Discussion

The majority of the currently utilized impact ionization coefficients are based on 4H measurements (see Fig. 20). Care has to be taken especially for publications prior to the year 2000, as those often are based on 6H^{69,292,474,475}. These outdated results have later found their way in various publications^{65,110,155,159,161}. In early publications⁶⁹ 6H was still used because 4H values were not available or simply^{163,476} because the early available fittings from Konstantinov *et al.*⁴⁴⁹, Raghunathan and Baliga⁴⁶³ deviated significantly. The results from Bakowski, Gustafsson, and Lindefelt⁶⁹ were later further changed by Lades⁶⁵ who calculated the parameters at 273 K and introduced a typographical error for the hole coefficient a , which was stated as 2.24×10^6 /cm instead of 3.24×10^6 /cm. We found additional more or less critical inaccuracies, which we all summarize in ??.

The most influential publications are arguably by Raghunathan and Baliga^{448,463} and Hatakeyama

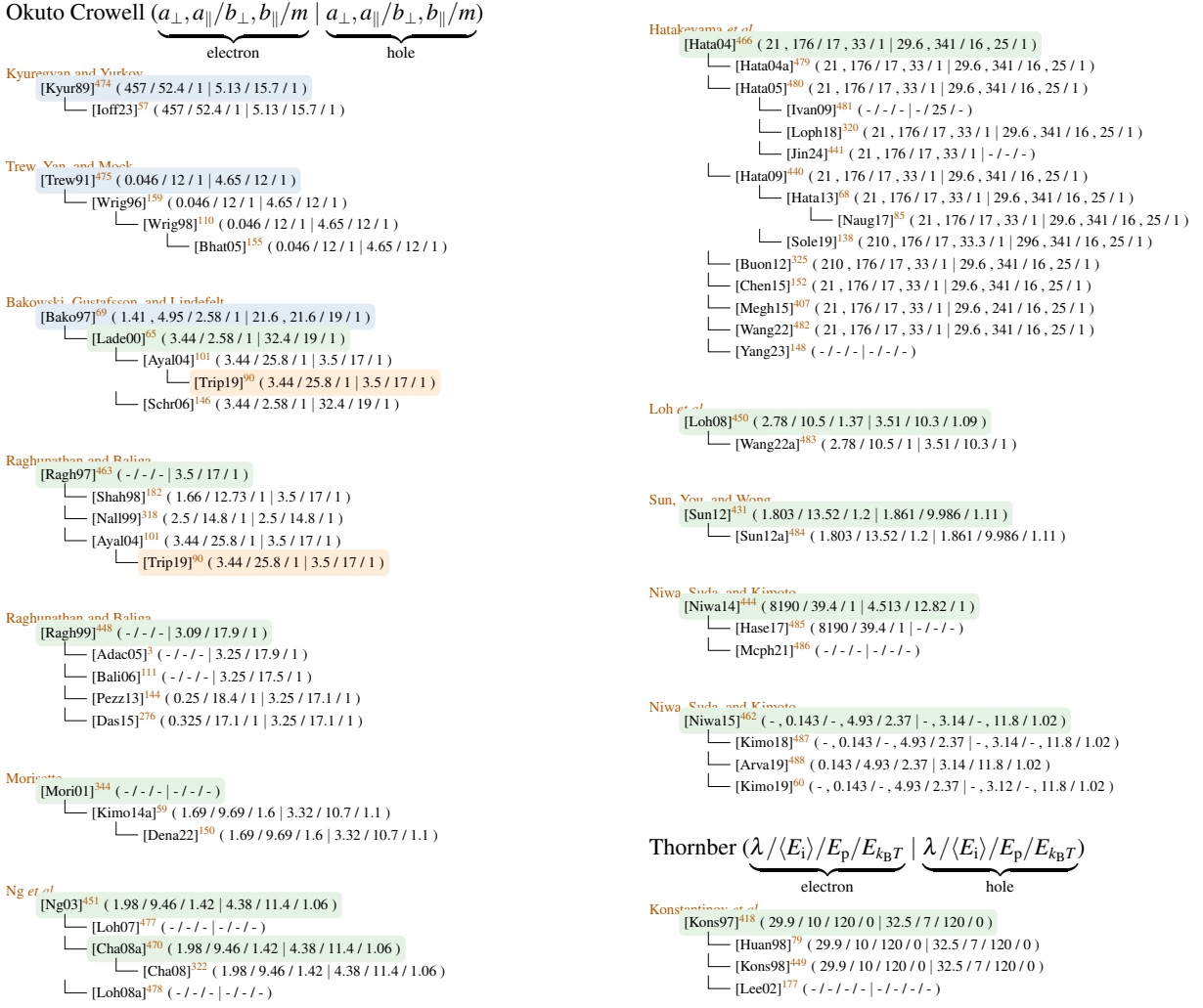


FIG. 20. Reference chain for impact ionization parameters. Publications with blue background are not focused on 4H-SiC, those in green are novel analyses on 4H-SiC and orange color indicates that the reference was guessed based on the values but not explicitly stated in the publication. The values for a and b were scaled by 1×10^6 for improved readability.

et al.⁴⁶⁶. However, twelve investigations in the last decade indicate that impact ionization is still an active area of research. Nevertheless, only few values for the impact ionization perpendicular to the c-axis are available. Since the available parameters suggest a higher multiplication and thus earlier breakdown in these directions, further in detail investigations are required in the future.

In contrast to Silicon, 4H-SiC shows higher hole than electron current amplification, i.e., $\beta > \alpha$ ^{3,180}, which is attributed to discontinuities in the electron spectrum¹⁶⁰. Consequently, the Shockley approximation of the "lucky electron" can only be applied to holes, as the electrons

energy can not continuously increase⁴¹⁸. Kimoto *et al.*⁴⁸⁷ name these "minigaps" as the reason for the low temperature dependence of α . Temperature analyses are, however, sparsely available. Some of the available data were years after the original publication proposed by other authors, e.g., by Cha and Sandvik³²² or by Steinmann *et al.*⁴⁷¹, who fitted the linear and quadratic temperature coefficients of the breakdown voltage. Nida and Grossner⁴⁴² present the high temperature evolution of some models.

Although models can be used for any arbitrary field strengths, they are most accurate within their often very narrow characterization range. In general, the highest accuracy is required around the critical electric field, i.e., where breakdown occurs. In the literature commonly 2–3 MV/cm^{23,72,103,121,123,137,139,389,490} are used, whereat some explicitly state a dependence on the doping concentration^{60,112,333,348,390,418,439,448,455,462,487,491–493}. Be advised that these values are, most commonly, determined for uniformly doped non-punch through diodes using power law approximations of the impact coefficients⁴⁴⁸. Consequently such values have to be interpreted with a grain of salt and have to be corrected according to the actual structure and doping level^{462,494}. Over short distances a higher field is required to achieve breakdown than for thick devices, where charges can multiply over long distances.

V. CHARGE CARRIER RECOMBINATION

In a semiconductor electron-hole pairs are continuously created, for example due to thermal processes, adding additional charge carriers. Their concentration is denoted as excess carrier Δ_N , non-equilibrium, generated^{495,496} or solely carrier concentration²⁵². Simultaneously to the generation, electron-hole pairs also recombine, such that the rate of change can be described as shown in Eq. (25)^{497–499}.

$$\frac{d\Delta_N}{dt} = D \frac{d^2\Delta_N}{dx^2} - R + G \quad (25)$$

The first term denotes the diffusion of charge carriers (D equals the ambipolar diffusion coefficient), R the recombination and G the generation rate. One of the effects accounting to the latter is impact ionization, which we already investigated in Section IV, or optical generation. In equilibrium, all the contributions compensate and the net change is zero.

In TCAD simulations it is essential to correctly model the localized change in charge carrier concentration, as it influences, among others, the conductivity and the internal electric fields. In this section we are, thus, going to review the relevant charge carrier recombination mechanisms

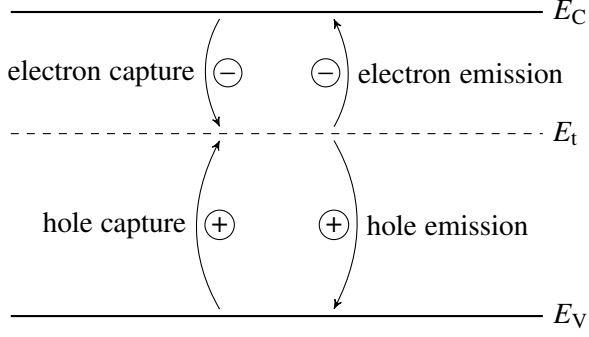


FIG. 21. Capture and emission of charge carriers described by R_{SRH} . E_t denotes the trap level energy.

in 4H-SiC. The time between two recombination events depends on several parameters that have to be clearly distinguished. Partially, the values are very sample depend and thus a wide range of values were found in the literature.

A. Theory

The decay of excess charge carriers towards the equilibrium value is described by the recombination rate R^{500} . It can be written as shown in Eq. (26)^{243,367,498,501,502} where R_{SRH} denotes the trap-assisted Shockley-Read-Hall, R_{bim} the bimolecular and R_{Auger} the Auger recombination rate²⁵⁵.

$$\begin{aligned} R &= R_{\text{SRH}} + R_{\text{bim}} + R_{\text{Auger}} \\ &= \frac{\Delta_N}{\tau_{\text{SRH}}} + \frac{\Delta_N}{\tau_{\text{bim}}} + \frac{\Delta_N}{\tau_{\text{Auger}}} = \frac{\Delta_N}{\tau_r} \end{aligned} \quad (26)$$

In the second line an alternative representation using lifetimes τ_x is shown¹⁵⁴, which denote the average time between two recombination events. The single contributions to the recombination will be shortly investigated in the sequel. For a more comprehensive description the interested reader is referred to the dedicated literature^{171,260,501,503}.

1. Shockley-Read-Hall Recombination

The term R_{SRH} denotes the successive capturing of a hole and an electron in a trap level with energy E_t inside the band gap^{501,504}, sometimes also called monomolecular recombination²⁵⁵. Due to the lower energy difference between trap and energy bands compared to the overall band

gap, the transition of a charge carrier to a trap is much more likely than a band-to-band transition. To describe this process in detail specific terms have been proposed in literature (see also Fig. 21)^{505–507}: *electron capture* denotes the transition of an electron from the conduction band into the trap while *electron emission* describes the reverse process. Similarly, during *hole capture* a hole rises from the valence band to the trap level, i.e., an electron drops from the trap into the valence band. *Hole emission* denotes the reverse case. Overall, during any capture process the electron loses energy, while during emission it gains some. In this context the electron/hole *capture cross sections* are used to quantify the possibility for an electron/hole capture.

The excessive energy released/consumed during these transitions is exchanged with lattice vibrations⁵⁰¹, whereat different phonon interactions are distinguished, e.g., multi- or cascade-phonon interaction^{503,508}. Among these the capture cross section and their respective temperature dependencies differ⁵⁰⁶.

The recombination rate R heavily depends on the material quality⁵⁰¹. Certain defects, e.g., impurities or damages in the lattice, are very effective "lifetime killers"⁵⁰⁹, meaning that they increase the recombination rate significantly. Lots of effort is undertaken to refine growth conditions to achieve cleaner samples and, thus, higher lifetimes^{243,510–528}. The recombination rate even varies across a single wafer. Typically it is smallest in the middle where the best growth conditions are available^{512,525,527,529–539}, but also in thick 4H-SiC layers variations were reported⁵⁴⁰. In fact, the recombination rate decreases at structural defect positions⁵⁴¹ but increases inversely linear with temperature^{542–544}.

For an accurate description of R_{SRH} detailed information, i.e., energy level, type (acceptor or donor) and cross section of the defects in the device are required. Many investigations in regard to these parameters have been published^{9,13–15,23,24,34,41,49–51,53,57,59–63,65,68–70,72,74–77,81,86,88,90,101,104,107,111,123,124}, making a comprehensive analysis within this review infeasible. Instead, we refer the interested reader to an analysis by Gaggl *et al.*⁶¹², who investigated defects in 4H-SiC. In regard to recombination, the most important ones are called $Z_{1/2}$ and $EH_{6/7}$ ^{604,610,613,614} and, presumably, denote different charge states of a carbon vacancy⁵⁵³.

The trap-assisted recombination can be split into the recombination in the bulk (R_{SRH}^b) and on the surface (R_{SRH}^s). Both occur simultaneously and are therefore often hard to separate^{501,615}. In the sequel we are going to investigate these in more detail.

a. Bulk Recombination Rate The Shockley-Read-Hall recombination of the bulk was mathematically first described by Shockley and Read⁵⁰⁵, Hall⁶¹⁶ as shown in Eq. (27)^{86,260,333,412,505,507,616}.

$$R_{\text{SRH}}^{\text{b}} = \frac{np - n_i^2}{\tau_p(n + n_1) + \tau_n(p + p_1)} \quad (27)$$

$$n_1 = \frac{1}{g_t} N_C \exp\left(-\frac{E_C - E_t}{k_B T}\right) \quad (28)$$

$$p_1 = g_t N_V \exp\left(-\frac{E_t - E_V}{k_B T}\right) \quad (29)$$

$$n_i = \sqrt{n_1 p_1} = \sqrt{N_C N_V} \exp\left(-\frac{E_C - E_V}{2k_B T}\right) = \sqrt{N_C N_V} \exp\left(-\frac{E_g}{2k_B T}\right) \quad (30)$$

$$\tau_{n,p} = (\sigma_{n,p} v_{\text{th}} N_t)^{-1} \quad (31)$$

Here, n_i denotes the intrinsic carrier concentration, $\tau_{n,p}$ the electron resp. hole lifetime, $\sigma_{n,p}$ the electron resp. hole cross section, N_t the trap concentration, $v_{\text{th}} = \sqrt{3k_B T / m_d^*}$ ^{203,507} the thermal velocity and g_t the trap degeneracy factor, which is often neglected as they are usually one³²⁵. E_t denotes the trap energy level, whereat Shockley and Read⁵⁰⁵ stated that this is actually an effective energy level that is derived from the actual one by considering the degeneracies of the empty (w_p) and full (w) trap, i.e., $E_t = E_t(\text{true}) + k_B T \ln(w_p/w)$. In TCAD tools either the lifetimes $\tau_{n,p}$ or the cross sections $\sigma_{n,p}$ can be provided as input, however, none of the investigated tools allows to specify the degeneracy factor at the moment.

It is also possible to define p_1 and n_1 as shown in Eq. (32)^{154,177,508}, i.e., by using the intrinsic carrier concentration and an effective Fermi level E_i , which must not be confused with the intrinsic Fermi level E_F used to calculate the actual carrier concentration $n = N_C \exp[(E_F - E_C)/k_B T]$ and $p = N_V \exp[(E_V - E_F)/k_B T]$. Care has to be taken in this case as the intrinsic carrier concentration n_i changes with the doping concentration due to band gap narrowing effects (see Section III).

$$\begin{aligned} n_1 &= \frac{1}{g_t} n_i \exp\left(-\frac{E_t - E_i}{k_B T}\right) \\ p_1 &= g_t n_i \exp\left(-\frac{E_i - E_t}{k_B T}\right) \end{aligned} \quad (32)$$

The SRH carrier lifetime is not constant but depends on the temperature and doping concentration $N_{A,D}$ ⁶¹⁷. The latter describes the increase of lattice defects, i.e., recombination centers, that accompany the doping process⁴¹² and has to be clearly distinguished from the excess carrier concentration Δ_N . The reduction of the lifetime can be described for each charge carrier separately using the empirical Scharfetter relation^{86,145,292,412,508,618–622} shown in Eq. (33). A more detailed analysis on the change of the lifetime for various relations of donor and acceptor concentrations

was recently provided by Shao *et al.*⁶²³. We want to highlight that dopants (see Section VI) themselves are a special form of defects, i.e., recombination centers, whose impact on the recombination can be described also with Eq. (27)²⁴⁷.

$$\tau = \frac{\tau_{\max}}{1 + \left(\frac{N_A + N_D}{N_{\text{ref}}}\right)^{\gamma}} \quad (33)$$

It is also common practice to determine the reduced lifetime in a more simplistic fashion from the defect concentration, e.g., $\tau(\mu\text{s}) = 1.5 \times 10^{13}/N_{\text{VC}}$ ^{613,624} and $\tau(\mu\text{s}) = 1.8 \times 10^{13}/N_{\text{VC}}$ ⁴⁸⁷ for carbon vacancies, and $\tau(\mu\text{s}) = 1.6 \times 10^{13}/N_{Z_{1/2}}$ ⁵⁹ and $\tau(\mu\text{s}) = 2 \times 10^{13}/N_{Z_{1/2}}$ ⁵¹⁸ for the $Z_{1/2}$ defect, instead of using Eq. (31)⁶²⁵.

At high temperatures the energetic charge carrier has to approach the center of the defect more closely to be captured⁶²¹. This implies that the lifetime increases with increasing temperature^{521,524,537,626}, which was extensively analyzed by Udal and Velmre⁶²⁷. The cross section changes in the order of T^{-x} ⁶²⁸, which leads, in conjunction with the change of the thermal velocity according to \sqrt{T} , to a power law description⁶²⁴. In TCAD tools the model shown in Eq. (34)^{629–631} is used, whereat τ_{T_0} denotes the lifetime at some reference temperature T_0 .

$$\tau_{\max} = \tau_{T_0} \left(\frac{T}{T_0} \right)^{\alpha} \quad (34)$$

Because the lifetime approaches zero for $T \rightarrow 0$ in this approximation a slightly modified version²⁴⁷ shown in Eq. (35) was proposed. By comparison we find $\tau_0 = \tau_{T_0}/2$ that is achieved for $T = 0\text{ K}$.

$$\tau_{\max} = \tau_0 \left(1 + \left(\frac{T}{T_0} \right)^{\alpha} \right) \quad (35)$$

We also found an exponential description using an activation energy E_{act} shown in Eq. (36)⁶²⁷, where τ_{∞} denotes the lifetime for $T \rightarrow \infty$.

$$\tau_{\max} = \tau_{\infty} \exp \left(\frac{-E_{\text{act}}}{k_B T} \right) \quad (36)$$

Since the meaning of τ_{∞} is hard to grasp, it can be replaced by $\tau_{T_0} \exp(E_{\text{act}}/k_B T_0)$ ^{59,632}, with τ_{T_0} the lifetime at $T = T_0$. For $E_{\text{act}} = 0.105\text{ eV}$ and $T_0 = 300\text{ K}$ we get $\exp(E_{\text{act}}/k_B T_0) = 57.9$ ^{59,632}. A very similar approach shown in Eq. (37)⁴⁹⁷ approaches a value of $51\tau_0$ for $T \rightarrow \infty$.

$$\tau_{\max} = \tau_0 \left(1 + \frac{100}{1 + \exp(E_{\text{act}}/k_B T)} \right) \quad (37)$$

The models in Eq. (36) and Eq. (37) have the disadvantage that the lifetime stalls for high temperatures. Consequently these are only suitable for moderate temperatures between 300–500 K⁶²⁷, which circumvented by the model shown in Eq. (38)^{82,318}.

$$\tau_{\max} = \tau_{T_0} \exp^{C\left(\frac{T}{T_0} - 1\right)} \quad (38)$$

A recent investigation by Lechner⁸² identified an initial increase in the lifetime followed by a decrease at high temperatures. Based on the research by Schenk⁶³¹ the fitting shown in Eq. (39)⁸² was proposed.

$$\tau_{\max} = \tau_{T_0} \left(\frac{T}{T_0} \right)^{T_{\text{coeff}}} \exp \left[-\alpha_{\tau} \left(\frac{T}{T_0} - 1 \right)^{\beta_{\tau}} \right] \quad (39)$$

Be aware that in state-of-the-art simulation tools only Eq. (34) and Eq. (38) are included.

b. Surface Recombination Rate Surface recombination includes mechanisms that occur on surfaces or interfaces due to imperfections or impurities at the transition between two materials. It includes many different surface types and thus also effects, such as semiconductor-oxide, semiconductor-semiconductor or oxides across the latter. Naturally, these can be heavily influenced by the chosen materials and growth conditions. The share of surfaces recombination on the overall recombination rate decreases with the thickness of the samples, because the ratio of surface to bulk volume decreases⁶²⁵.

In general, the surface recombination is written as the boundary condition of the diffusion term^{633–636} as shown in Eq. (40). A fantastic review on the causes, characterization methods and possible countermeasures of surface recombination is presented by Mao *et al.*⁴⁹⁹ and a theoretical analysis by Gulbinas *et al.*⁶³³.

$$D \frac{d\Delta_N(\mathbf{x}, t)}{d\mathbf{x}} = S_0 \Delta_N(\mathbf{x}, t) \quad (40)$$

Despite the tight correlation to the diffusion the surface recombination is described in TCAD tools by the SRH formalism, with the sole difference that instead of lifetimes the *surface recombination velocities* $s_{n,p}$ (see Eq. (41))^{260,325,412,501} that depend on the interface trap density N_{it} are used.

$$R_{\text{SRH}}^s = \frac{(n_s p_s - n_i^2)}{(n_s + n_i)/s_p + (p_s + p_i)/s_n} \quad (41)$$

$$s_n = \sigma_{ns} v_{\text{th}} N_{\text{it}} \quad (42)$$

$$s_p = \sigma_{ps} v_{\text{th}} N_{\text{it}} \quad (43)$$

As inputs, the TCAD tools expect s_n and s_p . Their dependency on the crystal faces^{535,615,634–636} is not included in state-of-the-art simulation tools yet. Some, however, provide the possibility to model a doping dependency but we found no reliable data for 4H-SiC in literature.

The surface recombination velocity again depends on the surface quality and the neighboring material. Therefore, there have been studies to improve the material quality^{495,615,633,637–643} by differing growth mechanisms or by irradiation⁵⁶⁸. Even a more elaborate model using trap regions inside the band gap was developed^{347,644,645}.

The temperature dependency of the surface recombination velocity was described by Klein *et al.*⁶²⁵, Kato *et al.*⁶³⁵ and can be modeled by Eq. (44)^{646,647}. $-E_{bb}$ denotes the band bending near the surface, which leads to accumulation of charge carriers of one type at the surface and effectively repelling the other type^{517,647}.

$$s_{\text{eff}}(T) = s_\infty \exp\left(\frac{-E_{bb}}{k_B T}\right) \quad (44)$$

2. Bimolecular Recombination

The term R_{bim} denotes the recombination rate due to the interaction of two particles, which can be described by Eq. (45)^{333,412} with B the bimolecular recombination coefficient^{154,498}.

$$R_{\text{bim}} = B(np - n_i^2) \quad (45)$$

We want to highlight that in literature this type of recombination is sometimes reduced to the radiative band-to-band recombination process emitting a photon³⁶⁷. Since 4H-SiC is an indirect semiconductor (see Section III) and this process, thus, always requires a phonon to absorb the momentum, radiative recombination is less important^{154,497,498,506,536}. In addition to the radiative band-to-band recombinations R_{bim} includes (i) recombinations between donor-acceptor pairs (DAP)^{243,648} (ii) the recombination of a charge carrier from the conduction/valence band and an unionized dopant (e.g. e-A)^{648,649} and (iii) the recombination of excitons (see Section III)³⁶⁷.

Trap-assisted Auger recombination (TAA)⁶⁵⁰ is also a bimolecular process but it is handled in differing fashions in the literature. TAA denotes the process when an electron (hole) interacts with a trap (capture resp. emission) and the additional/missing energy is exchanged with a particle of the same kind. Since two particles are involved many authors include this process in the bimolecular recombination coefficient^{31,255,367,651}, some in the Auger process^{61,652}, whereat others add it to SRH^{503,650,653}. The latter is also the only option to model TAA in existing TCAD tools, however,

for 4H-SiC no suitable values have been found. TAA is also used to explain the rather high values of the bimolecular recombination coefficient³⁶⁷. We want to highlight that in the literature a lot of additional trap-assisted Auger processes are mentioned, which have to be handled with care. For example, the excitonic Auger capture process described by Hangleiter⁵⁰⁴ is denoted as "markedly different" from TAA and should be regarded as an alternative explanation for multi-phonon/SRH recombination⁶⁵¹. Booker *et al.*⁵⁵³ describe a trap-Auger mechanism, where the energy of a hole captured in a neutral EH_{6,7} trap, which contains two electrons, is transferred to the other electron in the trap, ejecting it to the conduction band.

Little data about the temperature dependency of B is available. Tawara *et al.*⁵²⁴ present measurements for six different temperatures and state, that the value stays constant. If one would assume, however, the first data point as flawed, a clear decrease would be visible. Ščajev *et al.*²⁰⁵ state that the radiative recombination coefficient doubles in the range of 10–1000 K, which could also lead to an increase of B . For more definite statements, however, further investigations would be necessary.

3. Auger Recombination

At last, the term R_{Auger} , also called Auger recombination "(first discovered in atomic systems by Pierre Auger; soft g, please, the gentleman is French not German!)"⁵⁰³, denotes a three particle interaction where the excessive resp. missing energy and momentum is taken from/transferred to a third particle (either hole or electron). This process is an intrinsic property of the material⁵⁰¹ and dominates for high excessive charge carrier densities. It is described by Eq. (46)^{86,333,412,654} where C_n denotes the energy transfer to an electron and C_p the transfer to a hole²⁵⁵.

$$R_{\text{Auger}} = (C_n n + C_p p)(np - n_i^2) \quad (46)$$

The Auger recombination coefficients are also temperature dependent^{285,524}. Galeckas *et al.*²⁵⁵ describes this effect by Eq. (47).

$$C_n + C_p = \gamma_{30} \exp\left(-\frac{\alpha(T - 300\text{K})}{k_B T}\right) \quad (47)$$

Ščajev and Jarašiūnas⁴⁹⁷ received quite different results, as they argue that Galeckas *et al.*²⁵⁵ did not consider the in-depth profile. Instead the authors propose the model in Eq. (48), with

$B_{CE}(T) \propto T^{-1.5}$ the Coulomb enhancement coefficient and a_{SC} the screening parameter.

$$C(T, \Delta_N) = \left(C_0 + \frac{B_{CE}(T)}{\Delta_N} \right) / \left(1 + \frac{\Delta_N}{a_{SC} \times T} \right)^2 \quad (48)$$

Ščajev *et al.*³⁶⁷ mentioned a dependency of C with $\Delta_N^{-0.3}$ due to the screening of the Coulomb enhancement coefficient and Tanaka, Nagaya, and Kato⁶⁵² derived a dependency of $\Delta_N^{-0.68}$. The differences can be explained due to a deviating fitting.

Also the model used to describe the temperature induced changes of the Auger recombination coefficients in Silicon (shown in Eq. (49)) is used^{320,469}.

$$C_{n,p} = \left(A_{n,p} + B_{n,p} \left(\frac{T}{T_0} \right) + D_{n,p} \left(\frac{T}{T_0} \right)^2 \right) \left[1 + H_{n,p} \exp \left(-\frac{n,p}{N_{0n,p}} \right) \right] \quad (49)$$

4. Analysis

In the sequel we want to analyze the presented equations and extract further useful information. Some reader might have already noticed that all recombination rates contain the multiplicative factor shown in Eq. (50) with n_0, p_0 the intrinsic- and Δ_n, Δ_p the excessive carrier concentrations for electrons resp. holes.

$$(np - n_i^2) = (n_0 + \Delta_n)(p_0 + \Delta_p) - n_0 p_0 = n_0 \Delta_p + p_0 \Delta_n + \Delta_n \Delta_p \quad (50)$$

For a device without traps, i.e., $\Delta_p = \Delta_n = \Delta$, and for low-level (ll, $\Delta \ll n_0, p_0$) resp. high-level (hl, $\Delta \gg n_0, p_0$) injections the models can be significantly simplified^{171,260,333,501,651}, which is also important to correctly interpret the measurements results⁵⁰¹. After a short calculation we get, due to $R = \Delta_N / \tau_r$ (see Eq. (26)), for low-level injections the results shown in Eq. (51) and high-level in Eq. (52).

$$\tau_{SRH}^{ll} = \frac{\tau_p(n_0 + n_1) + \tau_n(p_0 + p_1)}{n_0 + p_0} \quad (51a)$$

$$\tau_{bim}^{ll} = \frac{1}{B(n_0 + p_0)} \quad (51b)$$

$$\tau_{Auger}^{ll} = \frac{1}{(C_n n_0 + C_p p_0)(n_0 + p_0)} \quad (51c)$$

$$\tau_{SRH}^{hl} = \tau_p + \tau_n \quad (52a)$$

$$\tau_{bim}^{hl} = \frac{1}{B\Delta} \quad (52b)$$

$$\tau_{Auger}^{hl} = \frac{1}{(C_n + C_p)\Delta^2} \quad (52c)$$

The results show that for SRH and Auger at high-injection levels always the sum of electron and hole parameters is achieved, whereat $\tau_p + \tau_n$ in Eq. (52) is also denoted as ambipolar lifetime^{59,400}. Separate measurements are only possible at low-injection level and with doped semiconductors, i.e., either $n_0 \gg p_0, p_1, n_1$ or $p_0 \gg n_0, n_1, p_1$. In that case one of the summands gets significantly smaller and can be ignored.

For doped semiconductors we can rewrite the high-level injection results from Eq. (52) as shown in Eq. (53)^{154,255,333,367,498,501–503,563,651}, which highlights that the introduced recombination terms actually represent a polynomial approximation of the recombination rate up to degree three in respect to the excess carrier concentration.

$$\begin{aligned} R = \Delta\tau^{-1} &= \Delta(\tau_{\text{SRH}}^{-1} + \tau_{\text{bim}}^{-1} + \tau_{\text{Auger}}^{-1}) \\ &= A\Delta + B\Delta^2 + C\Delta^3 \end{aligned} \quad (53)$$

Note that for no excess charge carriers, i.e., $\Delta = 0$, also $R = 0$. For relatively low excess charge carrier densities the SRH term dominates while for high densities the Auger process is most important.

All these simplifications are only valid for $\Delta \geq 0$. If $(np - n_i^2) < 0$ the recombination rate becomes negative, meaning that according to Eq. (25) charge carriers are generated. The corresponding rate of change can be described by using the so-called generation lifetime τ_g ^{260,333,500,614,655}.

However, a simple inversion is only meaningful for the SRH and Auger descriptions, because for bimolecular generation incoming photons are mandatory⁵⁰⁰. We want to highlight that often impact ionization (see Section IV) is stated as the inverse of Auger recombination^{171,508,656}. However, Selberherr⁴¹² states that there is a difference, namely the source of the energy. While impact ionization requires high current densities the inverse process of the Auger recombination only requires high charge carrier concentrations with negligible current flow. Due to these facts the recombination rates in TCAD tools, specifically bimolecular and Auger, often get deactivated when they drop below zero. For the Auger process some simulation tools allow to explicitly enable generation while the optical generation of charge carriers (inverse of bimolecular recombination) is implemented separately in the tools.

B. Results & Discussion

In the sequel the results of our analyses are presented. We did not include values when solely the effective lifetime was proposed^{366,534,655} or if it was not possible to clearly distinguish τ_n and

τ_p ^{367,657,658}. We also do not show values for different faces inside the crystal^{523,635}.

1. SRH Lifetime

The recombination lifetime can be measured either optically or electrically. Commonly used optical techniques include photoluminescence decay (PLD)^{537,575,617}, (transient) (time-resolved) free carrier absorption ((T)(TR-)FCA)^{205,255,367,497,502,511,536,651,659,660}, electron beam induced current (EBIC)⁵¹⁰, time-resolved photoinduced absorption (TRPA)²⁵⁵, time-resolved photoluminescence (TRPL)^{499,512,519,522–524,536,539,604,610,625,661}, time-resolved transient absorption (RTA), transient absorption spectroscopy (TAS)⁴⁹⁸, four wave mixing (FWM)²⁵², low-temperature photoluminescence (LTPL)^{617,622}, capacitance transient (C-t)⁶³⁸, differential transmittivity (DT)⁶²² and (microwave) photoconductance decay ((μ)-PCD)^{379,487,495,496,499,513–518,520,521,527–529,531,536,563,615,635,642,657,666}. For electrical measurements possible techniques are reverse recovery (RR)^{490,627,665,666}, thyristor turned off gate current (TTOGC)⁵⁴², short-circuit current/open-circuit voltage decay (SCCVD/OCVD)^{61,154,543,624,667–670}, diode current density (DCD)^{485,671,672}, bipolar transistor emitter current (BTEC)⁶⁷³ and diode forward voltage degradation (DFVD)⁶⁷⁴. Also utilized is fitting to measurement results in literature (FT)^{143,238,291} or simulations (SIM)⁵⁴⁴.

The achieved lifetime values depend on the utilized method⁶¹. Overall it has to be assured that the same quantity is measured, and that injection level and temperature are taken into account⁶¹. For example, Kato, Mori, and Ichimura⁶⁷⁵ claim that μ -PCD tends to overestimate the carrier lifetimes in high injection conditions and, similarly, Tawara *et al.*⁶⁰⁴ experienced that μ -PCD achieves longer lifetimes than the ones by TRPL. Deviations might also result from improper measurement setups, because, e.g., OCVD is limited to low and high injection regions only¹⁵⁴. For more detailed information, e.g., which carrier lifetime is extracted from the decay time for high and low injection by each measurement technique, the interested reader is referred to the dedicated literature^{59,536}.

A wide range of values for τ_n (see Table XI) and τ_p (see Table XII) are available in literature, whereat much more results for holes are available. In early days, Bakowski, Gustafsson, and Lindefelt⁶⁹ still had to use Silicon values due to a lack of data but since then many investigations have been conducted. Despite the wide range of values, the relation $\tau_n = 5\tau_p$, which was originally used for Si, is still utilized^{146,163,182,292,324,338,377,476,676,677}. Recently, $\tau_n = \tau_p$ was observed as well^{140,144,315,318,678–680}.

TABLE XI. Electron lifetime results. Column *inj.* denotes the carrier injection level, i.e., low (ll) resp. high (hl), and column *excess* the exact amount. A y in column *impr.* highlights that the shown value is the highest lifetime achieved in an optimization process.

ref.	τ_n	dop	conc.	T	inj.	excess	impr.	method
	[s]		[1/cm ³]	[K]		[1/cm ³]		
[Agar01] ⁵⁴²	6×10^{-7}	p	7×10^{14}	293	hl	-	-	TTOGC
[Ivan06a] ⁵⁴⁴	6.6×10^{-8}	p	2×10^{17}	300	-	-	-	SIM
[Alba10] ¹⁵⁴	8×10^{-9}	-	2.04×10^{17}	300	-	-	-	OCVD
[Haya11] ⁴⁹⁵	1.3×10^{-6}	Al	9×10^{14}	-	ll	1.5×10^{14}	y	uPCD
[Haya11a] ⁴⁹⁶	1.6×10^{-6}	p	9×10^{14}	300–525	ll	1.5×10^{14}	y	uPCD
[Haya12] ⁵¹³	1.7×10^{-6}	p	5.6×10^{14}	-	ll	1×10^{15}	y	uPCD
[Okud13a] ⁵²⁰	3.1×10^{-7}	Al	1×10^{18}	300	-	9.1×10^{15}	-	uPCD
[Dibe14] ⁶⁷¹	1×10^{-9}	-	-	-	hl	-	-	DCD
[Okud14] ⁵²¹	1×10^{-5}	Al	2×10^{14}	300	-	3.6×10^{16}	y	uPCD
[Liau15] ⁶²²	2×10^{-8}	Al	1×10^{17}	300	hl	-	-	DT
[Okud16] ⁶⁶³	1.2×10^{-5}	Al	1×10^{15}	300	-	3.6×10^{14}	y	uPCD
[Hase17] ⁴⁸⁵	4×10^{-7}	p	8×10^{14}	-	-	-	-	DCD
[Kato20] ⁶³⁵	1.2×10^{-6}	Al	6×10^{14}	300	ll	-	y	uPCD
[Koya20] ⁶⁷⁴	1.3×10^{-7}	p	1×10^{19}	-	-	-	-	DFVD
[Maxi23] ^{238 a}	6×10^{-6}	-	-	-	-	-	-	FT
[Zhan23a] ⁵²⁷	3.14×10^{-6}	Al	2×10^{14}	300	-	-	y	uPCD

^a value fitted to measurements by Kimoto *et al.*⁴⁸⁷

TABLE XII: Hole lifetime results. Column *inj.* denotes the carrier injection level, i.e., low (ll) resp. high (hl), and column *excess* the exact amount. A y in column *impr.* highlights that the shown value is the highest lifetime achieved in an optimization process.

ref.	τ_p	dop	conc.	T	inj.	excess	impr.	method
	[s]		[1/cm ³]	[K]		[1/cm ³]		
[Kord96] ⁵³⁷	2.1×10^{-6}	n	-	300	-	-	-	PLD
[Gale97] ²⁵⁵	2.6×10^{-7}	N	5×10^{15}	-	hl	-	-	TRPA
[Neud98] ⁴⁹⁰	7×10^{-7}	N	$(2\text{--}4) \times 10^{16}$	-	-	-	-	RR
[Gale99a] ⁵³³	5×10^{-7}	N	<1e16	-	-	-	-	FCA
[Ivan99] ⁵⁴³	6×10^{-7}	n	6×10^{14}	293	hl	-	-	OCVD
	3.8×10^{-6}	n	6×10^{14}	550	hl	-	-	OCVD
[Kimo99] ⁶⁶⁵	3.3×10^{-7}	N	5×10^{14}	-	-	-	-	RR

[Udal00] ⁶⁶⁶	5.2×10^{-8}	n	$(0.9\text{--}2.6) \times 10^{15}$	-	-	-	-	RR
[Cheo03] ⁶³⁸	1×10^{-6}	N	$(1\text{--}1.8) \times 10^{16}$	300	-	-	-	Ct
[Dome03] ⁶⁷³	3.5×10^{-9}	n	8.6×10^{15}	-	hl	-	-	BTEC
[Zhan03] ⁶¹⁰	3×10^{-7}	n	$(1\text{--}200) \times 10^{14}$	-	-	-	-	TRPL
[Levi04] ⁶⁶⁹	1.55×10^{-6}	n	3×10^{14}	293	hl	-	-	OCVD
[Tawa04] ⁶⁰⁴	$(0.26\text{--}6.8) \times 10^{-6}$	n	$(1.8\text{--}34) \times 10^{14}$	300\text{--}500	-	$(1.1\text{--}4.2) \times 10^{15}$	-	TRPL
[Resh05] ⁶¹	1×10^{-6}	n	7×10^{15}	-	-	-	-	OCVD
[Huh06] ⁵⁷⁵	5×10^{-7}	n	1×10^{14}	-	ll	1×10^{13}	-	PLD
[Ivan06b] ⁶⁶⁸	3.7×10^{-6}	n	2×10^{14}	300	hl	-	-	OCVD
[Jenn06] ⁵¹⁰	1.55×10^{-5}	N	5×10^{15}	-	-	-	-	EBIC
[Neim06] ²⁵²	1.2×10^{-8}	N	1×10^{16}	-	-	-	-	FWM
[Dann07] ⁵⁶³	2.5×10^{-6}	N	1.5×10^{15}	300	hl	$(2\text{--}20) \times 10^{16}$	y	uPCD
[Stor07] ⁵²²	2.18×10^{-7}	N	5×10^{15}	300	-	-	y	TRPL
[Udal07] ⁶²⁷	4.4×10^{-9}	n	7×10^{15}	297	-	-	-	RR
[Kimo08] ⁵¹⁷	8.6×10^{-6}	n	$(1\text{--}2) \times 10^{15}$	-	ll	5×10^{12}	-	uPCD
[Stor08] ⁵²³	9.9×10^{-7}	n	1×10^{14}	300	-	-	y	TRPL
[Hiyo09] ⁵²⁸	1.62×10^{-6}	N	$(1\text{--}5) \times 10^{15}$	-	hl	$(2\text{--}20) \times 10^{16}$	y	uPCD
[Resh09] ⁶⁶⁷	2.13×10^{-6}	n	$(1\text{--}1.2) \times 10^{15}$	-	hl	-	-	OCVD
[Alba10] ¹⁵⁴	1.5×10^{-11}	-	2.21×10^{17}	300	-	-	-	OCVD
[Kimo10] ⁵¹⁸	9.5×10^{-6}	n	$(0.9\text{--}1) \times 10^{15}$	-	hl	$(5\text{--}50) \times 10^{15}$	y	uPCD
[Kimo10a] ⁶⁴²	1.31×10^{-5}	N	7×10^{14}	-	hl	$(5\text{--}50) \times 10^{15}$	y	uPCD
[Klei10] ⁶²⁵	>100e-6	N	<1e16	222	ll	2×10^{14}	-	TRPL
[Miya10] ⁶⁶²	1.85×10^{-5}	N	7×10^{13}	-	ll	3×10^{12}	-	uPCD
[Haya11a] ⁴⁹⁶	4.6×10^{-6}	n	1.2×10^{15}	300\text{--}525	ll	1.5×10^{14}	y	uPCD
[Donn12] ^{291 681}	2.4×10^{-7}	N	1×10^{16}	-	-	-	-	FT
[Ichi12] ⁵¹⁴	3.32×10^{-5}	N	$(3\text{--}8) \times 10^{14}$	-	-	$(1\text{--}10) \times 10^{15}$	y	uPCD
[Kawa12] ⁵¹⁶	6.5×10^{-6}	n	1×10^{16}	300	-	1×10^{16}	y	uPCD
[Lilj13] ⁵¹²	1.6×10^{-6}	N	3×10^{15}	300	ll	-	y	TRPL
[Miya13] ⁵¹⁹	1.3×10^{-5}	N	$(2\text{--}3) \times 10^{14}$	300	-	-	y	TRPL
[Scaj13] ⁴⁹⁷	5.5×10^{-7}	n	4×10^{14}	-	ll	-	-	FCA
[Dibe14] ⁶⁷¹	1×10^{-8}	-	-	-	hl	-	-	DCD
[Usma14] ^{143 682}	1.3×10^{-6}	n	2×10^{14}	-	-	-	-	FT
[Chow15] ³⁷⁹	2.5×10^{-6}	n	2.5×10^{14}	300	hl	-	-	uPCD
[Kaji15] ⁵¹⁵	2.16×10^{-5}	N	2×10^{14}	-	-	1×10^{14}	y	uPCD
[Suva15] ⁶⁵⁹	3.5×10^{-7}	N	8×10^{15}	-	hl	6×10^{17}	-	FCA
[Puzz16] ⁶⁷²	1×10^{-6}	n	3×10^{15}	400	-	-	-	DCD
[Sait16] ⁶⁶⁴	2.6×10^{-5}	n	1×10^{14}	300	-	1.8×10^{17}	-	uPCD
[Tawa16] ⁵²⁴	3×10^{-7}	N	7.7×10^{17}	300	ll	-	-	TRPL
[Tsuc16] ⁶⁶¹	2.6×10^{-6}	n	1.4×10^{14}	-	-	-	-	TRPL
[Ayed17] ⁵⁰⁹	2×10^{-5}	N	1×10^{15}	-	-	-	y	-
[Lilj17] ⁵¹⁷	3.5×10^{-6}	N	1.3×10^{15}	300	ll	-	-	PLD
[Fang18] ⁴⁹⁸	$(11 \pm 3) \times 10^{-9}$	N	9.1×10^{18}	300	-	-	-	TAS
[Kimo18] ⁴⁸⁷	0.00011	n	1×10^{14}	-	-	$(1\text{--}10) \times 10^{14}$	y	uPCD
[Cui19] ⁵²⁹	1.05×10^{-6}	N	2×10^{13}	300	-	4×10^{16}	-	uPCD
[Mura19] ⁵³⁹	9.9×10^{-6}	N	1×10^{15}	293	ll	-	-	TRPL
[Kato20] ⁶³⁵	7×10^{-7}	N	$(1\text{--}10) \times 10^{15}$	300	ll	-	y	uPCD

[Naga20] ⁵⁰²	1×10^{-5}	N	1×10^{18}	293	hl	1.5×10^{18}	-	TR-FCA
[Sapi20] ⁶²⁴	1.9×10^{-5}	n	1×10^{16}	300	hl	-	-	OCVD
[Erle21] ⁵³¹	5×10^{-6}	N	$(5-10) \times 10^{14}$	-	ll	-	-	uPCD
[Mura21] ⁶⁴⁸	1.4×10^{-7}	N	2×10^{17}	293	ll	7×10^{14}	-	TRPL
[Maxi23] ^{238 683}	2×10^{-6}	-	-	-	-	-	-	FT
[Kato24] ⁶¹⁵	4.5×10^{-6}	n	1×10^{15}	300	-	$(5-50) \times 10^{15}$	-	uPCD
[Sozz24] ⁶⁷⁰	6.09×10^{-6}	n	1.5×10^{14}	298	hl	4×10^{17}	-	OCVD

This overview is already a simplification, as many publications present values for multiple operating conditions, i.e., temperature, doping concentration or excess carrier concentration. Only the best achieved values are shown here. For example Hayashi *et al.*⁴⁹⁶ provides measurements over injection level for two temperatures (300 K and 525 K). Grivickas *et al.*⁵¹¹ show measurements with different intensities but no actual values. The lifetime depends on all the mentioned parameters simultaneously, which makes a proper presentation very challenging. Therefore, we highlight each single dependency separately. For example, we depict the measured lifetimes with the respective doping densities if specified in the paper (see Fig. 22). A decreasing lifetime with increasing doping density can be observed, but no actual difference between electron and hole lifetime. However, all these values were most probably measured with differing excess carrier concentrations and at deviating temperatures.

Note that we explicitly show the injection level during the measurements, because for a high level only the sum $\tau_n + \tau_p$ is achieved^{575,659} (cp. Eq. (52)). Consequently, it can be expected that the lifetime increases when going from low to high injection level, until it eventually starts to decrease when the bimolecular or Auger recombination become dominant. This effect was explicitly shown in literature^{495,496,513,615}. Despite that, Kimoto *et al.*⁶⁸⁴ stated in 2016 that the injection-level dependence of SRH lifetimes is not known in SiC, calling for further research. In contrast, Ščajev and Jarašiūnas⁴⁹⁷ stated that the lifetime is almost injection level independent. Very different results were reported by Tawara *et al.*⁵²⁴, who saw a lifetime decrease, eventually approaching a constant value.

For thin samples the achieved recombination rate has diminishing resemblance to the bulk contribution R_{SRH}^b ⁵⁰¹, since the surface recombination R_{SRH}^s dominates. In any case it is always important to consider the impact of the surface during measurements⁵³⁶. Optimally the surface contribution is measured separately^{490,625,662,665}, which is, however, not always practical⁵³⁶. For sufficiently thick samples R_{SRH}^b can be determined directly, however, this demands extraordinarily

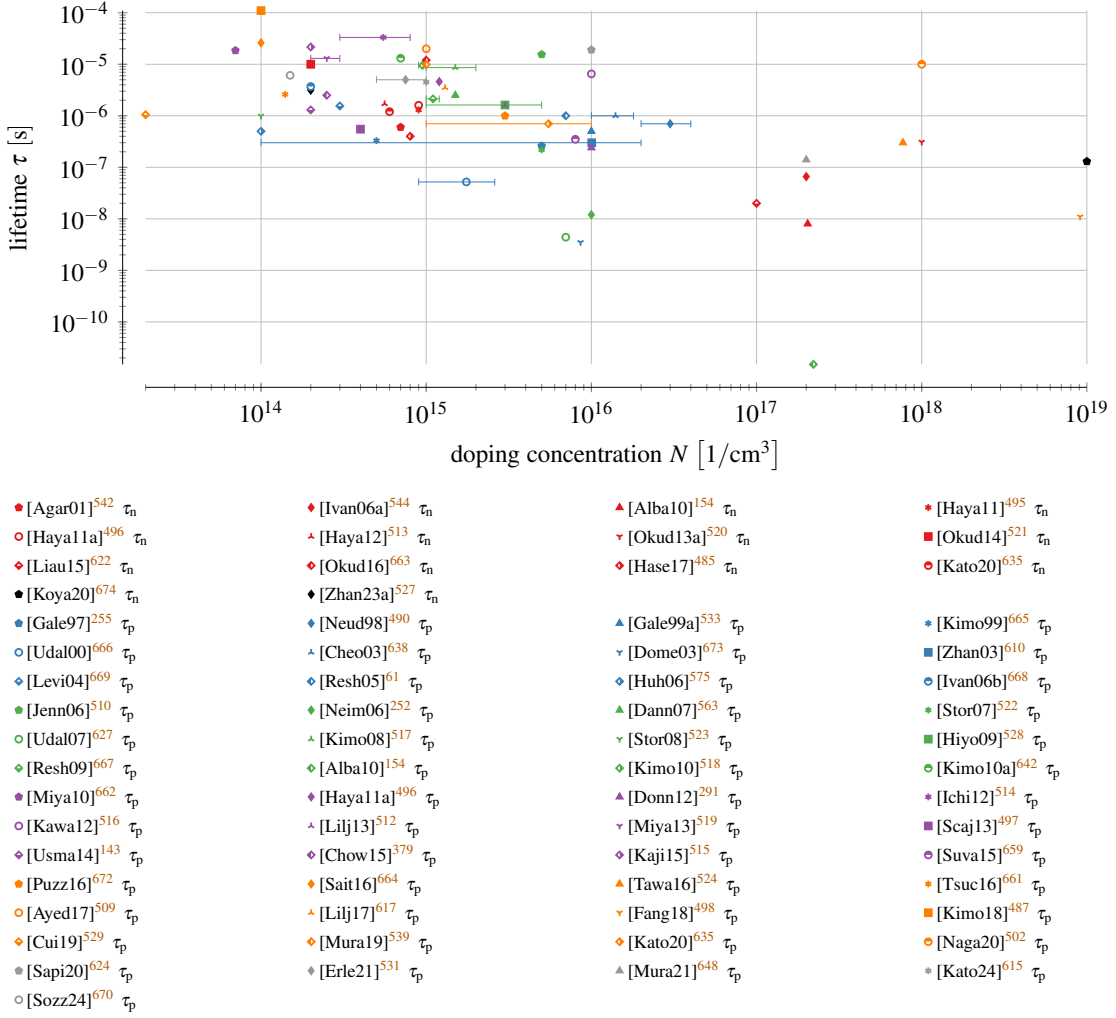


FIG. 22. Measurements of the minority charge carrier lifetime for the respective doping densities.

thick ones⁵⁰¹: Depending on the surface recombination velocity, thicknesses in the range of mm or even cm would be required²⁶⁰.

Finally, we also investigated the values that are referenced in literature (see Fig. 23). Overall, there are only very few references compared to the amount of fundamental investigations. This shows that the lifetime depends on many parameters and may differ considerably among samples. As mentioned before, very similar values for τ_n and τ_p are encountered.

2. Doping Dependency of SRH Lifetime

The decrease of the minority carrier lifetimes with doping concentration (cp. Fig. 22) is described by additional recombination centers (Scharfetter relation, Eq. (33)). We acquired multiple

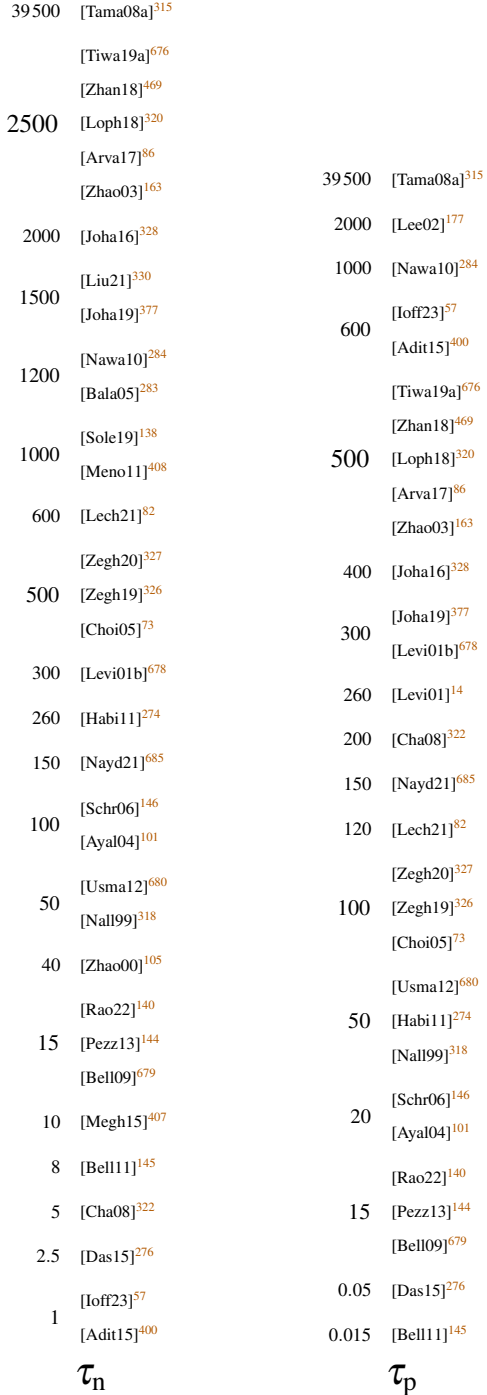


FIG. 23. Lifetime values referenced in literature.

parameter sets (see Table XIII) for the latter. In the 1990s no values for 4H-SiC values were available, so Ruff, Mitlehner, and Helbig²⁹² settled for a combination of Silicon based values gathered from various sources. Surprisingly, these parameters are still the most commonly ones used in literature (see Fig. 25). While some publications are well aware that Silicon data are used^{101,325,644}

TABLE XIII. Parameters for doping dependency according to the Scharfetter relation in Eq. (33).  are fittings to suitable measurements and  fittings to the excessive carrier concentrations.

ref.	electrons		holes	
	N_{ref} [1/cm ³]	γ [1]	N_{ref} [1/cm ³]	γ [1]
[Ruff94] ^{292 a}	3×10^{17}	0.3	3×10^{17}	0.3
[Nall99] ^{318 c}	1×10^{16}	1	1×10^{16}	1
[Levi01b] ⁶⁷⁸	7×10^{17}	1	-	-
[Choi05] ^{73 b}	5×10^{16}	1	5×10^{16}	1
[Donn12] ^{291 b f}	2×10^{18}	1.9	2×10^{18}	1.9
^g	4×10^{18}	1.4	4×10^{18}	1.4
[Liau15] ^{622 e}	5×10^{18}	1.2	-	-
[Lech21] ⁸²	7×10^{16}	1	7×10^{16}	1
[Maxi23] ^{238 d}	5×10^{15}	0.55	5×10^{15}	0.67

^a Silicon data from multiple sources combined

^b References Harris and Inspec ¹³ but no data found there. According to Albanese ¹⁵⁴ based on Silicon data.

^c fit to lifetime over excessive charge carrier densities ²⁵⁵

^d fit to measurements for changing doping concentration by Kimoto *et al.* ⁴⁸⁷

^e fit to own measurements for changing doping concentration

^f fit to lifetime over excessive charge carrier densities ⁶⁸⁶

^g fit to lifetime over excessive charge carrier densities ²⁵²

this information seems to was lost over the years.

The only fittings we could actually trace back to measurements of τ_{SRH} with varying doping concentration are the investigations by Liaugaudas *et al.* ⁶²², who did their own differential transmittivity measurements, and Maximenko ²³⁸, who fitted to the results of the μ -PCD measurements by Kimoto *et al.* ⁴⁸⁷. We also found dedicated measurements by Lilja *et al.* ⁶¹⁷ and Murata *et al.* ⁶⁴⁸, which, seemingly, were not yet used in any fitting. For other publications ^{73,82,678} we were simply unable to retrace the origin of the values, although often explicit references were provided.

There are often confusions between the doping and the excess charge carrier concentration. While both lead to a decrease in lifetime with increasing concentration the physical process causing that are fundamentally different. While more doping causes more recombination centers, more excess charge carrier lead to a higher contribution of bimolecular and Auger recombination. For

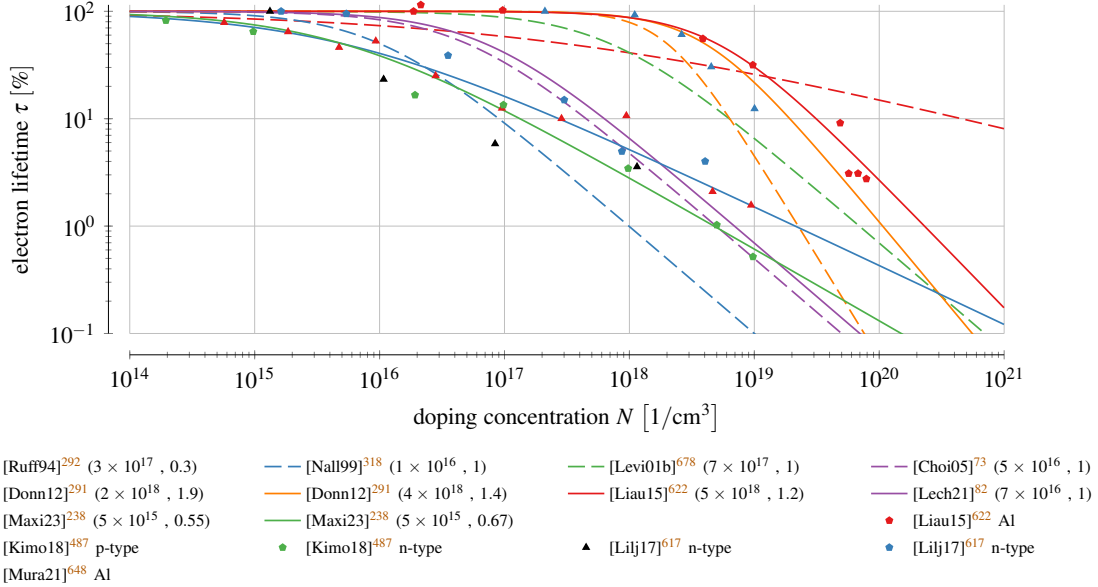


FIG. 24. Doping dependency according to the Scharfetter relation in Eq. (33). In brackets are the values for (N_{ref}, γ) . Only one graph is shown if electron and hole parameters are equal (see Table XIII). Solid non-opaque lines represent fitting to 4H-SiC measurement data.

example, Kimoto *et al.*⁴⁸⁷ adds bimolecular and Auger coefficients to a plot over the doping concentration. In addition, fittings of the Scharfetter relation versus an increasing excess charge carrier concentration were proposed^{291,318}. Although we believe that such a fitting is not reasonable we included the respective results in the table but highlighted them accordingly.

In a double logarithmic plot (see Fig. 24) the differences are well observable. There are differences in the onset of lifetime degradation, i.e., the value N_{ref} . For a specific reduction of the lifetime the respective doping can vary by up to three orders of magnitude. Also the rate of change deviates, whereat for the Silicon based model proposed by Ruff, Mitlehner, and Helbig²⁹² a significantly lower transition rate is observable. Interestingly also the models based on the measurements differ quite significantly. We also added some measurement result, which show significant variations and thus also lead to deviating fitting results.

In the literature the values by Ruff, Mitlehner, and Helbig²⁹² are still heavily utilized to describe the doping dependency (see Fig. 25), although these are not based on 4H. The dedicated fittings to 4H measurements have not been referenced so far.



FIG. 25. Reference chain for charge carrier recombination. ■ are fundamental investigations, ■ research not focused on 4H and ■ connections predicted from the used values.

3. Temperature Dependency of SRH Lifetime

There are various fantastic investigations on the changes of the lifetime with temperature^{615,635} some even distinguishing between surface and bulk lifetime⁶²⁵. Even various excess charge carriers in the range $(1\text{--}1000) \times 10^{16} \text{ 1/cm}^3$ were investigated⁶⁴⁹, whereat the behavior varies.

In the literature predominantly the power law descriptions of Eq. (34) and Eq. (35) are used (see Table XIV). The values for the exponent α thereby commonly vary between 1 and 2. Udal and Velmre⁶²⁷ stated a fitting in two regions, as the lifetime started to increase faster above 700 K.

TABLE XIV. temperature dependency parameters in literature. If only one value for $\alpha_{n,p}$ is stated no charge carrier specification was made in the publication.

ref.	α_n	α_p	T_0	E_{act}	C	conf.	equ.	method
	[1]	[1]	[K]	[eV]	[1]	[K]		
[Kord96] ^{537 a}	-	1.72	300	-	-	0–200	(34)	PLD
[Ivan99] ^{543 d}	-	-	-	0.11	-	300–500	(36)	OCVD
[Nall99] ^{318 b}	-	-	300	-	2.55	-	(38)	-
[Udal00] ⁶⁶⁶	-	2.2	300	-	-	200–450	(34)	RR
[Agar01] ^{542 d}	-	-	-	0.12	-	300–500	(36)	TTOGC
[Bala05] ²⁸³	5	-	300	-	-	-	(34)	-
[Levi05] ^{626 d}	-	-	-	0.08	-	300–500	(36)	-
[Ivan06a] ^{544 e}	-	-	-	0.105	-	300–500	(36)	SIM
[Udal07] ⁶²⁷	-	1.9	300	-	-	300–700	(34)	RR
	-	4.4	300	-	-	700–1000	(34)	RR
[Scaj13] ⁴⁹⁷	-	-	-	0.125	-	70–1000	(37)	FCA
[Dibe14] ⁶⁷¹	2.15	-	300	-	-	250–500	(34)	DCD
[Chow15] ^{379 c}	1.2	-	300	-	-	300–525	(34)	uPCD
[Rakh20] ²⁴⁷	-	8	450	-	-	100–700	(35)	-
	-	14	530	-	-	100–700	(35)	-
[Sapi20] ⁶²⁴	1.5	-	300	-	-	300–450	(34)	OCVD
[Tian20] ⁶⁷⁷	1.84	1.84	300	-	-	300–573	(34)	-
[Maxi23] ²³⁸	1.72	1.72	300	-	-	-	(34)	FT
[Sozz24] ⁶⁷⁰	1.7	-	298	-	-	300–450	(34)	OCVD

^a fitting provided in citing articles (see Fig. 25), Sapienza *et al.*⁶²⁴ fitted $\alpha = 1.9$

^b default value of many simulation tools, according to Lechner⁸² based on the research from Grasser *et al.*⁶⁹³

^c fitting done by Sapienza *et al.*⁶²⁴

^d fitting done by Udal and Velmre⁶²⁷

^e fitting done by Tamaki *et al.*⁶³²

Sapienza *et al.*⁶²⁴ achieved $\alpha = 1.5$ which is exactly the value expected for Coulomb-attractive charge recombination centers⁶²⁷.

More complex is the situation for the value $\alpha_{n,p} = 5^{143,283,284}$. Although we stated Balachandran, Chow, and Agarwal²⁸³ as the origin here we were actually not able to determine the origin

of this parameter. We suspect that it might have been the default value of a TCAD tool but we could not even confirm that. In the same sense we were not able to pinpoint the origin of the value $C = 2.55$ ³¹⁸ for Eq. (38). Although Lechner⁸² provided a reference⁶⁹³ we were not able to find anything in there either.

For the exponential based approaches the value of E_{act} is between 110–125 meV. Please note that for Eq. (39) a lot of parameters have been presented⁸². We calculated the average from the single sets and achieved the values shown in Eq. (54), where an initial increase followed by a decrease in the lifetime is visible.

$$T_{\text{coeff}} = 0.666, \quad \alpha_{\tau} = 0.06385, \quad \beta_{\tau} = 5.716 \quad (54)$$

A comparison of the single models (see Fig. 26) shows that for all the lifetime increases with increasing temperature. We also added some temperature measurements and scaled them such that the room temperature values are around $1\mu\text{s}$, which we fixed. Please be aware that we had to dismiss the values by Lophitis *et al.*³²⁰ as only the parameters but not the according equations were defined. We also do not show the results by Puzzanghera and Nipoti⁶⁷² as only minor deviations around the value at room temperature were achieved. Again we want to highlight that the plots have to be considered with a grain of salt as temperature changes depend on doping⁶⁴⁸. For high-level injection the sum of hole and electron lifetime is measured³⁷⁹, which, again, can have a differing temperature dependency. Sapienza *et al.*⁶²⁴ compares various sources in this respect^{87,537,627}.

The most prominent model in literature is the one proposed by Kordina *et al.*⁵³⁷ (see Fig. 25), which, was, however, only characterized up to 200 K.

4. Surface Recombination Velocity

The surface recombination velocity is, as the name indicates, not a bulk property but depends on many parameters such as crystal faces, i.e., Si-, C-, a- or m-face^{635,636}, and interface treatment. For these reasons we will only roughly cover this topic. Interesting analyses of the surface recombination velocity were published by Ščajev *et al.*³⁶⁷, Gulbinas *et al.*⁶³³, Mori, Kato, and Ichimura⁶³⁶.

In general, the surface recombination velocity has to be determined for each sample separately, due to the dependency on so many factors. It was pointed out that the injection level during

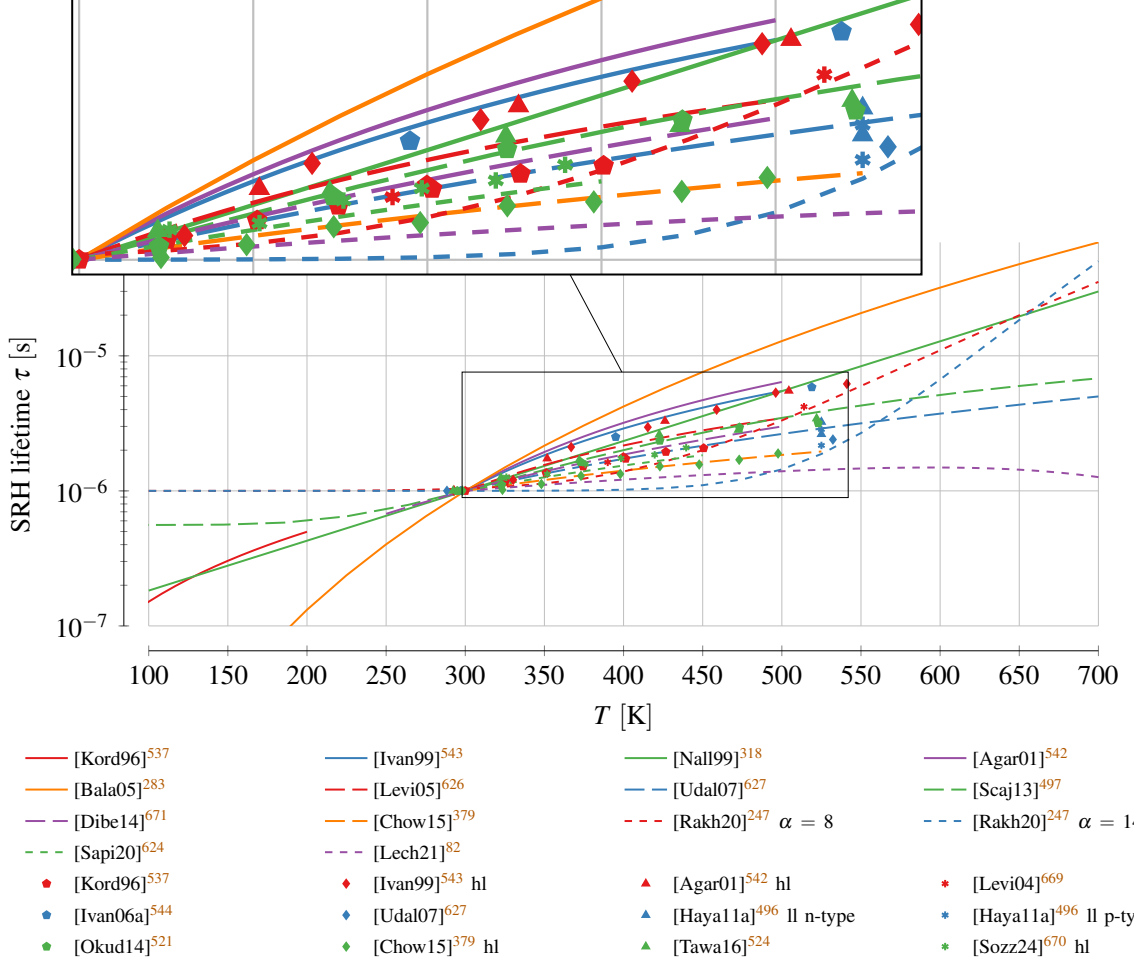


FIG. 26. Temperature Dependency of the SRH lifetime. Models are calibrated to hit 1 μ s at 300 K. Measurement results are scaled such that 1 μ s at (296 ± 4) K is achieved.

measurements has an impact^{260,367,615}, which was possibly explained by a band banding near the interface⁵¹⁷. Furthermore the surface recombination velocity is temperature dependent and increases with increasing temperature^{625,635}. Overall, suitable values in literature are mainly based on dedicated investigations (see Table XV) or are simply assumed, e.g., $s = 2.2 \times 10^5$ cm/s⁶⁴³, $s = 1 \times 10^3$ cm/s⁵¹⁴.

For the surface recombination velocity additional measurement methods to the earlier explained ones were used, for example colinear pump probe (CPP)⁶³³, non-equilibrium free-carrier density (NFCD)²⁸⁵, via the exponential prefactor in the current density (CD)^{639,695} or reverse recovery (RR)⁶⁶⁵. By changing the thickness of the devices the impact of the surfaces and their recombination velocities was extracted⁶³³ and sometimes even eliminated^{490,662}. An effective bulk lifetime of more than 1 μ s can, however, only directly measured within epitaxial layers thicker than

TABLE XV. Surface recombination velocity. A y in column *impr.* indicates that the velocities were achieved at the end of an optimization process.

ref.	<i>s</i> [cm/s]	<i>s_n</i> [cm/s]	<i>s_p</i> [cm/s]	type ^a	impr.	method
[Gale97] ²⁵⁵	-	-	$4 \times 10^4 / 1 \times 10^4$	S/I	-	FCA
[Neud98] ⁴⁹⁰	-	-	5×10^4	M	-	RR
[Gale99a] ⁵³³	-	-	$(5\text{--}8) \times 10^3$	S	y	FCA
[Kimo99] ⁶⁶⁵	-	-	5×10^4	M	-	CD
[Gale01] ⁵³⁴	$(5\text{--}500) \times 10^3$	-	-	S	y	TA
[Cheo03] ⁶³⁸	-	-	1–1000	S	y	Ct
[Huh06] ⁵⁷⁵	-	-	2.50×10^3	S	-	TRPL
[Ivan06a] ⁵⁴⁴	4200	-	-	M	-	CD
[Neim06] ²⁵²	-	-	$(4 \pm 1) \times 10^4$	S	-	FWM
[Griv07] ²⁸⁵	1×10^4	-	-	S	-	NFCD
[Klei08] ⁵³⁶	-	-	$(5\text{--}500) \times 10^3$	S	y	TFCA
[Klei10] ⁶²⁵	-	-	400–6940	S	-	TRPL
[Scaj10] ³⁶⁷	$(2\text{--}13) \times 10^3$	-	-	S	-	FCA
[Gulb11] ⁶³³	-	$(1.5\text{--}3) \times 10^4$	$(1\text{--}100) \times 10^4$	S	y	CPP
[Pour11] ⁶⁹⁴	-	1.07×10^3	$(1.07\text{--}57) \times 10^3$	S	y	FCA
[Kato12] ⁶³⁴	-	-	$(1\text{--}2) \times 10^3$	S	y	uPCD
[Mori14] ⁶³⁶	-	-	1500–7500	S	y	uPCD
[Suva15] ⁶⁵⁹	-	-	$(3.5\text{--}200) \times 10^4$	S/I	y	FCA
[Asad18] ⁶³⁹	$(6\text{--}120) \times 10^5$	-	-	M	y	CD
[Ichi18] ⁶⁴¹	-	300–6000	200–2500	S	y	uPCD
[Kato20] ⁶³⁵	-	400–1950	150–750	S	y	uPCD
[Xian21] ⁶⁹⁵	$((6 \pm 7)\text{--}58 \pm 5) \times 10^5$	-	-	M	y	CD
[Kato24] ⁶¹⁵	-	-	100–2500	S	y	uPCD

^a mesa structure (M), surface (S) or interface (I)

100 μm⁵⁹. Due to the numerous growth parameters⁶⁹⁴ a wide range of growth optimizations and surface treatments were proposed. Nevertheless, it seems that mechanically polishing surfaces, which leads to a significant roughness, delivers bad results (high velocities)⁵³⁶. The most recent values of < 200 cm/s indicate high surface qualities. The amount of publications in the recent years also shows that this is an active field of research.

Publications referencing other publications often combine multiple values to achieve reasonable values, e.g., $s = (1-100) \times 10^3 \text{ cm/s}$ ^{14,57}, $s = 2 \times 10^3 \text{ cm/s}$ ³⁷⁷, $s = 1 \times 10^4 \text{ cm/s}$ ⁶²², $s = 1 \times 10^3 \text{ cm/s}$ ^{502,652}, $s = 4 \times 10^4 \text{ cm/s}$ ⁴⁹⁷ and $s_n = s_p = 1 \times 10^5 \text{ cm/s}$ ⁶⁷³. Finally, we want to highlight that the values for 4H and 6H are fairly similar⁵³³.

5. Bimolecular Recombination

The bimolecular coefficient B was determined in several investigations (see Table XVI). The most influential is the one of Galeckas *et al.*²⁵⁵ (cp. Fig. 25), whereat Institute⁵⁷ states that the bimolecular factor is just an estimation. All the studies achieve a value of $(1.5 \pm 0.5) \times 10^{-12} \text{ cm}^3/\text{s}$. Exceptions were the investigation by Neimontas *et al.*²⁵², whose value is one order of magnitude bigger, and Murata *et al.*⁶⁴⁸, who achieved 3-4 times higher values. In some investigations^{497,502,635} deliberately only the radiative component with a value of $(1-3) \times 10^{-14} \text{ cm}^3/\text{s}$ ²⁰⁵ was used for the bimolecular parameter B . The rather high values of B compared to the radiative part is explained by the additionally included trap-assisted Auger recombination²⁵⁵ and electron-acceptor (e-A) recombination⁶⁴⁸.

6. Auger Recombination

The most fundamental research on Auger coefficients in 4H-SiC was conducted by Galeckas *et al.*²⁵⁵, who provided separate values for electrons (C_n) and holes (C_p). This is, so far, the only publications that did that. Following publications achieved, in general, similar combined coefficients (see Table XVII) and thus confirmed the results. Solely Grivickas *et al.*²⁸⁵ and Tawara *et al.*⁵²⁴ derived parameters that are one order of magnitude smaller. Interesting are also the results by Tanaka, Nagaya, and Kato⁶⁵², who identified a dependency of the Auger parameter on the excess carrier concentration Δ_N . In the investigations by Murata *et al.*⁶⁴⁸ Auger recombination turned out to be not important for an Aluminum doping concentration of $1 \times 10^{19}/\text{cm}^3$ but

TABLE XVI. Fundamental investigations of the bimolecular recombination parameter.

ref.	B [cm ³ /s]	T [K]	interval [1/cm ³]	method
[Gale97] ²⁵⁵	1.50×10^{-12}	300	$(1\text{--}1000) \times 10^{16}$	FCA
[Neim06] ²⁵²	$(3 \pm 1) \times 10^{-11}$	-	$(1\text{--}2000) \times 10^{16}$	FWM
[Scaj10] ³⁶⁷	$(1.2 \pm 0.2) \times 10^{-12}$	298	-	FCA
[Tawa16] ⁵²⁴	1.3×10^{-12}	300	$(3\text{--}70) \times 10^{17}$	TRPL
	0.94×10^{-12}	523	$(3\text{--}70) \times 10^{17}$	TRPL
[Mura21] ⁶⁴⁸	5.6×10^{-12}	293	$(1\text{--}100) \times 10^{17}$	TRPL
	4.5×10^{-12}	523	$(1\text{--}100) \times 10^{17}$	TRPL
[Tana23a] ⁶⁶⁰	$<2 \times 10^{-12}$	-	$(2\text{--}10) \times 10^{18}$	FCA

TABLE XVII. Auger recombination parameters.

ref.	C_n [cm ⁶ /s]	C_p [cm ⁶ /s]	T [K]	method	Δ_N [1/cm ³]
[Gale97] ²⁵⁵	$(5 \pm 1) \times 10^{-31}$	$(2 \pm 1) \times 10^{-31}$	300	FCA	-
[Griv07] ²⁸⁵	2×10^{-30}	-	75	FCA	-
[Scaj10] ³⁶⁷	$(7 \pm 4) \times 10^{-31}$		298	FCA	$(1\text{--}3) \times 10^{18}$
	$(0.8 \pm 0.2) \times 10^{-31}$		298	FCA	$(1\text{--}10) \times 10^{19}$
[Scaj13] ⁴⁹⁷	$(5 \pm 1) \times 10^{-31}$	-		FCA	-
[Tawa16] ⁵²⁴	1.6×10^{-30}	-	300	TRPL	-
	0.44×10^{-30}	-	523	TRPL	-
[Zhan18] ⁴⁶⁹	7.25×10^{-31}	1.21×10^{-31}	-	-	-
[Tana23] ^{652 a}	7.4×10^{-19}	$\Delta_N^{-0.68}$	-	FT	-
[Tana23a] ⁶⁶⁰	$<3 \times 10^{-31}$	-		FCA	-

^a fitting to measurements by Ščajev *et al.*³⁶⁷

considerable for a Nitrogen doping in mid $1 \times 10^{18}/\text{cm}^3$ range.

We want to highlight that there were also some values based on 6H⁶⁹¹ used for 4H^{82,101} and even some based on Silicon^{182,292} for 4H²⁷⁶. Zhao *et al.*¹⁰⁵ simply assumed $C_n = C_p = 1 \times 10^{-28} \text{ cm}^6/\text{s}$. For the results presented by Tawara *et al.*⁵²⁴ we concluded from the description of

TABLE XVIII. Parameters for Auger model shown in Eq. (49)

ref	type	A [cm ⁶ /s]	B [cm ⁶ /s]	D [cm ⁶ /s]	H	N ₀ [1/cm ³]	T ₀ [K]
. [Loph18] ³²⁰	electron	6.7×10^{-32}	2.45×10^{-31}	-2.2×10^{-32}	3.47	10^{18}	300
	hole	7.2×10^{-32}	4.5×10^{-33}	2.63×10^{-32}	8.26	10^{18}	300
[Zhan18] ⁴⁶⁹	electron	5×10^{-31}	2.45×10^{-31}	-2.2×10^{-32}	0	-	-
	hole	9.9×10^{-32}	4.5×10^{-33}	2.63×10^{-32}	0	-	-

samples and measurement (low injection and highly n-doped material) that C_n was measured and added it appropriately to the table.

For a comparison of the temperature dependency models in Eq. (47) and Eq. (48) we use the parameters shown in Eq. (55), Eq. (56) and Eq. (57).

$$\alpha = 0.45 \text{ meV/K} \quad (55)$$

$$B_{\text{CE}}(T) = 3.5 \times 10^{-9} T^{-3/2} \text{ cm}^3/\text{s} \quad (56)$$

$$a_{\text{SC}} = 7.8 \times 10^{16} \text{ K/cm}^3 \quad (57)$$

In a graphical representation (see Fig. 27) a contradiction among the models can be observed. Dedicated 4H-SiC models and measurements predict a decrease of C with increasing temperature, which confirms the prediction that Auger recombination is not significant for power devices operated at high temperatures Bellone *et al.*¹⁴⁵. In contrast, the models used for Silicon predict an increase of C .

Finally, Lophitis *et al.*³²⁰ present parameters for the model shown in Eq. (49) (see Table XVIII). We found these values also as default in some TCAD simulation suites, which, in general, correspond to Silicon. Thus, these values have to be handled with care.

For Auger recombination there is one main reference in literature, namely Galeckas *et al.*²⁵⁵ (see Fig. 25).

Finally, we combine all contributions to the lifetime into one plot, showing the lifetime over the excess carrier concentration (see Fig. 28). For the SRH lifetimes we added all measurements that clearly specified the excess carrier concentrations. In this log-log representation the bimolecular and Auger coefficients only cause a horizontal shift while the derivative (-1 for bimolecular, -2 for Auger) stays constant. Overall, it can be noted that the higher the value of τ_{SRH} the earlier and more pronounced the impact of the bimolecular recombination. A decrease due to Auger recombination

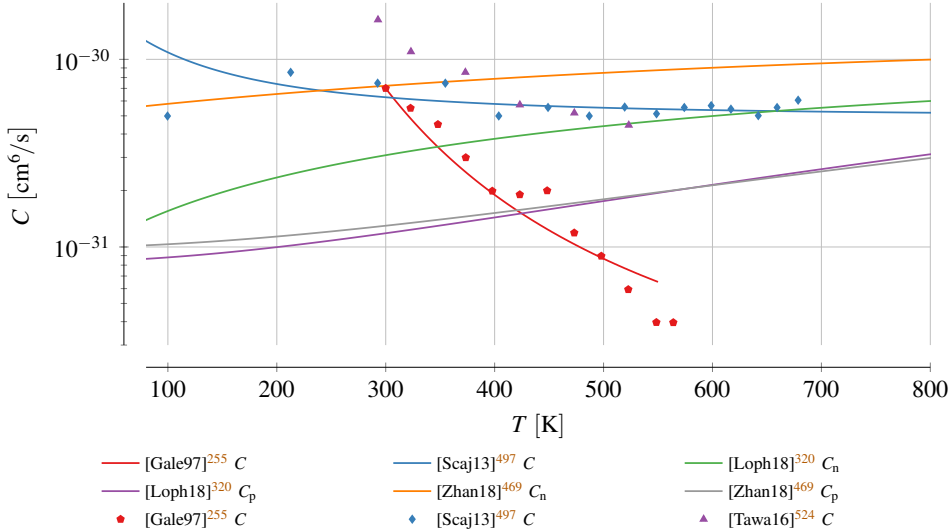


FIG. 27. Temperature dependency of the Auger recombination coefficients C_n and C_p for $\Delta_N = 2.5 \times 10^{18}/\text{cm}^3$

only gets significant for $\Delta_N > 10^{18}/\text{cm}^3$. Interestingly, there seem to be measurements that extract SRH values in regions where bimolecular resp. Auger recombination should be already very pronounced.

VI. INCOMPLETE IONIZATION

It is indispensable to add a doping to a semiconductor, i.e., to introduce impurity atoms, in order to create sophisticated electronic devices. These so-called dopants add energy levels near to the conduction (n-type doping) resp. valence band (p-type doping) such that free charge carrier can be injected at moderate temperatures. In this fashion the electrical characteristics of the material can be altered. Partial overviews on available doping elements and their respective activation energies in 4H-SiC are available^{13,14,23,53,72,74,75,120,123,162,249,259,332,333,360,397,552,562,607,696,697}. Uncommon elements were also investigated. Ab initio calculations by Miyata, Higashiguchi, and Hayafuji⁶⁹⁸ identified Arsenic⁶⁹⁹, Gallium⁷⁰⁰ or Antimony as, energy level wise, fitting. Group IV elements were investigated by Krieger *et al.*⁷⁰¹, Feng and Zhao²⁴⁹, Huang *et al.*⁵⁷⁴ focused on Tantalum and Chromium and Dalibor *et al.*⁵⁶¹, Dalibor and Schulz⁵⁶² on Vanadium. Additional factors such as the activation rates⁷⁰² or the impact of hydrogen⁵⁷³ might, however, prevent the deployment of these dopants.

Due to the wide bandgap of 4H-SiC the respective dopant activation energies are large such

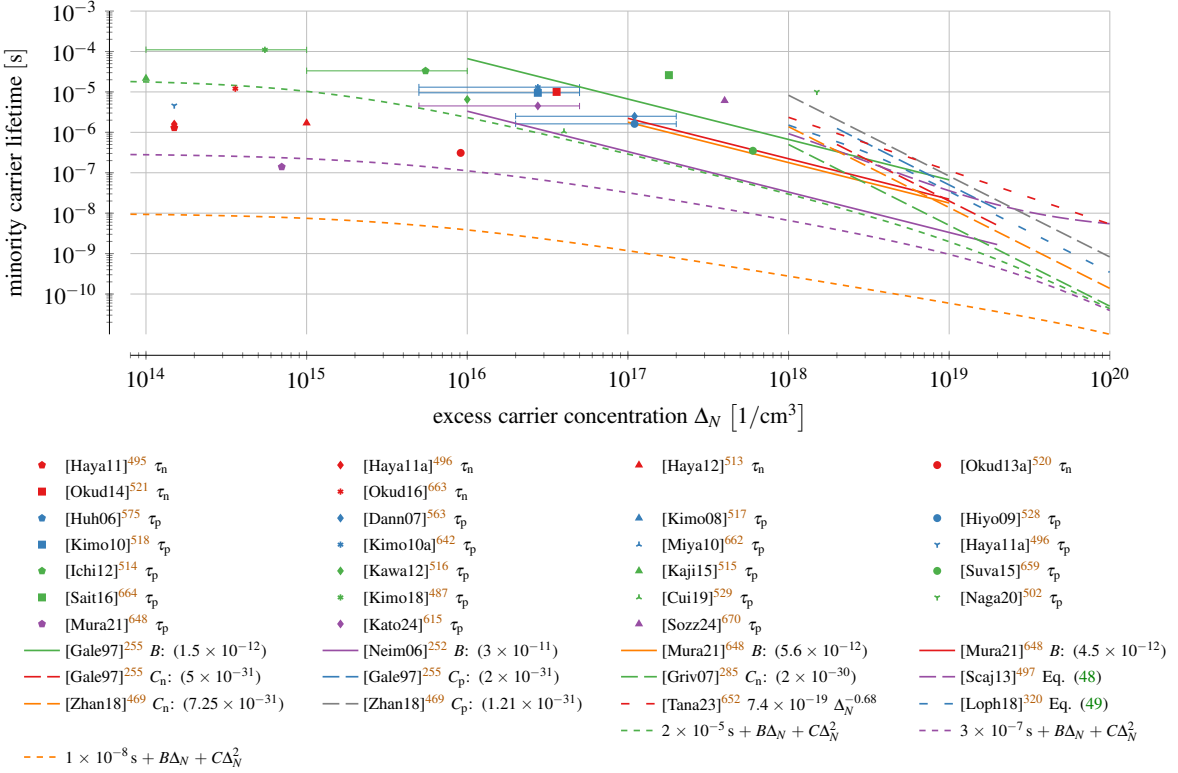


FIG. 28. Charge carrier lifetime considering the contributions of SRH, bimolecular (solid lines) and Auger (dashed lines). The overall recombination lifetime τ_r (dotted line) is shown for different values of τ_{SRH} , $\tau_{bim} = 3 \times 10^{-11} \text{ s}$ ²⁵² and $\tau_{Auger} = 2 \times 10^{-30} \text{ s}$.

that the often used assumption of full ionization is not applicable. Quite the opposite: incomplete ionization has to be carefully considered to correctly predict the amount of free charge carriers and, thus, achieve a realistic conductivity^{703,704}.

In this section we will, thus, review measurements, models and TCAD parameters used to described the amount of ionized dopants depending on temperature and doping concentration. We focus on the four most common doping species in 4H-SiC^{84,154,705}: Aluminum (analysis by Darmody and Goldsman¹³⁵) and Boron for p-type resp. Nitrogen and Phosphorous for n-type doping. We limit ourselves to simple model, e.g., a single energy level per lattice site (cubic or hexagonal). Depending on various parameters, e.g., binding type and location^{136,395,584,598} or whether the impurity is located in a non-neutral regions or not⁷⁰⁴, rather elaborate descriptions would be necessary to account otherwise²³⁵.

A. Theory

A good overview on the physical descriptions of incomplete ionization is provided by⁸⁴. In brief, the amount of ionized dopants can be modeled by the Fermi-Dirac distribution^{171,274,331,333,706}, also known as steady-state Gibbs distribution⁷⁰⁴, as

$$\begin{aligned} N_D^+ &= \frac{N_D}{1 + g_D \exp\left(\frac{E_{F,n} - E_D}{k_B T}\right)} \\ N_A^- &= \frac{N_A}{1 + g_A \exp\left(\frac{E_A - E_{F,p}}{k_B T}\right)} \end{aligned} \quad (58)$$

where N_A resp. N_D are the active acceptor resp. donor concentrations, E_A resp. E_D the acceptor resp. donor energy levels, $E_{F,n}$ resp. $E_{F,p}$ the electron resp. hole Fermi level and g_D resp. g_A the degeneracy factors. The latter denote the degeneracy of the energy levels²⁰¹, whereat in the literature commonly the values $g_A = 4$ (spin up and spin down plus two valence bands) and $g_D = 2$ (spin up and down)^{596,703} are used. There are, however, exception: Troffer⁶³ used $g_D = 6$, Scaburri⁸⁴, Laube *et al.*⁷⁰⁷ a spin degeneracy of $g_D = 4$ for Phosphorous, Balachandran, Chow, and Agarwal²⁸³, Nawaz²⁸⁴ $g_A = g_D = 3$, Persson and Lindefelt³⁹⁹ $g_A = 2$, Lv *et al.*⁷⁰⁸ $g_A = g_D = 2$ and Pernot *et al.*²³⁹ $g_k = 6$ resp. $g_h = 2$ for the cubic resp. hexagonal site of Nitrogen. There were also efforts to introduce a temperature dependency as $G_A(T)$ and $G_D(T)$ ^{23,49,62,63,84,589,709} based on the energy separation of excited states, whereat the description by Lophitis *et al.*³²⁰ (equ. (11)) deviates significantly.

If solely Boltzmann statistics are considered Eq. (58) can be simplified to^{68,84,101,123,325}

$$\begin{aligned} N_D^+ &= \frac{N_D}{1 + g_D \frac{n}{n_1}}, & n_1 &= N_C \exp\left(-\frac{\Delta E_D}{k_B T}\right) \\ N_A^- &= \frac{N_A}{1 + g_A \frac{p}{p_1}}, & p &= N_V \exp\left(-\frac{\Delta E_A}{k_B T}\right) \end{aligned} \quad (59)$$

with N_C resp. N_V the effective density of states in the conduction resp. valence band (see Section II) and $\Delta E_D = E_C - E_D$ resp. $\Delta E_A = E_A - E_V$ the ionization energies of donors and acceptors relative to the conduction (E_C) and valence band (E_V). This representation is often preferred in TCAD simulation tools, which commonly operate on charge carrier concentrations.

For completeness we want to highlight that using the neutrality equation⁸⁴

$$N_D^+(E_F) + p(E_F) = N_A^-(E_F) + n(E_F) \quad (60)$$

it is possible to even get rid of the carrier concentration. If we assume a highly donor doped material ($p(E_F)$ can be neglected) and no compensation ($N_A^-(E_F) = 0$) Eq. (60) results, by inserting Eq. (59) for N_D^+ , in a quadratic equation for n which can be solved to^{154,177,181,292,326,327,606}

$$N_D^+ = N_D \frac{-1 + \sqrt{1 + 4 g_D \frac{N_D}{N_C} \exp\left(\frac{\Delta E_D}{k_B T}\right)}}{2 g_D \frac{N_D}{N_C} \exp\left(\frac{\Delta E_D}{k_B T}\right)} . \quad (61)$$

The ionization energies also depend on the doping concentration. This can be explained by the changing potential energy of the charge carriers when they are closer to the ionized atoms, effectively shielding them⁷¹⁰. To model the decrease in the ionization energy the Pearson-Bardeen⁷¹⁰ expression

$$\Delta E(N) = \Delta E_0 - \alpha N^{1/3} \quad (62)$$

is used. Nice discussion of topic also by Schöner⁷¹¹, i.e., additional models described.

The literature is inconsistent on what dopants should be included into the overall doping concentration N in Eq. (62). Some authors include both donors and acceptors $N_A + N_D$ ^{68,325}, others only the respective donor concentration (N_A or N_D)^{15,50,578,589,712,713}, while a third group just uses the ionized ones⁵². Kajikawa⁷¹⁴ even argues that the compensating dopants, i.e., donors for the acceptor levels and vice versa, have the bigger impact and should be used instead of the overall donor and acceptor concentrations. There have also been proposals to include the compensating dopants into the factor α ^{84,715}. Finally, a completely different approach focuses on the degree of compensation depicted by a screening of free charge carriers^{84,716}, which introduces an additional temperature dependency.

An alternative approach to the Pearson-Bardeen expression in Eq. (62) is given by Altermatt, Schenk, and Heiser⁷¹⁷, Altermatt *et al.*⁷¹⁸, who used the logistic equation

$$\Delta E(N) = \frac{\Delta E_0}{1 + (N/N_E)^c} \quad (63)$$

to model the decrease in ionization energy, with N_E a reference concentration where the ionization energy is half its original value ΔE_0 . Darmody and Goldsman¹³⁵ argue that with Eq. (62) it is possible to shift the dopant level into the conduction/valence band and thus ionize all dopants immediately, which is neither physically reasonable nor possible with Eq. (63). Despite these arguments, the described approach has not yet found its way into the major simulation tools.

Dopants have differing ionization energies depending on whether they are located in a hexagonal or a cubic lattice site³⁴ (see ??). Consequently Eq. (59) has to be adapted to^{68,699}

$$N_D^+ = \frac{\frac{1}{2}N_D}{1 + g_D \frac{p}{N_C} \left(\frac{\Delta E_{Dh}}{k_B T} \right)} + \frac{\frac{1}{2}N_D}{1 + g_D \frac{p}{N_C} \left(\frac{\Delta E_{Dc}}{k_B T} \right)}$$

$$N_A^- = \frac{\frac{1}{2}N_A}{1 + g_A \frac{p}{N_V} \left(\frac{\Delta E_{Ah}}{k_B T} \right)} + \frac{\frac{1}{2}N_A}{1 + g_A \frac{p}{N_V} \left(\frac{\Delta E_{Ac}}{k_B T} \right)}$$

with E_{Dc} and E_{Dh} the cubic resp. hexagonal ionization energies for donors and E_{Ac} and E_{Ah} for acceptors. The factors $1/2$ denote that both lattice sites are equally probable¹⁰¹. In TCAD simulations it is often the case that these separate values are merged to an effective energy level, ending up once again in a description as shown in Eq. (59)^{69,155,292,325,332}. The effects of such simplifications have been investigated by Lades⁶⁵, Ayalew *et al.*⁵⁴⁹.

For more accurate approximation of dynamic processes around the dopant, i.e., (de)trapping of charge carriers, the electron and hole cross sections are crucial (see Section V). There are multiple description available in literature, which differ in their temperature scaling⁵⁰⁶. The multi-phonon capture model is independent of temperature^{711,719–721} while the cascade capture model is proportional to T^{-2} ^{256,711,722,723} (also [78Aba] in Schöner⁷¹¹). Kaindl *et al.*⁷²⁴ argue that the latter delivers a better fit. A scaling with T^{-3} was used by Kuznetsov and Zubrilov²⁴⁴. Note that we discovered large discrepancies between the single tools regarding which models are supported.

B. Results

Gorban *et al.*⁷²⁵ uses hexagonal value 66 of Ikeda, Matsunami, and Tanaka³⁴ to get cubic one. The most commonly method to determine the ionization energy of dopants in literature is to fit the neutrality equation, i.e., for p-type doping

$$p + N_K = \frac{N_A}{1 + \frac{g_A p}{N_V} \exp\left(\frac{\Delta E_A}{k_B T}\right)}.$$

to Hall measurements, e.g., conductivity or charge carrier concentration, for varying temperature^{15,49–51,62,63,202,231,239,256,392,557,560,576,579,580,584,586,590,594,596,603,605,606,700,713,714,726–740}. The compensation doping density N_K is only required for fitting purposes, such that we solely use N_A as the doping density to present our results. Due to the anisotropy of the Hall effect it is possible to achieve direction dependent ionization energies this way⁶². Other approaches based on Hall measurements include the fitting to the activation ratio⁷⁴¹ or free carrier concentration spectroscopy

(FCCS)^{578,589,742}. Further used electrical measurements are (thermal)^{295,743–745} admittance spectroscopy (AS)^{61–63,256,580,700,713,724}, electron spin resonance (ESR) measurement⁷⁴⁶, deep level transient spectroscopy (DLTS)^{62,244,610,747} and minority carrier transient spectroscopy (MCTS)⁶¹⁰, which are often combined with Hall measurements for more accurate results. Troffer⁶³ notes that DLTS is more sensitive but admittance spectroscopy allows to depict time constants below 1 μ s.

These electrical methods are complemented by optical ones, e.g., (fourier transform infrared) photothermal ionization spectroscopy (PTIS)²⁵⁰, donor-acceptor pair (DAP) luminescence^{34,41,251,398}, free to acceptor (FTA) spectroscopy³⁴, infrared absorption (IA)²⁰², photoluminescence (PL)^{317,404,406,580,602}, time-resolved spectroscopy (TRS)³¹⁷ or delay measurements (DM)³¹⁷. In these cases electrons are empowered and the resulting photon emission is recorded. The latter can be cause by transitions among traps or between traps and the conduction/valence band⁶². Note that different methods lead to slightly deviating results, even when applied to the same device²⁰². Also possible are calculations, e.g., Faulkner model (FM) calculations⁴², density functional theory (DFT)^{220,698}, effective mass approximation (EMA)²²⁴, first principles calculations (FPC)^{136,573,574} or *ab initio* supercell calculations (AISC)⁷⁴⁸. Finally, some authors define a value range based on measurements in literature^{65,101,154}, calculate an average values⁵⁸⁸ or fit to existing data^{68,82,135}.

In the sequel we are going to present the ionization energies ΔE_D resp. ΔE_A found in literature with their respective doping concentration. In order to draw the measurements we dropped uncertainties and replaced the sometimes stated exciton energy E_x with 20 meV (see Section III). We had to discard results where the samples were solely described as "high purity" or "unintentional doping"^{404,406,560,602} and Laube *et al.*⁷⁰⁷, which was superseded by a publication of the same authors. We mark results for the hexagonal lattice site by a trailing "h" and result for the cubic one by a trailing "c". The latter is often also denoted by the letter "k", which, most probably, corresponds to the german word "kubisch" for cubic. In fact, some of the literature is written in german^{62,63}, making it hard to retrace the results for the international community.

For Aluminum (see Fig. 29) many measurements and model fittings have been proposed. The values are equally distributed across the last three decades, meaning that the improvements in material quality did not result in significant changes. The model proposed by Achatz *et al.*⁷¹² uses the critical aluminum concentration for the doping-induced metal-insulator transition to set $\Delta E_A = 0$ and then fit the parameters. This is in contrast to the logistic equation in Eq. (63) used by Darmody and Goldsman¹³⁵, where a much slower decrease of ΔE_A below 100 meV can be observed.

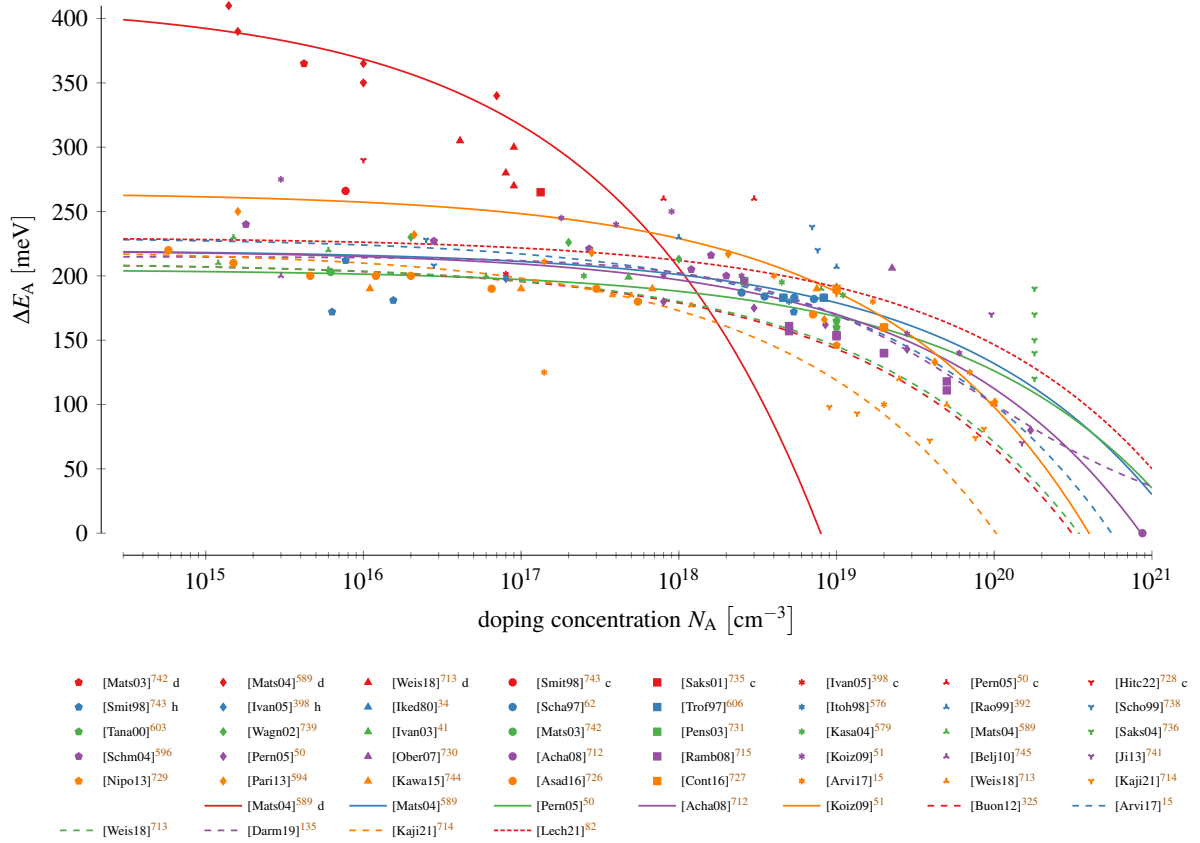


FIG. 29. Aluminum ionization energy. Marks refer to measurements and lines to fittings. The letter 'd' after the reference indicates a deep level whose origin is still discussed (see text). Colors are used solely to increase the readability.

For low-doped and compensated devices a second energy level is required to properly describe the measurements⁵⁰. The origin of this deep level is still discussed in literature. Matsuura *et al.*^{589,742} were not able to provide any explanation, Weiße *et al.*⁷¹³ suspect excited states of the aluminum ground state and Pernot, Contreras, and Camassel⁵⁰, Smith, Evwaraye, and Mitchel⁷⁴³ describe them as the cubic lattice site. In fact, Smith, Evwaraye, and Mitchel⁷⁴³ states that for higher concentration only the hexagonal site is measured. Nevertheless, in our plots we show the data as presented by the original authors, with the exceptions of the ones by Saks *et al.*⁷³⁵, which Pernot, Contreras, and Camassel⁵⁰ pointed out to denote the cubic lattice site.

Aluminum is the single dopant where a fitting using the logistic approximation (see Eq. (63)) was used. Darmody and Goldsman¹³⁵ achieved $\Delta E_0 = 214.86 \text{ meV}, N_E = 8.12 \times 10^{19}/\text{cm}^3$ and $c = 0.632$.

The available measurements for Boron (see Fig. 30) are very few and date back to the last

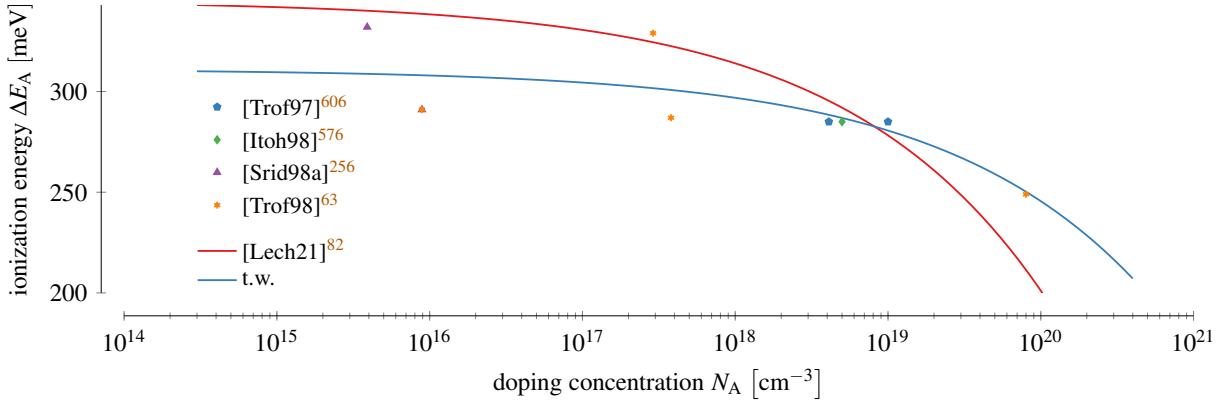


FIG. 30. Boron ionization energy. Marks refer to measurements and lines to fittings. Colors are used solely to increase the readability.

millennium. We suspect the main cause in the deep D-center^{63,135,136} that comes with a Boron doping. It introduces an energy level in a range of 495–630 meV^{34,63,244,251,256,610}, which results in a very effective recombination center. In some publications and also in some simulation tools the D-center level is used as the actual Boron one^{34,57,70,251,259,402,404,567}. Since only a single fitting according to Eq. (62) is available for Boron we used all the available data to generate an additional one (t.w.).

For the n-type donor Nitrogen (shown in Fig. 31) almost all publications distinguish between cubic and hexagonal site. However, there is also a big spread in the data, especially towards higher doping concentrations. The results suggest that the ionization energy does not decrease (especially for the cubic lattice site) even as the solubility limit ($1 \times 10^{19} \text{ cm}^3$ for annealing at 1700 K up to $3 \times 10^{20} \text{ cm}^3$ for annealing at 2500 K^{60,70,397,398,749}) is approached.

For Nitrogen only fittings according to Eq. (62) are available. Kagamihara *et al.*⁵⁷⁸ provided a fitting for both hexagonal and cubic lattice site, which were combined by Hatakeyama, Fukuda, and Okumura⁶⁸ to an effective ionization energy model. The remaining fittings also represent effective levels but are surprisingly low. In the case of Buono³²⁵ this can be explained by the selection of ΔE_0 , which was picked as the effective value of 65 meV determined by Bakowski, Gustafsson, and Lindefelt⁶⁹ based on the values from Götz *et al.*²⁰². The latter, as can be seen in the figure, were, however, determined for a doping of $1 \times 10^{17}/\text{cm}^3$ resp. $1 \times 10^{18}/\text{cm}^3$.

Compared to Nitrogen a lot less measurements are available for Phosphorous (see Fig. 32), all roughly two decades old. Again, hexagonal and cubic lattice site are always distinguished, but the results especially for the latter largely deviate. Due to the lack of fittings according to Eq. (62) we

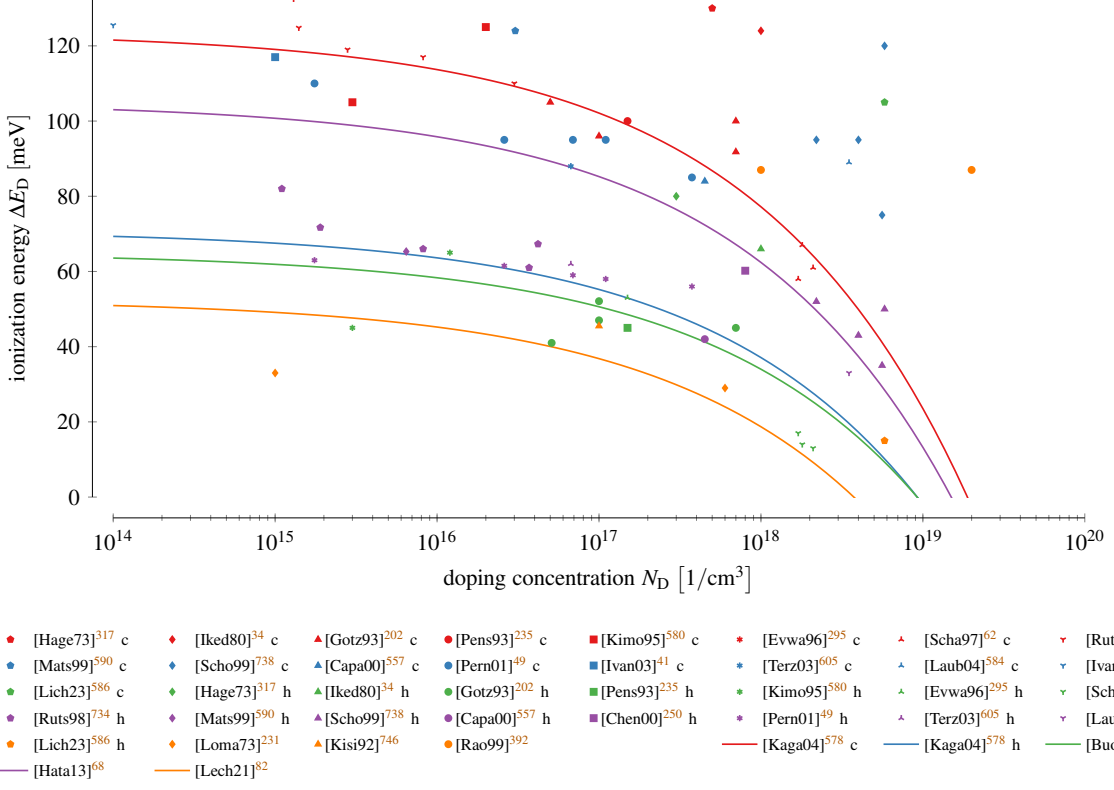


FIG. 31. Nitrogen ionization energy. Marks refer to measurements and lines to fittings. Colors are used solely to increase the readability.

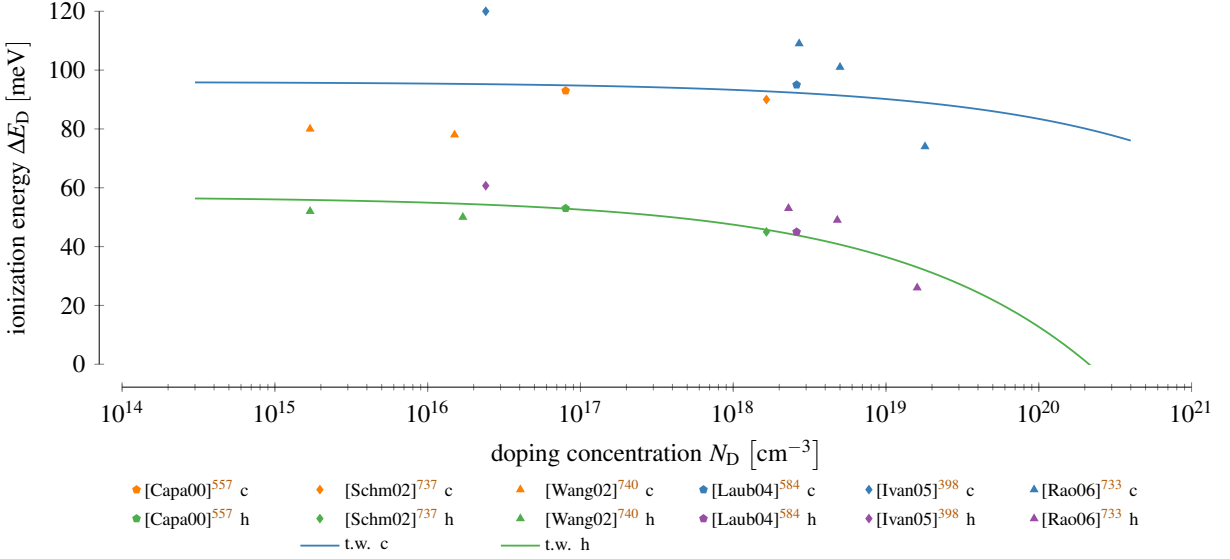


FIG. 32. Phosphorous ionization energy. Marks refer to measurements and lines to fittings. Colors are used solely to increase the readability.

used the available data to generate very crude fittings. Even as the solubility limit ($6 \times 10^{18} \text{ cm}^3$ for annealing at 1700 K up to $2 \times 10^{20} \text{ cm}^3$ for annealing at 2500 K^{60,70,397,398,749}) is reached high ionization energies for the cubic lattice site are observable.

The parameters for the Pearson-Bardeen model (see Eq. (62)) fittings, which were shown in Figs. 29 to 32, are summarized in Table XIX. We also added our own fitting parameters (t.w.). To take the described inconsistency for N in Eq. (62) into account column N denotes either the total doping (tot), the n- resp. p-type doping (dop), the compensation (comp) or fitting (fit). For the figures we used uniformly the specific doping concentration N_A resp. N_D (x-axis).

Cross-sections with varying temperature were heavily investigated at the end of the last century (see Table XX). The column σ denotes the cross section with the charge carrier in the energetically closer band (conduction or valence) because the interaction with the other band is significantly lower^{63,724}.

Finally we also investigated single energy values used in overviews or in TCAD simulations (see Fig. 33). We do not show fundamental values here as these are always linked to a specific doping concentration. For Aluminum many publications use a value that corresponds to the deeper (cubic site?) energy level. Also for Boron some values refer to the deep D-center. Altogether, a wide range of values is used, especially for Nitrogen, where again hexagonal and cubic sites are almost always distinguished. We want to highlight that for the Boron ionization energy of 293 meV^{86,320,704} no direct connection to any fundamental investigation could be inferred.

In some publications the dopant is not clearly specified. Instead only the acceptor and donor energy level are provided (see Fig. 34). While the acceptor values clearly correspond to Aluminum the n-type values could belong to both Nitrogen and Phosphorous.

C. Discussion

In contrast to other properties that have been investigated within this review, there exist a lot of fundamental studies and measurements for incomplete ionization. Nevertheless, the results acquired over the last decades deviate sometimes significantly, making it impossible to distill them to common values. This is, by the way, not caused by less mature samples in the past. Even by limiting our analysis to the last two decades we did reveal a large spread in measurement results. The situation is worsened by the fact that values for hexagonal and cubic lattice sites are often used without appropriate notation. In this fashion significant errors can be introduced, especially

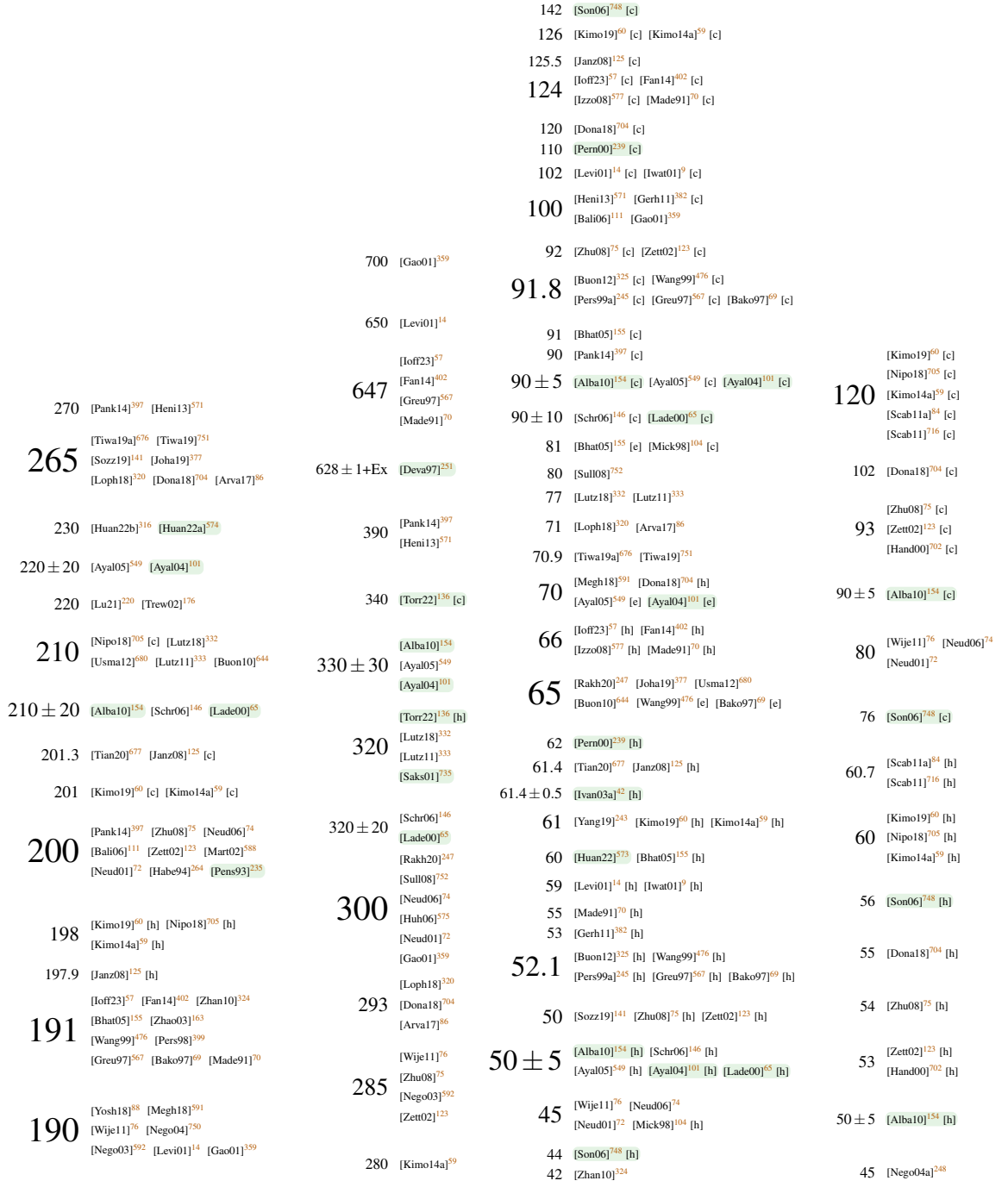


FIG. 33. Energy levels used in literature for each investigated dopant shown at the bottom. [c] marks cubic, [h] hexagonal and [e] effective values, i.e., a combination of hexagonal and cubic. Nodes with green background indicate a fundamental publication.

TABLE XIX. Parameters for the Pearson-Bardeen model (see Eq. (62)). Column N denotes how the factor N is interpreted: either as active dopants (dop), all dopants (tot), just the compensating ones (comp) or simply used in a fitting (fit). The site denotes besides hexagonal and cubic also a combined effective energy level (eff) and the deep level for Aluminium (deep). If left blank no information were stated in the paper.

ref.	N	site	ΔE	α
			[meV]	[meV cm]
Nitrogen				
[Kaga04] ⁵⁷⁸	dop	hex	70.9	3.38×10^{-5}
		cubic	123.7	4.65×10^{-5}
[Buon12] ³²⁵	tot	eff	65	3.1×10^{-5}
[Hata13] ⁶⁸	tot	eff	105	4.26×10^{-5}
[Lech21] ⁸²	tot		52.5	3.38×10^{-5}
Phosphorous				
t.w.	fit	hex	57	9.54×10^{-6}
		cubic	96	2.71×10^{-6}
Aluminum				
[Mats04] ⁵⁸⁹	dop		220	1.9×10^{-5}
[Pern05] ⁵⁰	dop		205	1.7×10^{-5}
[Acha08] ⁷¹²	dop		220	2.32×10^{-5}
[Koiz09] ⁵¹	dop		265	3.6×10^{-5}
[Buon12] ³²⁵	tot	eff	210	3.1×10^{-5}
[Arvi17] ¹⁵	dop		230 ± 10	$(2.8 \pm 0.3) \times 10^{-5}$
[Weis18] ⁷¹³	dop		210	3×10^{-5}
[Kaji21] ⁷¹⁴	comp		220	4.7×10^{-5}
[Lech21] ⁸²	tot		230	1.8×10^{-5}
Boron				
[Lech21] ⁸²	tot		345	3.1×10^{-5}
t.w.	fit		311	1.41×10^{-5}

for Boron where the deep levels is approximately twice the shallow one.

Overall, almost all publications utilize values determined from 4H-SiC measurements. Only

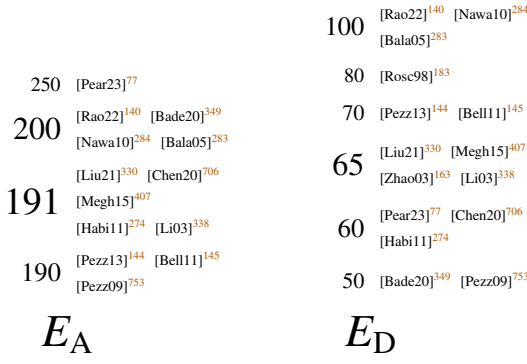


FIG. 34. Energy levels used in literature for acceptors and donors without closer specification of dopant element.

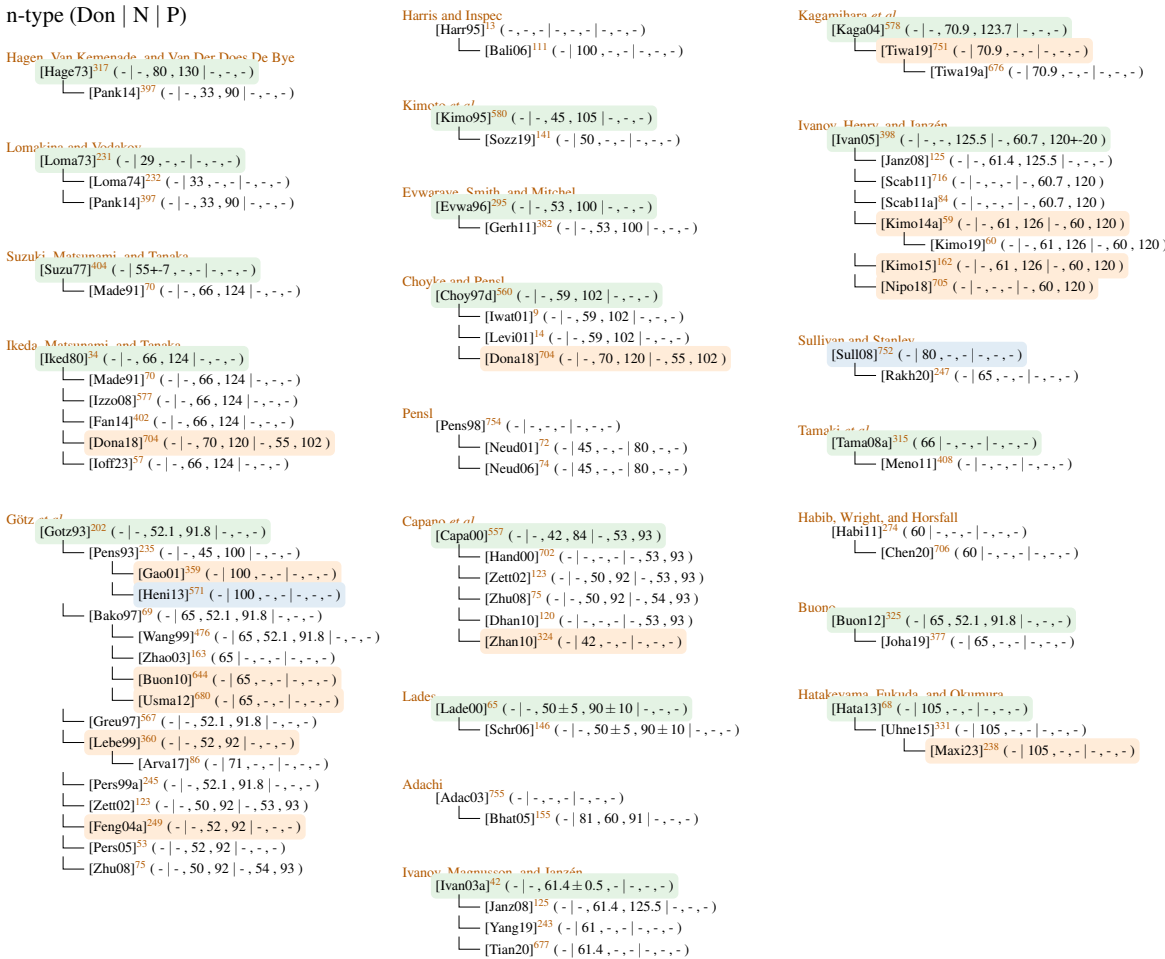


FIG. 35. Reference chain for n-type doping. Entries with green background show fundamental investigations, orange references we inferred based on the used data and blue investigation based not on 4H.

TABLE XX. Dopants and their respective cross sections with the charge carriers in the energetically closer band (conduction or valence). Different temperature dependencies are indicated in the column T^α . We found no data for Nitrogen.

ref.	site	T^α	ΔE [meV]	σ [cm 2]
Nitrogen				
[Kain99] ⁷²⁴	cubic	T^0	77	7.92×10^{-15}
		T^{-2}	90	3.57×10^{-10}
Aluminum				
[Kuzn95] ²⁴⁴		T^{-3}	229	8×10^{-13}
[Scha97] ⁶²		T^0	164–179	2.2–0.000 000 000 000 76
		T^{-2}	189–202	1.7–0.000 000 000 005 6
[Kain99] ⁷²⁴		T^0	189	2.58×10^{-13}
		T^{-2}	208	2.57×10^{-8}
[Resh05] ⁶¹		T^0	185	1×10^{-14}
		T^{-2}	210	1×10^{-13}
[Belj10] ⁷⁴⁵		T^0	200	1×10^{-12}
[Kawa15] ⁷⁴⁴		T^0	190	1.4×10^{-13}
[Kato22] ⁷⁴⁷		T^0	120–170	1–0.000 000 000 000 001 00
Boron				
[Srid98a] ²⁵⁶		T^0	259–262	-
		T^{-2}	284–295	-
[Trof98] ⁶³		T^0	292	6×10^{-15}
		T^{-2}	314	5×10^{-14}
[Kain99] ⁷²⁴		T^0	312	2.1×10^{-14}
		T^{-2}	375	9.69×10^{-9}
[Zhan03] ⁶¹⁰		T^0	230–280	2–0.000 000 000 000 30

seldomly 6H data were used^{247,575}, whereat the values match those from 4H publications^{86,320,704}. However, since the latter did not provide a reference for the picked values it is impossible to retrace where and how these values have been determined. Nevertheless we tried to create causality chains for n-type (see Fig. 35) p-type (see Fig. 36) values, whereat quite some values had to be inferred due to missing information.

For n-type doping the values published by Ikeda, Matsunami, and Tanaka³⁴ are widely used up until this day. Similarly, for p-type doping Götz *et al.*²⁰² provided for some time the values. However, recently the values by Ivanov, Magnusson, and Janzén⁴², Ivanov, Henry, and Janzén³⁹⁸

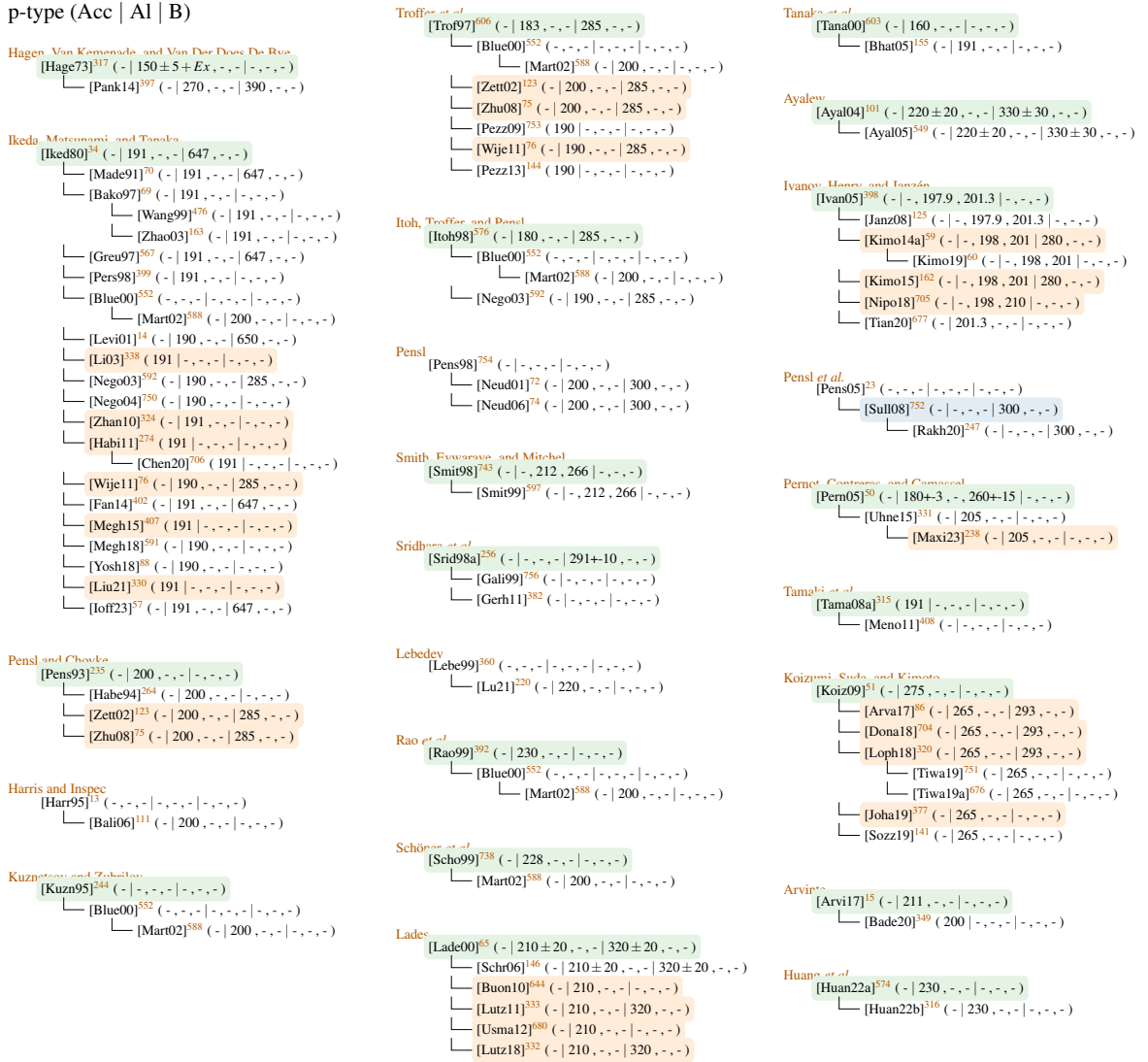


FIG. 36. Reference chain for p-type doping. Entries with green background show fundamental investigations, orange references we inferred based on the used data and blue investigation based not on 4H.

are dominantly cited.

The most research has been clearly directed towards Aluminum. Overall, future research should be denoted to (i) gather additional data for Phosphorous and Boron and (ii) condense the already achieved values. For this purpose we added our own fittings based on the gathered data for cubic and hexagonal lattice site as well as for all values together (effective value).

REFERENCES

- ¹E. Bellotti, *Advanced Modeling of Wide Band Gap Semiconductor Materials and Devices*, Ph.D. thesis, Georgia Institute of Technology (1999).
- ²V. Komarov, S. Wang, and J. Tang, in *Encyclopedia of RF and Microwave Engineering*, edited by K. Chang (Wiley, 2005) 1st ed.
- ³S. Adachi, *Properties of Group-IV, III-V and II-VI Semiconductors* (John Wiley, Chichester, England, 2005).
- ⁴J. Olivares, M. DeMiguel-Ramos, E. Iborra, M. Clement, T. Mirea, M. Moreira, and I. Katardjiev, in *2013 Joint European Frequency and Time Forum & International Frequency Control Symposium (EFTF/IFCS)* (IEEE, Prague, Czech Republic, 2013) pp. 118–121.
- ⁵W. Ching, Y.-N. Xu, P. Rulis, and L. Ouyang, *Materials Science and Engineering: A* **422**, 147 (2006).
- ⁶L. Patrick and W. J. Choyke, *Physical Review B* **2**, 2255 (1970).
- ⁷R. H. Lyddane, R. G. Sachs, and E. Teller, *Physical Review* **59**, 673 (1941).
- ⁸R. Ahuja, A. Ferreira Da Silva, C. Persson, J. M. Osorio-Guillén, I. Pepe, K. Järrendahl, O. P. A. Lindquist, N. V. Edwards, Q. Wahab, and B. Johansson, *Journal of Applied Physics* **91**, 2099 (2002).
- ⁹H. Iwata and K. M. Itoh, *Journal of Applied Physics* **89**, 6228 (2001).
- ¹⁰M. Hjelm, H.-E. Nilsson, A. Martinez, K. F. Brennan, and E. Bellotti, *Journal of Applied Physics* **93**, 1099 (2003).
- ¹¹R. Mickevičius and J. H. Zhao, *Materials Science Forum* **264–268**, 291 (1998).
- ¹²C. Persson and U. Lindefelt, *Journal of Applied Physics* **82**, 5496 (1997).
- ¹³G. L. Harris and Inspec, eds., *Properties of Silicon Carbide*, EMIS Datareviews Series No. 13 (INSPEC, the Inst. of Electrical Engineers, London, 1995).
- ¹⁴M. E. Levinshtein, S. L. Rumyantsev, and M. Shur, eds., *Properties of Advanced Semiconductor Materials: GaN, AlN, InN, BN, SiC, SiGe* (Wiley, New York, 2001).
- ¹⁵I.-R. Arvinte, *Investigation of Dopant Incorporation in Silicon Carbide Epilayers Grown by Chemical Vapor Deposition*, Ph.D. thesis, Universite Cote d'Azur (2017).
- ¹⁶H. Harima, S.-i. Nakashima, and T. Uemura, *Journal of Applied Physics* **78**, 1996 (1995).
- ¹⁷H. Harima, T. Hosoda, and S. Nakashima, *Materials Science Forum* **264–268**, 449 (1998).
- ¹⁸D. W. Feldman, J. H. Parker, W. J. Choyke, and L. Patrick, *Physical Review* **173**, 787 (1968).

- ¹⁹K. Karch, F. Bechstedt, P. Pavone, and D. Strauch, *Physical Review B* **53**, 13400 (1996).
- ²⁰G. Wellenhofer, K. Karch, P. Pavone, U. Rössler, and D. Strauch, *Physical Review B* **53**, 6071 (1996).
- ²¹B. Adolph, K. Tenelsen, V. I. Gavrilenko, and F. Bechstedt, *Physical Review B* **55**, 1422 (1997).
- ²²X. Peng-Shou, X. Chang-Kun, P. Hai-Bin, and X. Fa-Qiang, *Chinese Physics* **13**, 2126 (2004).
- ²³G. Pensl, F. Ciobanu, T. Frank, M. Krieger, S. Reshanov, F. Schmid, and M. Weidner, *International Journal of High Speed Electronics and Systems* **15**, 705 (2005).
- ²⁴J. Coutinho, V. J. B. Torres, K. Demmouche, and S. Öberg, *Physical Review B* **96**, 174105 (2017).
- ²⁵I. G. Ivanov, A. Stelmach, M. Kleverman, and E. Janzén, *Physical Review B* **73**, 045205 (2006).
- ²⁶J. G. Hartnett, D. Mouneyrac, J. Krupka, J.-M. Le Floch, M. E. Tobar, and D. Cros, *Journal of Applied Physics* **109**, 064107 (2011).
- ²⁷C. R. Jones, J. Dutta, G. Yu, and Y. Gao, *Journal of Infrared, Millimeter, and Terahertz Waves* **32**, 838 (2011).
- ²⁸L. Li, S. Reyes, M. J. Asadi, X. Wang, G. Fabi, E. Ozdemir, W. Wu, P. Fay, and J. C. M. Hwang, in *2023 100th ARFTG Microwave Measurement Conference (ARFTG)* (IEEE, Las Vegas, NV, USA, 2023) pp. 1–4.
- ²⁹M. Naftaly, J. F. Molloy, B. Magnusson, Y. M. Andreev, and G. V. Lanskii, *Optics Express* **24**, 2590 (2016).
- ³⁰A. T. Tarekegne, B. Zhou, K. Kaltenecker, K. Iwaszczuk, S. Clark, and P. U. Jepsen, *Optics Express* **27**, 3618 (2019).
- ³¹M.-m. Gao, L.-y. Fan, X.-y. Gong, J.-l. You, and Z.-z. Chen, *Journal of Applied Physics* **132**, 135702 (2022).
- ³²S. Ninomiya and S. Adachi, *Japanese Journal of Applied Physics* **33**, 2479 (1994).
- ³³L. Cheng, J.-Y. Yang, and W. Zheng, *ACS Applied Electronic Materials* **4**, 4140 (2022).
- ³⁴M. Ikeda, H. Matsunami, and T. Tanaka, *Physical Review B* **22**, 2842 (1980).
- ³⁵Q. Yang, Q. Liu, W. Xu, D. Zhou, F. Ren, R. Zhang, Y. Zheng, and H. Lu, *Solid-State Electronics* **187**, 108196 (2022).
- ³⁶J. M. Dutta, G. Yu, and C. R. Jones, in *2006 Joint 31st International Conference on Infrared Millimeter Wave* (IEEE, Shanghai, China, 2006) pp. 411–411.
- ³⁷S. Chen, M. Afsar, and D. Sakdatorn, *IEEE Transactions on Instrumentation and Measurement* **57**, 706 (2008).

- ³⁸L. Li, S. Reyes, M. J. Asadi, P. Fay, and J. C. M. Hwang, *Applied Physics Letters* **123**, 012105 (2023).
- ³⁹T. Li, L. Li, X. Wang, J. C. M. Hwang, S. Yanagimoto, and Y. Yanagimoto, *IEEE Journal of Microwaves* , 1 (2024).
- ⁴⁰Y. Yanagimoto, S. Yanagimoto, T. Li, and J. C. M. Hwang, in *2024 103rd ARFTG Microwave Measurement Conference (ARFTG)* (IEEE, Washington, DC, USA, 2024) pp. 1–4.
- ⁴¹I. G. Ivanov, B. Magnusson, and E. Janzén, *Physical Review B* **67**, 165211 (2003).
- ⁴²I. G. Ivanov, B. Magnusson, and E. Janzén, *Physical Review B* **67**, 165212 (2003).
- ⁴³A. Agarwal, S.-H. Ryu, and J. Palmour, in *Silicon Carbide*, edited by W. J. Choyke, H. Matsunami, and G. Pensl (Springer Berlin Heidelberg, Berlin, Heidelberg, 2004) pp. 785–811.
- ⁴⁴D. Hofman, J. Lely, and J. Volger, *Physica* **23**, 236 (1957).
- ⁴⁵A. Schöner, in *Silicon Carbide*, edited by W. J. Choyke, H. Matsunami, and G. Pensl (Springer Berlin Heidelberg, Berlin, Heidelberg, 2004) pp. 229–250.
- ⁴⁶I. Polaert, N. Benamara, J. Tao, T.-H. Vuong, M. Ferrato, and L. Estel, *Chemical Engineering and Processing: Process Intensification* **122**, 339 (2017).
- ⁴⁷J. Chen, Z. H. Levine, and J. W. Wilkins, *Physical Review B* **50**, 11514 (1994).
- ⁴⁸U. Lindefelt, *Journal of Applied Physics* **84**, 2628 (1998).
- ⁴⁹J. Pernot, W. Zawadzki, S. Contreras, J. L. Robert, E. Neyret, and L. Di Cioccio, *Journal of Applied Physics* **90**, 1869 (2001).
- ⁵⁰J. Pernot, S. Contreras, and J. Camassel, *Journal of Applied Physics* **98**, 023706 (2005).
- ⁵¹A. Koizumi, J. Suda, and T. Kimoto, *Journal of Applied Physics* **106**, 013716 (2009).
- ⁵²H. Tanaka, S. Asada, T. Kimoto, and J. Suda, *Journal of Applied Physics* **123**, 245704 (2018).
- ⁵³C. Persson and A. Ferreira Da Silva, in *Optoelectronic Devices: III Nitrides* (Elsevier, 2005) pp. 479–559.
- ⁵⁴T. A. Baeraky, *Egypt. J. Sol.* **25**, 263 (2002).
- ⁵⁵H.-J. Yang, J. Yuan, Y. Li, Z.-L. Hou, H.-B. Jin, X.-Y. Fang, and M.-S. Cao, *Solid State Communications* **163**, 1 (2013).
- ⁵⁶T. Chow and R. Tyagi, in *[1993] Proceedings of the 5th International Symposium on Power Semiconductor* (IEEE, Monterey, CA, USA, 1993) pp. 84–88.
- ⁵⁷I. Institute, “Silicon Carbide,” <http://www.ioffe.ru/SVA/NSM/Semicond/SiC/index.html> (2023).

- ⁵⁸P. T. B. Shaffer, *Applied Optics* **10**, 1034 (1971).
- ⁵⁹T. Kimoto and J. A. Cooper, *Fundamentals of Silicon Carbide Technology: Growth, Characterization, Deviation* 1st ed. (Wiley, 2014).
- ⁶⁰T. Kimoto, in *Wide Bandgap Semiconductor Power Devices* (Elsevier, 2019) pp. 21–42.
- ⁶¹S. Reshanov, *Device-relevant defect centers and minority carrier lifetime in 3C-, 4H- and 6H-SiC*, Ph.D. thesis, Friedrich-Alexander-Universität Erlangen-Nürnberg (2005).
- ⁶²M. Schadt, *Transporteigenschaften von Elektronen Und Löchern in Siliciumkarbid*, Ph.D. thesis, Friedrich-Alexander-Universität (1997).
- ⁶³T. Troffer, *Elektrische und optische Charakterisierung Bauelementrelevanter Dotierstoffe in Siliciumkarbid*, Ph.D. thesis, Friedrich-Alexander-Universität (1998).
- ⁶⁴N. W. Thibault, American Mineralogist **29**, 327 (1944), <https://pubs.geoscienceworld.org/msa/ammin/article-pdf/29/9-10/327/4243453/am-1944-327.pdf>.
- ⁶⁵M. Lades, *Modeling and Simulation of Wide Bandgap Semiconductor Devices: 4H/6H-SiC*, Ph.D. thesis, Technische Universität München (2000).
- ⁶⁶C. Persson, U. Lindefelt, and B. E. Sernelius, *Journal of Applied Physics* **86**, 4419 (1999).
- ⁶⁷N. T. Son, C. Persson, U. Lindefelt, W. M. Chen, B. K. Meyer, D. M. Hofmann, and E. Janzén, in *Silicon Carbide*, edited by W. J. Choyke, H. Matsunami, and G. Pensl (Springer Berlin Heidelberg, Berlin, Heidelberg, 2004) pp. 437–460.
- ⁶⁸T. Hatakeyama, K. Fukuda, and H. Okumura, *IEEE Transactions on Electron Devices* **60**, 613 (2013).
- ⁶⁹M. Bakowski, U. Gustafsson, and U. Lindefelt, *physica status solidi (a)* **162**, 421 (1997).
- ⁷⁰O. Madelung and R. Poerschke, eds., *Semiconductors: Group IV Elements and III-V Compounds*, Data in Science and Technology (Springer Berlin Heidelberg, Berlin, Heidelberg, 1991).
- ⁷¹B. Wenzien, P. Käckell, F. Bechstedt, and G. Cappellini, *Physical Review B* **52**, 10897 (1995).
- ⁷²P. Neudeck, in *Encyclopedia of Materials: Science and Technology* (Elsevier, 2001) pp. 8508–8519.
- ⁷³Y. Choi, H.-Y. Cha, L. Eastman, and M. Spencer, *IEEE Transactions on Electron Devices* **52**, 1940 (2005).
- ⁷⁴P. G. Neudeck (CRC Press, 2006).
- ⁷⁵X. Zhu, *ALTERNATIVE GROWTH AND INTERFACE PASSIVATION TECHNIQUES FOR SiO₂ ON 4H-SiC*, Ph.D. thesis, Auburn University (2008).
- ⁷⁶M. B. Wijesundara and R. Azevedo, *Silicon Carbide Microsystems for Harsh Environments*, MEMS Reference Shelf, Vol. 22 (Springer New York, New York, NY, 2011).

- ⁷⁷S. J. Pearton, X. Xia, F. Ren, M. A. J. Rasel, S. Stepanoff, N. Al-Mamun, A. Haque, and D. E. Wolfe, *Journal of Vacuum Science & Technology B* **41**, 030802 (2023).
- ⁷⁸J. Casady and R. Johnson, *Solid-State Electronics* **39**, 1409 (1996).
- ⁷⁹M. Huang, N. Goldsman, C.-H. Chang, I. Mayergoyz, J. M. McGarrity, and D. Woolard, *Journal of Applied Physics* **84**, 2065 (1998).
- ⁸⁰O. Madelung, ed., *Semiconductors — Basic Data* (Springer Berlin Heidelberg, Berlin, Heidelberg, 1996).
- ⁸¹T. Egilsson, J. P. Bergman, I. G. Ivanov, A. Henry, and E. Janzén, *Physical Review B* **59**, 1956 (1999).
- ⁸²B. Lechner, *Behaviour of 4H-SiC Power Semiconductor Devices under Extreme Operating Conditions*, Ph.D. thesis, Technische Universität München (2021).
- ⁸³N. Arpatzanis, A. Tsormpatzoglou, C. A. Dimitriadis, K. Zekentes, N. Camara, and M. Godlewski, *physica status solidi (a)* **203**, 2551 (2006).
- ⁸⁴R. Scaburri, *The Incomplete Ionization of Substitutional Dopants in Silicon Carbide*, Ph.D. thesis, Università di Bologna, Bologna (2011).
- ⁸⁵A. Naugarhiya, P. Wakhadkar, P. N. Kondekar, G. C. Patil, and R. M. Patrikar, *Journal of Computational Electronics* **16**, 190 (2017).
- ⁸⁶A. Arvanitopoulos, N. Lophitis, S. Perkins, K. N. Gyftakis, M. Belanche Guadas, and M. Antoniou, in *2017 IEEE 11th International Symposium on Diagnostics for Electrical Machines, Power Electronics and* (IEEE, Tinos, Greece, 2017) pp. 565–571.
- ⁸⁷R. Choudhary, M. Mehta, R. Singh Shekhawat, S. Singh, and D. Singh, *Materials Today: Proceedings* **46**, 5889 (2021).
- ⁸⁸H. Yoshioka and K. Hirata, *AIP Advances* **8**, 045217 (2018).
- ⁸⁹C. Miccoli and F. Iucolano, *Materials Science in Semiconductor Processing* **97**, 40 (2019).
- ⁹⁰S. Tripathi, C. Upadhyay, C. Nagaraj, A. Venkatesan, and K. Devan, *Nuclear Instruments and Methods in Physics Research Section A: Accelerators, Spectrometers, Detectors and Associated Equipment* **908**, 163 (2018).
- ⁹¹W. M. Klahold, W. J. Choyke, and R. P. Devaty, *Physical Review B* **102**, 205203 (2020).
- ⁹²A. Kovalchuk, J. Wozny, Z. Lisik, J. Podgorski, L. Ruta, A. Kubiak, and A. Boiadzhian, *Journal of Physics: Conference Series* **1534**, 012006 (2020).
- ⁹³A. Acharyya, *Applied Physics A* **123**, 629 (2017).
- ⁹⁴S. Banerjee, in *Advances in Terahertz Technology and Its Applications*, edited by S. Das,

- N. Anveshkumar, J. Dutta, and A. Biswas (Springer Singapore, Singapore, 2021) pp. 153–172.
- ⁹⁵H. Kim, *Transactions on Electrical and Electronic Materials* **25**, 141 (2024).
- ⁹⁶M. Bhatnagar and B. Baliga, *IEEE Transactions on Electron Devices* **40**, 645 (1993).
- ⁹⁷C. Codreanu, M. Avram, E. Carbunescu, and E. Iliescu, *Materials Science in Semiconductor Processing* **3**, 137 (2000).
- ⁹⁸C. Weitzel, J. Palmour, C. Carter, K. Moore, K. Nordquist, S. Allen, C. Thero, and M. Bhatnagar, *IEEE Transactions on Electron Devices* **43**, 1732 (Oct./1996).
- ⁹⁹H. Morkoç, S. Strite, G. B. Gao, M. E. Lin, B. Sverdlov, and M. Burns, *Journal of Applied Physics* **76**, 1363 (1994).
- ¹⁰⁰A. Burk, M. O'Loughlin, R. Siergiej, A. Agarwal, S. Sriram, R. Clarke, M. MacMillan, V. Balakrishna, and C. Brandt, *Solid-State Electronics* **43**, 1459 (1999).
- ¹⁰¹T. Ayalew, *SiC Semiconductor Devices Technology, Modeling, and Simulation*, Ph.D. thesis, TU Wien (2004).
- ¹⁰²S. Sriram, R. R. Siergiej, R. C. Clarke, A. K. Agarwal, and C. D. Brandt, *physica status solidi (a)* **162**, 441 (1997).
- ¹⁰³R. Han, X. Xu, X. Hu, N. Yu, J. Wang, Y. Tian, and W. Huang, *Optical Materials* **23**, 415 (2003).
- ¹⁰⁴R. Mickevičius and J. H. Zhao, *Journal of Applied Physics* **83**, 3161 (1998).
- ¹⁰⁵J. H. Zhao, V. Gruzinskis, Y. Luo, M. Weiner, M. Pan, P. Shiktorov, and E. Starikov, *Semiconductor Science and Technology* **15**, 1093 (2000).
- ¹⁰⁶A. Akturk, N. Goldsman, S. Potbhare, and A. Lelis, *Journal of Applied Physics* **105**, 033703 (2009).
- ¹⁰⁷B. Zippelius, *Elektrische Charakterisierung Bauelement-relevanter Defekte in 3C- Und 4H-Siliziumkarbid*, Ph.D. thesis, Friedrich-Alexander-Universität Erlangen-Nürnberg (2011).
- ¹⁰⁸C. Weitzel, *Materials Science Forum* **264–268**, 907 (1998).
- ¹⁰⁹F. Nava, G. Bertuccio, A. Cavallini, and E. Vittone, *Measurement Science and Technology* **19**, 102001 (2008).
- ¹¹⁰N. G. Wright, D. Morrison, C. M. Johnson, and A. G. O'Neill, *Materials Science Forum* **264–268**, 917 (1998).
- ¹¹¹B. J. Baliga, *Silicon Carbide Power Devices* (WORLD SCIENTIFIC, 2006).
- ¹¹²B. J. Baliga, *Fundamentals of Power Semiconductor Devices* (Springer International Publish-

ing, Cham, 2019).

- ¹¹³J. Y. Tsao, S. Chowdhury, M. A. Hollis, D. Jena, N. M. Johnson, K. A. Jones, R. J. Kaplar, S. Rajan, C. G. Van De Walle, E. Bellotti, C. L. Chua, R. Collazo, M. E. Coltrin, J. A. Cooper, K. R. Evans, S. Graham, T. A. Grotjohn, E. R. Heller, M. Higashiwaki, M. S. Islam, P. W. Juodawlkis, M. A. Khan, A. D. Koehler, J. H. Leach, U. K. Mishra, R. J. Nemanich, R. C. N. Pilawa-Podgurski, J. B. Shealy, Z. Sitar, M. J. Tadjer, A. F. Witulski, M. Wraback, and J. A. Simmons, [Advanced Electronic Materials 4, 1600501 \(2018\)](#).
- ¹¹⁴I. N. Jiya and R. Gouws, [Micromachines 11, 1116 \(2020\)](#).
- ¹¹⁵H.-E. Nilsson, E. Bellotti, M. Hjelm, K. F. Brennan, and C. Petersson, **Proceedings of the IMACS Conference, Sofia, Bulgaria, June 1999** (1999).
- ¹¹⁶E. Bellotti, H.-E. Nilsson, K. F. Brennan, P. P. Ruden, and R. Trew, [Journal of Applied Physics 87, 3864 \(2000\)](#).
- ¹¹⁷J. L. Vasconcelos, C. G. Rodrigues, and R. Luzzi, [Materials Science and Engineering: B 249, 114426 \(2019\)](#).
- ¹¹⁸C. G. Rodrigues, [Semiconductors 55, 625 \(2021\)](#).
- ¹¹⁹T. P. Chow, [Materials Science Forum 338–342, 1155 \(2000\)](#).
- ¹²⁰G. Dhanaraj, K. Byrappa, V. Prasad, and M. Dudley, eds., *Springer Handbook of Crystal Growth* (Springer Berlin Heidelberg, Berlin, Heidelberg, 2010).
- ¹²¹A. Elasser and T. Chow, [Proceedings of the IEEE 90, 969 \(2002\)](#).
- ¹²²M. Su, *Power Devices and Integrated Circuits Based on 4H-SiC Lateral JFETs*, Ph.D. thesis, New Brunswick Rutgers, New Jersey (2010).
- ¹²³C.-M. Zetterling, ed., *Process Technology for Silicon Carbide Devices*, EMIS Processing Series No. 2 (Institution of Electrical Engineers, London, 2002).
- ¹²⁴M. Östling, [Science China Information Sciences 54, 1087 \(2011\)](#).
- ¹²⁵E. Janzén, A. Gali, A. Henry, I. G. Ivanov, B. Magnusson, and N. T. Son, in *Defects in Microelectronic Materials and Devices* (CRC Press, 2008) pp. 615–669.
- ¹²⁶N. Kaminski, 2009 13th European Conference on Power Electronics and Applications **8** (2009).
- ¹²⁷N. Kaminski and O. Hilt, [IET Circuits, Devices & Systems 8, 227 \(2014\)](#).
- ¹²⁸C. Buttay, D. Planson, B. Allard, D. Bergogne, P. Bevilacqua, C. Joubert, M. Lazar, C. Martin, H. Morel, D. Tournier, and C. Raynaud, [Materials Science and Engineering: B 176, 283 \(2011\)](#).

- ¹²⁹S. Fujita, *Japanese Journal of Applied Physics* **54**, 030101 (2015).
- ¹³⁰P. G. Neudeck, in *Extreme Environment Electronics* (CRC Press, Taylor & Francis Group, 2013) pp. 225–232.
- ¹³¹A. Hassan, Y. Savaria, and M. Sawan, *IEEE Access* **6**, 78790 (2018).
- ¹³²M. Higashiwaki, K. Sasaki, A. Kuramata, T. Masui, and S. Yamakoshi, *physica status solidi (a)* **211**, 21 (2014).
- ¹³³G. Liu, B. R. Tuttle, and S. Dhar, *Applied Physics Reviews* **2**, 021307 (2015).
- ¹³⁴S. Rybalka, E.Yu. Krayushkina, A. Demidov, O. Shishkina, and B. Surin, *International Journal of Physical Research* **5**, 11 (2017).
- ¹³⁵C. Darmody and N. Goldsman, *Journal of Applied Physics* **126**, 145701 (2019).
- ¹³⁶V. J. B. Torres, I. Capan, and J. Coutinho, *Physical Review B* **106**, 224112 (2022).
- ¹³⁷S. J. Pearton, J. Yang, P. H. Cary, F. Ren, J. Kim, M. J. Tadjer, and M. A. Mastro, *Applied Physics Reviews* **5**, 011301 (2018).
- ¹³⁸V. Soler, *Design and Process Developments towards an Optimal 6.5 kV SiC Power MOSFET*, Ph.D. thesis, Universitat Politecnica de Catalunya (2019).
- ¹³⁹M. Yoder, *IEEE Transactions on Electron Devices* **43**, 1633 (Oct./1996).
- ¹⁴⁰S. Rao, E. D. Mallemace, and F. G. Della Corte, *Electronics* **11**, 1839 (2022).
- ¹⁴¹G. Sozzi, M. Puzzanghera, R. Menozzi, and R. Nipoti, *IEEE Transactions on Electron Devices* **66**, 3028 (2019).
- ¹⁴²R. Nipoti, G. Sozzi, M. Puzzanghera, and R. Menozzi, *MRS Advances* **1**, 3637 (2016).
- ¹⁴³M. Usman and M. Nawaz, *Solid-State Electronics* **92**, 5 (2014).
- ¹⁴⁴F. Pezzimenti, *IEEE Transactions on Electron Devices* **60**, 1404 (2013).
- ¹⁴⁵S. Bellone, F. G. Della Corte, L. F. Albanese, and F. Pezzimenti, *IEEE Transactions on Power Electronics* **26**, 2835 (2011).
- ¹⁴⁶D. Schröder, *Leistungselektronische Bauelemente* (Springer Berlin Heidelberg, Berlin, Heidelberg, 2006).
- ¹⁴⁷X. Dong, M. Huang, Y. Ma, C. Fu, M. He, Z. Yang, Y. Li, and M. Gong, *IEEE Transactions on Nuclear Science* , 1 (2024).
- ¹⁴⁸T. Yang, C. Fu, W. Song, Y. Tan, S. Xiao, C. Wang, K. Liu, X. Zhang, and X. Shi, *Nuclear Instruments and Methods in Physics Research Section A: Accelerators, Spectrometers, Detectors and Associated Equipment* **950**, 164503 (2020).
- ¹⁴⁹T. Yang, Y. Tan, C. Wang, X. Zhang, and X. Shi, “Simulation of the 4H-SiC Low Gain Avalanche Diode,” (2022), arXiv:2206.10191 [physics].

- ¹⁵⁰M. De Napoli, *Frontiers in Physics* **10**, 898833 (2022).
- ¹⁵¹M. Cabello, V. Soler, G. Rius, J. Montserrat, J. Rebollo, and P. Godignon, *Materials Science in Semiconductor Processing* **78**, 22 (2018).
- ¹⁵²Q. Chen, L. Yang, S. Wang, Y. Zhang, Y. Dai, and Y. Hao, *Applied Physics A* **118**, 1219 (2015).
- ¹⁵³H. A. Mantooth, in *Extreme Environment Electronics* (CRC Press, Taylor & Francis Group, 2013) pp. 243–252.
- ¹⁵⁴L. F. Albanese, *Characterization, Modeling and Simulation of 4H-SiC Power Diodes*, Ph.D. thesis, UniversitàdegliStudidiSalerno (2010).
- ¹⁵⁵P. Bhatnagar, A. B. Horsfall, N. G. Wright, C. M. Johnson, K. V. Vassilevski, and A. G. O'Neill, *Solid-State Electronics* **49**, 453 (2005).
- ¹⁵⁶M. W. Cole and P. Joshi, in *Silicon Carbide*, edited by Z. C. Feng and J. H. Zhao (Springer Berlin Heidelberg, Berlin, Heidelberg, 2004) pp. 517–536.
- ¹⁵⁷H. Iwata and K. M. Itoh, *Materials Science Forum* **338–342**, 729 (2000).
- ¹⁵⁸H. Iwata, K. M. Itoh, and G. Pensl, *Journal of Applied Physics* **88**, 1956 (2000).
- ¹⁵⁹N. Wright, in *IEE Colloquium on New Developments in Power Semiconductor Devices*, Vol. 1996 (IEE, London, UK, 1996) pp. 6–6.
- ¹⁶⁰H.-E. Nilsson, U. Sannemo, and C. S. Petersson, *Journal of Applied Physics* **80**, 3365 (1996).
- ¹⁶¹I. Neila Inglesias, “APPLYING NUMERICAL SIMULATION TO MODELS SiC SEMICONDUCTOR DEVICES,” (2012).
- ¹⁶²T. Kimoto, *Japanese Journal of Applied Physics* **54**, 040103 (2015).
- ¹⁶³J. Zhao, X. Li, K. Tone, P. Alexandrov, M. Pan, and M. Weiner, *Solid-State Electronics* **47**, 377 (2003).
- ¹⁶⁴A. Elasser, M. Kheraluwala, M. Ghezzo, R. Steigerwald, N. Evers, J. Kretchmer, and T. Chow, *IEEE Transactions on Industry Applications* **39**, 915 (2003).
- ¹⁶⁵A. Elasser, M. Ghezzo, N. Krishnamurthy, J. Kretchmer, A. Clock, D. Brown, and T. Chow, *Solid-State Electronics* **44**, 317 (2000).
- ¹⁶⁶V. Chelnokov and A. Syrkin, *Materials Science and Engineering: B* **46**, 248 (1997).
- ¹⁶⁷F. L. L. Nouketcha, Y. Cui, A. Lelis, R. Green, C. Darmody, J. Schuster, and N. Goldsman, *IEEE Transactions on Electron Devices* **67**, 3999 (2020).
- ¹⁶⁸A. A. Lebedev, *Radiation Effects in Silicon Carbide*, Materials Research Foundations No. volume 6 (2017) (Materials Research Forum LLC, Millersville, PA, USA, 2017).

- ¹⁶⁹T. P. Chow, I. Omura, M. Higashiwaki, H. Kawarada, and V. Pala, *IEEE Transactions on Electron Devices* **64**, 856 (2017).
- ¹⁷⁰J. A. Pellish and L. M. Cohn, in *Extreme Environment Electronics* (CRC Press, Taylor & Francis Group, 2013) pp. 49–58.
- ¹⁷¹S. M. Sze and K. K. Ng, *Physics of Semiconductor Devices*, 3rd ed. (Wiley-Interscience, Hoboken, N.J, 2007).
- ¹⁷²J. Millán, *IET Circuits, Devices & Systems* **1**, 372 (2007).
- ¹⁷³A. Pérez-Tomás, P. Brosselard, P. Godignon, J. Millán, N. Mestres, M. R. Jennings, J. A. Covington, and P. A. Mawby, *Journal of Applied Physics* **100**, 114508 (2006).
- ¹⁷⁴T. P. Chow, N. Ramungul, J. Fedison, and Y. Tang, in *Silicon Carbide*, edited by W. J. Choyke, H. Matsunami, and G. Pensl (Springer Berlin Heidelberg, Berlin, Heidelberg, 2004) pp. 737–767.
- ¹⁷⁵N. Zhang, *High Voltage GaN HEMTs with Low On-Resistance for Switching Applications*, Ph.D. thesis, UNIVERSITY of CALIFORNIA, Santa Barbara (2002).
- ¹⁷⁶R. Trew, *Proceedings of the IEEE* **90**, 1032 (2002).
- ¹⁷⁷S. K. Lee, *Processing and Characterization of Silicon Carbide (6H-SiC and 4H-SiC) Contacts for High Power and h...* (Mikroelektronik och informationsteknik, Kista, 2002).
- ¹⁷⁸R. Kemerley, H. Wallace, and M. Yoder, *Proceedings of the IEEE* **90**, 1059 (2002).
- ¹⁷⁹V. Dmitriev, T. P. Chow, S. P. DenBaars, M. S. Shur, and M. G. Spencer, “*High-Temperature Electronics in Europe;*” Tech. Rep. (Defense Technical Information Center, Fort Belvoir, VA, 2000).
- ¹⁸⁰T. Chow, V. Khemka, J. Fedison, N. Ramungul, K. Matocha, Y. Tang, and R. Gutmann, *Solid-State Electronics* **44**, 277 (2000).
- ¹⁸¹C. M. Zetterling, M. Östling, C. I. Harris, N. Nordell, K. Wongchotigul, and M. G. Spencer, *Materials Science Forum* **264–268**, 877 (1998).
- ¹⁸²P. B. Shah and K. A. Jones, *Journal of Applied Physics* **84**, 4625 (1998).
- ¹⁸³M. Roschke, F. Schwierz, G. Paasch, and D. Schipanski, *Materials Science Forum* **264–268**, 965 (1998).
- ¹⁸⁴E. Danielsson, C. I. Harris, C. M. Zetterling, and M. Östling, *Materials Science Forum* **264–268**, 805 (1998).
- ¹⁸⁵T. P. Chow, N. Ramungul, and M. Ghezzo, *MRS Proceedings* **483**, 89 (1997).
- ¹⁸⁶T. P. Chow and M. Ghezzo, *MRS Proceedings* **423**, 9 (1996).

- ¹⁸⁷B. Ozpineci, “Comparison of Wide-Bandgap Semiconductors for Power Electronics Applications,” Tech. Rep. ORNL/TM-2003/257, 885849 (Oak Ridge National Laboratory, 2004).
- ¹⁸⁸F. Bechstedt, *Materials Science Forum* **264–268**, 265 (1998).
- ¹⁸⁹W. M. Chen, N. T. Son, E. Janzén, D. M. Hofmann, and B. K. Meyer, *physica status solidi (a)* **162**, 79 (1997).
- ¹⁹⁰Y. M. Tairov and Y. A. Vodakov, in *Electroluminescence*, Vol. 17, edited by J. I. Pankove (Springer Berlin Heidelberg, Berlin, Heidelberg, 1977) pp. 31–61.
- ¹⁹¹G. Wellenhofer and U. Rössler, *physica status solidi (b)* **202**, 107 (1997).
- ¹⁹²N. T. Son, P. N. Hai, W. M. Chen, C. Hallin, B. Monemar, and E. Janzén, *Physical Review B* **61**, R10544 (2000).
- ¹⁹³C. Persson and U. Lindefelt, *Physical Review B* **54**, 10257 (1996).
- ¹⁹⁴K. Karch, G. Wellenhofer, P. Pavone, U. Rössler, and D. Strauch, “Structural and electronic properties of SiC polytypes,” (1995).
- ¹⁹⁵J. Dong and A.-B. Chen, in *SiC Power Materials*, Vol. 73, edited by R. Hull, R. M. Osgood, J. Parisi, H. Warlimont, and Z. C. Feng (Springer Berlin Heidelberg, Berlin, Heidelberg, 2004) pp. 63–87.
- ¹⁹⁶H. P. Iwata, U. Lindefelt, S. Öberg, and P. R. Briddon, *Physical Review B* **68**, 245309 (2003).
- ¹⁹⁷S. Nakashima and H. Harima, *physica status solidi (a)* **162**, 39 (1997).
- ¹⁹⁸Y. Kuroiwa, Y.-i. Matsushita, K. Harada, and F. Oba, *Applied Physics Letters* **115**, 112102 (2019).
- ¹⁹⁹W. Lambrecht, S. Limpijumnong, S. Rashkeev, and B. Segall, *physica status solidi (b)* **202**, 5 (1997).
- ²⁰⁰C. Raynaud, D. Tournier, H. Morel, and D. Planson, *Diamond and Related Materials* **19**, 1 (2010).
- ²⁰¹J. Blakemore, *Semiconductor Statistics* (Elsevier, 1962).
- ²⁰²W. Götz, A. Schöner, G. Pensl, W. Suttrop, W. J. Choyke, R. Stein, and S. Leibenzeder, *Journal of Applied Physics* **73**, 3332 (1993).
- ²⁰³W. Suttrop, *Aluminium, Bor und Stickstoff als Dotierstoffe in einkristallinem Siliziumkarbid SiC(6H)*, Ph.D. thesis, Friedrich-Alexander-Universität, Erlangen-Nürnberg (1991).
- ²⁰⁴C. Hemmingsson, N. T. Son, O. Kordina, J. P. Bergman, E. Janzén, J. L. Lindström, S. Savage, and N. Nordell, *Journal of Applied Physics* **81**, 6155 (1997).
- ²⁰⁵P. Ščajev, M. Karaliūnas, E. Kuokštis, and K. Jarašiūnas,

- Journal of Luminescence **134**, 588 (2013).
- ²⁰⁶V. K. Khanna, *Extreme-Temperature and Harsh-Environment Electronics: Physics, Technology and Applications*, second edition ed. (IOP Publishing, Bristol [England] (Temple Circus, Temple Way, Bristol BS1 6HG, UK), 2023).
- ²⁰⁷R. Ishikawa, M. Hara, H. Tanaka, M. Kaneko, and T. Kimoto, *Applied Physics Express* **14**, 061005 (2021).
- ²⁰⁸R. Ishikawa, H. Tanaka, M. Kaneko, and T. Kimoto, *Journal of Applied Physics* **135**, 075704 (2024).
- ²⁰⁹H. P. Iwata, *Applied Physics Letters* **82**, 598 (2003).
- ²¹⁰T. Kinoshita, K. M. Itoh, J. Muto, M. Schadt, G. Pensl, and K. Takeda, *Materials Science Forum* **264–268**, 295 (1998).
- ²¹¹O. Kordina, A. Henry, J. P. Bergman, N. T. Son, W. M. Chen, C. Hallin, and E. Janzén, *Applied Physics Letters* **66**, 1373 (1995).
- ²¹²J. Camassel and S. Juillaquet, *physica status solidi (b)* **245**, 1337 (2008).
- ²¹³J. T. Devreese, in *Digital Encyclopedia of Applied Physics*, edited by Wiley-VCH Verlag GmbH & Co. KGaA (Wiley, 2003) 1st ed.
- ²¹⁴G. D. Mahan, *Many-Particle Physics* (Springer US, Boston, MA, 1990).
- ²¹⁵H. Fröhlich, *Advances in Physics* **3**, 325 (1954).
- ²¹⁶K. Takahashi, A. Yoshikawa, and A. Sandhu, eds., *Wide Bandgap Semiconductors* (Springer Berlin Heidelberg, Berlin, Heidelberg, 2007).
- ²¹⁷K. Mikami, M. Kaneko, and T. Kimoto, *IEEE Electron Device Letters* , 1 (2024).
- ²¹⁸N. T. Son, W. M. Chen, O. Kordina, A. O. Konstantinov, B. Monemar, E. Janzén, D. M. Hofmann, D. Volm, M. Drechsler, and B. K. Meyer, *Applied Physics Letters* **66**, 1074 (1995).
- ²¹⁹P. Käckell, B. Wenzien, and F. Bechstedt, *Physical Review B* **50**, 10761 (1994).
- ²²⁰L. Lu, H. Zhang, X. Wu, J. Shi, and Y.-Y. Sun, *Chinese Physics B* **30**, 096806 (2021).
- ²²¹C. Persson and U. Lindefelt, *Journal of Applied Physics* **86**, 5036 (1999).
- ²²²G. L. Zhao and D. Bagayoko, *New Journal of Physics* **2**, 16 (2000).
- ²²³W. R. L. Lambrecht and B. Segall, *Physical Review B* **52**, R2249 (1995).
- ²²⁴A.-B. Chen and P. Srichaikul, *physica status solidi (b)* **202**, 81 (1997).
- ²²⁵G. Pennington and N. Goldsman, *Physical Review B* **64**, 045104 (2001).
- ²²⁶D. Volm, B. K. Meyer, D. M. Hofmann, W. M. Chen, N. T. Son, C. Persson, U. Lindefelt, O. Kordina, E. Sörman, A. O. Konstantinov, B. Monemar, and E. Janzén,

- Physical Review B **53**, 15409 (1996).
- ²²⁷C. Persson and U. Lindefelt, Journal of Applied Physics **83**, 266 (1998).
- ²²⁸G. Ng, *Computational Studies of 4H and 6H Silicon Carbide*, Ph.D. thesis, Arizona State University (2010).
- ²²⁹G. Ng, D. Vasileska, and D. Schroder, Superlattices and Microstructures **49**, 109 (2011).
- ²³⁰N. T. Son, P. Hai, W. Chen, C. Hallin, B. Monemar, and E. Janzén, Materials Science Forum **338–342**, 563 (2000).
- ²³¹G. Lomakina and Y. A. Vodakov, Sov. Phys. Solid State **15**, 83 (1973).
- ²³²G. Lomakina, in *In: Silicon Carbide-1973; Proceedings of the Third International Conference* (1974) pp. 520–526.
- ²³³L. Patrick, W. J. Choyke, and D. R. Hamilton, Physical Review **137**, A1515 (1965).
- ²³⁴M. Schadt, G. Pensl, R. P. Devaty, W. J. Choyke, R. Stein, and D. Stephani, Applied Physics Letters **65**, 3120 (1994).
- ²³⁵G. Pensl and W. Choyke, Physica B: Condensed Matter **185**, 264 (1993).
- ²³⁶A. Itoh, T. Kimoto, and H. Matsunami, IEEE Electron Device Letters **16**, 280 (1995).
- ²³⁷P. A. Ivanov, M. E. Levenshtein, J. W. Palmour, S. L. Rumyantsev, and R. Singh, Semiconductor Science and Technology **15**, 908 (2000).
- ²³⁸S. I. Maximenko, AIP Advances **13**, 105021 (2023).
- ²³⁹J. Pernot, S. Contreras, J. Camassel, J. L. Robert, W. Zawadzki, E. Neyret, and L. Di Cioccio, Applied Physics Letters **77**, 4359 (2000).
- ²⁴⁰G. Pennington and N. Goldsman, Journal of Applied Physics **95**, 4223 (2004).
- ²⁴¹V. Tilak, K. Matocha, and G. Dunne, IEEE Transactions on Electron Devices **54**, 2823 (2007).
- ²⁴²R. A. Faulkner, Physical Review **184**, 713 (1969).
- ²⁴³A. Yang, K. Murata, T. Miyazawa, T. Tawara, and H. Tsuchida, Journal of Applied Physics **126**, 055103 (2019).
- ²⁴⁴N. Kuznetsov and A. Zubrilov, Materials Science and Engineering: B **29**, 181 (1995).
- ²⁴⁵C. Persson, U. Lindefelt, and B. E. Sernelius, Physical Review B **60**, 16479 (1999).
- ²⁴⁶R. P. Joshi, Journal of Applied Physics **78**, 5518 (1995).
- ²⁴⁷S. Rakheja, L. Huang, S. Hau-Riege, S. E. Harrison, L. F. Voss, and A. M. Conway, IEEE Journal of the Electron Devices Society **8**, 1118 (2020).
- ²⁴⁸Y. Negoro, K. Katsumoto, T. Kimoto, and H. Matsunami, Journal of Applied Physics **96**, 224 (2004).

- ²⁴⁹Z. C. Feng and J. H. Zhao, eds., *Silicon Carbide: Materials, Processing, and Devices*, Opto-electronic Properties of Semiconductors and Superlattices No. v. 20 (Taylor & Francis, New York, 2004).
- ²⁵⁰C. Q. Chen, J. Zeman, F. Engelbrecht, C. Peppermüller, R. Helbig, Z. H. Chen, and G. Martinez, *Journal of Applied Physics* **87**, 3800 (2000).
- ²⁵¹R. P. Devaty and W. J. Choyke, *physica status solidi (a)* **162**, 5 (1997).
- ²⁵²K. Neimontas, T. Malinauskas, R. Aleksiejūnas, M. Sūdžius, K. Jarašiūnas, L. Storasta, J. P. Bergman, and E. Janzen, *Semiconductor Science and Technology* **21**, 952 (2006).
- ²⁵³M. Flores, F. Maia, V. Freire, J. Da Costa, and E. Da Silva, *Microelectronics Journal* **34**, 717 (2003).
- ²⁵⁴H. Van Daal, W. Knippenberg, and J. Wasscher, *Journal of Physics and Chemistry of Solids* **24**, 109 (1963).
- ²⁵⁵A. Galeckas, J. Linnros, V. Grivickas, U. Lindefelt, and C. Hallin, *Applied Physics Letters* **71**, 3269 (1997).
- ²⁵⁶S. G. Sridhara, L. L. Clemen, R. P. Devaty, W. J. Choyke, D. J. Larkin, H. S. Kong, T. Troffer, and G. Pensl, *Journal of Applied Physics* **83**, 7909 (1998).
- ²⁵⁷F. C. Beyer, *Deep Levels in SiC*, Ph.D. thesis, Linköping University (2011).
- ²⁵⁸A. Gsponer, M. Knopf, P. Gaggl, J. Burin, S. Waid, and T. Bergauer, *Nuclear Instruments and Methods in Physics Research Section A: Accelerators, Spectrometers, Detectors and Associated Equipment* **457**, 1 (2001).
- ²⁵⁹P. Kwasnicki, *Evaluation of Doping in 4H-SiC by Optical Spectroscopies*, Ph.D. thesis, UNIVERSITE MONTPELLIER II (2014).
- ²⁶⁰D. K. Schroder, *Semiconductor Material and Device Characterization*, 1st ed. (Wiley, 2005).
- ²⁶¹J. P. Wolfe and A. Mysyrowicz, *Scientific American* **250**, 98 (1984), 24969326.
- ²⁶²R. J. Elliott, *Physical Review* **108**, 1384 (1957).
- ²⁶³W. Choyke, in *Silicon Carbide—1968* (Elsevier, 1969) pp. S141–S152.
- ²⁶⁴Ch. Haberstroh, R. Helbig, and R. A. Stein, *Journal of Applied Physics* **76**, 509 (1994).
- ²⁶⁵A. Itoh, H. Akita, T. Kimoto, and H. Matsunami, *Applied Physics Letters* **65**, 1400 (1994).
- ²⁶⁶A. Itoh, T. K. Tsunenobu Kimoto, and H. M. Hiroyuki Matsunami, *Japanese Journal of Applied Physics* **35**, 4373 (1996).
- ²⁶⁷M. Ikeda and H. Matsunami, *Physica Status Solidi (a)* **58**, 657 (1980).
- ²⁶⁸G. B. Dubrovskii and V. I. Sankin, Sov. Phys. Solid State **17**, 1847 (1975).
- ²⁶⁹W. J. Choyke, L. Patrick, and D. Hamilton, 7th in conference on semicond. physics paris 1964,

- 7, 751 (1964).
- ²⁷⁰W. J. Choyke, D. R. Hamilton, and L. Patrick, *Physical Review* **133**, A1163 (1964).
- ²⁷¹G. Zanmarchi, 7th in conference on semicond. physics paris 1964, **7**, 57 (1964).
- ²⁷²W. J. Choyke, H. Matsunami, and G. Pensl, eds., *Silicon Carbide: Recent Major Advances*, Advanced Texts in Physics (Springer Berlin Heidelberg, Berlin, Heidelberg, 2004).
- ²⁷³R. Freer, ed., *The Physics and Chemistry of Carbides, Nitrides and Borides* (Springer Netherlands, Dordrecht, 1990).
- ²⁷⁴H. Habib, N. G. Wright, and A. B. Horsfall, *Advanced Materials Research* **413**, 229 (2011).
- ²⁷⁵H. Y. Fan, *Physical Review* **82**, 900 (1951).
- ²⁷⁶A. Das and S. P. Duttagupta, *Radiation Protection Dosimetry* **167**, 443 (2015).
- ²⁷⁷R. Pässler, *physica status solidi (b)* **200**, 155 (1997).
- ²⁷⁸R. Pässler, *Journal of Applied Physics* **83**, 3356 (1998).
- ²⁷⁹A. Galeckas, P. Grivickas, V. Grivickas, V. Bikbajevs, and J. Linnros, *physica status solidi (a)* **191**, 613 (2002).
- ²⁸⁰R. Pässler, *Physical Review B* **66**, 085201 (2002).
- ²⁸¹K. P. O'Donnell and X. Chen, *Applied Physics Letters* **58**, 2924 (1991).
- ²⁸²Y. P. Varshni, *Physica* **34**, 149 (1967).
- ²⁸³S. Balachandran, T. P. Chow, and A. K. Agarwal, *Materials Science Forum* **483–485**, 909 (2005).
- ²⁸⁴M. Nawaz, *Microelectronics Journal* **41**, 801 (2010).
- ²⁸⁵P. Grivickas, V. Grivickas, J. Linnros, and A. Galeckas, *Journal of Applied Physics* **101**, 123521 (2007).
- ²⁸⁶R. Pässler, *physica status solidi (b)* **216**, 975 (1999).
- ²⁸⁷L. Viña, S. Logothetidis, and M. Cardona, *Physical Review B* **30**, 1979 (1984).
- ²⁸⁸R. Pässler, *physica status solidi (b)* **236**, 710 (2003).
- ²⁸⁹E. F. Schubert, *Doping in III-V Semiconductors*, Cambridge Studies in Semiconductor Physics and Microelectronic Engineering No. 1 (Cambridge University Press, Cambridge [England] ; New York, NY, USA, 1993).
- ²⁹⁰S. Jain and D. Roulston, *Solid-State Electronics* **34**, 453 (1991).
- ²⁹¹G. Donnarumma, V. Palankovski, and S. Selberherr, in *Proceedings of the International Conference on Simulation of Semiconductor Processes and Devices (SISPAD)* (2012) pp. 125–128.
- ²⁹²M. Ruff, H. Mitlehner, and R. Helbig, *IEEE Transactions on Electron Devices* **41**, 1040 (1994).

- ²⁹³M. K. Mainali, P. Dulal, B. Shrestha, E. Amonette, A. Shan, and N. J. Podraza, *Surface Science Spectra* **31**, 026003 (2024).
- ²⁹⁴W. J. Choyke and L. Patrick, *Physical Review* **105**, 1721 (1957).
- ²⁹⁵A. O. Ewvaraye, S. R. Smith, and W. C. Mitchel, *Journal of Applied Physics* **79**, 7726 (1996).
- ²⁹⁶I. G. Ivanov, U. Lindefelt, A. Henry, O. Kordina, C. Hallin, M. Aroyo, T. Egilsson, and E. Janzén, *Physical Review B* **58**, 13634 (1998).
- ²⁹⁷I. G. Ivanov, J. Zhang, L. Storasta, and E. Janzén, *Materials Science Forum* **389–393**, 613 (2002).
- ²⁹⁸S. Sridhara, S. Bai, O. Shigiltchoff, R. P. Devaty, and W. J. Choyke, *Materials Science Forum* **338–342**, 567 (2000).
- ²⁹⁹D. Stefanakis and K. Zekentes, *Microelectronic Engineering* **116**, 65 (2014).
- ³⁰⁰W. H. Backes, P. A. Bobbert, and W. Van Haeringen, *Physical Review B* **49**, 7564 (1994).
- ³⁰¹H.-g. Junginger and W. Van Haeringen, *physica status solidi (b)* **37**, 709 (1970).
- ³⁰²W. Van Haeringen, P. Bobbert, and W. Backes, *physica status solidi (b)* **202**, 63 (1997).
- ³⁰³K. Yamaguchi, D. Kobayashi, T. Yamamoto, and K. Hirose, *Physica B: Condensed Matter* **532**, 99 (2018).
- ³⁰⁴G. B. Dubrovskii and A. A. Lepneva, *Sov. Phys. Solid State* **19**, 729 (1977).
- ³⁰⁵I. Shalish, I. B. Altfeder, and V. Narayananamurti, *Physical Review B* **65**, 073104 (2002).
- ³⁰⁶Explanation see text.
- ³⁰⁷According to shown band gap the data were extract from a 21R-SiC device although in⁶⁹ argued that it was 6H.
- ³⁰⁸Solely measurement for lowest temperature shown.
- ³⁰⁹V. I. Gavrilenko, A. V. Postnikov, N. I. Klyui, and V. G. Litovchenko, *physica status solidi (b)* **162**, 477 (1990).
- ³¹⁰C. H. Park, B.-H. Cheong, K.-H. Lee, and K. J. Chang, *Physical Review B* **49**, 4485 (1994).
- ³¹¹J. Käckel, *Siliziumkarbid - Strukturelle und elektronische Eigenschaften verschiedener Polytypen*, Ph.D. thesis, Friedrich-Schiller-Universität Jena (1996).
- ³¹²Model fitted to 6H-SiC results in⁷⁵⁸.
- ³¹³Model fitted to results in²⁶³.
- ³¹⁴Origin of Varshni parameters unknown.
- ³¹⁵T. Tamaki, G. G. Walden, Y. Sui, and J. A. Cooper, *IEEE Transactions on Electron Devices* **55**, 1920 (2008).

- ³¹⁶Y. Huang, R. Wang, Y. Zhang, D. Yang, and X. Pi, *Journal of Applied Physics* **131**, 185703 (2022).
- ³¹⁷S. Hagen, A. Van Kemenade, and J. Van Der Does De Bye, *Journal of Luminescence* **8**, 18 (1973).
- ³¹⁸F. Nallet, D. Planson, K. Isoird, M. Locatelli, and J. Chante, in *CAS '99 Proceedings. 1999 International Semiconductor Conference (Cat. No.99TH8389)*, Vol. 1 (IEEE, Sinaia, Romania, 1999) pp. 195–198.
- ³¹⁹R. Weingärtner, P. J. Wellmann, M. Bickermann, D. Hofmann, T. L. Straubinger, and A. Winacker, *Applied Physics Letters* **80**, 70 (2002).
- ³²⁰N. Lophitis, A. Arvanitopoulos, S. Perkins, and M. Antoniou, in *Disruptive Wide Bandgap Semiconductors, Related Technologies, and Their Applications*, edited by Y. K. Sharma (InTech, 2018).
- ³²¹P. Wellmann, S. Bushevoy, and R. Weingärtner, *Materials Science and Engineering: B* **80**, 352 (2001).
- ³²²H.-Y. Cha and P. M. Sandvik, *Japanese Journal of Applied Physics* **47**, 5423 (2008).
- ³²³B. Chen, Y. Yang, X. Xie, N. Wang, Z. Ma, K. Song, and X. Zhang, *Chinese Science Bulletin* **57**, 4427 (2012).
- ³²⁴Y.-R. Zhang, B. Zhang, Z.-J. Li, and X.-C. Deng, *Chinese Physics B* **19**, 067102 (2010).
- ³²⁵B. Buono, *Simulation and Characterization of Silicon Carbide Power Bipolar Junction Transistors*, Ph.D. thesis, KTH Royal Institute of Technology (2012).
- ³²⁶K. Zeghdar, L. Dehimi, F. Pezzimenti, S. Rao, and F. G. Della Corte, *Japanese Journal of Applied Physics* **58**, 014002 (2019).
- ³²⁷K. Zeghdar, L. Dehimi, F. Pezzimenti, M. L. Megherbi, and F. G. Della Corte, *Journal of Electronic Materials* **49**, 1322 (2020).
- ³²⁸D. Johannesson and M. Nawaz, *IEEE Transactions on Power Electronics* **31**, 4517 (2016).
- ³²⁹H. Lanyon and R. Tuft, *IEEE Transactions on Electron Devices* **26**, 1014 (1979).
- ³³⁰H. Liu, J. Wang, S. Liang, H. Yu, and W. Deng, *Semiconductor Science and Technology* **36**, 025009 (2021).
- ³³¹V. Uhnevionak, *Simulation and Modeling of Silicon-Carbide Devices*, Ph.D. thesis, Friedrich-Alexander-Universität (2015).
- ³³²J. Lutz, U. Scheuermann, H. Schlangenotto, and R. De Doncker, “Power Semiconductor Devices—Key Components for Efficient Electrical Energy Conversion Systems,” in *Semiconductor Power Devices* (Springer International Publishing, Cham, 2018) pp. 1–20.

- ³³³J. Lutz, H. Schlangenotto, U. Scheuermann, and R. De Doncker, *Semiconductor Power Devices: Physics, Characteristics, Reliability* (Springer Berlin Heidelberg, Berlin, Heidelberg, 2011).
- ³³⁴M. Jiménez-Ramos, A. García Osuna, M. Rodriguez-Ramos, E. Viezzer, G. Pellegrini, P. Godignon, J. Rafí, G. Rius, and J. García López, *Radiation Physics and Chemistry* **214**, 111283 (2024).
- ³³⁵T. R. Garcia, A. Kumar, B. Reinke, T. E. Blue, and W. Windl, *Applied Physics Letters* **103**, 152108 (2013).
- ³³⁶P. Masri, *Surface Science Reports* **48**, 1 (2002).
- ³³⁷J. A. Freitas, in *Properties of Silicon Carbide*, EMIS Datareviews Series No. 13, edited by G. L. Harris and Inspec (INSPEC, the Inst. of Electrical Engineers, London, 1995) pp. 29–41.
- ³³⁸X. Li, Y. Luo, L. Fursin, J. Zhao, M. Pan, P. Alexandrov, and M. Weiner, *Solid-State Electronics* **47**, 233 (2003).
- ³³⁹T. Egilsson, I. G. Ivanov, N. T. Son, G. Henry, A., J. P. Bergman, and E. Janzén, in *Silicon Carbide*, edited by Z. C. Feng and J. H. Zhao (Springer Berlin Heidelberg, Berlin, Heidelberg, 2004) pp. 517–536.
- ³⁴⁰R. C. Marshall, J. W. Faust, C. E. Ryan, A. F. C. R. L. (U.S.), and University of South Carolina, eds., *Silicon Carbide—1973: Proceedings*, 1st ed. (University of South Carolina Press, Columbia, 1974).
- ³⁴¹S. Sandeep and R. Komaragiri, in *India International Conference on Power Electronics 2010 (IICPE2010)* (IEEE, New Delhi, India, 2011) pp. 1–5.
- ³⁴²B. Zat’ko, L. Hrubčín, A. Šagátová, J. Osvald, P. Boháček, E. Kováčová, Y. Halahovets, S. V. Rozov, and V. Sandukovskij, *Applied Surface Science* **536**, 147801 (2021).
- ³⁴³G. Rescher, G. Pobegen, T. Aichinger, and T. Grasser, *IEEE Transactions on Electron Devices* **65**, 1419 (2018).
- ³⁴⁴D. T. Morisette, *Development of Robust Power Schottky Barrier Diodes in Silicon Carbide*, Ph.D. thesis, Purdue University (2001).
- ³⁴⁵J. Hudgins, G. Simin, E. Santi, and M. Khan, *IEEE Transactions on Power Electronics* **18**, 907 (2003).
- ³⁴⁶K. C. Mandal, P. G. Muzykov, R. M. Krishna, and J. R. Terry, *IEEE Transactions on Nuclear Science* **59**, 1591 (2012).
- ³⁴⁷V. V. Afanas’ev, M. Bassler, G. Pensl, M. J. Schulz, and E. Stein Von Kamienski, *Journal of Applied Physics* **79**, 3108 (1996).

- ³⁴⁸M. Shur, S. L. Rumyantsev, and M. E. Levinshtein, eds., *SiC Materials and Devices*, Selected Topics in Electronics and Systems No. v. 40 (World Scientific, New Jersey ; London, 2006).
- ³⁴⁹S. J. Bader, H. Lee, R. Chaudhuri, S. Huang, A. Hickman, A. Molnar, H. G. Xing, D. Jena, H. W. Then, N. Chowdhury, and T. Palacios, [IEEE Transactions on Electron Devices](#) **67**, 4010 (2020).
- ³⁵⁰D. Mukherjee and M. Neto, *Recent Advances in SiC/Diamond Composite Devices* (IOP Publishing, 2023).
- ³⁵¹X. Guo, Q. Xun, Z. Li, and S. Du, [Micromachines](#) **10**, 406 (2019).
- ³⁵²H. A. Mantooth, K. Peng, E. Santi, and J. L. Hudgins, [IEEE Transactions on Electron Devices](#) **62**, 423 (2015).
- ³⁵³J. D. Cressler and H. A. Mantooth, *Extreme Environment Electronics* (CRC Press, Taylor & Francis Group, Boca Raton, 2013).
- ³⁵⁴M. B. J. Wijesundara and R. G. Azevedo, “System Integration,” in *Silicon Carbide Microsystems for Harsh Environments*, Vol. 22 (Springer New York, New York, NY, 2011) pp. 189–230.
- ³⁵⁵V. Cimalla, J. Pezoldt, and O. Ambacher, [Journal of Physics D: Applied Physics](#) **40**, S19 (2007).
- ³⁵⁶M. J. Kumar and V. Parihar, [Microelectronic Engineering](#) **81**, 90 (2005).
- ³⁵⁷K. Bertilsson, *Simulation and Optimization of SiC Field Effect Transistors*, Ph.D. thesis, Mikroelektronik och informationsteknik / KTH, Microelectronics and Information Technology, IMIT / KTH, Microelectronics and Information Technology, IMIT (2004).
- ³⁵⁸A. Powell and L. Rowland, [Proceedings of the IEEE](#) **90**, 942 (2002).
- ³⁵⁹Y. Gao, S. I. Soloviev, T. S. Sudarshan, and C.-C. Tin, [Journal of Applied Physics](#) **90**, 5647 (2001).
- ³⁶⁰A. A. Lebedev, [Semiconductors](#) **33**, 107 (1999).
- ³⁶¹R. J. Trew, [physica status solidi \(a\)](#) **162**, 409 (1997).
- ³⁶²P. G. Neudeck, [Journal of Electronic Materials](#) **24**, 283 (1995).
- ³⁶³R. Karsthof, M. E. Bathen, A. Galeckas, and L. Vines, [Physical Review B](#) **102**, 184111 (2020).
- ³⁶⁴G. Lioliou, M. Mazzillo, A. Sciuto, and A. Barnett, [Optics Express](#) **23**, 21657 (2015).
- ³⁶⁵P. B. Klein, [physica status solidi \(a\)](#) **206**, 2257 (2009).
- ³⁶⁶D. Werber, P. Borthen, and G. Wachutka, [Materials Science Forum](#) **556–557**, 905 (2007).
- ³⁶⁷P. Ščajev, V. Gudelis, K. Jarašiūnas, and P. B. Klein, [Journal of Applied Physics](#) **108**, 023705 (2010).

- ³⁶⁸B. Ng, J. David, D. Massey, R. Tozer, G. Rees, F. Yan, J. H. Zhao, and M. Weiner, *Materials Science Forum* **457–460**, 1069 (2004).
- ³⁶⁹A. Agarwal, S. Seshadri, J. Casady, S. Mani, M. MacMillan, N. Saks, A. Burk, G. Augustine, V. Balakrishna, P. Sanger, C. Brandt, and R. Rodrigues, *Diamond and Related Materials* **8**, 295 (1999).
- ³⁷⁰J. Shenoy, J. Cooper, and M. Melloch, *IEEE Electron Device Letters* **18**, 93 (1997).
- ³⁷¹A. Agarwal, G. Augustine, V. Balakrishna, C. Brandt, A. Burk, Li-Shu Chen, R. Clarke, P. Esker, H. Hobgood, R. Hopkins, A. Morse, L. Rowland, S. Seshadri, R. Siergiej, T. Smith, and S. Sriram, in *International Electron Devices Meeting. Technical Digest* (IEEE, San Francisco, CA, USA, 1996) pp. 225–230.
- ³⁷²Wolfspeed, “Silicon Carbide and Nitride Materials Catalog,” (2023).
- ³⁷³C. Langpoklakpam, A.-C. Liu, K.-H. Chu, L.-H. Hsu, W.-C. Lee, S.-C. Chen, C.-W. Sun, M.-H. Shih, K.-Y. Lee, and H.-C. Kuo, *Crystals* **12**, 245 (2022).
- ³⁷⁴I. Capan, *Electronics* **11**, 532 (2022).
- ³⁷⁵J. V. Berens, *Carrier Mobility and Reliability of 4H-SiC Trench MOSFETs*, Ph.D. thesis, TU Wien (2021).
- ³⁷⁶H. Matsunami, *Proceedings of the Japan Academy, Series B* **96**, 235 (2020).
- ³⁷⁷D. Johannesson, M. Nawaz, and H. P. Nee, *Materials Science Forum* **963**, 670 (2019).
- ³⁷⁸G. Rescher, *Behavior of SiC-MOSFETs under Temperature and Voltage Stress*, Ph.D. thesis, TU Wien (2018).
- ³⁷⁹S. Chowdhury, C. Hitchcock, R. Dahal, I. B. Bhat, and T. P. Chow, in *2015 IEEE 27th International Symposium on Power Semiconductor Devices & IC's (ISPSD)* (IEEE, Hong Kong, China, 2015) pp. 353–356.
- ³⁸⁰M. B. J. Wijesundara and R. G. Azevedo, “Introduction,” in *Silicon Carbide Microsystems for Harsh Environments*, Vol. 22 (Springer New York, New York, NY, 2011) pp. 1–32.
- ³⁸¹V. R. Manikam and Kuan Yew Cheong, *IEEE Transactions on Components, Packaging and Manufacturing* (2004).
- ³⁸²R. Gerhardt, ed., *Properties and Applications of Silicon Carbide* (IntechOpen, 2011).
- ³⁸³C. M. Tanner, J. Choi, and J. P. Chang, *Journal of Applied Physics* **101**, 034108 (2007).
- ³⁸⁴M. Willander, M. Friesel, Q.-u. Wahab, and B. Straumal, *Journal of Materials Science: Materials in Electronics* **17**, 1 (2006).
- ³⁸⁵M. Philip and A. O'Neill, in *2006 Conference on Optoelectronic and Microelectronic Materials and Device* (2006).

- (IEEE, Perth, Australia, 2006) pp. 137–140.
- ³⁸⁶T. P. Chow, *Microelectronic Engineering* **83**, 112 (2006).
- ³⁸⁷S. Dhar, Y. W. Song, L. C. Feldman, T. Isaacs-Smith, C. C. Tin, J. R. Williams, G. Chung, T. Nishimura, D. Starodub, T. Gustafsson, and E. Garfunkel, *Applied Physics Letters* **84**, 1498 (2004).
- ³⁸⁸J. Kohlscheen, Y. N. Emirov, M. M. Beerbom, J. T. Wolan, S. E. Saddow, G. Chung, M. F. MacMillan, and R. Schlaf, *Journal of Applied Physics* **94**, 3931 (2003).
- ³⁸⁹M. Werner and W. Fahrner, *IEEE Transactions on Industrial Electronics* **48**, 249 (2001).
- ³⁹⁰A. Hefner, R. Singh, Jih-Sheg Lai, D. Berning, S. Bouche, and C. Chapuy, *IEEE Transactions on Power Electronics* **16**, 273 (2001).
- ³⁹¹H. Matsunami and T. Kimoto, *Materials Science and Engineering: R: Reports* **20**, 125 (1997).
- ³⁹²M. V. Rao, J. B. Tucker, M. C. Ridgway, O. W. Holland, N. Papanicolaou, and J. Mittereder, *Journal of Applied Physics* **86**, 752 (1999).
- ³⁹³D. Baierhofer, in *ESSDERC 2019 - 49th European Solid-State Device Research Conference (ESSDERC)* (IEEE, Cracow, Poland, 2019) pp. 31–34.
- ³⁹⁴J. W. Kleppinger, S. K. Chaudhuri, O. Karadavut, and K. C. Mandal, *Journal of Applied Physics* **129**, 244501 (2021).
- ³⁹⁵F. Bechstedt, J. Furthmüller, U. Grossner, and C. Raffy, in *Silicon Carbide*, edited by W. J. Choyke, H. Matsunami, and G. Pensl (Springer Berlin Heidelberg, Berlin, Heidelberg, 2004) pp. 3–25.
- ³⁹⁶H. Choi, “Overview of Silicon Carbide Power Devices,” (2016).
- ³⁹⁷J. I. Pankove, ed., *Electroluminescence*, softcover reprint of the original 1st ed. 1977 ed. (Springer Berlin, Berlin, 2014).
- ³⁹⁸I. G. Ivanov, A. Henry, and E. Janzén, *Physical Review B* **71**, 241201 (2005).
- ³⁹⁹C. Persson and U. Lindefelt, *Materials Science Forum* **264–268**, 275 (1998).
- ⁴⁰⁰A. Aditya, S. Khandelwal, C. Mukherjee, A. Khan, S. Panda, and B. Maji, in *2015 International Conference on Recent Developments in Control, Automation and Power Engineering (I* (IEEE, Noida, India, 2015) pp. 61–65.
- ⁴⁰¹S. Zollner, J. G. Chen, E. Duda, T. Wetteroth, S. R. Wilson, and J. N. Hilfiker, *Journal of Applied Physics* **85**, 8353 (1999).
- ⁴⁰²J. Fan and P. K. Chu, “General Properties of Bulk SiC,” in *Silicon Carbide Nanostructures* (Springer International Publishing, Cham, 2014) pp. 7–114.

- ⁴⁰³S. Yoshida, in *Properties of Silicon Carbide*, EMIS Datareviews Series No. 13, edited by G. L. Harris and Inspec (INSPEC, the Inst. of Electrical Engineers, London, 1995) pp. 29–41.
- ⁴⁰⁴A. Suzuki, H. Matsunami, and T. Tanaka, *Journal of The Electrochemical Society* **124**, 241 (1977).
- ⁴⁰⁵L. Patrick, D. R. Hamilton, and W. J. Choyke, *Physical Review* **143**, 526 (1966).
- ⁴⁰⁶H. Matsunami, A. Suzuki, and T. Tanaka, in *In: Silicon Carbide-1973; Proceedings of the Third International Conference* (1974) pp. 618–625.
- ⁴⁰⁷M. L. Megherbi, L. Dehimi, W. terghini, F. Pezzimenti, and F. G. Della Corte, *Courrier du Savoir* **19**, 71 (2015).
- ⁴⁰⁸K. G. Menon, A. Nakajima, L. Ngwendson, and E. M. Sankara Narayanan, *IEEE Electron Device Letters* **32**, 1272 (2011).
- ⁴⁰⁹G. Wolfowicz, C. P. Anderson, A. L. Yeats, S. J. Whiteley, J. Niklas, O. G. Poluektov, F. J. Heremans, and D. D. Awschalom, *Nature Communications* **8**, 1876 (2017).
- ⁴¹⁰B. Nedzvetskii, B. V. Novikov, N. K. Prokof'eva, and M. B. Reifman, *Sov. Phys. Solid State* **2**, 914 (1969).
- ⁴¹¹F. Capasso, in *Semiconductors and Semimetals*, Vol. 22 (Elsevier, 1985) pp. 1–172.
- ⁴¹²S. Selberherr, *Analysis and Simulation of Semiconductor Devices* (Springer Vienna, Vienna, 1984).
- ⁴¹³A. G. Chynoweth, *Physical Review* **109**, 1537 (1958).
- ⁴¹⁴A. G. Chynoweth, *Journal of Applied Physics* **31**, 1161 (1960).
- ⁴¹⁵R. Van Overstraeten and H. De Man, *Solid-State Electronics* **13**, 583 (1970).
- ⁴¹⁶P. A. Wolff, *Physical Review* **95**, 1415 (1954).
- ⁴¹⁷W. Shockley, *Solid-State Electronics* **2**, 35 (1961).
- ⁴¹⁸A. O. Konstantinov, Q. Wahab, N. Nordell, and U. Lindefelt, *Applied Physics Letters* **71**, 90 (1997).
- ⁴¹⁹T. Lackner, *Solid-State Electronics* **34**, 33 (1991).
- ⁴²⁰G. A. Baraff, *Physical Review* **128**, 2507 (1962).
- ⁴²¹K. K. Thornber, *Journal of Applied Physics* **52**, 279 (1981).
- ⁴²²Y. Okuto and C. R. Crowell, *Physical Review B* **6**, 3076 (1972).
- ⁴²³Y. Okuto and C. Crowell, *Solid-State Electronics* **18**, 161 (1975).
- ⁴²⁴M. Valdinoci, D. Ventura, M. Vecchi, M. Rudan, G. Bacarani, F. Illien, A. Stricker, and L. Zullino, in *1999 International Conference on Simulation of Semiconductor Processes and Devices. SISPAD'99 (IEEE)*

- (Japan Soc. Appl. Phys, Kyoto, Japan, 1999) pp. 27–30.
- ⁴²⁵A. Acharyya and J. P. Banerjee, *Journal of Computational Electronics* **13**, 917 (2014).
- ⁴²⁶K. Brennan, E. Bellotti, M. Farahmand, H.-E. Nilsson, P. Ruden, and Yumin Zhang, *IEEE Transactions on Electron Devices* **47**, 1882 (Oct./2000).
- ⁴²⁷R. Fujita, K. Konaga, Y. Ueoka, Y. Kamakura, N. Mori, and T. Kotani, in *2017 International Conference on Simulation of Semiconductor Processes and Devices (SISPAD)* (IEEE, Kamakura, Japan, 2017) pp. 289–292.
- ⁴²⁸H.-E. Nilsson, E. Bellotti, K. Brennan, and M. Hjelm, *Materials Science Forum* **338–342**, 765 (2000).
- ⁴²⁹C. C. Sun, A. H. You, and E. K. Wong, in *MALAYSIA ANNUAL PHYSICS CONFERENCE 2010 (PERFIK-2010)* (Damai Laut, (Malaysia), 2011) pp. 277–280.
- ⁴³⁰H. Tanaka, T. Kimoto, and N. Mori, *Journal of Applied Physics* **131**, 225701 (2022).
- ⁴³¹C. Sun, A. You, and E. Wong, *The European Physical Journal Applied Physics* **60**, 10204 (2012).
- ⁴³²A. Concannon, F. Piccinini, A. Mathewson, and C. Lombardi, in *Proceedings of International Electron Devices Meeting* (IEEE, Washington, DC, USA, 1995) pp. 289–292.
- ⁴³³K. Katayama and T. Toyabe, in *International Technical Digest on Electron Devices Meeting* (IEEE, Washington, DC, USA, 1989) pp. 135–138.
- ⁴³⁴R. Raghunathan and B. J. Baliga, *Applied Physics Letters* **72**, 3196 (1998).
- ⁴³⁵P. Mukherjee, S. K. R. Hossain, A. Acharyya, and A. Biswas, *Applied Physics A* **126**, 127 (2020).
- ⁴³⁶P. Mukherjee, D. Chatterjee, and A. Acharyya, *Journal of Computational Electronics* **16**, 503 (2017).
- ⁴³⁷W. Bartsch, R. Schörner, and K. O. Dohnke, *Materials Science Forum* **645–648**, 909 (2010).
- ⁴³⁸Z. Stum, Y. Tang, H. Naik, and T. P. Chow, *Materials Science Forum* **778–780**, 467 (2014).
- ⁴³⁹S.-i. Nakamura, H. Kumagai, T. Kimoto, and H. Matsunami, *Applied Physics Letters* **80**, 3355 (2002).
- ⁴⁴⁰T. Hatakeyama, *physica status solidi (a)* **206**, 2284 (2009).
- ⁴⁴¹S. Jin, K. Lee, W. Choi, C. Park, S. Yi, H. Fujii, J. Yoo, Y. Park, J. Jeong, and D. S. Kim, *IEEE Transactions on Electron Devices* , 1 (2024).
- ⁴⁴²S. Nida and U. Grossner, *IEEE Transactions on Electron Devices* **66**, 1899 (2019).
- ⁴⁴³C. R. Crowell and S. M. Sze, *Applied Physics Letters* **9**, 242 (1966).
- ⁴⁴⁴H. Niwa, J. Suda, and T. Kimoto, *Materials Science Forum* **778–780**, 461 (2014).

- ⁴⁴⁵H. Hamad, C. Raynaud, P. Bevilacqua, S. Scharnholz, and D. Planson, *Materials Science Forum* **821–823**, 223 (2015).
- ⁴⁴⁶C. Banc, E. Bano, T. Ouisse, O. Noblanc, and C. Brylinski, *Materials Science Forum* **389–393**, 1371 (2002).
- ⁴⁴⁷J. S. Cheong, M. M. Hayat, Xinxin Zhou, and J. P. R. David, *IEEE Transactions on Electron Devices* **62**, 1946 (2015).
- ⁴⁴⁸R. Raghunathan and B. Baliga, *Solid-State Electronics* **43**, 199 (1999).
- ⁴⁴⁹A. O. Konstantinov, Q. Wahab, N. Nordell, and U. Lindefelt, *Journal of Electronic Materials* **27**, 335 (1998).
- ⁴⁵⁰W. S. Loh, B. K. Ng, J. S. Ng, S. I. Soloviev, H.-Y. Cha, P. M. Sandvik, C. M. Johnson, and J. P. R. David, *IEEE Transactions on Electron Devices* **55**, 1984 (2008).
- ⁴⁵¹B. Ng, J. David, R. Tozer, G. Rees, Feng Yan, Jian H. Zhao, and M. Weiner, *IEEE Transactions on Electron Devices* **50**, 1724 (2003).
- ⁴⁵²D. Nguyen, C. Raynaud, N. Dheilly, M. Lazar, D. Tournier, P. Brosselard, and D. Planson, *Diamond and Related Materials* **20**, 395 (2011).
- ⁴⁵³D. Nguyen, C. Raynaud, M. Lazar, G. Pâques, S. Scharnholz, N. Dheilly, D. Tournier, and D. Planson, *Materials Science Forum* **717–720**, 545 (2012).
- ⁴⁵⁴D. Stefanakis, X. Chi, T. Maeda, M. Kaneko, and T. Kimoto, *IEEE Transactions on Electron Devices* **67**, 3740 (2020).
- ⁴⁵⁵Y. Zhao, H. Niwa, and T. Kimoto, *Japanese Journal of Applied Physics* **58**, 018001 (2019).
- ⁴⁵⁶A. S. Kyuregyan, *Semiconductors* **50**, 289 (2016).
- ⁴⁵⁷J. E. Green, W. S. Loh, A. R. J. Marshall, B. K. Ng, R. C. Tozer, J. P. R. David, S. I. Soloviev, and P. M. Sandvik, *IEEE Transactions on Electron Devices* **59**, 1030 (2012).
- ⁴⁵⁸P. L. Cheang, E. K. Wong, and L. L. Teo, *Journal of Electronic Materials* **50**, 5259 (2021).
- ⁴⁵⁹L. Zhu, P. A. Losee, T. P. Chow, K. A. Jones, C. Scozzie, M. H. Ervin, P. B. Shah, M. A. Derenge, R. Vispute, T. Venkatesan, and A. K. Agarwal, *Materials Science Forum* **527–529**, 1367 (2006).
- ⁴⁶⁰D. Stefanakis, N. Makris, K. Zekentes, and D. Tassis, *IEEE Transactions on Electron Devices* **68**, 2582 (2021).
- ⁴⁶¹H.-E. Nilsson, A. Martinez, U. Sannemo, M. Hjelm, E. Bellotti, and K. Brennan, *Physica B: Condensed Matter* **314**, 68 (2002).
- ⁴⁶²H. Niwa, J. Suda, and T. Kimoto, *IEEE Transactions on Electron Devices* **62**, 3326 (2015).

- ⁴⁶³R. Raghunathan and B. Baliga, in *Proceedings of 9th International Symposium on Power Semiconductor Devices and ICs (ISPSD)* (IEEE, Weimar, Germany, 1997) pp. 173–176.
- ⁴⁶⁴D. C. Sheridan, G. Niu, J. Merrett, J. D. Cressler, C. Ellis, and C.-C. Tin, *Solid-State Electronics* **44**, 1367 (2000).
- ⁴⁶⁵K. Bertilsson, H.-E. Nilsson, and C. Petersson, in *COMPEL 2000. 7th Workshop on Computers in Power Electronics. Proceedings (Cat. No.00TH8535)* (IEEE, Blacksburg, VA, USA, 2000) pp. 118–120.
- ⁴⁶⁶T. Hatakeyama, T. Watanabe, T. Shinohe, K. Kojima, K. Arai, and N. Sano, *Applied Physics Letters* **85**, 1380 (2004).
- ⁴⁶⁷W. Loh, J. David, B. Ng, S. I. Soloviev, P. M. Sandvik, J. Ng, and C. M. Johnson, *Materials Science Forum* **615–617**, 311 (2009).
- ⁴⁶⁸R. K. Sharma, P. Hazdra, and S. Popelka, *IEEE Transactions on Nuclear Science* **62**, 534 (2015).
- ⁴⁶⁹X. Zhang and N. You, in *2018 IEEE 3rd International Conference on Integrated Circuits and Microsystems (ICIM)* (IEEE, Shanghai, 2018) pp. 60–63.
- ⁴⁷⁰H.-Y. Cha, S. Soloviev, S. Zelakiewicz, P. Waldrab, and P. M. Sandvik, *IEEE Sensors Journal* **8**, 233 (2008).
- ⁴⁷¹P. Steinmann, B. Hull, I.-H. Ji, D. Lichtenwalner, and E. Van Brunt, *Journal of Applied Physics* **133**, 235705 (2023).
- ⁴⁷²T. Kimoto, M. Kaneko, K. Tachiki, K. Ito, R. Ishikawa, X. Chi, D. Stefanakis, T. Kobayashi, and H. Tanaka, in *2021 IEEE International Electron Devices Meeting (IEDM)* (IEEE, San Francisco, CA, USA, 2021) pp. 36.1.1–36.1.4.
- ⁴⁷³X. Guo, A. Beck, Xiaowei Li, J. Campbell, D. Emerson, and J. Sumakeris, *IEEE Journal of Quantum Electronics* **41**, 562 (2005).
- ⁴⁷⁴A. Kyuregyan and S. Yurkov, Sov. Phys. Solid State **23**, 1126 (1989).
- ⁴⁷⁵R. Trew, J.-B. Yan, and P. Mock, *Proceedings of the IEEE* **79**, 598 (1991).
- ⁴⁷⁶J. Wang and B. W. Williams, *Semiconductor Science and Technology* **14**, 1088 (1999).
- ⁴⁷⁷W. Loh, C. M. Johnson, J. Ng, P. M. Sandvik, S. Arthur, S. I. Soloviev, and J. David, *Materials Science Forum* **556–557**, 339 (2007).
- ⁴⁷⁸W. S. Loh, E. Z. J. Goh, K. Vassilevski, I. Nikitina, J. P. R. David, N. G. Wright, and C. M. Johnson, *MRS Proceedings* **1069**, 1069 (2008).
- ⁴⁷⁹T. Hatakeyama, T. Watanabe, K. Kojima, N. Sano, T. Shinohe, and K. Arai, *MRS Proceedings* **815**, J9.3 (2004).

- 480 T. Hatakeyama, J. Nishio, C. Ota, and T. Shinohe, in *2005 International Conference On Simulation of Semiconductor Processes and Devices* (IEEE, Tokyo, Japan, 2005) pp. 171–174.
- 481 A. Ivanov, M. Mynbaeva, A. Sadokhin, N. Strokan, and A. Lebedev, *Nuclear Instruments and Methods in Physics Research Section A: Accelerators, Spectrometers, Detectors and Associated Equipment* **926**, 163001 (2019).
- 482 C. Wang, X. Li, L. Li, X. Deng, W. Zhang, L. Zheng, Y. Zou, W. Qian, Z. Li, and B. Zhang, *IEEE Electron Device Letters* **43**, 2025 (2022).
- 483 Y. Wang, J.-c. Zhou, M. Lin, X.-j. Li, J.-Q. Yang, and F. Cao, *IEEE Journal of the Electron Devices Society* **10**, 373 (2022).
- 484 C. C. Sun, A. H. You, and E. K. Wong, in *2012 10th IEEE International Conference on Semiconductor Electronics* (IEEE, Kuala Lumpur, Malaysia, 2012) pp. 366–369.
- 485 J. Hasegawa, L. Pace, L. V. Phung, M. Hatano, and D. Planson, *IEEE Transactions on Electron Devices* **64**, 1203 (2017).
- 486 J. A. McPherson, C. W. Hitchcock, T. Paul Chow, W. Ji, and A. A. Woodworth, *IEEE Transactions on Nuclear Science* **68**, 651 (2021).
- 487 T. Kimoto, H. Niwa, T. Okuda, E. Saito, Y. Zhao, S. Asada, and J. Suda, *Journal of Physics D: Applied Physics* **51**, 363001 (2018).
- 488 A. E. Arvanitopoulos, M. Antoniou, S. Perkins, M. Jennings, M. B. Guadas, K. N. Gyftakis, and N. Lophitis, *IEEE Transactions on Industry Applications* **55**, 4080 (2019).
- 489 B. Ng, F. Yan, J. David, R. Tozer, G. Rees, C. Qin, and J. Zhao, *IEEE Photonics Technology Letters* **14**, 1342 (2002).
- 490 P. G. Neudeck, *Journal of Electronic Materials* **27**, 317 (1998).
- 491 J. Palmour, R. Singh, R. Glass, O. Kordina, and C. Carter, in *Proceedings of 9th International Symposium on Power Semiconductor Devices and IC's* (IEEE, Weimar, Germany, 1997) pp. 25–32.
- 492 D. Peters, P. Friedrichs, H. Mitlehner, R. Schoerner, U. Weinert, B. Weis, and D. Stephani, in *12th International Symposium on Power Semiconductor Devices & ICs. Proceedings (Cat. No.00CH37094)* (IEEE, Toulouse, France, 2000) pp. 241–244.
- 493 R. Singh, J. Cooper, M. Melloch, T. Chow, and J. Palmour, *IEEE Transactions on Electron Devices* **49**, 665 (2002).
- 494 O. Slobodyan, J. Flicker, J. Dickerson, J. Shoemaker, A. Binder, T. Smith, S. Goodnick, R. Kaplar, and M. Hollis, *Journal of Materials Research* **37**, 849 (2022).

- ⁴⁹⁵T. Hayashi, K. Asano, J. Suda, and T. Kimoto, *Journal of Applied Physics* **109**, 114502 (2011).
- ⁴⁹⁶T. Hayashi, K. Asano, J. Suda, and T. Kimoto, *Journal of Applied Physics* **109**, 014505 (2011).
- ⁴⁹⁷P. Ščajev and K. Jarašiūnas, *Journal of Physics D: Applied Physics* **46**, 265304 (2013).
- ⁴⁹⁸Y. Fang, X. Wu, J. Yang, G. Chen, Y. Chen, Q. Wu, and Y. Song, *Applied Physics Letters* **112**, 201904 (2018).
- ⁴⁹⁹W. Mao, C. Cui, H. Xiong, N. Zhang, S. Liu, M. Dou, L. Song, D. Yang, and X. Pi, *Semiconductor Science and Technology* **38**, 073001 (2023).
- ⁵⁰⁰D. Schroder, *IEEE Transactions on Electron Devices* **29**, 1336 (1982).
- ⁵⁰¹Y. Arafat, F. M. Mohammedy, and M. M. Shahidul Hassan, *International Journal of Optoelectronic Engineering* **2**, 5 (2012).
- ⁵⁰²K. Nagaya, T. Hirayama, T. Tawara, K. Murata, H. Tsuchida, A. Miyasaka, K. Kojima, T. Kato, H. Okumura, and M. Kato, *Journal of Applied Physics* **128**, 105702 (2020).
- ⁵⁰³P. T. Landsberg, *Recombination in Semiconductors*, 1st ed. (Cambridge University Press, 1992).
- ⁵⁰⁴A. Hangleiter, *Physical Review B* **37**, 2594 (1988).
- ⁵⁰⁵W. Shockley and W. T. Read, *Physical Review* **87**, 835 (1952).
- ⁵⁰⁶I. D. Booker, *Carrier Lifetime Relevant Deep Levels in SiC*, Linköping Studies in Science and Technology. Dissertations, Vol. 1714 (Linköping University Electronic Press, Linköping, 2015).
- ⁵⁰⁷H. C. De Graaff and F. M. Klaassen, *Compact Transistor Modelling for Circuit Design*, edited by S. Selberherr, Computational Microelectronics (Springer Vienna, Vienna, 1990).
- ⁵⁰⁸J. Fossum and D. Lee, *Solid-State Electronics* **25**, 741 (1982).
- ⁵⁰⁹H. M. Ayedh, R. Nipoti, A. Hallén, and B. G. Svensson, *Journal of Applied Physics* **122**, 025701 (2017).
- ⁵¹⁰J. R. Jenny, D. P. Malta, V. F. Tsvetkov, M. K. Das, H. McD. Hobgood, C. H. Carter, R. J. Kumar, J. M. Borrego, R. J. Gutmann, and R. Aavikko, *Journal of Applied Physics* **100**, 113710 (2006).
- ⁵¹¹P. Grivickas, A. Galeckas, J. Linnros, M. Syväjärvi, R. Yakimova, V. Grivickas, and J. Tellefsen, *Materials Science in Semiconductor Processing* **4**, 191 (2001).
- ⁵¹²L. Lilja, I. D. Booker, J. U. Hassan, E. Janzén, and J. P. Bergman, *Journal of Crystal Growth* **381**, 43 (2013).
- ⁵¹³T. Hayashi, K. Asano, J. Suda, and T. Kimoto, *Journal of Applied Physics* **112**, 064503 (2012).

- ⁵¹⁴S. Ichikawa, K. Kawahara, J. Suda, and T. Kimoto, *Applied Physics Express* **5**, 101301 (2012).
- ⁵¹⁵N. Kaji, H. Niwa, J. Suda, and T. Kimoto, *IEEE Transactions on Electron Devices* **62**, 374 (2015).
- ⁵¹⁶K. Kawahara, J. Suda, and T. Kimoto, *Journal of Applied Physics* **111**, 053710 (2012).
- ⁵¹⁷T. Kimoto, K. Danno, and J. Suda, *physica status solidi (b)* **245**, 1327 (2008).
- ⁵¹⁸T. Kimoto, T. Hiyoshi, T. Hayashi, and J. Suda, *Journal of Applied Physics* **108**, 083721 (2010).
- ⁵¹⁹T. Miyazawa and H. Tsuchida, *Journal of Applied Physics* **113**, 083714 (2013).
- ⁵²⁰T. Okuda, T. Kimoto, and J. Suda, *Applied Physics Express* **6**, 121301 (2013).
- ⁵²¹T. Okuda, T. Miyazawa, H. Tsuchida, T. Kimoto, and J. Suda, *Applied Physics Express* **7**, 085501 (2014).
- ⁵²²L. Storasta and H. Tsuchida, *Applied Physics Letters* **90**, 062116 (2007).
- ⁵²³L. Storasta, H. Tsuchida, T. Miyazawa, and T. Ohshima, *Journal of Applied Physics* **103**, 013705 (2008).
- ⁵²⁴T. Tawara, T. Miyazawa, M. Ryo, M. Miyazato, T. Fujimoto, K. Takenaka, S. Matsunaga, M. Miyajima, A. Otsuki, Y. Yonezawa, T. Kato, H. Okumura, T. Kimoto, and H. Tsuchida, *Journal of Applied Physics* **120**, 115101 (2016).
- ⁵²⁵H. Tsuchida, I. Kamata, T. Miyazawa, M. Ito, X. Zhang, and M. Nagano, *Materials Science in Semiconductor Processing* **78**, 2 (2018).
- ⁵²⁶M. Wang, M. Yang, W. Liu, S. Yang, J. Liu, C. Han, L. Geng, and Y. Hao, *Applied Physics Express* **13**, 111002 (2020).
- ⁵²⁷R. Zhang, R. Hong, J. Han, H. Ting, X. Li, J. Cai, X. Chen, D. Fu, D. Lin, M. Zhang, S. Wu, Y. Zhang, Z. Wu, and F. Zhang, *Chinese Physics B* **32**, 067205 (2023).
- ⁵²⁸T. Hiyoshi and T. Kimoto, *Applied Physics Express* **2**, 041101 (2009).
- ⁵²⁹Y. Cui, J. Li, K. Zhou, X. Zhang, and G. Sun, *Diamond and Related Materials* **92**, 25 (2019).
- ⁵³⁰J. Erlekampf, B. Kallinger, J. Weiße, M. Rommel, P. Berwian, J. Friedrich, and T. Erlbacher, *Journal of Applied Physics* **126**, 045701 (2019).
- ⁵³¹J. Erlekampf, M. Rommel, K. Rosshirt-Lilla, B. Kallinger, P. Berwian, J. Friedrich, and T. Erlbacher, *Journal of Crystal Growth* **560–561**, 126033 (2021).
- ⁵³²A. Galeckas, V. Grivickas, J. Linnros, H. Bleichner, and C. Hallin, *Journal of Applied Physics* **81**, 3522 (1997).
- ⁵³³A. Galeckas, J. Linnros, M. Frischholz, K. Rottner, N. Nordell, S. Karlsson, and V. Grivickas, *Materials Science and Engineering: B* **61–62**, 239 (1999).

- ⁵³⁴A. Galeckas, J. Linnros, M. Frischholz, and V. Grivickas, *Applied Physics Letters* **79**, 365 (2001).
- ⁵³⁵M. Kato, M. Kawai, T. Mori, M. Ichimura, S. Sumie, and H. Hashizume, *Japanese Journal of Applied Physics* **46**, 5057 (2007).
- ⁵³⁶P. B. Klein, *Journal of Applied Physics* **103**, 033702 (2008).
- ⁵³⁷O. Kordina, J. P. Bergman, C. Hallin, and E. Janzén, *Applied Physics Letters* **69**, 679 (1996).
- ⁵³⁸J. Hassan and J. P. Bergman, *Journal of Applied Physics* **105**, 123518 (2009).
- ⁵³⁹K. Murata, T. Tawara, A. Yang, R. Takanashi, T. Miyazawa, and H. Tsuchida, *Journal of Applied Physics* **126**, 045711 (2019).
- ⁵⁴⁰N. A. Mahadik, R. E. Stahlbush, P. B. Klein, A. Khachatrian, S. Buchner, and S. G. Block, *Applied Physics Letters* **111**, 221904 (2017).
- ⁵⁴¹T. Mori, M. Kato, H. Watanabe, M. Ichimura, E. Arai, S. Sumie, and H. Hashizume, *Japanese Journal of Applied Physics* **44**, 8333 (2005).
- ⁵⁴²A. K. Agarwal, P. A. Ivanov, M. E. Levenshtein, J. W. Palmour, S. L. Rumyantsev, and S.-H. Ryu, *Semiconductor Science and Technology* **16**, 260 (2001).
- ⁵⁴³P. Ivanov, M. Levenshtein, K. Irvine, O. Kordina, J. Palmour, S. Rumyantsev, and R. Singh, *Electronics Letters* **35**, 1382 (1999).
- ⁵⁴⁴P. Ivanov, M. Levenshtein, A. Agarwal, S. Krishnaswami, and J. Palmour, *IEEE Transactions on Electron Devices* **53**, 1245 (2006).
- ⁵⁴⁵D. Åberg, A. Hallén, and B. Svensson, *Physica B: Condensed Matter* **273–274**, 672 (1999).
- ⁵⁴⁶G. Alfieri, E. V. Monakhov, B. G. Svensson, and M. K. Linnarsson, *Journal of Applied Physics* **98**, 043518 (2005).
- ⁵⁴⁷G. Alfieri and A. Mihaila, *Journal of Physics: Condensed Matter* **32**, 465703 (2020).
- ⁵⁴⁸M. Anikin, A. A. Lebedev, A. Syrkin, and A. Suvorov, *Sov. Phys. Semicond.* **19**, 1847 (1985).
- ⁵⁴⁹T. Ayalew, T. Grasser, H. Kosina, and S. Selberherr, *Materials Science Forum* **483–485**, 845 (2005).
- ⁵⁵⁰H. M. Ayedh, V. Bobal, R. Nipoti, A. Hallén, and B. G. Svensson, *Materials Science Forum* **858**, 331 (2016).
- ⁵⁵¹M. E. Bathen, A. Galeckas, J. Müting, H. M. Ayedh, U. Grossner, J. Coutinho, Y. K. Frodason, and L. Vines, *npj Quantum Information* **5**, 111 (2019).
- ⁵⁵²J. M. Bluet, J. Pernot, J. Camassel, S. Contreras, J. L. Robert, J. F. Michaud, and T. Billon, *Journal of Applied Physics* **88**, 1971 (2000).

- ⁵⁵³I. D. Booker, E. Janzén, N. T. Son, J. Hassan, P. Stenberg, and E. Ö. Sveinbjörnsson, *Journal of Applied Physics* **119**, 235703 (2016).
- ⁵⁵⁴T. Brodar, L. Bakrač, I. Capan, T. Ohshima, L. Snoj, V. Radulović, and Ž. Pastuović, *Crystals* **10**, 845 (2020).
- ⁵⁵⁵I. Capan, T. Brodar, J. Coutinho, T. Ohshima, V. P. Markevich, and A. R. Peaker, *Journal of Applied Physics* **124**, 245701 (2018).
- ⁵⁵⁶I. Capan, T. Brodar, Ž. Pastuović, R. Siegele, T. Ohshima, S.-i. Sato, T. Makino, L. Snoj, V. Radulović, J. Coutinho, V. J. B. Torres, and K. Demmouche, *Journal of Applied Physics* **123**, 161597 (2018).
- ⁵⁵⁷M. A. Capano, J. A. Cooper, M. R. Melloch, A. Saxler, and W. C. Mitchel, *Journal of Applied Physics* **87**, 8773 (2000).
- ⁵⁵⁸A. Castaldini, A. Cavallini, L. Rigutti, and F. Nava, *Applied Physics Letters* **85**, 3780 (2004).
- ⁵⁵⁹S. K. Chaudhuri, O. Karadavut, J. W. Kleppinger, and K. C. Mandal, *Journal of Applied Physics* **130**, 074501 (2021).
- ⁵⁶⁰W. Choyke and G. Pensl, *MRS Bulletin* **22**, 25 (1997).
- ⁵⁶¹T. Dalibor, G. Pensl, T. Kimoto, H. Matsunami, S. Sridhara, R. P. Devaty, and W. J. Choyke, *Diamond and Related Materials* **6**, 1333 (1997).
- ⁵⁶²T. Dalibor and M. Schulz, eds., *Numerical Data and Functional Relationships in Science and Technology. Subvol. A2: Gruppe 3: Kristall- Und Festkörperphysik = Group 3: Crystal and Solid State Physics Vol. 41, Semiconductors Impurities and Defects in Group IV Elements, IV-IV and III-V Compounds. Part Beta: Group IV-IV and III-V Compounds / Ed. by M. Schulz; Authors: T. Dalibor*, Vol. 41 (Springer, Berlin Heidelberg, 2003).
- ⁵⁶³K. Danno, D. Nakamura, and T. Kimoto, *Applied Physics Letters* **90**, 202109 (2007).
- ⁵⁶⁴K. Danno and T. Kimoto, *Journal of Applied Physics* **100**, 113728 (2006).
- ⁵⁶⁵M. L. David, G. Alfieri, E. M. Monakhov, A. Hallén, C. Blanchard, B. G. Svensson, and J. F. Barbot, *Journal of Applied Physics* **95**, 4728 (2004).
- ⁵⁶⁶J. Doyle, M. Aboelfotoh, B. Svensson, A. Schöner, and N. Nordell, *Diamond and Related Materials* **6**, 1388 (1997).
- ⁵⁶⁷S. Greulich-Weber, *physica status solidi (a)* **162**, 95 (1997).
- ⁵⁶⁸P. Hazdra and S. Popelka, *Materials Science Forum* **897**, 463 (2017).
- ⁵⁶⁹P. Hazdra, P. Smrkovsky, J. Vobecky, and A. Mihaila, *IEEE Transactions on Electron Devices* **68**, 202 (2021).

- ⁵⁷⁰C. G. Hemmingsson, N. T. Son, A. Ellison, J. Zhang, and E. Janzén, *Physical Review B* **58**, R10119 (1998).
- ⁵⁷¹H. K. Henisch and R. Roy, *Silicon Carbide—1968: Proceedings of the International Conference on Silicon Carbide, University Park, Pennsylvania, October 20-23, 1968* (Elsevier, 2013).
- ⁵⁷²T. Hornos, A. Gali, and B. G. Svensson, *Materials Science Forum* **679–680**, 261 (2011).
- ⁵⁷³Y. Huang, R. Wang, Y. Zhang, D. Yang, and X. Pi, *Chinese Physics B* **31**, 056108 (2022).
- ⁵⁷⁴Y. Huang, R. Wang, Y. Qian, Y. Zhang, D. Yang, and X. Pi, *Chinese Physics B* **31**, 046104 (2022).
- ⁵⁷⁵S. W. Huh, J. J. Sumakeris, A. Polyakov, M. Skowronski, P. B. Klein, B. Shanabrook, and M. J. O’Loughlin, *Materials Science Forum* **527–529**, 493 (2006).
- ⁵⁷⁶H. Itoh, T. Troffer, and G. Pensl, *Materials Science Forum* **264–268**, 685 (1998).
- ⁵⁷⁷G. Izzo, G. Litrico, L. Calcagno, G. Foti, and F. La Via, *Journal of Applied Physics* **104**, 093711 (2008).
- ⁵⁷⁸S. Kagamihara, H. Matsuura, T. Hatakeyama, T. Watanabe, M. Kushibe, T. Shinohe, and K. Arai, *Journal of Applied Physics* **96**, 5601 (2004).
- ⁵⁷⁹L. Kasamakova-Kolaklieva, L. Storasta, I. G. Ivanov, B. Magnusson, S. Contreras, C. Consejo, J. Pernot, M. Zielinski, and E. Janzén, *Materials Science Forum* **457–460**, 677 (2004).
- ⁵⁸⁰T. Kimoto, A. Itoh, H. Matsunami, S. Sridhara, L. L. Clemen, R. P. Devaty, W. J. Choyke, T. Dalibor, C. Peppermüller, and G. Pensl, *Applied Physics Letters* **67**, 2833 (1995).
- ⁵⁸¹T. Kimoto, K. Hashimoto, and H. Matsunami, *Japanese Journal of Applied Physics* **42**, 7294 (2003).
- ⁵⁸²T. Kimoto, A. Itoh, and H. Matsunami, *physica status solidi (b)* **202**, 247 (1997).
- ⁵⁸³P. B. Klein, B. V. Shanabrook, S. W. Huh, A. Y. Polyakov, M. Skowronski, J. J. Sumakeris, and M. J. O’Loughlin, *Applied Physics Letters* **88**, 052110 (2006).
- ⁵⁸⁴M. Laube, F. Schmid, K. Semmelroth, G. Pensl, R. P. Devaty, W. J. Choyke, G. Wagner, and M. Maier, in *Silicon Carbide*, edited by W. J. Choyke, H. Matsunami, and G. Pensl (Springer Berlin Heidelberg, Berlin, Heidelberg, 2004) pp. 493–515.
- ⁵⁸⁵F. La Via, G. Galvagno, F. Roccaforte, A. Ruggiero, and L. Calcagno, *Applied Physics Letters* **87**, 142105 (2005).
- ⁵⁸⁶D. J. Lichtenwalner, J. H. Park, S. Rogers, H. Dixit, A. Scholtze, S. Bubel, and S. H. Ryu, *Materials Science Forum* **1089**, 3 (2023).
- ⁵⁸⁷K. C. Mandal, J. W. Kleppinger, and S. K. Chaudhuri, *Micromachines* **11**, 254 (2020).
- ⁵⁸⁸A. Martinez, U. Lindefelt, M. Hjelm, and H.-E. Nilsson,

- Journal of Applied Physics **91**, 1359 (2002).
- ⁵⁸⁹H. Matsuura, M. Komeda, S. Kagamihara, H. Iwata, R. Ishihara, T. Hatakeyama, T. Watanabe, K. Kojima, T. Shinohe, and K. Arai, *Journal of Applied Physics* **96**, 2708 (2004).
- ⁵⁹⁰H. Matsuura, T. K. Tsunenobu Kimoto, and H. M. Hiroyuki Matsunami, *Japanese Journal of Applied Physics* **38**, 4013 (1999).
- ⁵⁹¹M. L. Megherbi, F. Pezzimenti, L. Dehimi, M. A. Saadoune, and F. G. Della Corte, *IEEE Transactions on Electron Devices* **65**, 3371 (2018).
- ⁵⁹²Y. Negoro, T. Kimoto, and H. Matsunami, *Electronics and Communications in Japan (Part II: Electronics)* **8**.
- ⁵⁹³K. V. Nguyen, M. A. Mannan, and K. C. Mandal, *IEEE Transactions on Nuclear Science* **62**, 3199 (2015).
- ⁵⁹⁴A. Parisini and R. Nipoti, *Journal of Applied Physics* **114**, 243703 (2013).
- ⁵⁹⁵Ž. Pastuović, R. Siegele, I. Capan, T. Brodar, S.-i. Sato, and T. Ohshima, *Journal of Physics: Condensed Matter* **29**, 475701 (2017).
- ⁵⁹⁶F. Schmid, M. Krieger, M. Laube, G. Pensl, and G. Wagner, in *Silicon Carbide*, edited by W. J. Choyke, H. Matsunami, and G. Pensl (Springer Berlin Heidelberg, Berlin, Heidelberg, 2004) pp. 517–536.
- ⁵⁹⁷S. R. Smith, A. O. Evvaraye, W. C. Mitchel, and M. A. Capano, *Journal of Electronic Materials* **28**, 190 (1999).
- ⁵⁹⁸N. T. Son, Mt. Wagner, C. G. Hemmingsson, L. Storasta, B. Magnusson, W. M. Chen, S. Greulich-Weber, J.-M. Spaeth, and E. Janzén, in *Silicon Carbide*, edited by W. J. Choyke, H. Matsunami, and G. Pensl (Springer Berlin Heidelberg, Berlin, Heidelberg, 2004) pp. 461–492.
- ⁵⁹⁹N. T. Son, X. T. Trinh, L. S. Løvlie, B. G. Svensson, K. Kawahara, J. Suda, T. Kimoto, T. Umeda, J. Isoya, T. Makino, T. Ohshima, and E. Janzén, *Physical Review Letters* **109**, 187603 (2012).
- ⁶⁰⁰L. Storasta, J. P. Bergman, E. Janzén, A. Henry, and J. Lu, *Journal of Applied Physics* **96**, 4909 (2004).
- ⁶⁰¹L. Storasta, P. Bergman, E. Janzén, and C. Hallin, *Materials Science Forum* **389–393**, 549 (2002).
- ⁶⁰²A. Suzuki, H. Matsunami, and T. Tanaka, *Japanese Journal of Applied Physics* **12**, 1083 (1973).
- ⁶⁰³Y. Tanaka, N. Kobayashi, H. Okumura, R. Suzuki, T. Ohdaira, M. Hasegawa, M. Ogura, S. Yoshida, and H. Tanoue, *Materials Science Forum* **338–342**, 909 (2000).

- ⁶⁰⁴T. Tawara, H. Tsuchida, S. Izumi, I. Kamata, and K. Izumi, *Materials Science Forum* **457–460**, 565 (2004).
- ⁶⁰⁵P. Terziyska, C. Blanc, J. Pernot, H. Peyre, S. Contreras, G. Bastide, J. L. Robert, J. Camassel, E. Morvan, C. Dua, and C. C. Brylinski, *physica status solidi (a)* **195**, 243 (2003).
- ⁶⁰⁶T. Troffer, M. Schadt, T. Frank, H. Itoh, G. Pensl, J. Heindl, H. P. Strunk, and M. Maier, *physica status solidi (a)* **162**, 277 (1997).
- ⁶⁰⁷R. Wang, Y. Huang, D. Yang, and X. Pi, *Applied Physics Letters* **122**, 180501 (2023).
- ⁶⁰⁸X. Xu, L. Zhang, L. Li, Z. Li, J. Li, J. Zhang, and P. Dong, *Discover Nano* **18**, 128 (2023).
- ⁶⁰⁹X. Yan, P. Li, L. Kang, S.-H. Wei, and B. Huang, *Journal of Applied Physics* **127**, 085702 (2020).
- ⁶¹⁰J. Zhang, L. Storasta, J. P. Bergman, N. T. Son, and E. Janzén, *Journal of Applied Physics* **93**, 4708 (2003).
- ⁶¹¹B. Zippelius, J. Suda, and T. Kimoto, *Journal of Applied Physics* **111**, 033515 (2012).
- ⁶¹²P. Gaggl, J. Burin, A. Gsponer, S.-E. Waid, R. Thalmeier, and T. Bergauer, *Nuclear Instruments and Methods in Physics Research Section A: Accelerators, Spectrometers, Detectors and Targets* **850**, 160 (2017).
- ⁶¹³S. Yamashita and T. Kimoto, *Applied Physics Express* **13**, 011006 (2020).
- ⁶¹⁴M. J. Marinella, D. K. Schroder, G. Chung, M. J. Loboda, T. Isaacs-Smith, and J. R. Williams, *IEEE Transactions on Electron Devices* **57**, 1910 (2010).
- ⁶¹⁵M. Kato, A. Ogawa, L. Han, and T. Kato, *Materials Science in Semiconductor Processing* **170**, 107980 (2020).
- ⁶¹⁶R. N. Hall, *Physical Review* **87**, 387 (1952).
- ⁶¹⁷L. Lilja, I. Farkas, I. Booker, J. Ul Hassan, E. Janzén, and J. P. Bergman, *Materials Science Forum* **897**, 238 (2017).
- ⁶¹⁸D. Scharfetter and R. Johnston, *IEEE Transactions on Electron Devices* **14**, 634 (1967).
- ⁶¹⁹D. Roulston, N. Arora, and S. Chamberlain, *IEEE Transactions on Electron Devices* **29**, 284 (1982).
- ⁶²⁰M. Law, E. Solley, M. Liang, and D. Burk, *IEEE Electron Device Letters* **12**, 401 (1991).
- ⁶²¹M. Tyagi and R. Van Overstraeten, *Solid-State Electronics* **26**, 577 (1983).
- ⁶²²G. Liaugaudas, D. Dargis, P. Kwasnicki, H. Peyre, R. Arvinte, S. Juillaguet, M. Zielinski, and K. Jarašiūnas, *Materials Science Forum* **821–823**, 249 (2015).
- ⁶²³H. Shao, X. Yang, D. Wang, X. Li, X. Chen, G. Hu, H. Li, X. Xiong, X. Xie, X. Hu, and X. Xu, *Journal of Electronic Materials* **53**, 2429 (2024).
- ⁶²⁴S. Sapienza, G. Sozzi, D. Santoro, P. Cova, N. Delmonte, G. Verrini, and G. Chiorboli, *Microelectronics Reliability* **113**, 113937 (2020).

- 625 P. B. Klein, R. Myers-Ward, K.-K. Lew, B. L. VanMil, C. R. Eddy, D. K. Gaskill, A. Shrivastava, and T. S. Sudarshan, *Journal of Applied Physics* **108**, 033713 (2010).
- 626 M. E. Levinshtein, P. A. Ivanov, M. S. Boltovets, V. A. Krivutsa, J. W. Palmour, M. K. Das, and B. A. Hull, *Solid-State Electronics* **49**, 1228 (2005).
- 627 A. Udal and E. Velmre, *Materials Science Forum* **556–557**, 375 (2007).
- 628 R. Wu and A. Peaker, *Solid-State Electronics* **25**, 643 (1982).
- 629 H. Goebel and K. Hoffmann, in *Proceedings of the 4th International Symposium on Power Semiconductor I* (IEEE, Tokyo, Japan, 1992) pp. 130–135.
- 630 D. Klaassen, *Solid-State Electronics* **35**, 961 (1992).
- 631 A. Schenk, *Solid-State Electronics* **35**, 1585 (1992).
- 632 T. Tamaki, G. G. Walden, Y. Sui, and J. A. Cooper, *IEEE Transactions on Electron Devices* **55**, 1928 (2008).
- 633 K. Gulbinas, V. Grivickas, H. P. Mahabadi, M. Usman, and A. Hallén, *Materials Science* **17**, 119 (2011).
- 634 M. Kato, A. Yoshida, and M. Ichimura, *Japanese Journal of Applied Physics* **51**, 02BP12 (2012).
- 635 M. Kato, Z. Xinchi, K. Kohama, S. Fukaya, and M. Ichimura, *Journal of Applied Physics* **127**, 195702 (2020).
- 636 Y. Mori, M. Kato, and M. Ichimura, *Journal of Physics D: Applied Physics* **47**, 335102 (2014).
- 637 G. Y. Chung, M. J. Loboda, M. Marinella, D. Schroder, T. Isaacs-Smith, and J. R. Williams, *Materials Science Forum* **615–617**, 283 (2009).
- 638 K. Y. Cheong, S. Dimitrijev, and Jisheng Han, *IEEE Transactions on Electron Devices* **50**, 1433 (2003).
- 639 S. Asada, J. Suda, and T. Kimoto, *IEEE Transactions on Electron Devices* **65**, 4786 (2018).
- 640 T. Hayashi, T. Okuda, J. Suda, and T. Kimoto, *Japanese Journal of Applied Physics* **53**, 111301 (2014).
- 641 Y. Ichikawa, M. Ichimura, T. Kimoto, and M. Kato, *ECS Journal of Solid State Science and Technology* **7**, Q127 (2018).
- 642 T. Kimoto, Y. Nanen, T. Hayashi, and J. Suda, *Applied Physics Express* **3**, 121201 (2010).
- 643 K. Nonaka, A. Horiuchi, Y. Negoro, K. Iwanaga, S. Yokoyama, H. Hashimoto, M. Sato, Y. Maeyama, M. Shimizu, and H. Iwakuro, *physica status solidi (a)* **206**, 2457 (2009).
- 644 B. Buono, R. Ghandi, M. Domeij, B. G. Malm, C.-M. Zetterling, and M. Ostling, *IEEE Transactions on Electron Devices* **57**, 704 (2010).
- 645 V. V. Afanasev, M. Bassler, G. Pensl, and M. Schulz, *physica status solidi (a)* **162**, 321 (1997).

- ⁶⁴⁶D. Fitzgerald and A. Grove, *Surface Science* **9**, 347 (1968).
- ⁶⁴⁷E. Yablonovitch, D. L. Allara, C. C. Chang, T. Gmitter, and T. B. Bright, *Physical Review Letters* **57**, 249 (1986).
- ⁶⁴⁸K. Murata, T. Tawara, A. Yang, R. Takanashi, T. Miyazawa, and H. Tsuchida, *Journal of Applied Physics* **129**, 025702 (2021).
- ⁶⁴⁹K. Tanaka and M. Kato, *Japanese Journal of Applied Physics* **63**, 011002 (2024).
- ⁶⁵⁰J. Fossum, R. Mertens, D. Lee, and J. Nijs, *Solid-State Electronics* **26**, 569 (1983).
- ⁶⁵¹J. Linnros, *Journal of Applied Physics* **84**, 275 (1998).
- ⁶⁵²K. Tanaka, K. Nagaya, and M. Kato, *Japanese Journal of Applied Physics* **62**, SC1017 (2023).
- ⁶⁵³P. T. Landsberg and G. S. Kousik, *Journal of Applied Physics* **56**, 1696 (1984).
- ⁶⁵⁴J. Dziewior and W. Schmid, *Applied Physics Letters* **31**, 346 (1977).
- ⁶⁵⁵G. Y. Chung, M. J. Loboda, M. Marinella, D. Schroder, P. B. Klein, T. Isaacs-Smith, and J. Williams, *Materials Science Forum* **600–603**, 485 (2008).
- ⁶⁵⁶M. Ruff, *Elektronische Bauelemente Aus Siliziumkarbid (SiC) : Physikalische Grundlagen Und Numerische Simulation*, Ph.D. thesis, Friedrich-Alexander-Universität, Erlangen-Nürnberg (1993).
- ⁶⁵⁷C. Hettler, C. James, J. Dickens, and A. Neuber, in *2010 IEEE International Power Modulator and High Voltage Conference* (IEEE, Atlanta, GA, USA, 2010) pp. 34–37.
- ⁶⁵⁸C. Hettler, W. W. Sullivan Iii, and J. Dickens, *Materials Science Forum* **717–720**, 301 (2012).
- ⁶⁵⁹S. S. Suvanam, K. Gulbinas, M. Usman, M. K. Linnarson, D. M. Martin, J. Linnros, V. Grivickas, and A. Hallén, *Journal of Applied Physics* **117**, 105309 (2015).
- ⁶⁶⁰K. Tanaka and M. Kato, *AIP Advances* **13**, 085220 (2023).
- ⁶⁶¹H. Tsuchida, I. Kamata, M. Ito, T. Miyazawa, H. Uehigashi, K. Fukada, H. Fujibayashi, M. Naitou, K. Hara, H. Osawa, T. Sugiura, and T. Kozawa, *Materials Science Forum* **858**, 119 (2016).
- ⁶⁶²T. Miyazawa, M. Ito, and H. Tsuchida, *Applied Physics Letters* **97**, 202106 (2010).
- ⁶⁶³T. Okuda, T. Kobayashi, T. Kimoto, and J. Suda, *Applied Physics Express* **9**, 051301 (2016).
- ⁶⁶⁴E. Saito, J. Suda, and T. Kimoto, *Applied Physics Express* **9**, 061303 (2016).
- ⁶⁶⁵T. Kimoto, N. Miyamoto, and H. Matsunami, *Materials Science and Engineering: B* **61–62**, 349 (1999).
- ⁶⁶⁶A. Udal and E. Velmre, *Materials Science Forum* **338–342**, 781 (2000).
- ⁶⁶⁷S. A. Reshanov, W. Bartsch, B. Zippelius, and G. Pensl,

- Materials Science Forum **615–617**, 699 (2009).
- ⁶⁶⁸P. A. Ivanov, M. E. Levenshtein, J. W. Palmour, M. K. Das, and B. A. Hull, *Solid-State Electronics* **50**, 1368 (2006).
- ⁶⁶⁹M. E. Levenshtein, T. T. Mnatsakanov, P. A. Ivanov, R. Singh, J. W. Palmour, and S. N. Yurkov, *Solid-State Electronics* **48**, 807 (2004).
- ⁶⁷⁰G. Sozzi, S. Sapienza, G. Chiorboli, L. Vines, A. Hallén, and R. Nipoti, *IEEE Access* , 1 (2024).
- ⁶⁷¹L. Di Benedetto, G. D. Licciardo, R. Nipoti, and S. Bellone, *IEEE Electron Device Letters* **35**, 244 (2014).
- ⁶⁷²M. Puzzanghera and R. Nipoti, *Materials Science Forum* **858**, 773 (2016).
- ⁶⁷³M. Domeij, E. Danielsson, W. Liu, U. Zimmermann, C.-M. Zetterling, and M. Ostling, in *ISPSD '03. 2003 IEEE 15th International Symposium on Power Semiconductor Devices and ICs, 2003. Proceedings* (IEEE, Cambridge, UK, 2003) pp. 375–378.
- ⁶⁷⁴A. Koyama, M. Sometani, K. Takenaka, K. Nakayama, A. Miyasaka, K. Kojima, K. Eto, T. Kato, J. Senzaki, Y. Yonezawa, and H. Okumura, *Japanese Journal of Applied Physics* **59**, SGGD14 (2020).
- ⁶⁷⁵M. Kato, Y. Mori, and M. Ichimura, *Materials Science Forum* **778–780**, 293 (2014).
- ⁶⁷⁶A. K. Tiwari, M. Antoniou, N. Lophitis, S. Perkin, T. Trajkovic, and F. Udrea, *IEEE Transactions on Electron Devices* **66**, 3066 (2019).
- ⁶⁷⁷K. Tian, J. Xia, K. Elgammal, A. Schöner, W. Kaplan, R. Karhu, J. Ul-Hassan, and A. Hallén, *Materials Science in Semiconductor Processing* **115**, 105097 (2020).
- ⁶⁷⁸M. E. Levenshtein, T. T. Mnatsakanov, P. A. Ivanov, A. K. Agarwal, J. W. Palmour, S. L. Rumyantsev, A. G. Tandoev, and S. N. Yurkov, *Solid-State Electronics* **45**, 453 (2001).
- ⁶⁷⁹S. Bellone, L. F. Albanese, and G.-D. Licciardo, *IEEE Transactions on Electron Devices* **56**, 2902 (2009).
- ⁶⁸⁰M. Usman, B. Buono, and A. Hallen, *IEEE Transactions on Electron Devices* **59**, 3371 (2012).
- ⁶⁸¹Value fitted to results by Galeckas *et al.*²⁵⁵.
- ⁶⁸²Value fitted to forward current measurements by Ryu *et al.*⁷⁵⁷.
- ⁶⁸³Value fitted to measurements by Kimoto *et al.*⁴⁸⁷.
- ⁶⁸⁴T. Kimoto, K. Yamada, H. Niwa, and J. Suda, *Energies* **9**, 908 (2016).
- ⁶⁸⁵K. Naydenov, N. Donato, and F. Udrea, *Engineering Research Express* **3**, 035008 (2021).
- ⁶⁸⁶A. Galeckas, J. Linnros, V. Grivickas, U. Lindefelt, and C. Hallin,

- Materials Science Forum **264–268**, 533 (1998).
- ⁶⁸⁷B. Kakarla, A. Tsibizov, R. Stark, I. K. Badstubner, and U. Grossner, in *2020 32nd International Symposium on Power Semiconductor Devices and ICs (ISPDS)* (IEEE, Vienna, Austria, 2020) pp. 234–237.
- ⁶⁸⁸S. Bellone and L. Di Benedetto, *IEEE Transactions on Power Electronics* **29**, 2174 (2014).
- ⁶⁸⁹L. Di Benedetto, N. Rinaldi, G. D. Licciardo, R. Liguori, A. Rubino, A. May, and M. Rommel, in *2024 International Semiconductor Conference (CAS)* (IEEE, Sinaia, Romania, 2024) pp. 23–28.
- ⁶⁹⁰S. Asada, T. Miyazawa, and H. Tsuchida, *IEEE Transactions on Electron Devices* **68**, 3468 (2021).
- ⁶⁹¹N. Ramungul, V. Khemka, T. P. Chow, M. Ghezzo, and J. W. Kretchmer, Materials Science Forum **264–268**, 1065 (1998).
- ⁶⁹²R. Nipoti, A. Parisini, G. Sozzi, M. Puzzanghera, A. Parisini, and A. Carnera, *ECS Journal of Solid State Science and Technology* **5**, P621 (2016).
- ⁶⁹³T. Grasser, B. Kaczer, W. Goes, Th. Aichinger, Ph. Hehenberger, and M. Nelhiebel, in *2009 IEEE International Reliability Physics Symposium* (IEEE, Montreal, QC, Canada, 2009) pp. 33–44.
- ⁶⁹⁴H. Pourbagheri Mahabadi, *Optical Studies of Surface Recombination Velocity in 4H-SiC Epitaxial Layer*, Master's thesis, KTH, School of Information and Communication Technology (ICT) / KTH, School of Information and Communication Technology (ICT) (2011).
- ⁶⁹⁵A. Xiang, *IEEE Transactions on Nanotechnology* **20**, 28 (2021).
- ⁶⁹⁶I. G. Atabaev, Kh. N. Juraev, and M. U. Hajiev, *Journal of Spectroscopy* **2018**, 1 (2018).
- ⁶⁹⁷V. Heera, D. Panknin, and W. Skorupa, *Applied Surface Science* **184**, 307 (2001).
- ⁶⁹⁸M. Miyata, Y. Higashiguchi, and Y. Hayafuji, *Journal of Applied Physics* **104**, 123702 (2008).
- ⁶⁹⁹J. Senzaki, K. Fukuda, Y. Ishida, Y. Tanaka, H. Tanoue, N. Kobayashi, T. Tanaka, and K. Arai, *MRS Proceedings* **622**, T6.7.1 (2000).
- ⁷⁰⁰T. Troffer, G. Pensl, A. Schöner, A. Henry, C. Hallin, Kordina, and E. Janzén, Materials Science Forum **264–268** (1998), 10.4028/www.scientific.net/MSF.264-268.557.
- ⁷⁰¹M. Krieger, M. Rühl, T. Sledziewski, G. Ellrott, T. Palm, H. B. Weber, and M. Bockstedte, Materials Science Forum **858**, 301 (2016).
- ⁷⁰²E. M. Handy, M. V. Rao, O. W. Holland, K. A. Jones, M. A. Derenge, and N. Papanicolaou, *Journal of Applied Physics* **88**, 5630 (2000).
- ⁷⁰³G. Xiao, J. Lee, J. Liou, and A. Ortiz-Conde, *Microelectronics Reliability* **39**, 1299 (1999).

- 70⁴N. Donato and F. Udrea, *IEEE Transactions on Electron Devices* **65**, 4469 (2018).
- 70⁵R. Nipoti, H. M. Ayedh, and B. G. Svensson, *Materials Science in Semiconductor Processing* **78**, 13 (2018).
- 70⁶Q. Chen, W. He, C. Cheng, and Y. Xue, *Journal of Physics: Conference Series* **1649**, 012048 (2020).
- 70⁷M. Laube, F. Schmid, G. Pensl, G. Wagner, M. Linnarsson, and M. Maier, *Journal of Applied Physics* **92**, 549 (2002).
- 70⁸Z. Lv, J. Li, L. Dong, and J. Zang, in *2023 International Conference on Telecommunications, Electronics and Computer Engineering (ICTEC)* (IEEE, Lisbon, Portugal, 2023) pp. 269–273.
- 70⁹H. Matsuura, *Materials Science Forum* **389–393**, 679 (2002).
- 71⁰G. L. Pearson and J. Bardeen, *Physical Review* **75**, 865 (1949).
- 71¹A. Schöner, *Elektrische Charakterisierung von Flächen Und Tiefen Störstellen in 4H-, 6H- Und 15R-Siliziumkarbid*, Ph.D. thesis, FriedrichAlexander-Universität (1994).
- 71²P. Achatz, J. Pernot, C. Marcenat, J. Kacmarcik, G. Ferro, and E. Bustarret, *Applied Physics Letters* **92**, 072103 (2008).
- 71³J. Weiße, M. Hauck, T. Sledziewski, M. Tschiesche, M. Krieger, A. J. Bauer, H. Mitlehner, L. Frey, and T. Erlbacher, *Materials Science Forum* **924**, 184 (2018).
- 71⁴Y. Kajikawa, *Journal of Electronic Materials* **50**, 1247 (2021).
- 71⁵M. Rambach, A. J. Bauer, and H. Ryssel, *physica status solidi (b)* **245**, 1315 (2008).
- 71⁶R. Scaburri, A. Desalvo, and R. Nipoti, *Materials Science Forum* **679–680**, 397 (2011).
- 71⁷P. P. Altermatt, A. Schenk, and G. Heiser, *Journal of Applied Physics* **100**, 113714 (2006).
- 71⁸P. P. Altermatt, A. Schenk, B. Schmithüsen, and G. Heiser, *Journal of Applied Physics* **100**, 113715 (2006).
- 71⁹P. T. Landsberg, *physica status solidi (b)* **41**, 457 (1970).
- 72⁰B. K. Ridley, *Journal of Physics C: Solid State Physics* **11**, 2323 (1978).
- 72¹M. Lades, W. Kaindl, N. Kaminski, E. Niemann, and G. Wachutka, *IEEE Transactions on Electron Devices* **46**, 598 (1999).
- 72²M. Lax, *Physical Review* **119**, 1502 (1960).
- 72³V. N. Abakumov, V. I. Perel, and I. N. Yassievich, *Nonradiative Recombination in Semiconductors*, Modern Problems in Condensed Matter Sciences No. v. 33 (North-Holland ; Sole distributors for the USA and Canada, Elsevier Science Pub. Co, Amsterdam ; New York : New York, NY, USA, 1991).
- 72⁴W. Kaindl, M. Lades, N. Kaminski, E. Niemann, and G. Wachutka, *Journal of Electronic Materials* **28**, 154 (1999).

- ⁷²⁵I. S. Gorban, A. P. Krokhmal', V. I. Levin, A. S. Skirda, Yu. M. Tairov, and V. F. Tsetkov, Sov. Phys. Semiconductors **21**, 119 (1987).
- ⁷²⁶S. Asada, T. Okuda, T. Kimoto, and J. Suda, *Applied Physics Express* **9**, 041301 (2016).
- ⁷²⁷S. Contreras, L. Konczewicz, P. Kwasnicki, R. Arvinte, H. Peyre, T. Chassagne, M. Zielinski, M. Kayambaki, S. Juillaguet, and K. Zekentes, *Materials Science Forum* **858**, 249 (2016).
- ⁷²⁸C. Hitchcock, R. Ghandi, P. Deeb, S. Kennerly, M. Torky, and T. P. Chow, *Materials Science Forum* **1062**, 422 (2022).
- ⁷²⁹R. Nipoti, R. Scaburri, A. Hallén, and A. Parisini, *Journal of Materials Research* **28**, 17 (2013).
- ⁷³⁰M. Obernhofer, M. Krieger, F. Schmid, H. B. Weber, G. Pensl, and A. Schöner, *Materials Science Forum* **556–557**, 343 (2007).
- ⁷³¹G. Pensl, F. Schmid, F. Ciobanu, M. Laube, S. A. Reshanov, N. Schulze, K. Semmelroth, A. Schöner, G. Wagner, and H. Nagasawa, *Materials Science Forum* **433–436**, 365 (2003).
- ⁷³²M. Rambach, L. Frey, A. J. Bauer, and H. Ryssel, *Materials Science Forum* **527–529**, 827 (2006).
- ⁷³³S. Rao, T. P. Chow, and I. Bhat, *Materials Science Forum* **527–529**, 597 (2006).
- ⁷³⁴G. Rutsch, R. P. Devaty, W. J. Choyke, D. W. Langer, and L. B. Rowland, *Journal of Applied Physics* **84**, 2062 (1998).
- ⁷³⁵N. S. Saks, A. K. Agarwal, S.-H. Ryu, and J. W. Palmour, *Journal of Applied Physics* **90**, 2796 (2001).
- ⁷³⁶N. S. Saks, A. V. Suvorov, and D. C. Capell, *Applied Physics Letters* **84**, 5195 (2004).
- ⁷³⁷F. Schmid, M. Laube, G. Pensl, G. Wagner, and M. Maier, *Journal of Applied Physics* **91**, 9182 (2002).
- ⁷³⁸A. Schöner, S. Karlsson, T. Schmitt, N. Nordell, M. Linnarsson, and K. Rottner, *Materials Science and Engineering: B* **61–62**, 389 (1999).
- ⁷³⁹G. Wagner, W. Leitenberger, K. Irmscher, F. Schmid, M. Laube, and G. Pensl, *Materials Science Forum* **389–393**, 207 (2002).
- ⁷⁴⁰R. Wang, I. B. Bhat, and T. P. Chow, *Journal of Applied Physics* **92**, 7587 (2002).
- ⁷⁴¹S. Y. Ji, K. Kojima, Y. Ishida, H. Tsuchida, S. Yoshida, and H. Okumura, *Materials Science Forum* **740–742**, 181 (2013).
- ⁷⁴²H. Matsuura, K. Aso, S. Kagamihara, H. Iwata, T. Ishida, and K. Nishikawa, *Applied Physics Letters* **83**, 4981 (2003).
- ⁷⁴³S. Smith, A. Evwaraye, and W. Mitchel, *MRS Proceedings* **510**, 193 (1998).

- ⁷⁴⁴K. Kawahara, H. Watanabe, N. Miura, S. Nakata, and S. Yamakawa, *Materials Science Forum* **821–823**, 403 (2015).
- ⁷⁴⁵S. Beljakowa, S. A. Reshanov, B. Zippelius, M. Krieger, G. Pensl, K. Danno, T. Kimoto, S. Onoda, T. Ohshima, F. Yan, R. P. Devaty, and W. J. Choyke, *Materials Science Forum* **645–648**, 427 (2010).
- ⁷⁴⁶C. Kisielowski, K. Maier, J. Schneider, and V. Oding, *Materials Science Forum* **83–87**, 1171 (1992).
- ⁷⁴⁷M. Kato, J. Di, Y. Ohkouchi, T. Mizuno, M. Ichimura, and K. Kojima, *Materials Today Communications* **31**, 103648 (2022).
- ⁷⁴⁸N. T. Son, A. Henry, J. Isoya, M. Katagiri, T. Umeda, A. Gali, and E. Janzén, *Physical Review B* **73**, 075201 (2006).
- ⁷⁴⁹M. Bockstedte, A. Mattausch, and O. Pankratov, *Applied Physics Letters* **85**, 58 (2004).
- ⁷⁵⁰Y. Negoro, T. Kimoto, H. Matsunami, F. Schmid, and G. Pensl, *Journal of Applied Physics* **96**, 4916 (2004).
- ⁷⁵¹A. K. Tiwari, F. Udrea, N. Lophitis, and M. Antoniou, in *2019 31st International Symposium on Power Semiconductor Devices and ICs (ISPSD)* (IEEE, Shanghai, China, 2019) pp. 175–178.
- ⁷⁵²J. Sullivan and J. Stanley, *IEEE Transactions on Plasma Science* **36**, 2528 (2008).
- ⁷⁵³F. Pezzimenti, L. F. Albanese, S. Bellone, and F. G. D. Corte, in *2009 IEEE Bipolar/BiCMOS Circuits and Technology Meeting* (IEEE, Capri, Italy, 2009) pp. 214–217.
- ⁷⁵⁴G. Pensl, ed., *Silicon Carbide, III-nitrides and Related Materials: Proceedings of the 7th International Conference on Silicon Carbide, III-Nitrides and Related Materials, Stockholm, Sweden, September 1997*, Materials Science Forum No. 264/268 (1998).
- ⁷⁵⁵K. Adachi, *Simulation and Modelling of Power Devices Based on 4H Silicon Carbide*, Ph.D. thesis, University of Newcastle (2003).
- ⁷⁵⁶A. Gali, P. Deák, R. P. Devaty, and W. J. Choyke, *Physical Review B* **60**, 10620 (1999).
- ⁷⁵⁷S.-H. Ryu, C. Capell, L. Cheng, C. Jonas, A. Gupta, M. Donofrio, J. Clayton, M. O'Loughlin, A. Burk, D. Grider, A. Agarwal, J. Palmour, A. Hefner, and S. Bhattacharya, in *2012 IEEE Energy Conversion Congress and Exposition (ECCE)* (IEEE, Raleigh, NC, USA, 2012) pp. 3603–3608.
- ⁷⁵⁸W. J. Choyke and L. Patrick, *Physical Review* **127**, 1868 (1962).